Quantitative analysis of geological controls on incised-valley-fill geometry and stratigraphic architecture

Ru Wang

Submitted in accordance with the requirements for the degree of
Doctor of Philosophy

The University of Leeds
School of Earth and Environment

February, 2020

The candidate confirms that the work submitted is her own, except where work which has formed part of jointly-authored publications has been included. The contribution of the candidate and the other authors to this work has been explicitly indicated below. The candidate confirms that appropriate credit has been given within the thesis where reference has been made to the work of others.

The thesis comprises three chapters that were prepared for publication and have been subsequently modified for inclusion in this thesis. The current status of these components of the thesis, at the time of submission, is as follows:

Chapter 3:

Wang, R., Colombera, L., Mountney, N.P., 2019. Geologic controls on the geometry of incised-valley fills: Insights from a global dataset of late-Quaternary examples. Sedimentology, 66, 2134-2168. DOI: 10.1111/sed.12596.

Wang, R. – Main author. Responsible for data collection, processing, collation and interpretation, and writing of the manuscript.

Colombera, L. – Data processing using the Shallow-Marine Architecture Knowledge Store (SMAKS) database developed by the Shallow-Marine Research Group at the University of Leeds. In-depth discussion and detailed review of the manuscript.

Mountney, N.P. – In-depth discussion and detailed review of the manuscript.

Chapter 4:

Wang, R., Colombera, L., Mountney, N.P., 2020. Quantitative analysis of the stratigraphic architecture of incised-valley fills: a global comparison of Quaternary systems. Earth-Science Reviews, 102988, 1-25. DOI: 10.1016/j.earscirev.2019.102988.

Wang, R. – Main author. Responsible for data collection, processing, collation and interpretation, and writing of the manuscript.

Colombera, L. – Data processing using the Shallow-Marine Architecture Knowledge Store (SMAKS) database developed by the Shallow-Marine Research Group at the University of Leeds. In-depth discussion and detailed review of the manuscript.

Mountney, N.P. – In-depth discussion and detailed review of the manuscript.

Chapter 5:

Wang, R., Colombera, L., Mountney, N.P., (in review). Palaeohydrologic characteristics and palaeogeographic reconstructions of incised-valley-fill systems: insights from the Namurian successions of the United Kingdom and Ireland. Submitted to Sedimentology.

Wang, R. – Main author. Responsible for data collection, processing, collation and interpretation, and writing of the manuscript.

Colombera, L. – Data processing using the Fluvial Architecture Knowledge Transfer System (FAKTS) database developed by the Fluvial Research Group at the University of Leeds. In-depth discussion and detailed review of the manuscript.

Mountney, N.P. – Detailed review of the manuscript.

Acknowledgements

First, I would like to thank my supervisors Nigel Mountney and Luca Colombera for providing the opportunity to work on this PhD research project and for all of the guidance and support throughout my PhD. A special thank you to Luca for the hours spent in discussing and proofreading my manuscripts in the last three years. I also want to thank Nigel for the guidance in grant application and providing the opportunity to present my research all over the world.

China Scholarship Council is thanked for its financial support through my study. FRG-ERG and SMRG sponsors and partners AkerBP, Areva (now Orano), BHPBilliton, Cairn India (Vedanta), ConocoPhillips, Chevron, Debmarine, Engie, Equinor, Murphy Oil, Nexen-CNOOC, Occidental, Petrotechnical Data Systems, Saudi Aramco, Shell, Tullow Oil, Woodside and YPF are thanked for their additional financial support. I am grateful for IAS to provide a Postgraduate Research Grant that enabled field data collection for part of this study in Pembrokeshire, Wales. IAS and SEPM are thanked for provision of travel grants to SEPM 2020 conference. Soma Budai is thanked for fieldwork assistance. Roman Soltan is thanked for providing papers on the geology of the Pennine Basin and sharing his experience of fieldwork techniques. Xin Zhao is thanked for giving advice on statistical methods. Anna Clough from the IT department at University of Leeds is thanked for offering guidance on the utilization of ArcGIS. This research also benefits greatly from various training courses provided by University of Leeds, such as Outdoor first-aid course, Introduction to Digital Maps, Statistics and Introduction to Data Science.

I am also grateful for all the experiences and opportunities I have received throughout my PhD studies, notably demonstrating in lab classes and fieldwork , and for the pleasant times I had during conferences, especially ICFS and AAPG. Special thanks are given to all those long-term and professional fellows in ICFS, for opening the gate to the world of sedimentologists and getting me interested in a career life in academia. I was really awed by your passion and determination in exploring the truth in science.

Thank you for members of FRG-ERG for the support and accompany in the past three years, notably Yan Na, Sonia Campos-Soto, Jose Montero, Dave Somerville and Simon Jackson. I would also like to thank my friends, in particular, Xueting Wang, for being my longest and best friend through 11 years of sharing joys and sorrows. A final special thank you is for my family for years of unconditional support, encouragement and hugs, especially my parents for the everlasting trust no matter what choice I made.

Abstract

Incised-valley systems are common features in coastal and shelf regions. Assessments of factors possibly controlling the geometry of incised valleys commonly either focus on experimental or numerical models, or are based on consideration of individual examples. Classical facies models characterizing the internal fills of incised valleys are largely conceptual, descriptive and qualitative, and are mostly limited to individual examples. Here, novel database-driven quantitative analysis of 151 late-Quaternary incised-valley fills (IVFs) is undertaken, aiming at exploring the relative roles of possible controls in determining the geometry and stratigraphic architecture of IVFs. The resulting knowledge is then applied to further our understanding of the significance of ancient IVFs in the older geological record: a data synthesis of 18 Namurian (Serpukhovian to Bashkirian) IVFs from the United Kingdom and Ireland is performed to characterize the palaeohydrologic characteristics of the formative rivers feeding these incised valleys, and to attempt a refinement of the regional palaeogeographic reconstructions. Results indicate that various factors including relative sea-level change operate to control the geometry of IVFs, notably basin physiography, drainage-basin size, climate, substrate type and tectonics. Upstream controls (e.g., drainage area and dominant vegetation type in the catchment) appear to be more important in determining valley geometry, compared to the characteristics of the receiving basin (e.g., basin physiography, substrates and shoreline hydrodynamics), especially for passive margins. Significant variability in stratigraphic architectures of IVFs is identified that is not accounted for by classical facies and sequence-stratigraphic models. Factors other than relative sea-level fluctuations – such as continental-margin type, drainage area, IVF geometry, basin physiography and shoreline hydrodynamics – are demonstrated to be responsible for the observed variability in the internal architecture of IVFs. Facies architecture recorded in the Namurian IVF fluvial deposits indicate that their formative palaeorivers were likely perennial and characterized by relatively low discharge variability. This study challenges some paradigms embedded in sequence-stratigraphic thinking, notably the notion that the degree of exposure of the shelf dictates the magnitude of vertical incision preserved in sequence boundaries, and the view that magnitude and location of valley incision are primarily determined by the coastal-prism convexity at the highstand shoreline, if the sea-level does not drop below the shelf break. The results also have significant implications for improved understanding of source-to-sink scaling and have important applied significance in subsurface-reservoir prediction and characterization.

Contents

List of tables

List of figures

Abbreviations

1D	one-dimensional
2D	two-dimensional
3D	three-dimensional
SMAKS	Shallow-Marine Architecture Knowledge Store
FAKTS	Fluvial Architecture Knowledge Transfer System
IVF	incised-valley fill
LGM	Last Glacial Maximum
LI	Last Interglacial
LST	Lowstand Systems Tract
TST	Transgressive Systems Tract
HST	Highstand Systems Tract
UK	United Kingdom

1 Introduction

1.1 Project rationale

Incised-valley systems have long been recognized as common features developed in shelf and coastal regions. They are typically defined as fluvially eroded, elongate palaeotopographic lows formed by river incision that is itself driven by relative sea-level fall; the valleys are then subsequently infilled with sediment during subsequent relative sea-level rise (Posamentier and Allen, 1999; Zaitlin et al, 1994; Blum et al., 2013). Compared to the adjacent continental shelf regions, the internal fills of nearshore incised-valley systems generally form important archives of critical stratigraphic information on environmental change in coastal regions, notably in relation to changes in sea level and climate (e.g. Mattheus and Rodriguez, 2011; Wetzel et al., 2017). Due to the subject to severe physical reworking such as wave erosions and/or sediment starvation, the adjacent shelf areas tend to have a less complete sedimentary record (Boyd et al., 2006; Simms et al., 2010; Mattheus and Rodriguez, 2011). In this regard, the infills of incised valleys have also been of great interest to research scientists in the field of sequence stratigraphy because they can provide a detailed record of the sedimentary response to changes in sea level and related environmental factors such as climate and rate and timing of sediment supply to shorelines (e.g., Lin et al., 2005; Dalrymple, 2006; Chaumillon et al., 2010). Moreover, incised-valley-fill systems have important applied significance, as they can form potential hydrocarbon reservoirs themselves, and can be considered as reference for prediction of downdip lowstand delta and deep-marine sand accumulations (Dalrymple et al. 1994; Shanley and McCabe, 1994; Zaitlin et al., 1994; Blum et al., 2013). Additionally, present-day estuaries and rias that notably develop at the mouths of incised valleys during the episodes of relative sea-level rise, are of considerable economic and ecological importance; the response of these flooded incised-valley systems to on-going sea-level change, and to changes in other external controls can significantly influence the cities, human populations, associated coastal infrastructure and industries (e.g., ports and large-scale fisheries) located in or adjacent to these areas (Kennish, 1991; Chaumillon et al., 2010; Zhang et al., 2014; Marlianingrum et al., 2019).

In consideration of the scientific, economic and ecological importance of incised-valley-fill systems, a wide variety of research has focused on the characterization of

the stratigraphic organization of incised-valley fills (e.g., Roy, 1984; Dalrymple et al., 1992; Allen and Posamentier, 1993, 1994b; Zaitlin et al., 1994; Boyd et al., 2006; Blum et al., 2013). Nevertheless, relatively few studies have been performed to explore and evaluate potential geological controls on the geometry of nearshore incised-valley systems. Of those studies that have been undertaken, most either concentrate on experimental or numerical models (Talling, 1998; Strong and Paola, 2006, 2008; Martin et al., 2011), or are based on case studies of individual examples (e.g. Posamentier, 2001; Weber et al., 2004; Ishihara and Sugai, 2017), or consider a limited number of examples located in a single area (e.g. Mattheus 2007; Mattheus and Rodriguez, 2011; Phillips, 2011; Chaumillon et al., 2008). Furthermore, widely employed traditional facies models characterizing the internal fills of nearshore incised valleys (e.g., Dalrymple et al., 1992; Allen and Posamentier, 1994b; Zaitlin et al., 1994) are typically conceptual, descriptive and qualitative, and are mostly constrained to individual examples.

Identifying and quantifying the nature and impact of many different geological boundary conditions on the geometry and stratigraphic architecture of incised-valley-fill systems is not straightforward because the preserved geological record of incised-valley-fill systems is highly varied. Only by means of quantitative statistical analysis of very large composite datasets that incorporate the attributes of a wide variety of examples, can critical insight be gained to an improved understanding of the relative roles of many different geological controls in determining the geometry and stratigraphic architecture of incised-valley-fill systems. In this PhD research project, a novel database-driven approach is employed to attempt to address this issue stated above. In particular, in the first part of this Thesis, attention is focused on quantitative analysis of late-Quaternary examples. This is because the controlling factors on valley-fill characteristics and evolution can be constrained more closely for recent sea-level cycles compared to those in the ancient past. In a successive part of the Thesis, the resultant database-conditioned models derived from late-Quaternary examples are applied to tentatively reconstruct characteristics of river systems from the preserved alluvial stratigraphic record. This is achieved through an examination of examples of incised valley-fills present in the Namurian successions of the United Kingdom (UK) and Ireland. The facies architecture of these ancient examples is employed to help decipher palaeohydraulic characteristics of their formative rivers and to attempt a refinement of regional palaeogeographic reconstructions.

1.2 Aim and Objectives

The overarching aim of this research project is to gain an improved understanding of the relative roles of possible geological controls in determining the geometry and stratigraphic architecture of incised-valley-fill systems, and to present the implications of these results for sequence-stratigraphic models, source-to-sink studies and of their applied significance. Specific objectives of this research are summarised as follows:

(i) to evaluate the relative roles of possible geological controls in determining the dimensions of incised-valley fills;

(ii) to perform a comprehensive quantitative statistical analysis on the basis of data relating to the geometry, spatial relationships, stacking patterns, and lithological heterogeneity of deposits that form the infill of late-Quaternary incised valleys documented in the published literature and through one original field study;

(iii) to evaluate the relative roles of possible geological controls in determining the stratigraphic architecture of incised-valley fills;

(iv) to present implications of the results based on late-Quaternary examples for sequence-stratigraphic models, source-to-sink studies and subsurface-reservoir prediction and characterization;

(v) to apply scaling relationships derived from late-Quaternary examples to reconstruct characteristics of river systems from the ancient rock record, and together with complementary analyses of facies architecture to decipher their palaeohydraulic characteristics;

(vi) to present implications for regional palaeogeographic reconstructions, when estimation of contributing drainage-basin area is considered in combination with existing provenance studies and sedimentological data.

1.3 Methods

In this work, quantitative statistical analyses based on two relational databases, the Shallow-Marine Architecture Knowledge Store (SMAKS; Colombera et al., 2016) and the Fluvial Architecture Knowledge Transfer System (FAKTS; Colombera et al., 2012), have been performed in order to achieve the Thesis aim stated above. Data population into the SMAKS and FAKTS databases has been a key activity of this PhD project: all the datasets utilized for the quantitative analyses presented in this

PhD Thesis have been coded into their respective relational databases (FAKTS and SMAKS) as part of this research.

The SMAKS database is employed to investigate the relative roles of different geological controls in determining the dimensions and stratigraphic architecture of incised-valley-fill systems through a literature compilation of late-Quaternary examples. Data on the geometry, spatial relationships, stacking patterns, and lithological heterogeneity of deposits that form the infill of late-Quaternary incised valleys, dimensions of late-Quaternary incised-valley fills and parameters that describe their context and controlling factors are extracted from published literature, standardized into common formats and subsequently included into the SMAKS database (**Fig. 1.1**). SMAKS incorporates quantitative data on the sedimentary architecture and geomorphic organization of shallow-marine and paralic siliciclastic depositional systems. It stores quantitative data relating to geological entities of varied nature and scale (i.e., surfaces, depositional tracts, architectural elements, sequence stratigraphic surfaces, sequence stratigraphic units, facies units, geomorphic elements) (**Fig. 1.2**), and to their associated depositional systems, themselves classified on several parameters (e.g., shelf width, delta catchment area) tied to metadata (e.g., data types, data sources).

In this work, the FAKTS database is utilized to store and analyse data on fluvial successions forming parts of Namurian incised-valley fills in the UK and Ireland; these data are then used to quantitatively estimate palaeohydrological characteristics of the formative rivers and to attempt to refine the regional palaeogeographic reconstructions for the basins that hosted them. Data on the sedimentology of fluvial deposits forming the majority of these IVFs are extracted from the published literature and through a field study (Farewell Rock, Pembrokeshire, South Wales), and digitized to a common standard for inclusion in FAKTS (**Fig. 1.1**). FAKTS commonly captures data on the geometry, spatial relationships, and hierarchical relationships of genetic units such as ‘depositional elements’, ‘architectural elements’ and ‘facies units’ (**Fig. 1.3**); these genetic units are assigned to subsets of fluvial systems, which can be classified on a series of boundary conditions (e.g., climate, tectonic setting, catchment area) and metadata (e.g., data quality, data types). Facies units in FAKTS represent lithofacies classified according to grainsize and sedimentary structures, and are constrained by bounding surfaces that correspond to a change in lithofacies type or palaeocurrent direction, or to erosional contacts or element boundaries (Colombera et al., 2013).

As part of this PhD, a field study was conducted in Pembrokeshire, South Wales, which focused on the Upper Sandstone Group, a succession of Namurian age. The

study area is located in a peripheral foreland basin. Outcrops in this area reveal the internal sedimentary anatomy of one Namurian incised-valley fill in different locations, and hence provided an excellent opportunity for a field study with which to examine the internal fills of incised valleys. The fieldwork focused on the acquisition of quantitative and qualitative data of the geometry, spatial relationships, stacking patterns, and lithologic heterogeneity of architectural elements representative of a variety of subenvironments and sequence stratigraphic units that form the infill of an incised-valley fill. Field photomosaics, GPS measurements and architectural panels were taken at four outcrop localities (Amroth, Settling Nose, First Point near Tenby and Waterwynch Bay near Tenby), and data on lithofacies (**Fig. 1.4**), geometry and palaeocurrent distribution of the studied successions were collected. Grain-size data were obtained visually using a hand lens and a grain-size card. Additionally, measured sections also recorded the frequency and thickness of cross-sets of dune-scale cross strata, the thickness of architectural storeys, and the inclination and accretion direction of dipping beds forming the internal components of barform elements. Quantitative data relating to the measured thickness of lithofacies, measured thickness of dune-scale cross sets, bar- and channel-story geometries and dominance of sedimentary structures in this field work were extracted and utilized as shown in Chapter 5 to help decipher the palaeohydrological characteristics of the ancient rivers feeding this incised-valley fill, and to attempt to refine the regional palaeogeographic reconstructions of Namurian basins.

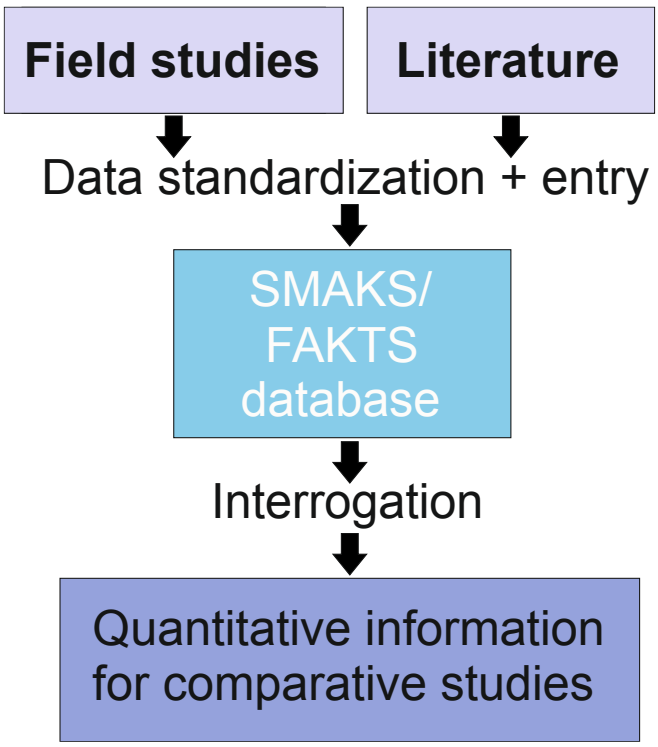

Fig. 1.1. *Flow chart demonstrating the workflow for data entry into and retrieval from the SMAKS and FAKTS databases.*

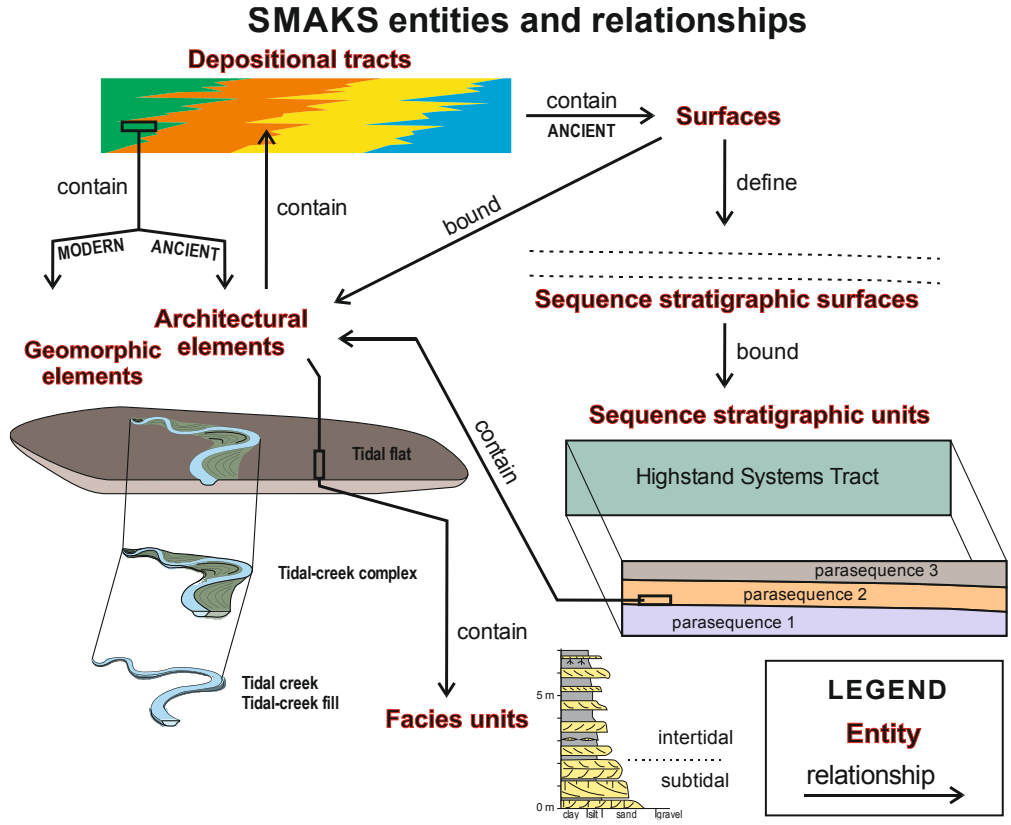

Fig. 1.2. *Schematic diagram depicting SMAKS entities and relationships that may exist between them. Modified after Colombera et al. (2016).*

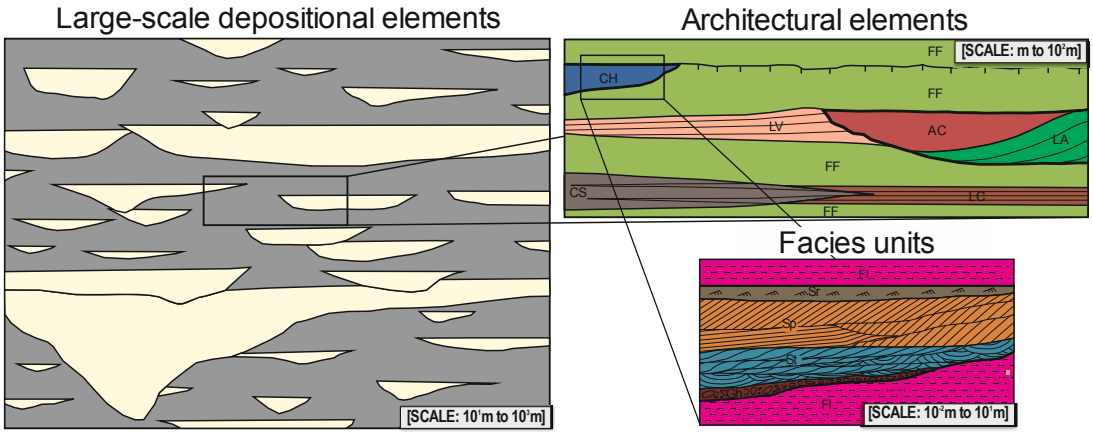

Fig. 1.3. *Definition sketch illustrating the main scales of observation and hierarchical relationships of sedimentary genetic units such as 'depositional elements', 'architectural elements' and 'facies units' stored in FAKTS database. Modified after Colombera et al. (2013).*

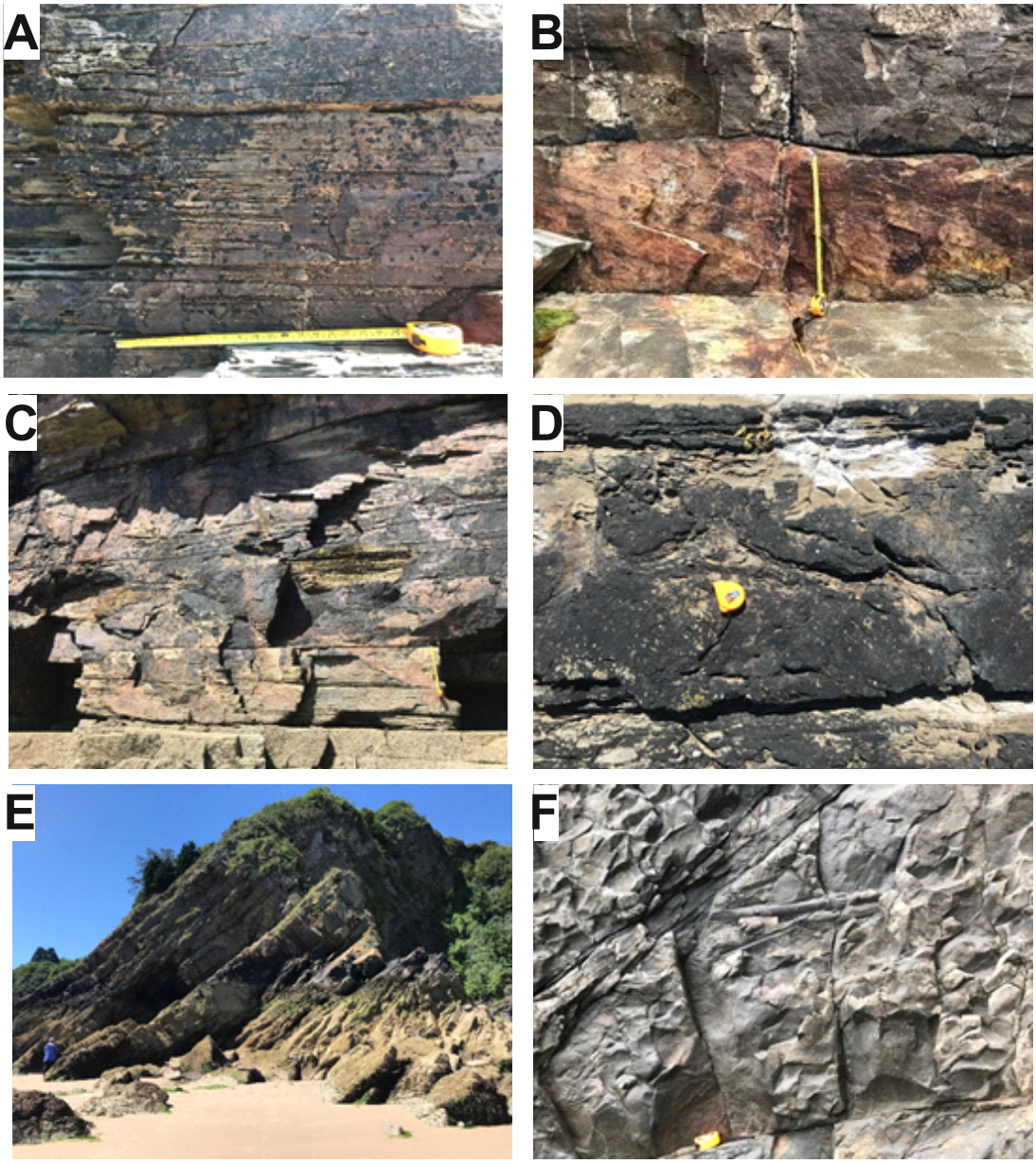

Fig. 1.4. *Facies types and associations observed in the Farewell Rock, Upper Sandstone Group, in South Wales. (A) Sr; ripple-laminated fine sandstone. (B) Sp; planar cross-stratified sandstone. (C) Sl; low-angle cross-bedded sandstone. (D) Sd; soft-sediment deformed sandstone. (E) Sp; planar cross-stratified sandstone. (F) C; Carbonaceous mudstone rich in organic-matter debris. Facies codes adapted from Colombera et al. (2013).*

In consideration of the diversity of data relating to the morphometric parameters of incised-valley fills, classification of in-valley architectural elements and corresponding geological boundary conditions reported in the primary data sources, these data were standardized into common formats prior to their inclusion into the databases (**Fig. 1.5**) for scope of comparative analysis. This included re-formatting

some classification schemes and re-defining the terminologies. For scopes of future analysis and to enable audit trail, the information and nomenclatures adopted in the primary data sources are also recorded, though these are not used in the presentation of the results in this PhD Thesis. Additionally, the perceived data quality and reliability from the original source work are recorded as a series of data quality indices (DQIs) (Colombera et al., 2012) on the basis of a threefold ranking system (rating datasets and attributes as A, B or C level, in order of decreasing quality) following established criteria (Baas et al. 2005). However, it is worth noting that these standardizations might carry uncertainties and are based on some assumptions. For instance, in this work, the morphometric parameters of incised-valley fills from the primary data sources were either derived from the text or measured directly on figures. Specifically, for datasets based on 2D or 3D high-resolution seismic data, conversions from two-way travel time (t) in the primary seismic sections to depth (h) were performed based on the seismic velocities (v) reported in the original source work, utilizing the simple geophysical relationship that $h = v*t/2$. For cases where the converting velocities are unavailable but for which the depth corresponding to a given two-way travel time recorded in the seismic sections is documented in the primary text, a calculation of the relationships between depth and two-way travel time was undertaken. Furthermore, based on the type of continental margin at the location where the incised-valley fills were characterized, the incised-valley fills are classified as being associated with continental margins that are passive, active or unclassified, according to the global distribution map of passive and active margins by Mann (2015). Additionally, in this research project, the distinction between inner shelf and outer shelf is based on bathymetry rather than process regime. The inner shelf is defined as the bathymetric tract extending from the present-day shoreline to the 25 m isobath, while the outer shelf is defined as the bathymetric tract extending from the 25 m isobath to the shelf break. For practical purposes, the 25-m isobath is chosen as the boundary between inner and outer shelf in this PhD Thesis because it is considered as a representative value of mean storm wave base (Katz et al., 2013).

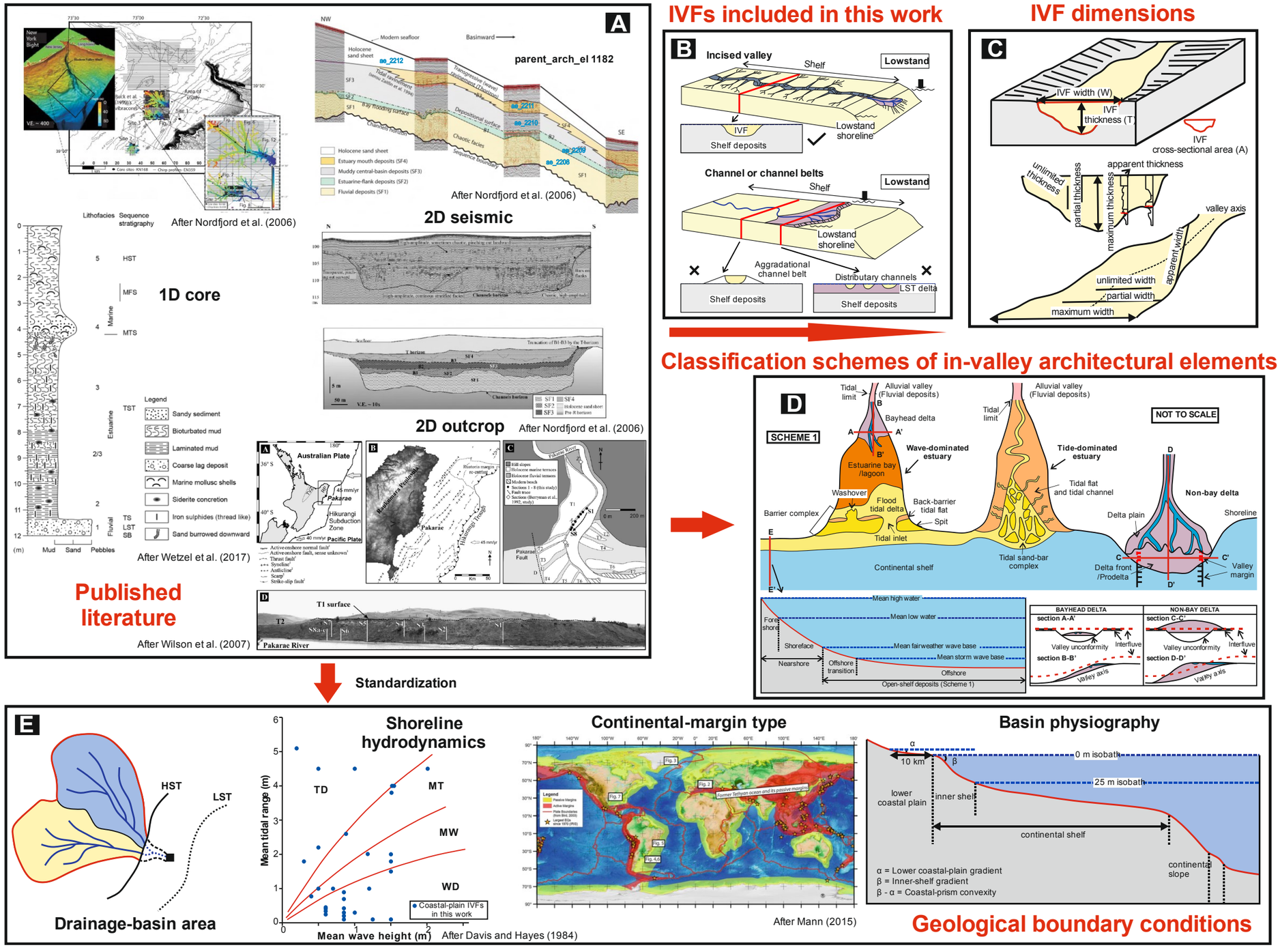

Fig. 1.5. *Diagram illustrating worked through examples from images and information in the published literature (A) to the standardized data (C-E) prior to their inclusion into the databases in this work. Channel belts in relation to river propagation on the shelf at lowstand and distributary channels relating to lowstand deltas, which might be misinterpreted into incised-valley fills in the primary sources, are not included in this work (B). In (D), only the classification scheme of in-valley architectural elements by (sub-)environment of deposition is illustrated here for presentation purposes.*

1.4 Thesis outline

This thesis contains seven chapters: Chapter 1 and Chapter 2 constitute the introductory part of the research project and include a detailed review of the background to the research topics. Specific research topics are subsequently explored and discussed in detail in Chapters 3-5. The scientific background, aim and objectives, and discussion of each sub-project are presented individually within each data chapter (3-5), and in this regard each chapter can be read as a stand-alone piece of work. In Chapters 3 and 4, attention is given to quantitative analysis of late-Quaternary examples, where deposits and controlling factors can be constrained closely. Chapter 3 focuses on the investigation of the possible geological controls on the geometry of incised-valley-fill systems and Chapter 4 concentrates on the exploration and evaluation of the relative roles of different geological controls in determining the stratigraphic architecture of incised-valley-fill systems. In Chapter 5, the focus is turned to analysis of incised-valley fills of Namurian age, from successions in the United Kingdom and Ireland. The facies architecture of these ancient examples is utilized to help decipher palaeohydraulic characteristics of their formative rivers, and to attempt a refinement of regional palaeogeographic reconstructions. Chapter 6 integrates the main findings in Chapters 3-5 and presents a wider discussion of the implications of these results, which are finally synthesised as the conclusions in Chapter 7.

Chapter 1: Introduction

The current chapter outlines the research rationale, overarching project aim and objectives. It also summarises the philosophy that underpins the project in relation to the data collection and analytical methods employed in this Thesis. Finally, it provides a brief introduction to the SMAKS and FAKTS databases utilized in this work.

Chapter 2: Literature Review

The second chapter provides an overview of published literature on the research topics explored in this work. This includes: i) an overview of external controls (sea-level change, climate and tectonics) on fluvial geometry and architecture, with an emphasis on the extent of sea-level influence along longitudinal profiles, and on the facies signature of discharge variability in the preserved alluvial stratigraphic record; and ii) an introduction to the current understanding of incised-valley-fill systems, notably the mechanisms of formation and evolution of incised-valley-fill systems,

the overall stratigraphic architecture of the internal fills of valley systems, and their significance from a source-to-sink perspective.

Chapter 3: Geologic controls on the geometry of incised-valley fills: insights from a global dataset of late-Quaternary examples

(Paper 1: Geologic controls on the geometry of incised-valley fills: Insights from a global dataset of late-Quaternary examples. Sedimentology, 66, 2134-2168. DOI: 10.1111/sed.12596)

The third chapter presents a database-driven statistical analysis of 151 late-Quaternary incised-valley fills, undertaken to investigate the geological controls on their geometry. Data on the geometry of late-Quaternary incised-valley fills and on variables describing their context and controlling factors form a large literature compilation. These quantitative data are analysed by means of statistical methods to evaluate the relative roles of different geological controls that might act to determine incised-valley-fill dimensions. The implications of the results for sequence stratigraphy and for hydrocarbon-reservoir prediction and characterization are also presented and discussed.

Chapter 4: Quantitative analysis of the stratigraphic architecture of incised-valley fills: a global comparison of Quaternary systems

(Paper 2: Quantitative analysis of the stratigraphic architecture of incised-valley fills: a global comparison of Quaternary systems. Earth-Science Reviews, 102988, 1-25. DOI: 10.1016/j.earscirev.2019.102988)

The fourth chapter focuses on the assessment of the general validity and predictive value of widely adopted facies models for incised-valley fills and investigation of the relative importance of possible controls on their stratigraphic organization. This is achieved using a database-driven quantitative statistical analysis of 87 late-Quaternary incised-valley fills. On the basis of a large composite dataset from the published literature stored in the SMAKS database, the geometry and proportion of systems tracts, and of architectural elements of different hierarchies within incised-valley fills are quantified. These characteristics are analysed to assess how they vary in relation to parameters that represent potential controlling factors: relative sea-level stage, continental-margin type, contributing drainage-basin area, valley geometry, basin physiography, and hydrodynamic conditions at the shoreline.

Chapter 5: Palaeohydrologic characteristics and palaeogeographic reconstructions of incised-valley-fill systems: insights from the Namurian successions of the United Kingdom and Ireland

(Paper 3: Palaeohydrologic characteristics and palaeogeographic reconstructions of incised-valley-fill systems: insights from the Namurian successions of the United Kingdom and Ireland. Submitted to Sedimentology, in review.)

The fifth chapter concentrates on a data synthesis of 18 Namurian (Carboniferous) sandstone-dominated fluvial successions from the United Kingdom and Ireland, interpreted to form the majority of the infill of cross-shelf incised valleys. The aim is to characterize the palaeohydrologic characteristics of the formative river systems feeding the IVFs and to attempt a refinement of the regional palaeogeographic reconstructions for the basins that hosted them. This is accomplished via the quantitative statistical analyses of facies proportions, of thickness distribution of dune-scale cross-strata, and of the geometry of the valley fills, with consideration of incised-valley-fill scaling relationships for late-Quaternary systems presented in Chapter 3.

Chapter 6: Discussion

The sixth chapter integrates the main findings presented in Chapters 3-5 of this Thesis and presents a discussion of the implications of the results for sequence-stratigraphic models and source-to-sink analysis, and of their applied significance.

Chapter 7: Conclusions and future work

The final chapter provides a short summary of the research, presenting conclusions pertinent to the overarching thesis aim and stated research objectives. Recommendations are also made for possible areas of future research, which might be undertaken to further build upon the findings presented and discussed in this Thesis.

2 Literature review

2.1 Allogenic controls on fluvial sedimentation

Fluvial systems respond to a wide range of external forcing mechanisms, including eustasy, climate change and tectonism (Shanley and McCabe, 1994; Blum and Törnqvist, 2000; Catuneanu, 2006; **Fig. 2.1**). These three external controls might operate on a sedimentary basin at any one time, but they do not need to be independent (Miall, 2014). Of considerable importance is the recognition of the distinction between downstream controls and upstream controls. In downstream reaches, rivers are influenced by base level; this equates to sea level in marine basins, lake level in some inland basins, or the level of a tectonic rim of a basin through which a river flows (Miall, 2014). Upstream controls include climate and tectonism. Climate affects fluvial discharge and vegetation cover, and therefore exerts a key control on sediment supply (Miall, 2014). Tectonism controls the relief in the source area and regional slope and consequently has a major influence on the calibre and quantity of the sediment being delivered (Miall, 2014). It is worth noting that climate and tectonism can also act as downstream controls through their effects on wave, tides and currents and rates of basin subsidence, respectively (Catuneanu, 2006).

The concept of river base level in the field of geomorphology and its outgrowth that led to the development of related concepts such as fluvial equilibrium longitudinal profile have played key roles in the development of an improved understanding of fluvial response to external controls. Powell (1875) introduced the concept of “base level” to refer to the lower limit to which a river can erode, with his defined “ultimate base level” being determined by sea level. Gilbert (1877) introduced the concept of “graded stream”, suggesting that rivers tend to aggrade or degrade as they strive for a ‘’graded’’ or equilibrium condition. Mackin (1948, p. 471) proposed the fundamental concept of fluvial equilibrium longitudinal profile as a “graded or dynamic equilibrium surface wherein the slope is adjusted so that there is neither net sediment aggradation nor erosion through time and that the sediment load entering the system from upstream equals the load leaving the system from downstream”, which can adjust to grade-altering factors propagating throughout the system (e.g., increased or decreased water discharge, increased or decreased sediment supply, base-level drop).

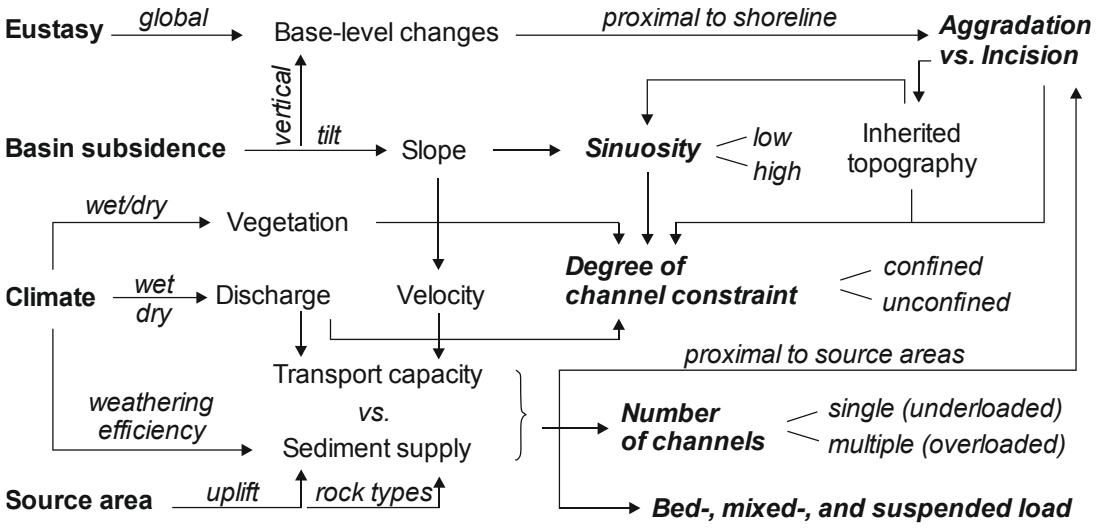

***Fig. 2.1**. Allogenic sedimentary controls on fluvial morphology, geometry and architecture. Fluvial processes of aggradation or degradation are a function of downstream controls (e.g., sea-level change, basin subsidence) and upstream controls (e.g., climate, source area uplift). Note that climate might also be a downstream control through its effects on waves, tides and currents. The controls on four key parameters widely adopted to characterize fluvial systems (sediment load type, sinuosity, degree of channel constraint and number of channels) are also shown in this diagram. Modified from Catuneanu (2006).*

2.1.1 Downstream controls

Fluvial response to downstream controls, particularly relative sea-level (RSL) change, has been intensively explored since the 1980s. As sea level is the ultimate base level in systems that meet a marine shoreline, the longitudinal profile of a shore-reaching river will rise or fall as a function of sea-level rise or fall and differences between the gradient of the original fluvial longitudinal profile and newly exposed land (Posamentier and Vail, 1988; Leckie, 1994; **Fig. 2.2**). Such changes and responses may be expressed and recorded by fluvial processes of aggradation or degradation (**Fig. 2.2**). However, other researchers (Schumm, 1993; Wescott, 1993) show that eustatic variations do not always significantly change the overall gradient of coeval river profiles and thus do not universally require an aggradational or degradational response, for example in cases where the profile is merely lengthened but its overall shape remains unchanged (see Emery and Myers, 1996, for a summary).

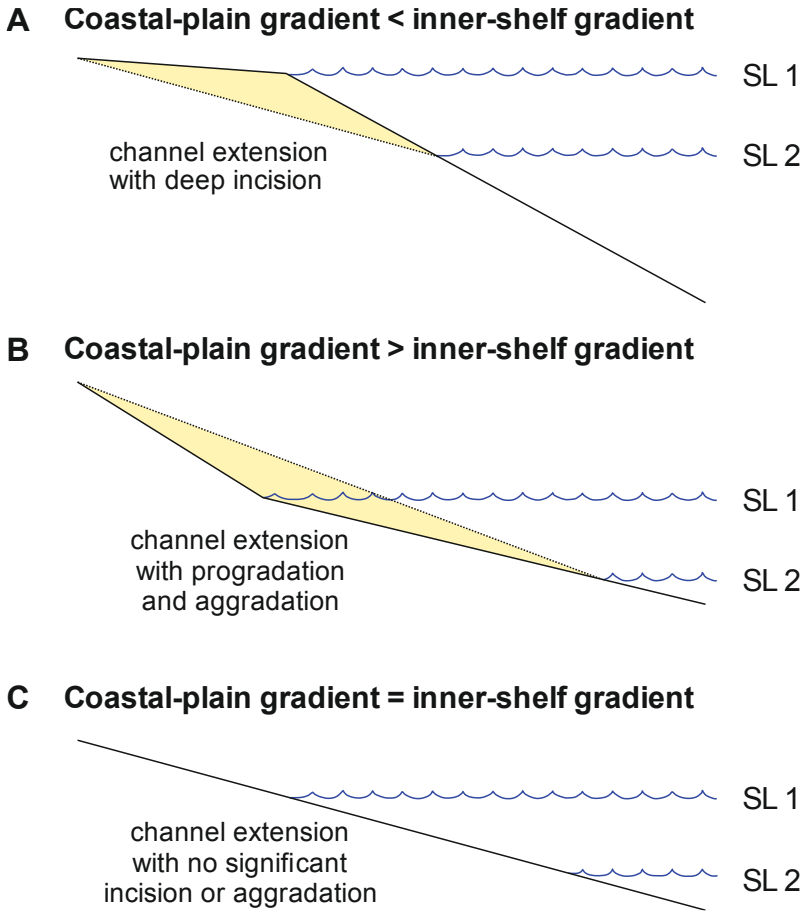

Fig. 2.2. *Simple conceptual generic models illustrating fluvial response to sea-level fall in relation to different combinations of coastal-plain and continental-shelf gradients. (A) Channel incision through coastal prism due to sea-level fall across a shelf that has a gradient steeper than the coastal plain; (B) Channel extension with no significant incision or aggradation due to no difference between coastal plain and exposed shelf as sea-level falls; (C) Channel extension with aggradation and progradation due to gentler gradients exposed on the inner shelf compared to coastal-plain gradients as sea-level falls. Adapted from Summerfield (1985).*

These discussions on downstream base-level controls on fluvial sedimentation have spawned a suite of widely used fluvial sequence-stratigraphic models (e.g., Wright and Marriott, 1993; Shanley and McCabe, 1994; Legarreta and Uliana, 1998; **Fig. 2.3-2.5**). These models typically attempt to fit to and extend an earlier generation of sequence stratigraphic models and concepts that apply to marine strata (e.g., Vail et al., 1977; Jervey, 1988; Posamentier and Vail, 1988; Posamentier et al., 1988); fluvial deposits are therefore attempted to be linked to the standard lowstand, transgressive and highstand systems tracts (LST, TST, HST). Within these models, relative sea-level change is argued to play a dominant role in controlling sedimentary system behaviour and the resultant nature of the

accumulated stratigraphic record. These fluvial sequence stratigraphic models (**Fig. 2.3-2.5**) tend to link fluvial strata with contemporaneous shorelines either on the basis of apparently interbedded fluvial and marine strata, or of the recognition of systematic vertical changes in channel sandbody stacking patterns. In detail, fluvial systems tend to incise when a relative fall in sea level occurs, which can promote subaerial erosion and the formation of incised valleys. When a relative rise in sea level takes place, channel belts and associated overbank deposits tend to stack progressively on the basal erosional surface as systems aggrade to fill available accommodation. During late lowstand, typically normal regression, the slow rate of accommodation creation compared to the rate of sediment supply could lead to high amalgamation of channel belts; during relative sea-level rise, typically normal transgression, high accommodation creation rate could result in low connectivity of the channel belts and typically estuarine sediments being preserved in the valley-fill deposits. Based on outcrop studies conducted on Cretaceous strata of the Western Interior foreland basin of Utah, USA, Shanley and McCabe (1993, 1994) developed a widely used “early” fluvial sequence stratigraphic model (**Fig. 3**), which envisages valley incision and formation of terrace deposits occurring during stages of base-level fall, which are then followed by valley filling, in the form of amalgamated fluvial deposits first, followed by tidally influenced fluvial deposits as the rate of RSL rise accelerates during the TST, and finally by low net-to-gross fluvial deposits as the rate of RSL rise decelerates during the HST. Wright and Marriott (1993) proposed a similar generic sequence stratigraphic model (**Fig. 2.4**) with emphasis on the relationships between fluvial architecture, palaeosols and accommodation, which relates mainly to floodplain sedimentation. During the lowstand systems tract (LST), fluvial deposits are characterized by amalgamated channel deposits, which are confined within an incised valley. Mature, well-drained soils usually develop on marginal terraces because of subaerial exposure. During the transgressive systems tract (TST), increased accommodation rates favour a higher preservation potential for thick floodplain deposits with isolated channel bodies and formation of hydromorphic soils and these deposits tend to occur beyond the confines of the incised-valley fill. During the highstand systems tract (HST), as the rate of sea-level rise slows, resulting in a decrease of the rate of accommodation creation, fluvial deposits are characterized by sand bodies that become increasingly laterally amalgamated, with a much lower proportion of floodplain fines and with the development of mature soils. Legarreta and Uliana (1991, 1998) proposed a model (**Fig. 2.5**) for Cretaceous continental basins in Argentina, which includes (i) a lowstand systems tract, in which deposits are areally restricted and characterized by sandy to gravelly bed-load deposits organized as amalgamated, upward-coarsening and thickening channel-fill complexes; (ii) a transgressive systems tract,

in which deposits are characterized by a mixture of bed-load and suspension- load deposits arranged as upward-fining and upward-thinning bedsets and are interpreted to reflect increased accommodation during periods of stratigraphic base-level rise; and (iii) a highstand systems tract, for which deposits are composed of sediments of suspended-load origin and a greater occurrence of soil profiles, suggesting limited accommodation and a landscape of reduced surface gradient.

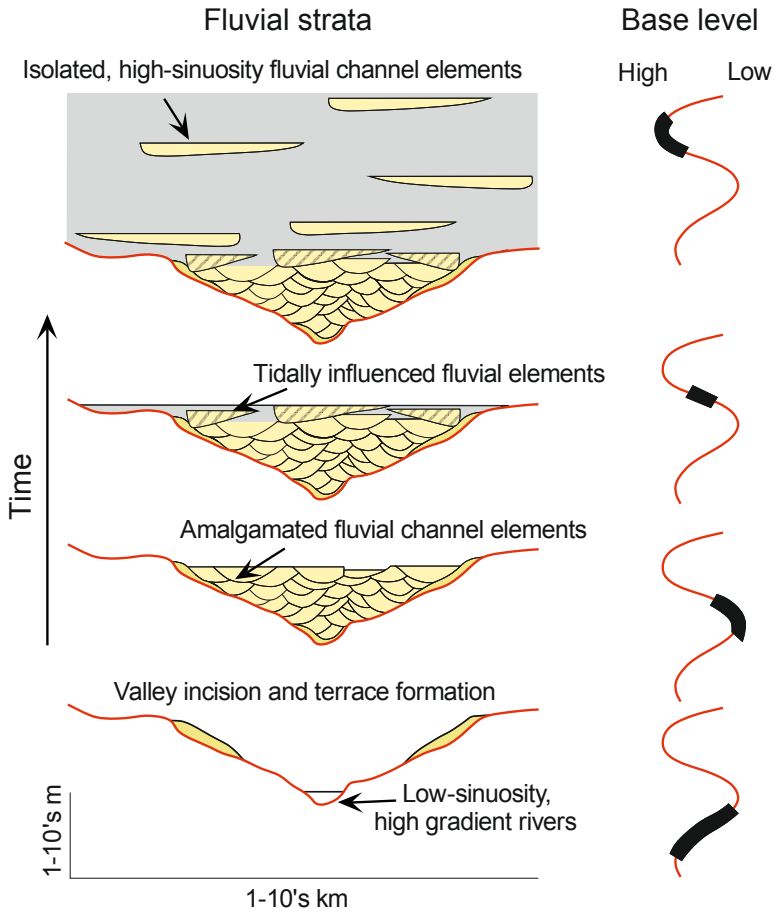

Fig. 2.3. *Shanley and McCabe (1993, 1994) fluvial sequence stratigraphic model depicting the development of depositional sequences in mixed fluvial-coastal-marine strata of the Cretaceous Western Interior basin of the USA, in response to base-level changes. The diagram illustrates the concept of incision and complete sediment bypass during base-level fall, followed by valley filling, first with amalgamated fluvial deposits, then tidally influenced strata and finally low net-to-gross fluvial successions composed of largely disconnected fluvial channel sandbodies.*

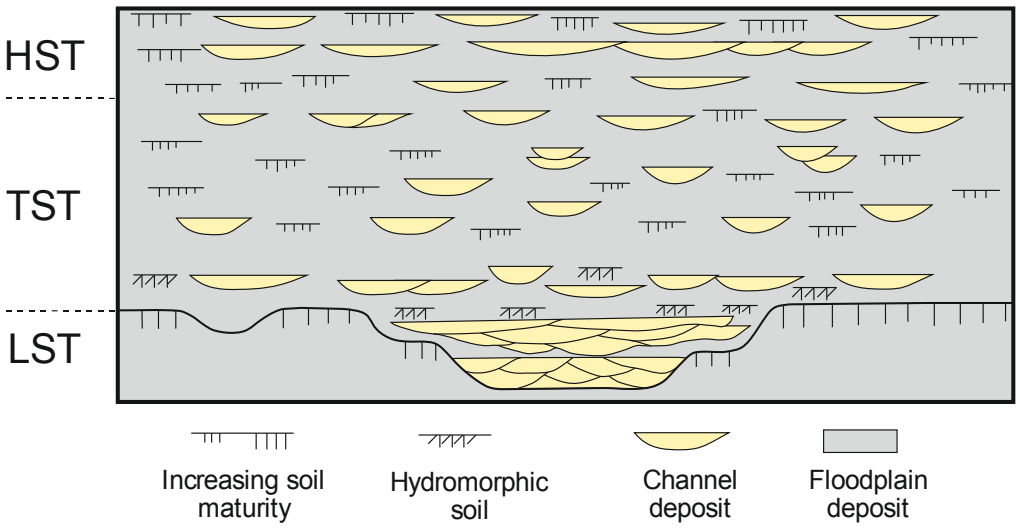

Fig. 2.4. *Wright and Marriott (1993) fluvial sequence stratigraphic model illustrating simple architectural and pedogenic relationships for a fluvial sequence deposited during a third-order base-level fall-rise (type 1 sequence boundary of Posamentier and Vail, 1988). LST= lowstand systems tract; TST= transgressive systems tract; HST = highstand systems tract.*

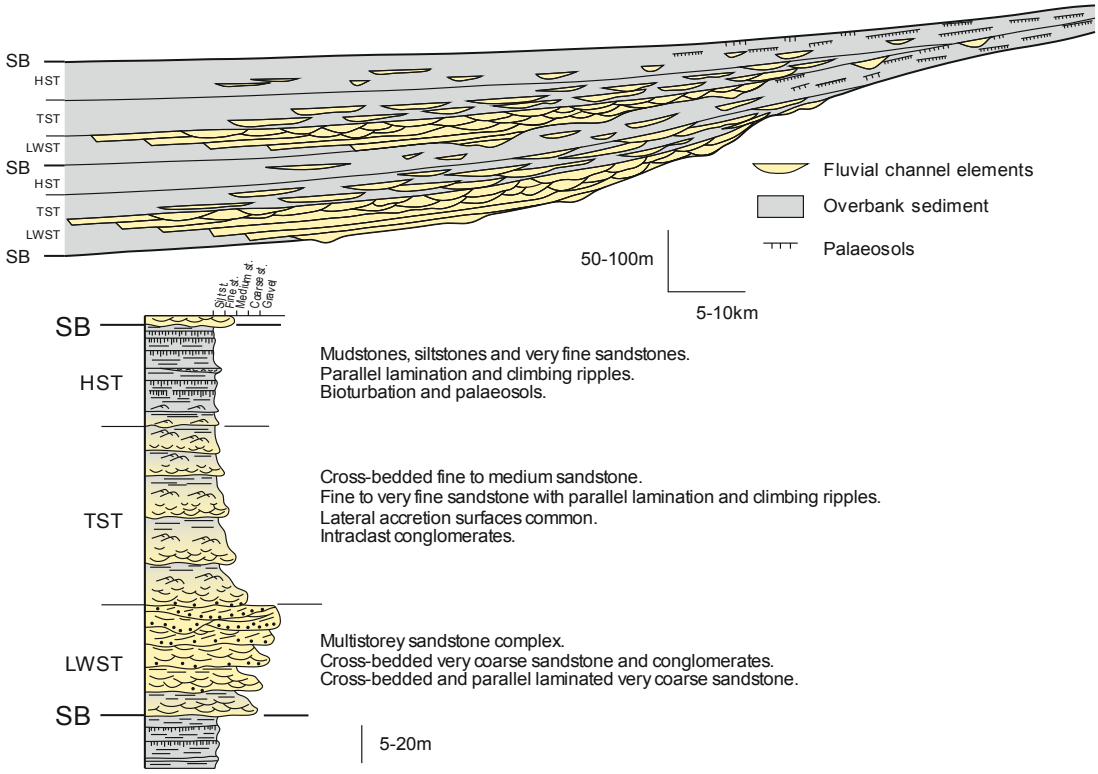

Fig. 2.5. *Legarreta and Uliana (1998) fluvial sequence stratigraphic model illustrating hinterland fluvial depositional sequences on the basis of Cretaceous non-marine strata in Argentina. These sequences are comprised of three recognizable systems tracts. Lowstand wedge systems tract (LWST) deposits are characterized by bed-load sandy to gravelly deposits with an overall coarsening upwards pattern. The transgressive systems tract (TST) is characterized by a mixture of bed-load and suspension-load deposits with an overall fining upwards pattern. The highstand systems tract (HST) is dominated by suspension-load deposits and an increase in the occurrence of soil profiles. These characteristics represent a depositional regime with limited accommodation space.*

The effects of sea-level change on river longitudinal profiles, and thus fluvial processes, decrease upstream from the coastline and can propagate only a limited distance (Fisk, 1944; Blum, 1993; Shanley and McCabe, 1994; Tornqvist, 1998; Blum and Tornqvist, 2000). Landward of this zone, the dominance of upstream controls progressively increases. Blum and Törnqvist (2000) recognized the upstream limits of sea-level influence as the upstream extent of coastal onlap due to sea-level rise (**Fig. 2.6**) and based on study of late-Quaternary coastal-plain examples, emphasize that this distance is highly variable across different scales of river-system size and is negatively correlated to channel slope. Blum et al. (2013) suggest the minimum onlap distance scales with the equilibrium backwater length

L_b (*sensu* Paola and Mohrig, 1996), given by $L_b = h_f / S$, where h_f denotes flow depth and S denotes channel slope. The upstream extent of sea-level influence range from hundreds of kilometres for large, low-gradient river systems to a few kilometres for small and steep river systems (**Fig. 2.7**). Recently, significant research interest has focused on the ''backwater zone'' and its potential influence in alluvial stratigraphy in the ancient rock record (Lamb et al., 2012; Blum et al., 2013). The upstream limit of the backwater zone is placed where the river bed drops below the sea level, leading to river-flow deceleration (Lamb et al., 2012). As rivers enter the backwater zone, bedload transport and deposition drop markedly (Chatanantavet et al. 2012). Studies in the preserved alluvial stratigraphic record suggest that the transition into the backwater zone can be identified by distinctive facies changes (e.g., Petter, 2011; Colombera et al., 2016).

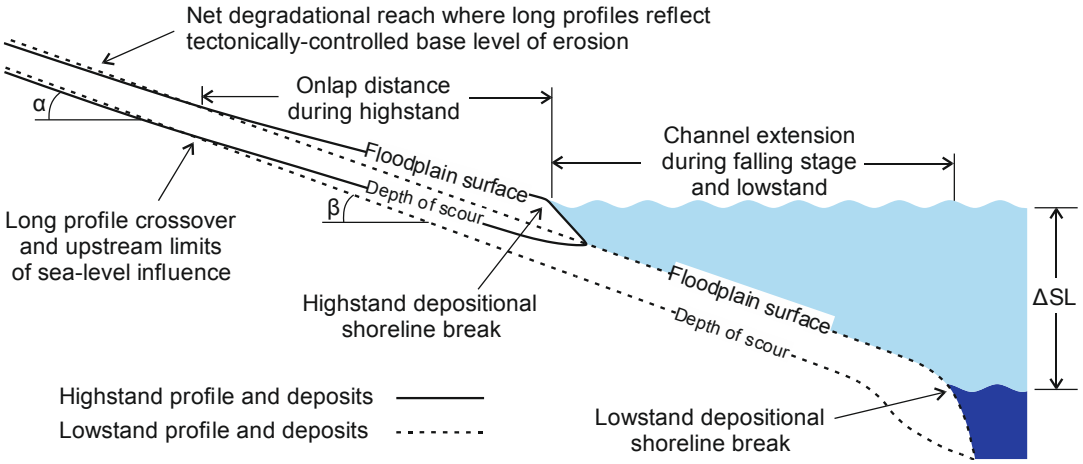

Fig. 2.6. *Definition sketch for fluvial response to sea-level change along a continental margin with a distinct highstand depositional shoreline break. Diagram illustrates concepts of channel extension during sea-level fall and lowstand, vs. upstream limits of onlap during sea-level rise and highstand. (figure and caption from Blum and Törnqvist, 2000, Fig. 2.13, p. 18).*

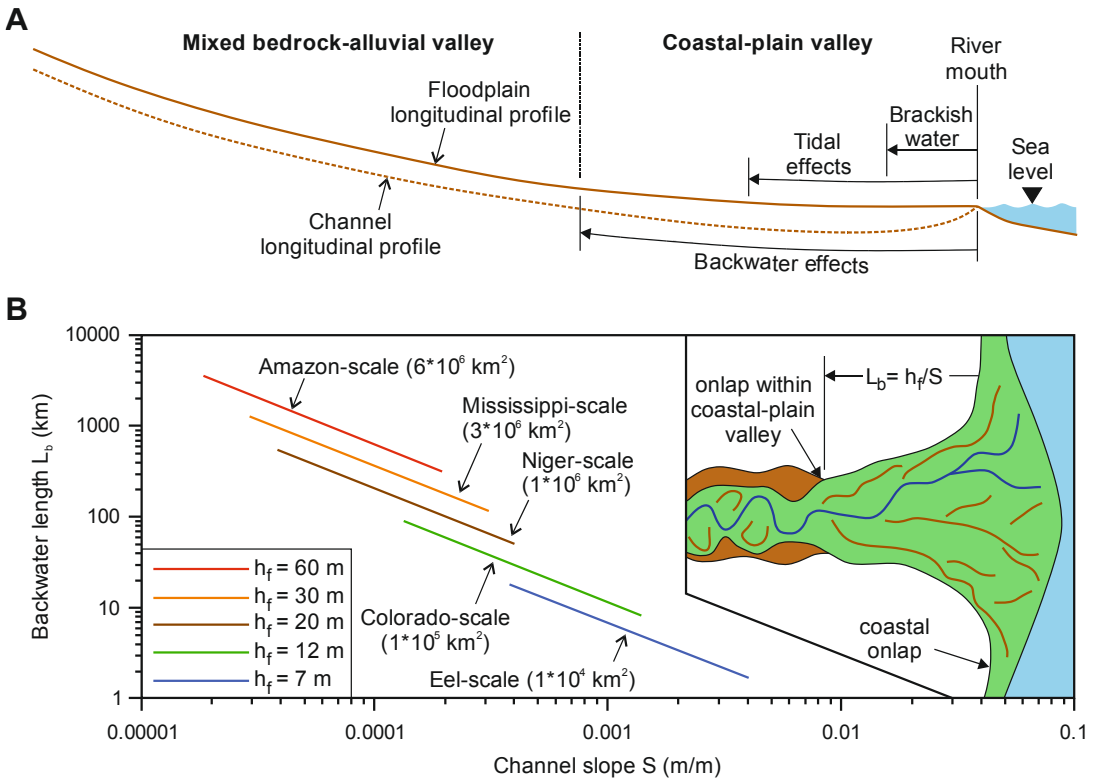

Fig. 2.7. *Definition sketch highlighting the concept of backwater length. (A) Longitudinal line drawing illustrating general relationships between floodplain, channel long profiles, and the upstream limits of brackish water, tidal effects and backwater conditions. Modified from Blum et al. (2013); originally after Li et al. (2006). (B) Plan-view line drawing for backwater zone and cross-plot between backwater length vs. channel slope for river systems with variable sizes of drainage-basin area, and flow depths. Modified from Blum et al. (2013).*

2.1.2 Upstream controls

Outside of the limit of the influence of sea-level changes, upstream controls including climate and tectonics can play dominant roles in governing the geometry and architecture of fluvial strata. Climate and tectonics can operate across the whole extent of the fluvial longitudinal profile, i.e., from source areas to the basin margins; however, they tend to be most evident in deposits upstream the limit of backwater effect, as in the downstream regions within the limit of sea-level influence, their effects are prone to be masked by the effects of base-level changes.

2.1.2.1 Climate

The control of climate on fluvial architecture and geometry can be realized in a number of ways (**Fig. 2.1**), including variations of temperature, humidity, precipitation, flood frequency and magnitude, and evaporation rates. These parameters can in turn have a major influence on vegetation cover, weathering and

erosion patterns, and rates of sediment supply. Cecil (1990) and Perlmutter and Matthews (1990) proposed general models illustrating the sedimentological behaviour of depositional systems in response to climate change. Temperate, seasonal wet/dry climates tend to be associated with maximum sediment yields; very humid climates dominated by thick vegetation cover tend to be characterized by decreased sediment yield and favour the formation of peat/coal; arid climates tend to be associated with low sediment yield and are dominant by the development of pedogenic carbonates and evaporites in low-lying areas. Sedimentary behaviour of fluvial channels is determined by the balance between stream power and sediment supply (Lane, 1955; Blum and Törnqvist, 2000; **Fig. 2.8**). Stream power is primarily a function of water discharge, which might be steady or flashy over time, and might be associated with different climatic regimes. Sediment supply can be determined by many factors, with climate being a primary influence. The same authors thus concluded that given a river system which has reached a dynamic equilibrium, an increase in sediment supply will lead to channel aggradation whereas an increase in discharge will lead to channel degradation.

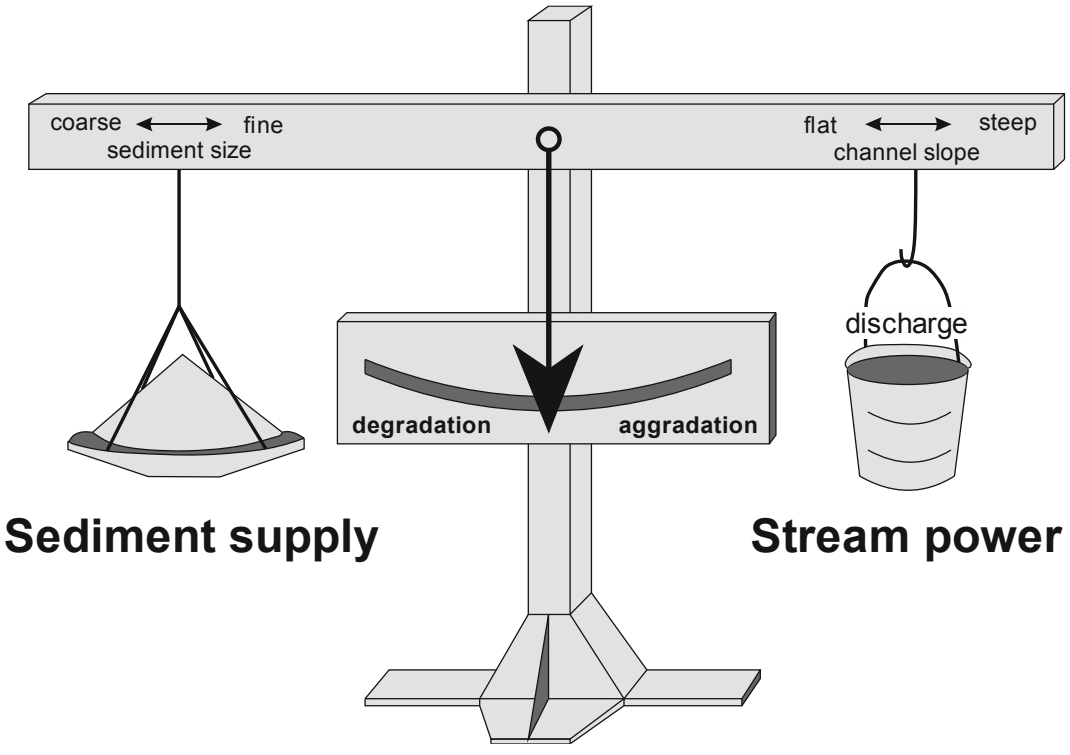

Fig. 2.8. *Balance model for fluvial sedimentological behaviours (aggradation or degradation) with respect to the relationship between water discharge and sediment supply. Modified from Blum and Törnqvist (2000); originally after Lane (1955).*

Fluvial processes in response to longer-term climate-controlled sea-level changes accompanying glacial and interglacial cycles have also been explored (Blum, 1993; Blum and Törnqvist, 2000; Foreman et al., 2012). Typically, deglaciation corresponds to an increase in water discharge, which in turn leads to fluvial incision. By contrast, glacial maxima correspond to a decrease in water discharge, which in turn leads to fluvial aggradation. Based on work on Late Cenozoic record of the Gulf Coast rivers, Blum (1993) and Blum and Törnqvist (2000) developed a climate-driven model, which indicated that fluvial cycles driven by climate fluctuations may be totally out of phase relative to those controlled by base-level changes (**Fig. 2.9**).

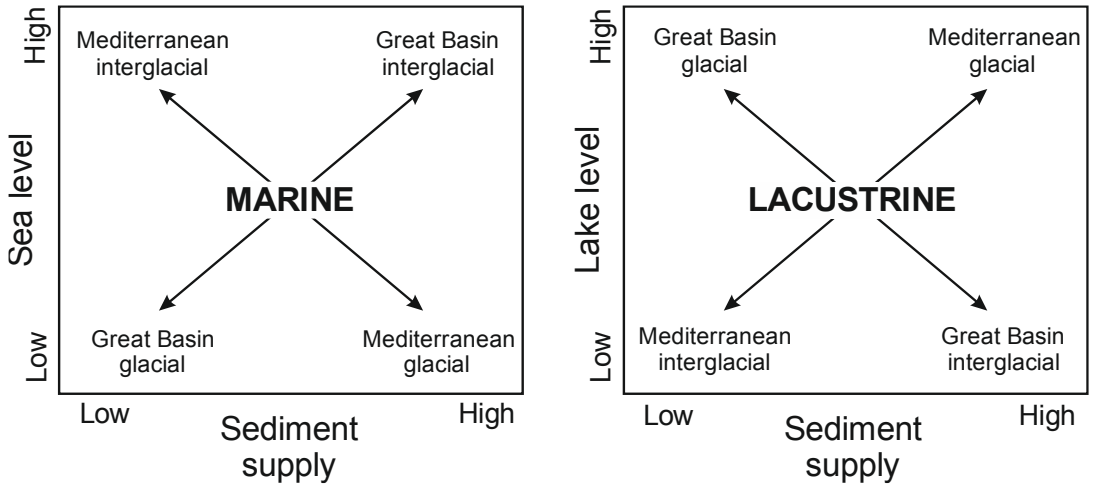

Fig. 2.9. *Model for changes in sediment supply in Mediterranean vs. USA Great Basin climates during glacial and interglacial periods. The diagram on the left illustrates conditions that might apply to a marine basin, whereas the diagram on the right illustrates conditions for a lacustrine basin. Both diagrams illustrate a succession of possible out-of-phase responses. Figure and caption from Blum and Törnqvist (2000); originally after Leeder et al. (1998).*

Another issue of fundamental significance is the recognition of climatic controls on sedimentation in the ancient record. Miall (1996) discussed a suite of problems that might arise regarding this issue: (i) Large variation in fluvial discharge could leave recognizable effects in the facies record, but the time scale of variation might be difficult to resolve. (ii) The climate prevailing in the source area might be different from that in the receiving sedimentary basin. Flow hydraulics of a river and the resultant facies architecture of the deposits are primarily influenced by the climate of the sediment source area, whereas floodplains and the finer-grained deposits are largely determined by the climate of the depositional basin. (iii) Topographic effects

might exert a control on the local or regional climates, which might complicate the stratigraphic record. (iv) Climate is often recognized in the ancient rock record based on evidence of vegetation, either as remains of the vegetation itself (e.g. preserved leaf debris or rhizoliths), or by the effects vegetation exerts on sediment supply, bank erodibility, channel style etc. However, vegetation patterns have evolved throughout the Earth history and therefore modern analogues have a limited applicability to the ancient past, especially in parts of the Palaeozoic when land plants had only recently colonised the land masses and had only shallow root systems (e.g., Santos et al., 2017).

In the past decade, some research efforts (Fielding et al., 2009 and 2018; Plink-Björklund, 2015; Nicholas et al., 2016; Trower et al., 2018; Colombera and Mountney, 2019; Ganti et al., 2019b; Leary and Ganti, 2020) have focused on the possible control of discharge variability on alluvial stratigraphy from bedform to basin scales, attempting to decipher climate change within the fluvial deposits through facies and architectural analysis of the ancient record. Nicholas et al. (2016) employed physics-based numerical modelling to investigate relationships between morphology and dynamics in large rivers. They highlighted that discharge variability and flood duration played critical roles in preserved alluvial stratigraphy at the macroform scale, suggesting that the plan-view classification of fluvial deposits may not be a reliable guide to the alluvial stratigraphic record. Fielding et al. (2018) proposed to use the coefficient of variation of annual peak flood discharge CVQp to classify rivers in consideration of the importance of river-discharge variability as a control on the alluvial stratigraphic record. On the basis of analysis of 26 modern rivers with both available long-term gauging records and published descriptions of subsurface sedimentary architecture, the same authors suggested that rivers might be categorized into 5 groups with very low (<0.20), low (0.20–0.40), moderate (0.40–0.60), high (0.60–0.90), or very high (>0.90) annual peak discharge variability. Each class of river is proposed to link to a distinctive facies association: rivers with very low and low peak discharge variability are characterized by the dominance of cross stratifications and well-preserved macroforms; rivers with moderate values of CVQp preserve mostly cross stratifications, but records of macroforms decrease and are mostly modified by reworking; rivers with high and very high values of CVQp are dominated by Froude transcritical and supercritical flow structures and typically lack macroform structures, abundant in situ trees, transported large, woody debris, and pedogenically modified mud partings.

Flume experiments on dune evolution in steady and unsteady flows by Leary and Ganti (2020) indicate that flood discharge variability can exert an important control on the preservation of cross strata and concluded that variations in the thickness of

dune-scale cross sets in the preserved alluvial stratigraphic record can provide critical information on the ratio of the timescales of formative flood variability and bedform adjustment, and hence can act as a potential signature of bedform disequilibrium in the alluvial stratigraphic record.

2.1.2.2 Tectonics

Tectonic processes can control fluvial geometry and facies architecture through their influence on relative sea-level changes, basin physiography, relief of the source area and regional slope, which in turn could exert key control on sediment yield and transport capacity.

Fluvial cycles could also be driven by high-frequency tectonic cycles of subsidence and uplift superimposed on a longer-term climatic background. Models for such fluvial sequences need to be developed for specific tectonic settings considering the considerable differences of the mechanisms and patterns of subsidence and uplift among different types of sedimentary basins. For example, Catuneanu and Elango (2001) established a fluvial sedimentation model (**Fig. 2.10A**) for the foredeep portion of retroarc foreland systems based on the orogenic cycles of thrusting and quiescence in the adjacent fold-thrust belts predicted from fluvial sequences (Catuneanu and Elango, 2001; **Fig. 2.10B**) of the Balfour Formation of the Beaufort Group of the Karoo Basin, South Africa.

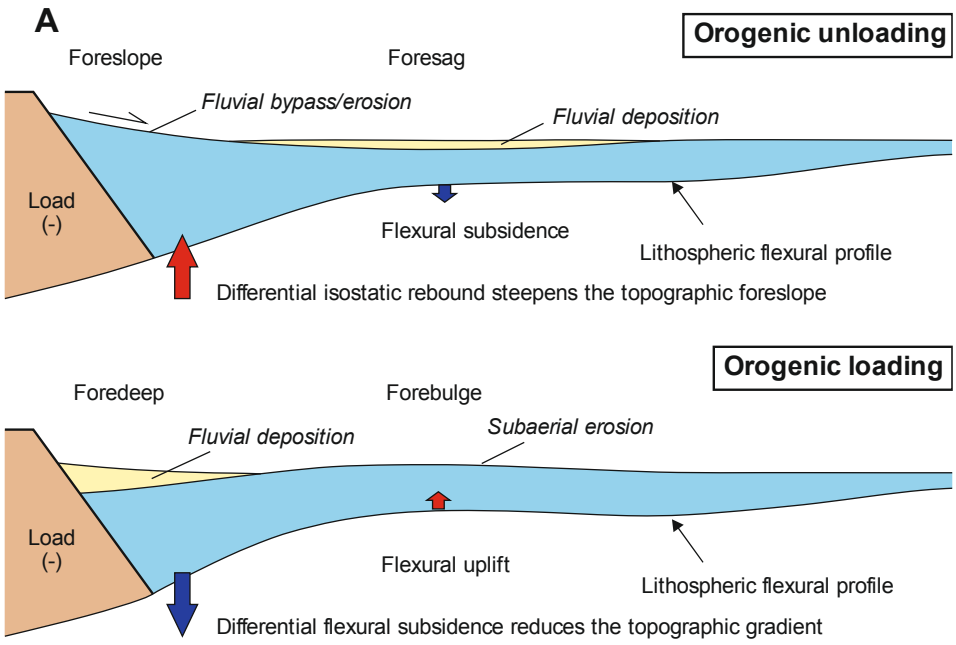
A
Orogenic unloading
Foreslope
Foresag
Fluvial bypass/erosion
Fluvial deposition
Load
(-)
Flexural subsidence
Lithospheric flexural profile
Differential isostatic rebound steepens the topographic foreslope
Orogenic loading
Foredeep
Forebulge
Fluvial deposition
Subaerial erosion
Load
(-)
Flexural uplift
Lithospheric flexural profile
Differential flexural subsidence reduces the topographic gradient

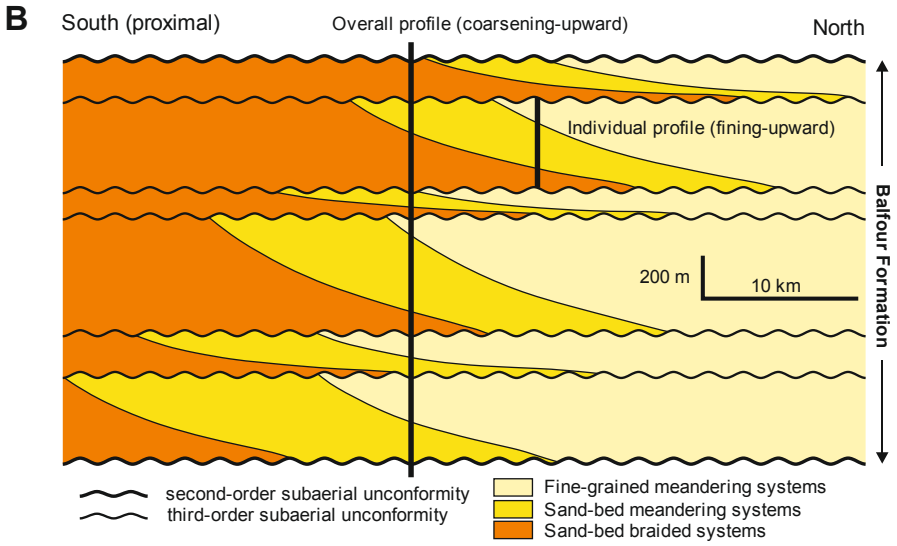
B
South (proximal)
Overall profile (coarsening-upward)
North
Individual profile (fining-upward)
200 m
10 km
Balfour Formation
second-order subaerial unconformity
third-order subaerial unconformity
Fine-grained meandering systems
Sand-bed meandering systems
Sand-bed braided systems

Fig. 2.10. *(A) Fluvial sedimentation model for a retroarc foreland system during the overfilled phase (sensu Sinclair and Allen, 1992), emphasizing changes in the relationship between accommodation and sedimentation. Orogenic unloading results in flexural uplift and steepening of the topographic slope (foreslope). Orogenic loading leads to differential subsidence and the lowering of the topographic gradient. The depocenter therefore moves from the foredeep zone, during orogenic loading, to the foresag zone during unloading. Modified from Catuneanu and Elango (2001). (B) Fluvial depositional sequences of the Balfour Formation, Karoo Basin, South Africa. Note that each sequence displays a fining upward profile, due to the change with time in fluvial styles from higher to lower-energy systems. At the same time, the overall vertical profile of the formation is coarsening-upward in response to the progradation of the orogenic front. The change from low- to high-accommodation conditions during the deposition of each sequence is gradational. Figure and caption from Catuneanu (2006); originally after Catuneanu and Elango (2001).*

However, these models (**Fig. 2.3-2.5, Fig. 2.10A**) may oversimplify the relationship between external forcing mechanisms and fluvial architecture. Based on the study of Cretaceous Dakota Group strata, USA, Holbrook et al. (2006) established the so-called “buffers and buttresses” model (**Fig. 2.11**) to account for both downstream and upstream controls on fluvial architecture and geometry. This model can be amended to existing fluvial sequence stratigraphic models to capture dip-oriented changes in fluvial facies and architecture upstream from a coastline. A buttress represents some fixed point indicating the downstream controls (such as sea-level for marine basins, lake level for inland basins, or the level of the tectonic rim through which the river flows out of a basin). The buffer zone is the available instantaneous preservation space for the fluvial system, which is constrained by the maximum depth of local channel scour and the maximum height of river aggradation under prevailing conditions of water discharge and sediment load. The buffer zone can expand or contract vertically in response to changes in upstream controls (climate change and tectonism) (**Fig. 2.12**), which can exert important controls on the water and sediment flux of the river. The river system will aggrade or erode towards a new dynamically maintained equilibrium longitudinal profile that balances the water and sediment supply and the rate of change in accommodation.

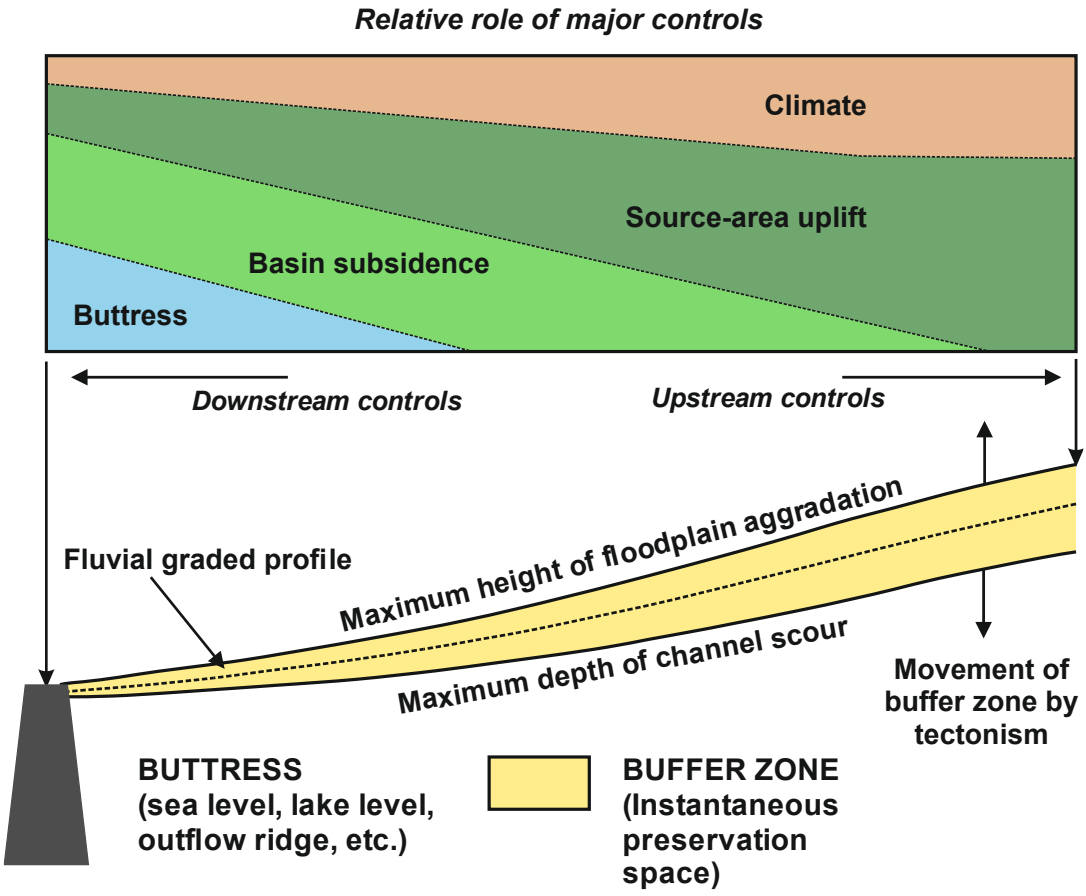

Fig. 2.11. *Definition sketch illustrating allogenic controls on fluvial geometry and architecture along dip-oriented profiles. The diagram is intended to indicate how the balance between upstream (tectonic, climatic) and downstream (base-level) controls changes from coastal shoreline to the source area. The relative roles of major controls are based on Shanley and McCabe (1994). The buffers and buttresses concepts are based on Holbrook et al. (2006). Figure modified from Miall (2014).*

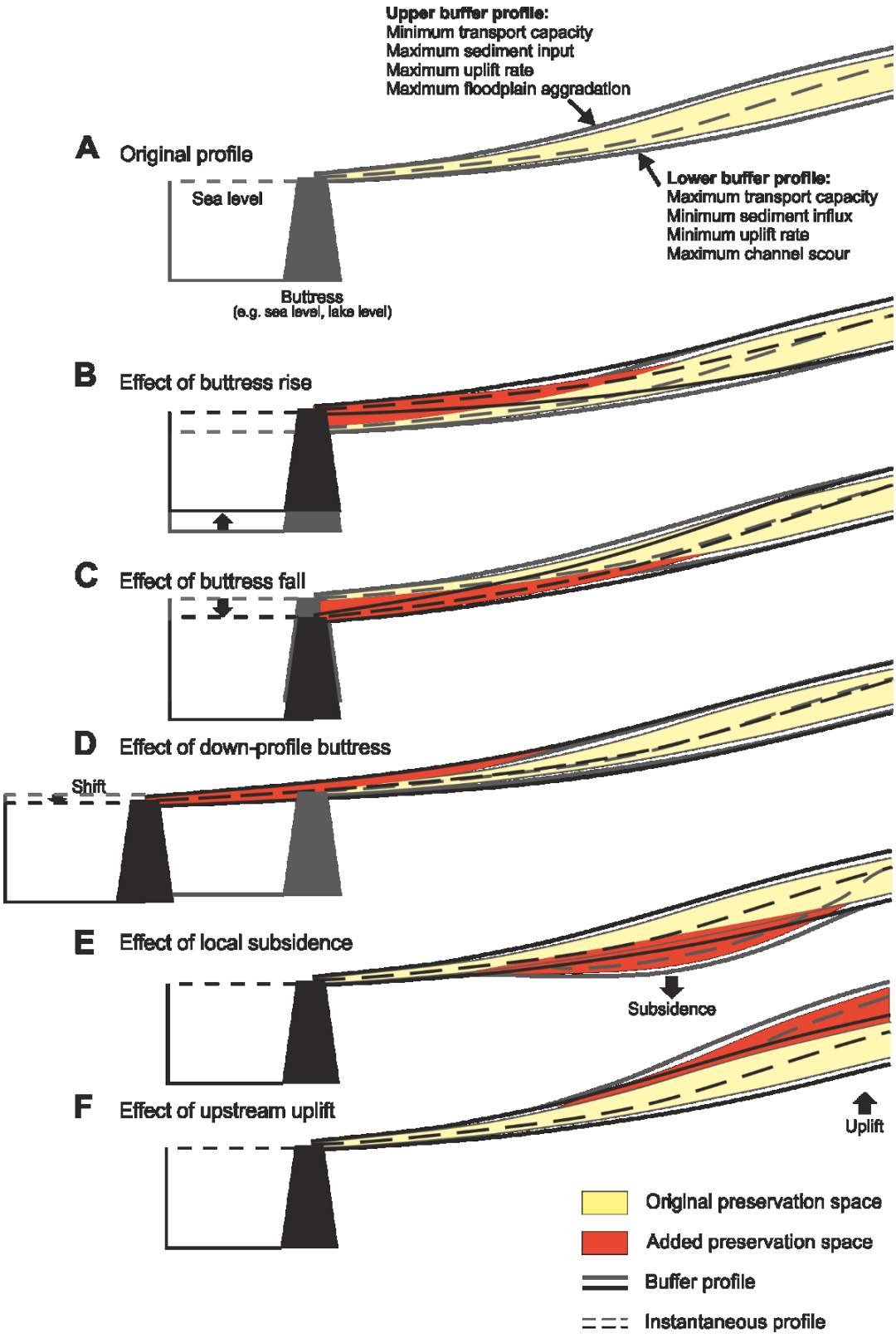
Upper buffer profile:
Minimum transport capacity
Maximum sediment input
Maximum uplift rate
Maximum floodplain aggradation
A Original profile
Sea level
Lower buffer profile:
Maximum transport capacity
Minimum sediment influx
Minimum uplift rate
Maximum channel scour
Buttress
(e.g. sea level, lake level)
B Effect of buttress rise
C Effect of buttress fall
D Effect of down-profile buttress
Shift
E Effect of local subsidence
Subsidence
F Effect of upstream uplift
Uplift
Original preservation space
Added preservation space
Buffer profile
Instantaneous profile

Fig. 2.12. *Range of effects on both a single river profile and enveloping buffer zone because of changes in the sea level buttress and because of local uplift and subsidence. Preservation space between the upper and lower buffer profiles record fluvial deposition because of variation in the instantaneous profile over short durations because of fluctuations in sediment and water supply ratios. Rise and fall of the buffer zone because of changes in base level and tectonics raise and lower river profiles and thus further add or remove accommodation for sediment preservation, respectively. Modified partly from Stuart (2015); originally after Holbrook et al. (2006).*

2.2 Incised-valley systems

As fluvial graded profiles respond to rises and falls in base level and other upstream controls, river vertical incision may lead to the formation of incised valleys (Easterbook, 1999). Generally, incised valleys are described as elongate topographic lows whereby smaller rivers feeding them lack the discharge to constantly flood beyond the valley incision and onto the interfluves (Gibling et al., 2011). According to the location with respect to the source-to-sink systems and the dominant processes and controls, Blum et al. (2013) classified the general fluvial valley systems into 4 categories: bedrock, mixed bedrock-alluvial, coastal-plain and cross-shelf incised valleys (**Fig. 2.13**). Bedrock and mixed bedrock-alluvial valleys typically occur in areas dominated by tectonic uplift and are in a long-term state of incision and deepening, with channels incising into bedrock (Howard et al., 1994; Howard, 1998). Coastal-plain valleys are fully alluvial, extending from the highstand shoreline to the upstream limits of sea-level influence. Cross-shelf valleys extend between the highstand shoreline and the shelf margin and are exposed to fluvial and marine processes. These coastal-plain and cross-shelf valleys are the subject of this work. Nearshore incised valleys are defined as fluvially eroded, elongate palaeotopographic lows developed in shelf and coastal settings in response to relative sea-level fall, and subsequently inundated, infilled and reworked by fluvial, coastal and marine processes during episodes of relative sea-level rise (Posamentier and Allen, 1999; Zaitlin et al, 1994; Blum et al., 2013). The basal erosional surface of incised valleys along with their correlative interfluve surfaces has long been considered as a regional, sequence-bounding unconformity that represent significant hiatuses in deposition (e.g., Vail et al., 1977, Posamentier and Vail, 1988; Posamentier et al., 1988; Van Wagoner et al., 1990).

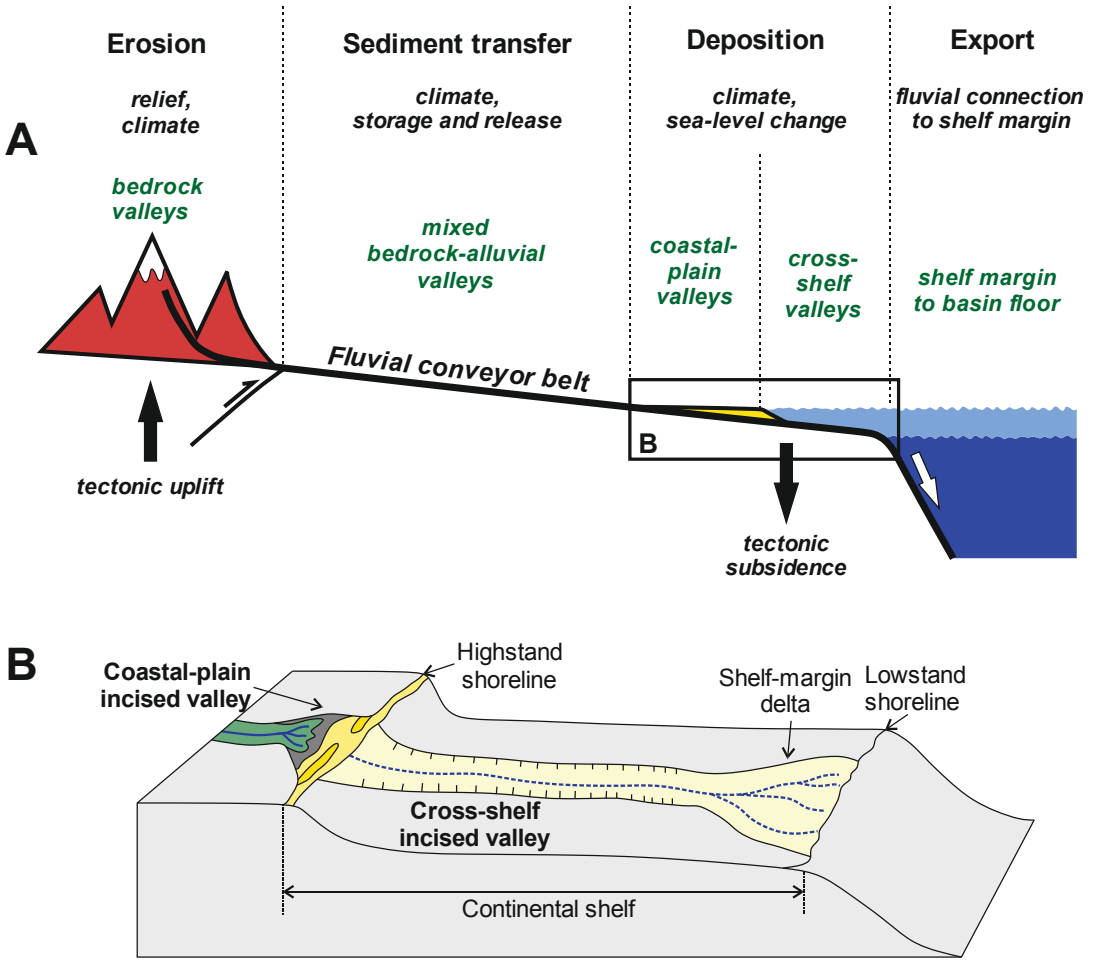

Fig. 2.13. *Definition sketch (A) illustrating the classification of fluvial valley systems and corresponding dominant processes and controls from the source area to the depositional basin. Modified from Blum and Womack (2009). Inset map (B) illustrates the position of coastal-plain incised valley and cross-shelf incised valley in a plan-view profile.*

2.2.1 Formation and evolution of incised-valley systems

Incised valleys have long been considered to form in two episodes: (i) incision, sediment bypass through the valley, and deposition at the lowstand coastline or beyond during periods of relative sea-level fall; and (ii) deposition within valleys during periods of relative sea-level late lowstand and sea-level rise (Posamentier and Vail, 1988; Posamentier et al., 1988; Van Wagoner et al., 1990; Zaitlin et al., 1994). However, recent experimental and computational modelling (Strong and Paola, 2006, 2008; Martin et al., 2009) and well-dated Quaternary systems (Blum and Price, 1998; Blum et al., 2013) challenge this view and support an alternative notion (**Fig. 2.14**): the basal surface of incised-valley fills are highly diachronous, composite erosional features resulting from multiple episodes of punctuated channel incisions accompanied by lateral migration, channel-belt deposition and

valley-wall reshaping through a sea-level cycle. The bounding surfaces of valley fills are generally unlikely to have existed as topographic surfaces in their original landscapes. Valley deepening is driven by vertical channel incision, whereas valley widening is largely driven by lateral migration of channels and valley sidewall destabilization (Strong and Paola, 2006, 2008; Martin et al., 2011; Blum et al., 2013).

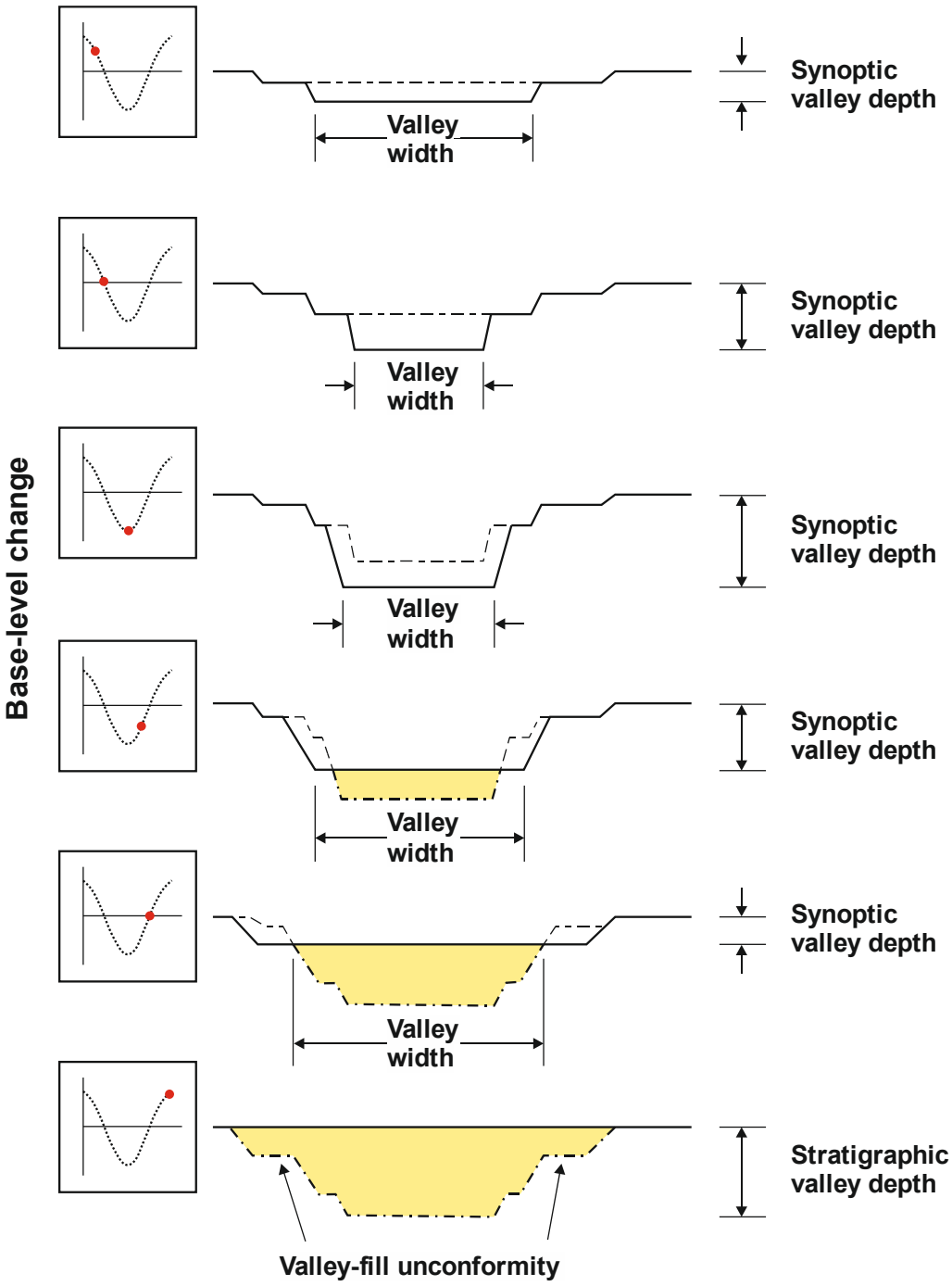

Fig. 2.14. *Diagram of the evolution of valley width and depth in experimental settings (modified from Blum et al., 2013; originally from Strong and Paola, 2009), highlighting the formation and evolution of the basal surface of incised-valley fills, constantly reworked by erosion and deposition through a base-level cycle. See text for details.*

2.2.2 Stratigraphic architecture of incised-valley fills

Classical facies models (e.g., Dalrymple et al., 1992; Allen and Posamentier, 1994b; Zaitlin et al., 1994) for incised-valley fills commonly link internal fills of

valleys with estuarine facies successions that form during shoreline transgression, generally corresponding to relative sea-level rise. These facies models for coastal-plain incised-valley development and infill (**Fig. 2.15-2.17**) are widely adopted and typically envisage three segments: (i) a seaward segment (segment 1) comprising basal fluvial deposits overlain by estuarine deposits and capped by fully marine deposits; (ii) a medial segment (segment 2) recording a drowned-valley estuarine complex that existed around the time of maximum transgression, overlying a lowstand to transgressive succession of fluvial and estuarine deposits; and (iii) a proximal landward segment (segment 3) mostly occupied by fluvial systems throughout its depositional history, whereby the fluvial style changes due to variations in the rate of base level change (**Fig. 2.16 and Fig. 2.17**).

However, Blum et al. (2013) highlight that incised-valley fills associated with marine shoreline systems may or may not contain estuarine facies successions: the scale of valley fills within the limit of sea-level influence might be overly underestimated if only the extent containing estuarine successions are considered, as backwater effects can extend significantly upstream from estuarine limits (see **Fig. 2.7**). Based on field studies of ancient and Quaternary systems, they summarize that the internal fills of coastal-plain incised valleys (**Fig. 2.18**) are typically composed of an amalgamated lower valley fill, dominated by amalgamated sand bodies that rest on the classically defined sequence boundary, overlain by a non-amalgamated (low-net) upper valley fill, characterized by ribbon- and sheet-like sand bodies that are more isolated within mud-dominated successions.

In summary, the widely adopted drowned-valley estuarine facies models (Dalrymple et al., 1992; Allen and Posamentier, 1994b; Zaitlin et al., 1994; **Fig. 2.16 and Fig. 2.17**) are biased by being derived from small coastal-plain valley systems with limited sediment supply. It is recognized that facies models should be a distillation of existing case studies, and that they are intended to represent the common trends rather than the only possible stratigraphic expression; however variability can be expected and deviations from the classical model may be significant depending on the range of geological boundary conditions (Boyd et al., 2006). For example, valley fills entirely filled by fluvial deposits might indicate that the rate of fluvial sediment supply are high compared to the rate of creation of accommodation by relative sea-level rise, or that the location of the studied valleys is situated far inland upstream of the estuarine effects (e.g., segment 3 in **Fig. 2.16**). The detailed characterization provided by Blum et al. (2013), therefore, can be considered as a refinement for the facies model for the proximal landward segment (segment 3 in **Fig. 2.16**) of incised-valley fills by Zaitlin et al. (1994).

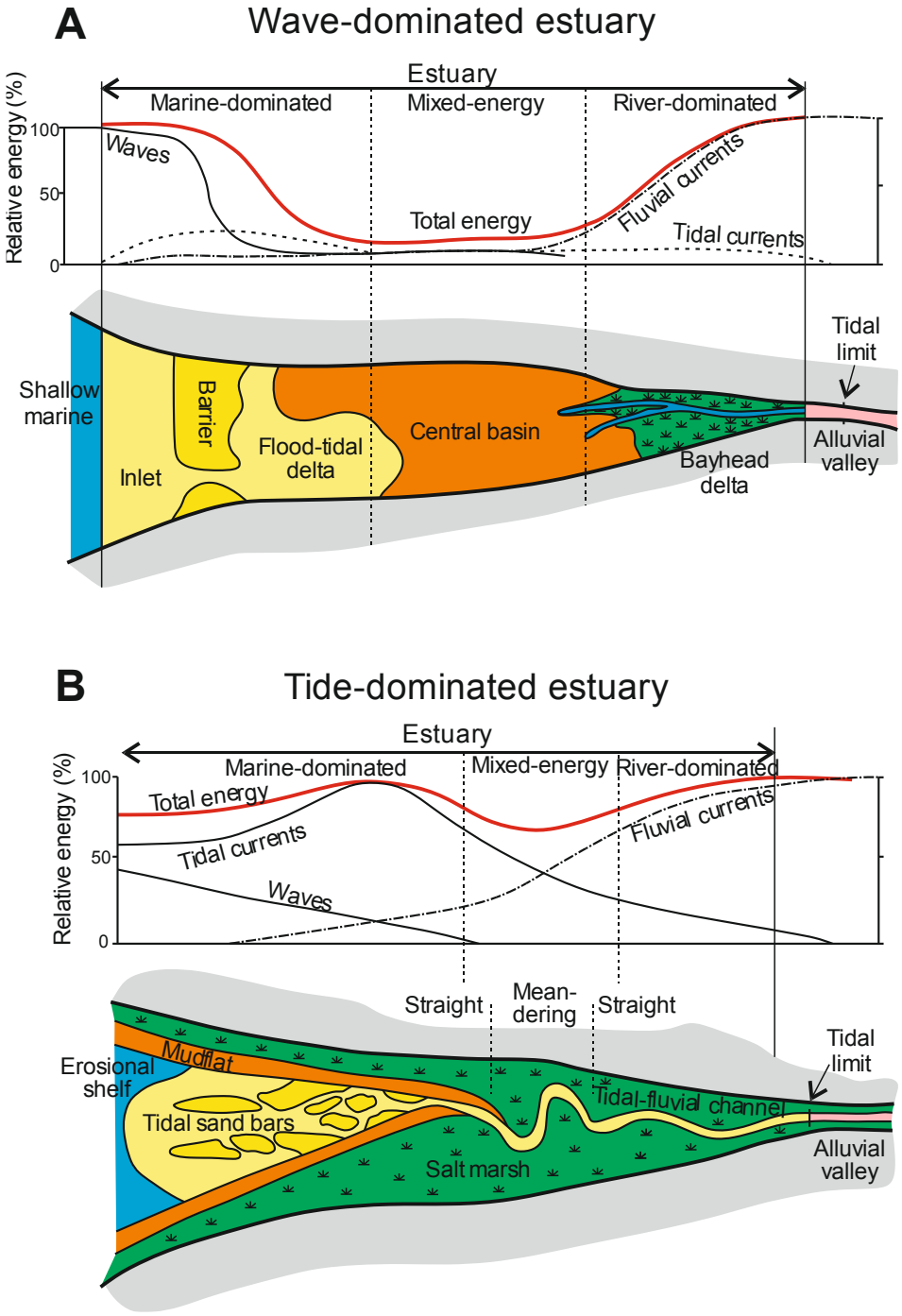

Fig. 2.15. *Diagram illustrating the distribution of energy types and plan-view morphological components within an idealized wave-dominated estuary (A) and tide-dominated estuary. MSL = mean sea level. Modified from Dalrymple et al. (1992).*

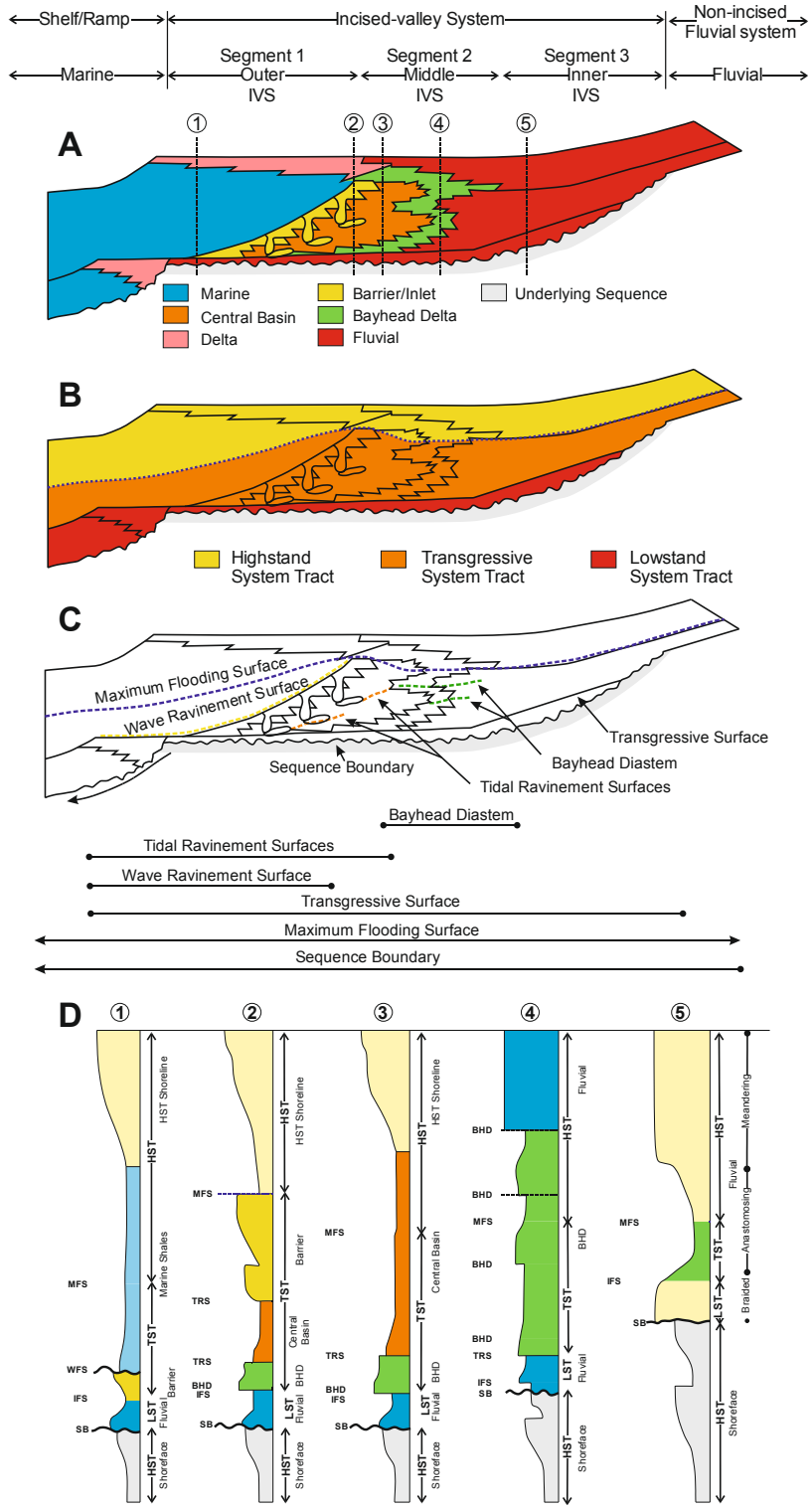

Fig. 2.16. *Idealized longitudinal section of a simple incised-valley-fill system illustrating the distribution of (A) depositional environments, (B) systems tracts, and (C) key stratigraphic surfaces. A wave-dominated estuary has been considered in this model. Segments 1 and 3 are typically much longer than segment 2, and are compressed here for presentation purposes. Also displayed in (D) are five representative vertical sections of facies and sequence-stratigraphic surfaces, whose locations have been shown in (A). Modified from Zaitlin et al. (1994).*

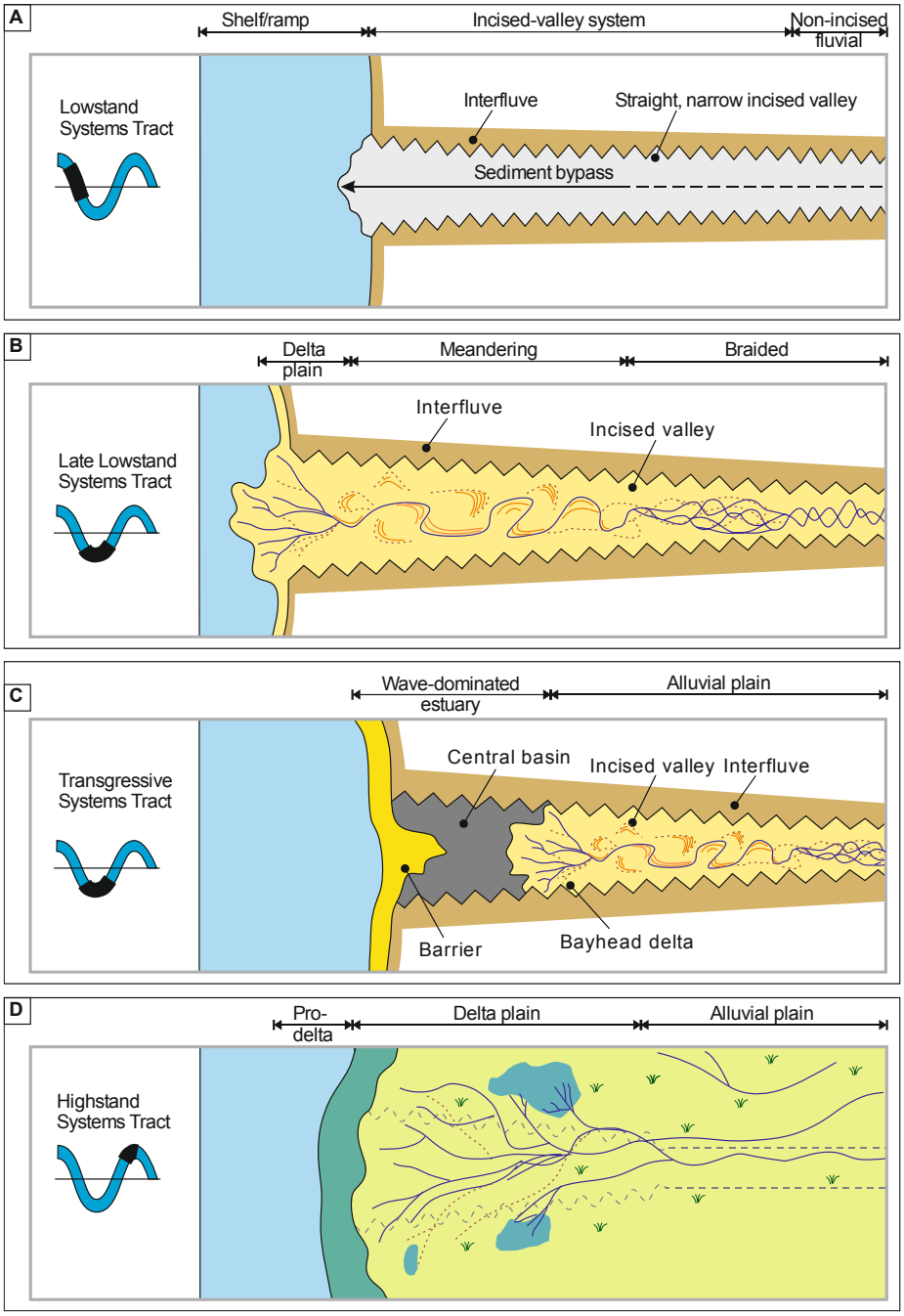

Fig. 2.17. *Idealized plan-view map of a simple incised-valley-fill system showing its evolution in a complete sea-level cycle. (A) Lowstand systems tract time illustrating valley incision near the shoreline with complete sediment bypass. (B) Late lowstand systems tract time illustrating the development of a lowstand delta at the mouth of the incised valley and the beginning of fluvial deposition in the incised-valley system. (C) Transgressive systems tract time illustrating the establishment of a tripartite, wave-dominated estuarine system within the incised-valley system. (D) Highstand systems tract time illustrating the development of a progradational delta system beyond the margins of the buried incised valley. Modified from Stuart (2015); originally after Zaitlin et al. (1994).*

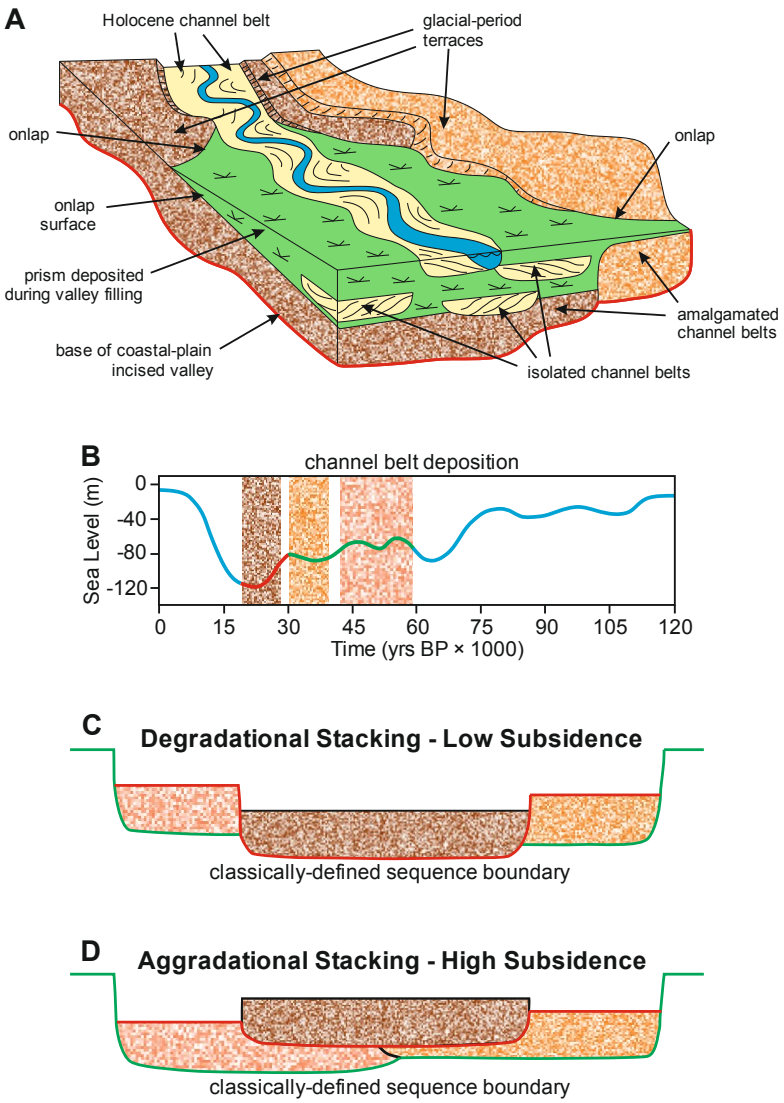

Fig. 2.18. *(A) Schematic diagram illustrating the stratigraphic architecture of coastal-plain incised-valley fills (modified from Blum et al., 2013; originally after Blum and Womack, 2009), highlighting distinctive difference between amalgamated (high-net) basal components, and non-amalgamated (low-net) upper components. The amalgamated component is shown here as displaying a degradational stacking pattern for presentation purposes. Heavy red line corresponds to the diachronous basal valley-fill surface. Contrasting stacking patterns of channel-belt sand bodies for the amalgamated basal components during relative sea-level fall and lowstand. (B) Schematic sea-level curve for 100 kyr glacio-eustatic cycle, indicating time periods of channel-belt deposition. (C) Degradational stacking pattern typical of passive continental margins. (D) Aggradational stacking pattern typical of the Po or Rhine systems. Heavy green line corresponds to valley incision during initial relative sea-level fall, and represents the surface that traces up and out of the valley to the surface of subaerial exposure. Heavy red line corresponds to the base of channel belts formed during sea-level lowstand and the maximum basinward extension. Modified from Blum et al. (2013).*

2.2.3 Incised valleys and source-to-sink system

Incised-valley systems have long been considered features that play a key role in transferring sediments from hinterland regions to deep-marine environments during lowstand (**Fig. 2.13 and Fig. 2.19**), which makes them a useful reference for exploration of sediment linkages to down-dip, relatively coarse-grained lowstand deltas or basin-floor fans (Mitchum 1985; Van Wagoner et al., 1988, 1990; Posamentier, 2001; Törnqvist et al., 2006; Blum and Törnqvist, 2000).

The question of how and when incised-valley systems regulate sediment supply to downdip components of the sediment dispersal system is contentious. A notion deeply embedded in sequence-stratigraphic models is that relative sea-level fall can promote the upstream-propagation of stream rejuvenation and lead to valley incision, driving the remobilization of sediments from the coastal plain and the newly emergent shelf that would feed distal components of the sediment dispersal system. This incision and complete sediment bypass pattern of sediment supply was referred to as a ‘’vacuum cleaner’’ model by Blum and Törnqvist (2000), compared to a ‘’conveyor belt’’ model (**Fig. 2.20**), where sediment supply are constantly delivered to the downdip components of the sediment dispersal system derived from a large hinterland drainage basin. Based on estimation of sediment supply and valley dimensions of coastal-plain valleys of the Colorado river, Gulf of Mexico Coast, Blum and Törnqvist (2000) show that the total volume of sediments produced by ‘’vacuum cleaner’’ excavation of a valley during the last glacio-eustatic sea-level fall and lowstand were an order of magnitude less than the volume delivered by the conveyor belt during the same interval of time. A global compilation and empirical model for sediment supply by Syvitski and Milliman (2007) indicates that contributing drainage-basin areas and relief are first-order controls on sediment supply, with climatic parameters being of second-order. Moreover, important morphometric scaling relationships have been identified by Sømme et al. (2009a, 2009b) between the size of drainage-basin areas, fluvial components and shelf to deep-water systems including strong positive relationships between drainage-basin area, river channel lengths and gradients, shelf widths and the scale of basin-floor fans.

Another issue of considerable significance for sediment supply is the amalgamation of drainage-basin areas as rivers traverse coastal plains and newly emergent shelves during relative sea-level fall (Mulder and Syvitski, 1996) in view of the important control of drainage-basin area on sediment supply. The greatly enlarged drainage areas due to amalgamation of drainage basins during lowstand have been commonly recognized in late-Quaternary coastal systems (Blum and Womack, 2009; **Fig. 2.21**). Mulder and Syvitski (1996) and Burgess and Hovius (1998) have

demonstrated that the amalgamation of drainage-basin areas across broad shelves during lowstand will increase the volume of individual point-source sediment inputs to the basin margin and beyond, and that there will be fewer point sources than what might be expected during highstand. However, Blum and Törnqvist (2000) highlight that for smaller rivers with narrow shelves, or for Greenhouse periods in the Earth history, the potential for drainage-basin amalgamation might be considerably less because of significantly shorter transit distances (**Fig. 2.22**).

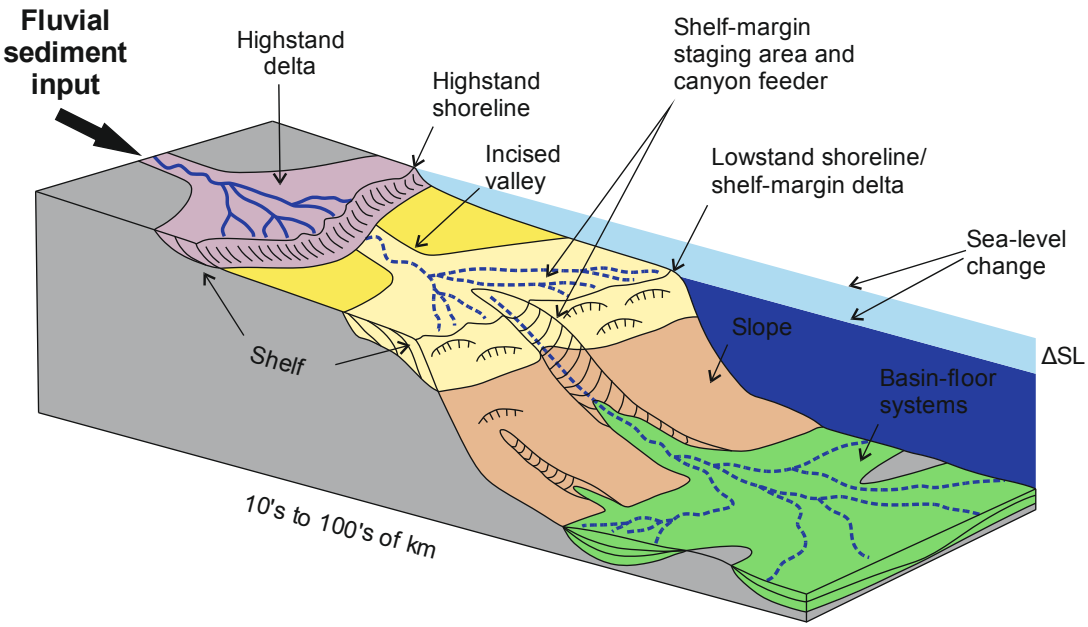

Fig. 2.19. *Definition sketch highlighting the major components of the source-to-sink system (modified from Blum and Womack, 2009; originally after Posamentier and Kolla, 2003). Note that sediment dispersal to the shelf margin and deep basin is determined by processes that control sediment supply to the shelf margin and processes that control dispersal farther downdip.*

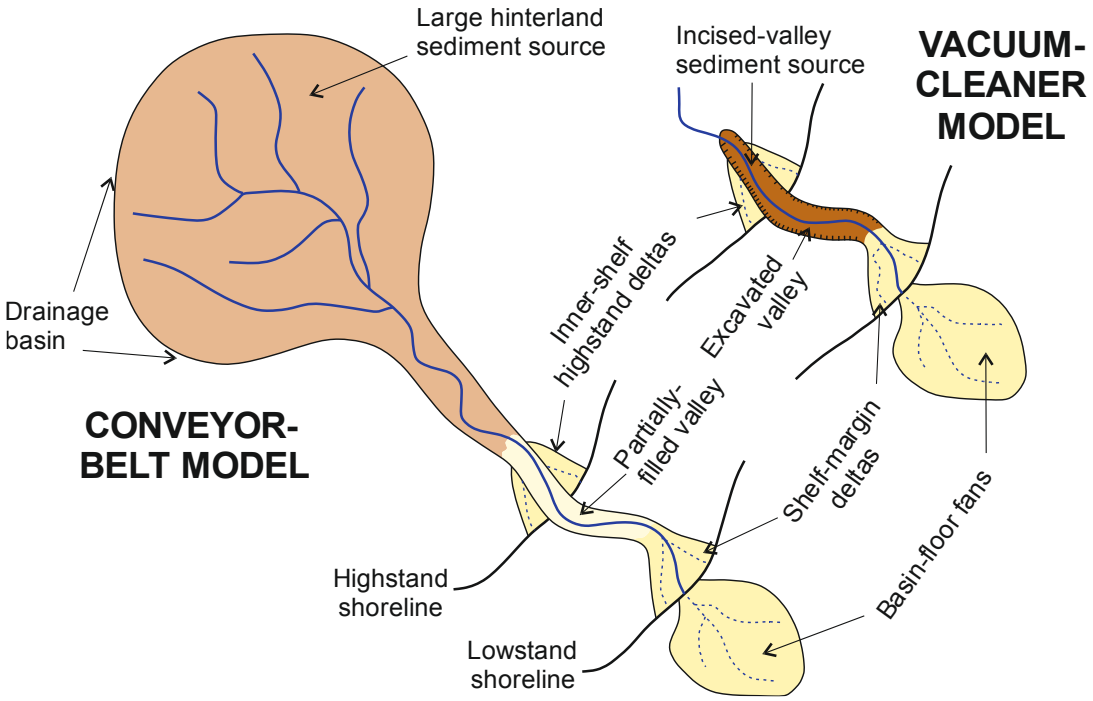

Fig. 2.20. *Schematic diagram illustrating typical contrasts between conveyor-belt vs. vacuum-cleaner models for sediment supply to basin margins. The conveyor belt derives sediments by continuous feed from a large hinterland drainage network, and is not necessarily linked to deep incision with complete sediment bypass during the episodes of sea-level fall, whereas the vacuum cleaner derives all sediments from more distal parts of the basin by excavation of a coastal-plain incised-valley system. Modified from Blum et al. (2013); originally after Blum and Törnqvist (2000).*

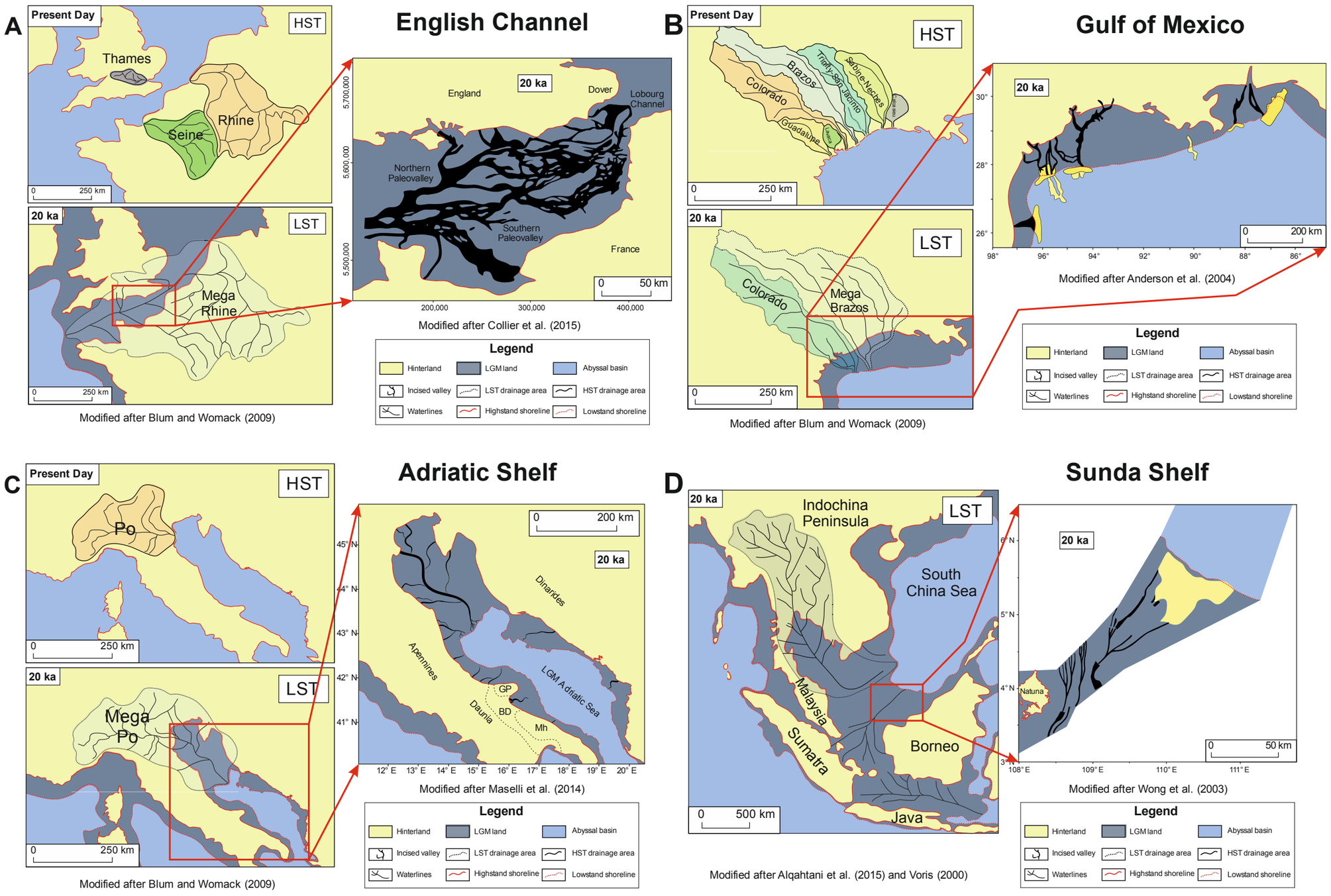

Fig. 2.21. *Diagram illustrating changes in drainage-basin areas between present day and the last glacial maximum (LGM). Inset maps indicate the configuration of incised valleys transiting the newly exposed shelf in respective areas at LGM. Modified partly from Blum and Womack (2009), Collier et al. (2015), Anderson et al. (2004), Maselli et al. (2014) and Wong et al. (2003).*

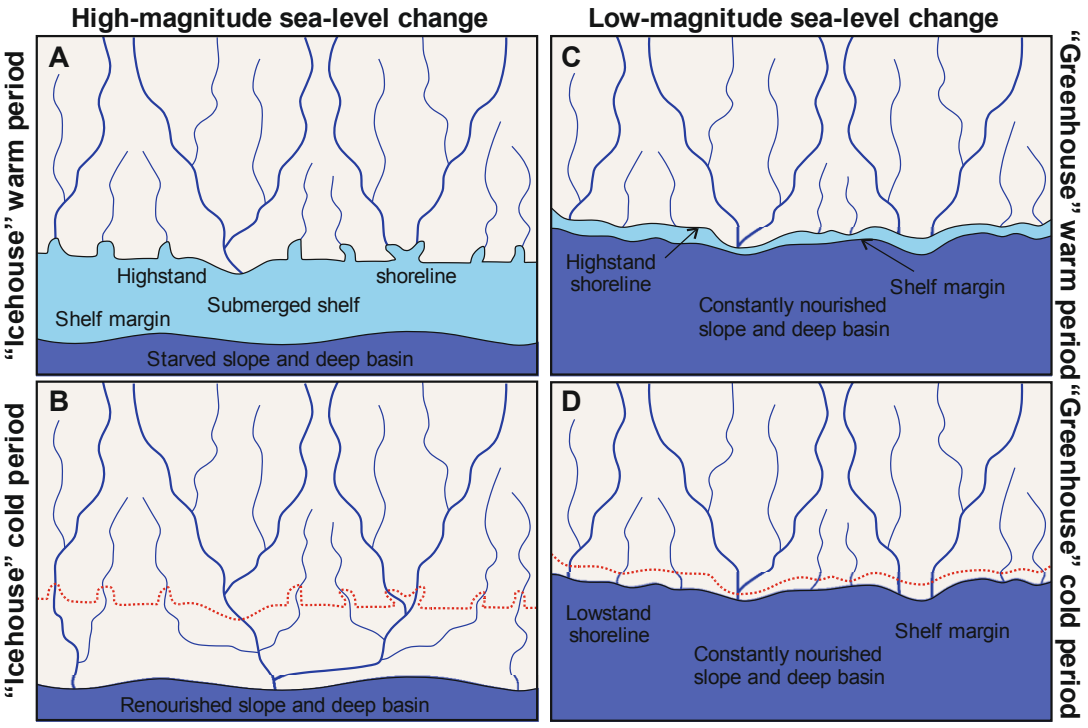

Fig. 2.22. *Schematic diagram illustrating generic models for the amalgamation of drainage-basin areas, or the lack thereof, in icehouse and greenhouse periods of Earth history. (A) "Icehouse" highstand, where all rivers discharge to the inner part of a broad submerged shelf and therefore the shelf slope and deep basin is sediment starved. (B) "Icehouse" lowstand, where smaller rivers merge into larger trunk rivers as they transverse the newly emergent shelf. (C) "Greenhouse" highstand, where all rivers feed into a very narrow shelf, and fluvial sediment is constantly delivered to the shelf slope and deep basin. (D) "Greenhouse" lowstand, where amalgamation of drainage-basin areas may not occur. Modified from Blum et al. (2013); originally after Blum and Womack (2009).*

2.3 Magnitude and frequency of climate and sea-level change

2.3.1 The Quaternary

The Milankovitch theory of climate change (Milankovitch, 1941; de Boer and Smith, 1994) has been widely invoked to explain and account for global changes in ice volumes and corresponding fluctuations of eustatic sea level, especially since studies of oxygen isotopes in deep-sea sediments were utilized for the analysis of glacial-interglacial cycles. On the basis of oxygen-isotope records in deep-sea foraminifera, Hays et al. (1976) illustrated that fluctuations in global ice volume and resultant eustatic sea level followed the periodicities of ca. 400, 100, 43, 23, and 19

kyr, which are predicted by the Milankovitch theory and proposed to be triggered by the long-term quasi-periodic changes in the orbital parameters of Earth relative to the Sun (eccentricity, obliquity and precession). Currently, the Earth's eccentricity cycles with a period of ca. 100 kyr, whereas obliquity has a period of ca. 43 kyr and precession periodicity of ca. 23 kyr and 19 kyr.

Eustatic sea-level change during the Quaternary Icehouse period is characterized by asymmetric, high-frequency (<400 kyr), high-magnitude (>50 m) sea-level cycles with superimposed cycles of shorter frequencies and magnitude. During the middle to late Pleistocene, full glacial–interglacial cycles followed 100-kyr changes in the eccentricity of Earth's orbit around the Sun. Amplitudes of eustatic sea-level change for these cycles were typically larger than 100 m (Miller et al., 2005). Prior to that, amplitudes were generally ca. 50 m (Miller et al., 2005) and full glacial–interglacial cycles occurred with a periodicity of ca. 43 kyr, following changes in the axial tilt of the Earth with respect to the Earth's orbital plane (Shackleton and Opdyke, 1973; Imbrie and Imbrie, 1979; Martinsen et al., 1987; Lisiecki and Raymo, 2005). The ~20 kyr cycles (23 and 19 kyr) are superimposed on full glacial–interglacial cycles and determine both the seasonal distribution of solar radiation reaching the top of the Earth's atmosphere and the strength of atmospheric circulation features, such as monsoon climates (Prell and Kutzbach, 1992). These cycles are thought to contribute to a stepped character of the higher-order sea-level falling limbs, whereas the rising phase of higher-order limbs is commonly uninterrupted by this lower-order modulation. Additionally, research on ice cores and the marine record indicates that significant global climate changes at the scale of 10^3 and 10^4 years are superimposed on Milankovitch orbit-forcing cycles (Bond et al., 1997), which have also been demonstrated to manifest in the terrestrial biosphere by pollen data (e.g. Harrison and Goni, 2010). During the middle to late Pleistocene, mean eustatic sea level is reported to have been ca. -62 m (**Fig. 2.23A**) and rates of eustatic sea-level fluctuations are estimated to be generally <±3 mm/yr (**Fig. 2.23C**); 45% of the last 10^6 years experienced sea-level rise and ca. 55% experienced eustatic sea-level fall (**Fig. 2.23C**). The asymmetric character of Quaternary sea-level curves (**Fig. 2.23E**) has been explained by the dynamics of continental ice caps: as continental ice caps develop, they tend to contribute to a prolonged period of eustatic sea-level fall; when the ice-masses melt, they do so over a much shorter time period and thus lead to rapid episodes of sea-level rise. Furthermore, it is worth noting that end-member states of full glacial or full interglacial climate and sea-level conditions are rare as they only represent a small percentage (20%) of the last million years (Porter, 1989). These observations support the notion that conditions of eustatic sea-level fluctuation is the rule, not an exception (Blum et al., 2013).

In the first part of this PhD Thesis, the focus is on late-Quaternary incised-valley fills, especially those formed during the last complete 100 kyr glacial–interglacial cycle, from ca. 120 ka to present. This is in consideration of the fact that during this most recent period, global climate and sea-level changes and other boundary conditions, such as climates in the catchments, tectonic settings and receiving basin physiography, can be constrained closely. The penultimate interglacial period, with the global ice-volume minima and sea-level maxima, lasted from ca. 120 to 74 ka and was typically referred to as marine isotope stage 5 (MIS 5). This period was further divided into five substages, from MIS 5e to MIS 5a: MIS 5e, the last interglacial maximum, occurred from ca. 120–115 ka, when global eustatic sea level reached elevations of +3 to 6 m (relative to modern sea level); MIS 5d–5a witnessed fluctuations in eustatic sea level between −60 and−20 m. MIS 4–2, which are typically considered to correspond to the last glacial period, lasted from ca. 74 to 15 ka, when the glacio-eustatic sea level fluctuated but typically fell from −60 to −130 m. MIS 2, the last glacial maximum (LGM), with maxima in global ice volumes and minima in sea level at −130 to −120 m, occurred from ca. 25 to 18 ka. Late MIS 2 and early MIS 1, from ca. 18 to 6 ka, were characterized by rapid melting of global ice caps and the corresponding rapid sea-level rise. After this time, global eustatic sea level has remained close to the state at present-day time (Lambeck and Chappell, 2001; Siddall et al., 2003; Church et al., 2008).

One issue of considerable significance is that climate change and sea-level change in local or regional areas tend to be much more complicated than what depicted by the global record. In the past 20 kyr, many local regions have shown significant deviations in magnitude and/or direction from global climatic conditions (Wright et al., 1993; Kutzbach et al., 1997). Relative sea-level changes of local to regional importance can demonstrate significant departures from eustatic sea-level changes in both rate and magnitude, and sometimes in polarity (Lambeck, 1993a,b; Shennan et al., 2000, 2002; Peltier et al., 2002; Shennan and Horton, 2002; Milne et al., 2006; Shennan et al., 2006). The causative mechanisms of these discrepancies are varied, and include local to regional tectonics, local land subsidence, mantle response to development and melting of ice sheets, melting of local land ice, glacio- and hydro-isostatic deformation of shorelines, sediment compaction, hydrodynamics (Peltier and Andrews, 1976; Tushingham and Peltier, 1992; Lambeck, 1993a, b; Fleming et al., 1998; Peltier, 1998).

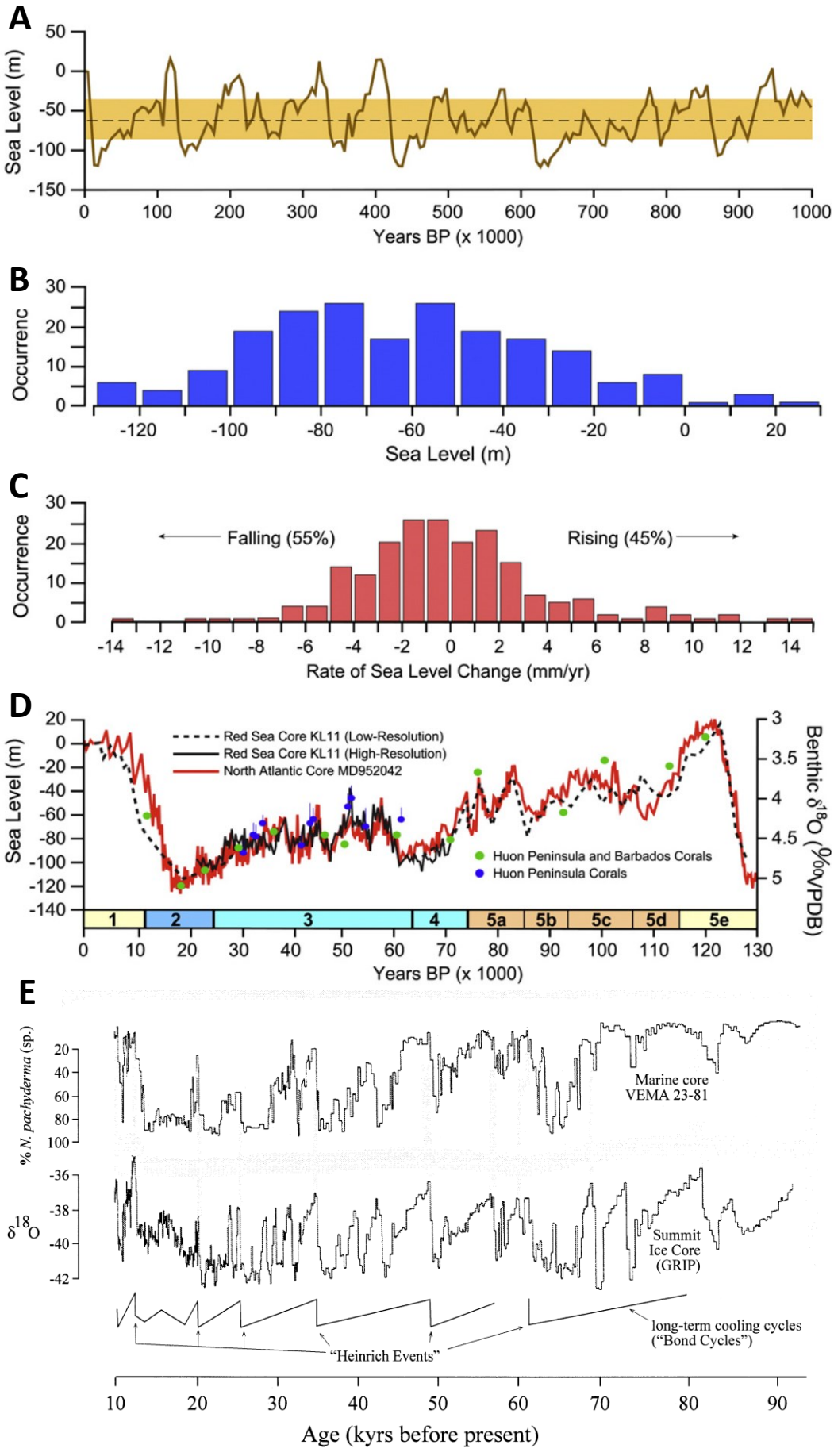
A
Sea Level (m)
50
0
-50
-100
-150
0
100
200
300
400
500
600
700
800
900
1000
Years BP (x 1000)
B
Occurrenc
30
20
10
0
-120
-100
-80
-60
-40
-20
0
20
Sea Level (m)
C
Occurrence
30
20
10
0
Falling (55%)
Rising (45%)
-14
-12
-10
-8
-6
-4
-2
0
2
4
6
8
10
12
14
Rate of Sea Level Change (mm/yr)
D
Sea Level (m)
20
0
-20
-40
-60
-80
-100
-120
-140
Red Sea Core KL11 (Low-Resolution)
Red Sea Core KL11 (High-Resolution)
North Atlantic Core MD952042
Huon Peninsula and Barbados Corals
Huon Peninsula Corals
1
2
3
4
5a
5b
5c
5d
5e
0
10
20
30
40
50
60
70
80
90
100
110
120
130
Years BP (x 1000)
Benthic δ18O (‰VPDB)
3
3.5
4
4.5
5
E
% N. pachyderma (sp.)
20
40
60
80
100
Marine core
VEMA 23-81
δ18O
-36
-38
-40
-42
Summit
Ice Core
(GRIP)
"Heinrich Events"
long-term cooling cycles
("Bond Cycles")
10
20
30
40
50
60
70
80
90
Age (kyrs before present)

Fig. 2.23. *(A) Eustatic sea-level curve during the last 1 Ma. Dashed line denotes the mean value of sea-level position relative to modern sea level and orange box shows the range of sea-level positions that represent 60% of time in the past 1 million years (Myr). (B) Histogram illustrating the distribution of sea-level positions in the past 1 Myr. Note that the frequency of occurrence of sea-level positions here is recorded for every 5 kyr. (C) Histogram illustrating the distribution of rates of sea-level change in the past 1 Myr. Note that frequency of occurrence of sea-level fluctuation rate here is recorded for every 5 kyr. (D) Fluctuations of eustatic sea levels during the last 130 kyr. Note that key Marine Isotope Stages (from MIS 5e through MIS 1) are shown in the bottom colour bars; these are referred to throughout this work. Figure and caption after Blum et al. (2013). (E) Diagram of the proportion variation of the planktonic cold-water foraminifera in marine core VM 23-81 and oxygen-isotope records in deep-water sediments in the last 90 kyr, emphasizing the asymmetric character of the eustatic sea-level curve in the last 100-kyr glacial-interglacial cycle. After Blum and Törnqvist (2000), originally after Bond et al. (1993).*

2.3.2 Pre-Quaternary

It has long been considered that during the Phanerozoic period, the Earth's climate alternated between icehouse and greenhouse conditions, which were separated by transitional climates (Frakes et al., 1992; **Fig. 2.24**). Icehouse conditions were characterized by high-frequency (4th-order) and high-magnitude (> 100 m) sea-level oscillations and operated in tandem with the waxing and waning of continental ice sheets. By contrast, greenhouse conditions were typically characterized by high-frequency but limited amplitude (< 10 m) sea-level fluctuations (Lehrmann and Goldhammer, 1999; Séranne, 1999). Only for a relatively small part of the Earth's history during the Phanerozoic did the global climate resemble that of the Quaternary icehouse world (**Fig. 2.24**), and these times include the Carboniferous (Fielding et al., 2006) and the late Paleogene to Neogene (Abreu and Anderson, 1998).

However, Milankovitch-scale radiation-driving climate change is an intrinsic part of Earth–Sun relations (Berger et al., 1989; Berger and Loutre, 1994) and might have operated significantly throughout the Phanerozoic (Barron and Moore, 1994), although with variable periodicity, amplitude and phasing relations (Blum and Törnqvist, 2000). The wavelengths of relative sea-level changes for the 100 kyr eccentricity cycle have been recognized to differ little at 500 Ma compared to those operating in the late Quaternary, whereas the obliquity (currently 41 kyr) and precession cycles (currently 23 and 19 kyr) are considered to have shortened since

500 Ma (ca. 30 kyr for obliquity cycles; 19 kyr and 16 kyr for precession cycles) (Berger et al., 1989; Berger and Loutre, 1994). Nevertheless, this external forcing might also have different manifestations between greenhouse conditions and icehouse conditions (Frakes et al., 1992). Therefore, care should be taken when extrapolating any relationships observed in the geological record of the late Quaternary to the more ancient rock record, especially for geological times dominated by greenhouse conditions.

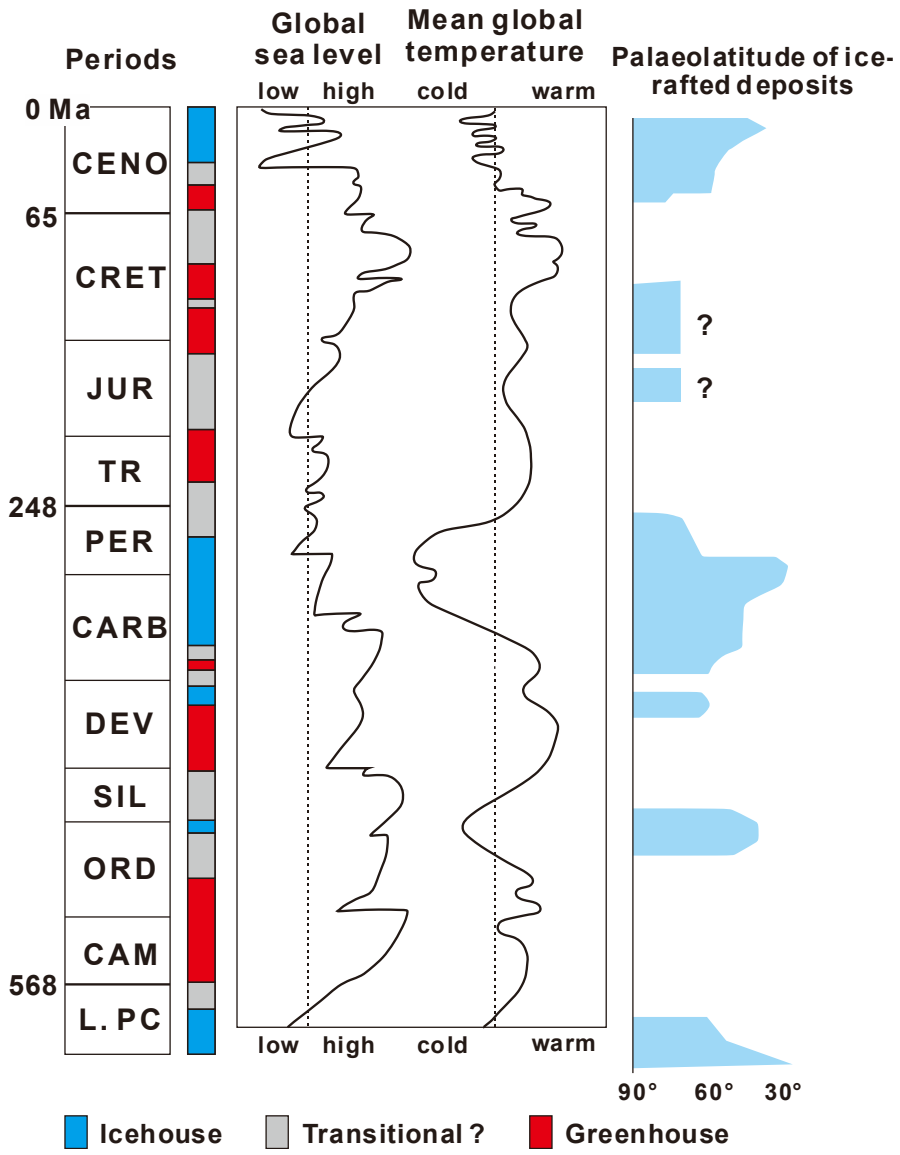

Fig. 2.24. *Diagram illustrating Earth's climates and eustatic fluctuations throughout the Phanerozoic. Greenhouse-Icehouse portion of the diagram modified from Frakes and Francis (1988), Frakes et al. (1992) and Read (1995). The portion of the diagram relating to palaeolatitude of ice-rafted deposits is modified from Frakes and Francis (1988). Global sea-level curve and mean global temperature curve after Frakes et al. (1992).*

2.4 Summary

Understanding of controls that govern channel incision and lateral migration during relative sea-level fall and rise is necessary for exploring the geological controls on incised-valley-fill dimensions, as valley deepening is driven by vertical channel incision, whereas valley widening is largely driven by lateral migration of channels and valley sidewall destabilization. Evaluating the different roles of upstream controls and downstream controls on the alluvial stratigraphic record can provide guidelines to decipher the prevailing boundary conditions in Earth history from the ancient record.

In the following chapters (Chapters 3 and 4), geological controls on the geometry and stratigraphic architecture of incised-valley-fill systems are explored based on quantitative analysis of late-Quaternary examples, where deposits and controlling factors can be well constrained, in order to gain an improved understanding of the relative roles of different controls on valley-fill geometry and stratigraphic architecture. In Chapter 5, the resultant database-conditioned models from late-Quaternary examples have been applied to reconstruct characteristics of river systems from the ancient rock record, i.e., to Namurian incised-valley fills of the United Kingdom and Ireland. The facies architecture of these ancient examples is employed to help decipher palaeohydraulic characteristics of their formative rivers and to attempt a refinement of regional palaeogeographic reconstructions.

3 Geological controls on the geometry of incised-valley fills: Insights from a global dataset of late-Quaternary examples

3.1 Summary

Incised valleys that develop due to relative sea-level change are common features of continental shelves and coastal plains. Assessment of the factors that control the geometry of incised-valley fills has hitherto largely relied on conceptual, experimental or numerical models, else has been grounded on case studies of individual depositional systems. Here, a database-driven statistical analysis of 151 late-Quaternary incised-valley fills has been performed, the aim being to investigate the geological controls on their geometry.

Results of this analysis have been interpreted with consideration of the role of different processes in determining the geometry of incised-valley fills through their effect on the degree and rate of river incision, and on river size and mobility. The studied incised-valley fills developed along active margins are thicker and wider, on average, than those along passive margins, suggesting that tectonic setting exerts a control on the geometry of incised-valley fills, likely through effects on relative sea-level change and river behaviour, and in relation to distinct characteristics of basin physiography, water discharge and modes of sediment delivery. Valley-fill geometry is positively correlated with the associated drainage-basin size, confirming the dominant role of water discharge. Climate is also inferred to exert a potential control on valley-fill dimensions, possibly through modulations of temperature, peak precipitation, vegetation and permafrost, which would in turn affect water discharge, rates of sediment supply and valley-margin stability. Shelves with slope breaks that are currently deeper than 120 m contain incised-valley fills that are thicker and wider, on average, than those hosted on shelves with breaks shallower than 120 m. No correlation exists between valley-fill thickness and present-day coastal-prism convexity, which is measured as the difference in gradient between lower coastal plains and inner shelves.

These findings challenge some concepts embedded in sequence stratigraphic thinking, and have significant implications for analysis and improved understanding

of source-to-sink sediment route-ways, and for attempting predictions of the occurrence and characteristics of hydrocarbon reservoirs.

3.2 Introduction

Incised valleys are common features of continental shelves and coastal plains. In these settings, valleys develop as fluvially eroded, elongated palaeotopographic lows in response to relative sea-level fall that causes rivers to incise their bed in an attempt to reach a new lowered equilibrium profile (Summerfield, 1985; Posamentier and Allen, 1999; Blum and Törnqvist, 2000; Holbrook et al., 2006; Blum et al., 2013). The resultant valleys are subsequently inundated by the sea during a following episode of sea-level rise, typically leading to the development of estuaries in the nearshore (Zaitlin et al., 1994). As transgression proceeds, both the valley margins and the sedimentary infill in the base of the valley itself may be reworked by coastal and marine processes (Roy, 1984; Dalrymple et al., 1992; Allen and Posamentier, 1993; Zaitlin et al., 1994; Strong and Paola, 2008; Blum and Törnqvist, 2000; Blum et al., 2013). Valley systems that are cut in response to relative sea-level change possess greater potential for sediment accommodation than time-equivalent interfluve areas, and the infill of such valleys typically records a complex history of infilling via sedimentation in a range of environments as sea level rises (Thomas and Anderson, 1994; Rodriguez et al., 2005; Simms et al., 2007a).

Although incision and development of valleys in the nearshore region occurs during episodes of relative sea-level fall, valley development may continue during lowstand times as rivers seek to re-equilibrate (Summerfield, 1985; Blum and Price, 1998; Posamentier and Allen, 1999; Blum and Törnqvist, 2000; Holbrook et al., 2006; Strong and Paola, 2008; Martin et al., 2011; Blum et al., 2013). The lower part of the valley fill usually records sediment accumulation via fluvial systems both during the falling-stage and lowstand systems tracts (Blum and Price, 1998; Strong and Paola, 2008; Martin et al., 2011; Blum et al., 2013). However, the majority of the fill of valley systems consists of a relatively complete record of deposition during the lowstand and early transgressive system tracts, whereby slowly rising sea level locally reduces the fluvial gradient close to the valley shoreline and encourages accumulation (Posamentier and Allen, 1999; Blum and Törnqvist, 2000; Holbrook et al., 2006; Blum et al., 2013). Thus, the sedimentary fill of these types of valleys might provide critical information about earth-surface processes, related depositional history, and its controls, such as the rate of relative sea-level change and its effects on sediment distribution and depositional environments (Posamentier

and Vail, 1988; Wright and Marriott, 1993; Shanley and McCabe, 1994; Dalrymple et al. 1994; Zaitlin et al., 1994; Legarreta and Uliana, 1998; Blum et al., 2013). Furthermore, incised-valley systems play key roles in transferring sediments from hinterland regions to deep-marine environments during lowstands, which makes them a useful reference for exploration of sediment linkages to down-dip, coarse-grained lowstand deltas or basin-floor fans (Mitchum 1985; Van Wagoner et al., 1988, 1990; Posamentier, 2001; Törnqvist et al., 2006; Blum and Törnqvist, 2000). Typically, incised valleys are initially filled with coarse-grained fluvial deposits at their base during relative sea-level fall and lowstand, and are subsequently filled by estuarine and marine deposits during the following sea-level rise (Roy, 1984; Dalrymple et al., 1992; Allen and Posamentier, 1993; Wright and Marriott, 1993; Shanley and McCabe, 1993, 1994; Dalrymple et al. 1994; Zaitlin et al., 1994; Blum and Törnqvist, 2000; Blum et al., 2013). Thus, many valley fills are sand prone, which makes them potential hydrocarbon reservoirs and groundwater aquifers (Wright and Marriott, 1993; Shanley and McCabe, 1994; Dalrymple et al. 1994; Zaitlin et al., 1994; Blum et al., 2013), and possible sources of sand for beach renourishment.

Extensive research has been undertaken previously to characterize the internal fill of near-shore incised valleys (e.g., Fisk, 1944; Zaitlin et al., 1994; Wright and Marriott, 1993; Allen and Posamentier, 1993; Shanley and McCabe, 1994; Dalrymple et al., 1994, 2006; Legarreta and Uliana, 1998; Blum et al., 2013). Numerous conceptual, numerical and experimental models have been devised, and scaling relationships identified from modern or ancient case studies, to investigate mechanisms of fluvial channel incision, lateral migration and associated drivers over short timescales ($< 10^3$ yr) (e.g. Hooke, 1979, 1980; Nanson and Hickin, 1983; Fielding and Crane, 1987; Bridge and Mackey, 1993; Mackey and Bridge, 1995; Lawler et al., 1999; Richard et al., 2005; Shanley, 2004; Fielding et al., 2006; Gibling 2006; Blum et al., 2013). However, only a limited number of studies have hitherto focused on geological controls that determine the geometry of near-shore incised valleys and their fills; the results of such studies largely consist of conceptual, experimental, or numerical models (Talling, 1998; Posamentier and Allen, 1999; Strong and Paola, 2006, 2008; Martin et al., 2011), or are based on case studies of individual incised-valley systems (e.g. Posamentier, 2001; Weber et al., 2004; Ishihara and Sugai, 2017) or of multiple valley systems in a single region (e.g. Mattheus 2007; Mattheus and Rodriguez, 2011; Phillips, 2011; Chaumillon et al., 2008).

In this study, a database-driven statistical analysis has been performed with the aim to investigate the geological controls on the geometry of incised-valley fills. The

study is based on a compilation of late-Quaternary incised-valley fills, especially – but not only – those formed during the last glacio-eustatic cycle; the studied examples are representative of different climatic and tectonic settings, and are distributed globally. By restricting the scope of investigation to late-Quaternary examples, the controlling factors on valley characteristics and evolution can be constrained closely. It is therefore possible to relate valley-fill geometry to magnitude of sea-level change, drainage-basin size, drainage-basin vegetation type, physiography of the receiving basin, climate, substrate lithology and tectonics. These variables are generally poorly constrained for most ancient successions. Specific objectives of this work are as follows: (i) to gain an improved understanding of geological controls on valley-fill dimensions; (ii) to evaluate the relative roles of different controls on valley incision and widening; (iii) to present implications of the results for sequence stratigraphy and for hydrocarbon-reservoir prediction and characterization.

3.3 Background

Observations from experiments (Strong and Paola, 2006, 2008) and investigation of late-Quaternary incised valleys, such as those along the Texas coastal plain (Blum and Price, 1998; Blum et al., 2013), reveal the diachronous nature of the basal surfaces of incised-valley fills; these surfaces do not typically represent relict geomorphic surfaces, but rather amalgamated erosional features resulting from multiple episodes of punctuated channel incisions accompanied by lateral migration, channel-belt deposition and valley-wall reshaping during relative sea-level fall and lowstand. Valley deepening is driven by vertical channel incision, whereas valley widening is largely driven by lateral migration of channels and valley sidewall destabilization (Strong and Paola, 2006, 2008; Martin et al., 2011; Blum et al., 2013). Insight on controls that govern channel incision and lateral migration during relative sea-level fall and rise is therefore useful for exploring the geological controls on incised-valley-fill dimensions. Process-based studies argue that along the continental margins, fluvial incision initiates when a steeper-gradient surface with respect to the fluvial equilibrium profile is exposed during relative sea-level fall (Summerfield, 1985; Leckie, 1994; Talling, 1998; Posamentier and Allen, 1999; Blum and Törnqvist, 2000; Holbrook et al., 2006; Blum et al., 2013). The onset of incision generally occurs at the highstand coastline or at the shelf-slope break when exposed by sea-level fall. Fluvial systems tend to reach their graded profile by landward propagation of retreating knickpoints (Summerfield, 1985; Posamentier and Allen, 1999; Blum and Törnqvist, 2000; Holbrook et al., 2006). Knickpoint

migration rates have been shown to be strongly controlled by water discharge (Schumm et al., 1984; Loget and Van Den Driessche, 2009) and substrate characteristics (Van Heijst and Postma, 2001; Loget and Van Den Driessche, 2009). Thus, both the magnitude of sea-level fall and the physiography of the basin determine the largest vertical adjustment of a river system through valley incision, whereas water discharge and substrate characteristics dominate the degree to which, and rate at which, fluvial systems approach the equilibrium profile (Paola et al., 1992). However, rivers might not incise during relative sea-level fall if the shelf is broad and of a gradient similar to, or less than, that of the adjacent coastal plain, and if water discharge is relatively small (cf. Woolfe et al., 1998). Valley downcutting might also take place under conditions of marine transgression, for example because of tectonic and isostatic uplift of coastal plains, or due to rapid coastal erosion by waves and longshore drift (cf. Leckie 1994). Channel lateral migration rates have been shown to be strongly controlled by water discharge (Hooke, 1979, 1980; Nanson and Hickin, 1983; Lawler et al., 1999; Richard et al., 2005), sediment supply (Sheets et al., 2002; Peakall et al., 2007; Braudrick et al., 2009; Martin et al., 2011), bed material size (Nanson and Hickin, 1986; Richard et al., 2005) and bank stability (Hickin and Nanson, 1975; Nanson and Hickin 1983; Hickin and Nanson, 1984; Lawler et al., 1999; Richard et al., 2005).

Many authors have summarized the fundamental controlling factors that govern valley geometry; principal among these are the rate and magnitude of base-level fall, basin physiography (gradients along the depositional profile and shelf-break depth), climate, substrate characteristics and tectonics (Schumm, 1993; Talling, 1998; Posamentier and Allen, 1999; Holbrook and Schumm, 1999; Blum and Törnqvist, 2000; Posamentier, 2001; Van Heijst and Postma, 2001; Gibling 2006; Strong and Paola, 2006, 2008; Loget and Van Den Driessche, 2009; Martin et al., 2011; Blum et al., 2013).

A number of studies have concentrated on the impact of relative sea-level fall on the formation and morphology of incised valleys (Blum and Törnqvist, 2000; Strong and Paola, 2006, 2008; Martin et al., 2011; Blum et al., 2013). Strong and Paola (2006, 2008) explored the evolution in valley morphology and the emergence of stratigraphic feedbacks in response to relative sea-level fall through experiments that included (i) an isolated slow cycle, where ‘slow’ is defined with respect to a theoretical equilibrium time that is direct function of basin length (Paola et al., 1992), (ii) an isolated rapid cycle, and (iii) several superimposed rapid cycles, given steady passive-margin style subsidence and constant sediment and water supplies. Physical experiments by Strong and Paola (2006, 2008) indicate that relatively slow sea-level fall could lead to the formation of broader and flatter erosional surfaces,

whereas relatively rapid sea-level fall tends to encourage the development of deeper incised valley systems. The same authors also demonstrate that the magnitude of relative sea-level fall primarily determines the valley depth, whereas the rate of relative sea-level fall is a fundamental control on valley width by controlling the duration of time over which the valley-fill boundaries can be shaped. Based on observations from experiments, numerical modelling and field data, Martin et al. (2011) focused on the downstream changes in valley dimensions, indicating that valley width and valley depth tend to increase downstream towards the shoreline position at the beginning of base-level fall, and interpreting such downstream valley widening as related to increased sediment influx from valley excavation, acting independently from relative sea-level changes or initial surface topography. Furthermore, Martin et al. (2011) highlight that both valley depth and valley width increase with the magnitude of relative base-level fall, and that valley widening closely follows valley incision and extension temporally during relative sea-level fall.

The physiography of the depositional profile over which incised valleys develop has been shown to play an important role in valley incision and widening (Summerfield, 1985; Talling, 1998; Posamentier and Allen, 1999; Posamentier, 2001; Blum and Törnqvist, 2000; Törnqvist et al., 2006; Blum et al., 2013). Along the continental margins, the onset of valley incision tends to commence when a convex-up topography is exposed during relative sea-level fall (Summerfield, 1985; Talling, 1998; Blum and Törnqvist, 2000; Blum et al., 2013). Such topographic profiles are typical of the highstand coastline and shelf-slope break. Several authors (Talling, 1998; Posamentier and Allen, 1999; Posamentier, 2001; Törnqvist et al., 2006) have argued that when sea level falls below the shelf break, incised valleys will form across the entire shelf. By contrast, when sea level falls but does not expose the shelf break, incised-valley development will be limited to the region of the coastal prism. Based on observations of present-day gradient profiles along passive margins and margins associated with foreland basins, Talling (1998) further illustrates that if the sea level remains above the shelf break, valley incision will be governed primarily by the geometry of the coastal prism and valley incision will tend to increase with the coastal-prism convexity. Moreover, the magnitude of valley incision is expected to increase basinward towards the highstand shoreline, and then decrease towards the shelf break; the maximum degree of incision is thought to occur at the highstand shoreline (Talling, 1998).

Climate is known to control valley morphology and valley-fill dimensions in a complex manner. It dictates the supply of water and sediment to a river, mediated by effects on variables such as temperature, precipitation, vegetation, and presence

of permafrost, particularly through their influence on surface runoff characteristics, which are themselves related to the magnitude and frequency of floods (Blum et al., 1994; Blum and Törnqvist, 2000; Bogaart et al., 2003a, b; Vandenberghe, 2003; Blum et al., 2013). Through analysis of the geometry of late-Quaternary incised-valley systems along the passive continental margins of the northern Gulf of Mexico and of the US mid-Atlantic coast, Mattheus et al. (2007), Mattheus and Rodriguez (2011) and Phillips (2011) show that valley dimensions (valley depth, width and cross-sectional area) are primarily controlled by their drainage-basin area, which is a proxy for the water discharge of their formative rivers; shelf-break depth and coastal-plain and shelf gradients are secondary controls.

Tectonic processes also control valley dimensions, notably through their influence on relative sea-level changes, basin physiography and sediment delivery rates, and indirectly by affecting the drainage-basin climate (Posamentier and Allen, 1999; Jain and Tandon, 2003; Ishihara et al., 2011, 2012; Wohl et al., 2012; Tropeano et al., 2013; Vandenberghe, 2003; Ishihara and Sugai, 2017). Studies on several palaeovalleys (Sugai and Sugiyama, 1998, 1999; Makinouchi et al., 2006; Ishihara et al., 2012; Ishihara and Sugai, 2017) developed on coastal plains in Japan show that tectonic uplift or subsidence act to enhance or reduce, respectively, the effect of sea-level fall on valley dimensions for a given episode of eustatic sea-level fall; local tectonic uplift is generally associated with well-developed terraces and narrow valley floors, whereas local tectonic subsidence is primarily linked to poorly delineated terraces and wide valley floors.

Additionally, wave or tidal erosion causing ravinement during the transgressive stage of incised valley infilling might greatly modify the dimensions of incised-valley fills (e.g. Lericolais et al., 2001; Mattheus and Rodriguez, 2011; Blum et al., 2013).

Existing conceptual models or experimental studies have tended to focus on consideration of one overarching factor (e.g. relative sea-level change) as a control on the geometry of incised-valley fills, whilst treating other parameters as constant. Yet, this is known not to be the case in natural systems. A more comprehensive assessment of controlling factors on the geometry of incised-valley fills is attempted here by means of a comparison of data from multiple case studies, enabled by a database approach.

3.4 Methods

To evaluate the relative roles of different geological controls that influence valley incision and widening, in this work a statistical analysis of relationships between

late-Quaternary incised-valley fills and parameters that describe their context and controlling factors has been undertaken based on data derived from a literature compilation. Data have been coded in a relational database, the Shallow-Marine Architecture Knowledge Store (SMAKS; Colombera et al., 2016), which stores data on the sedimentary architecture and geomorphic organization of shallow-marine and paralic siliciclastic depositional systems. SMAKS includes quantitative data on geological entities of varied nature and scale, and on their associated depositional systems, which can be classified on multiple parameters (e.g., shelf width, delta catchment area) tied to metadata (e.g., data types, data sources).

This study utilizes data on 151 classified late-Quaternary incised-valley fills, 135 of which developed during the last glacial-interglacial cycle (LGC), and 16 of which are of pre-LGC age. The primary data have been extracted from 67 published literature sources. A detailed account of all the case studies included in this work, their associated bibliographic references and the types of data is reported in Table 3.1, and the location of the studied incised-valley fills is shown in Fig. 3.1. The datasets that underpin this work are available as part of the supporting information that is available to download as an accompaniment to this paper (see Supplementary Material).

The importance of controls on valley-fill dimensions has been assessed through (i) comparison of descriptive statistics and associated statistical tests and (ii) determination of correlation between variables, as outlined below.

Table 3.1. *Case studies stored in the SMAKS database on late-Quaternary incised-valley fills. The table illustrates published literature sources, data types and the age of formation (as LGC or pre-LGC) for each case study. Case-study identification numbers (ID) relate to those coded in the SMAKS database and are referred to in following figures. N = number of incised-valley-fill elements developed for each case study, at or before the LGC.*

ID	Case study	Data source	Data types	N	Age
31	Composite database, Gulf of mexico and Atlantic Ocean, USA	Mattheus and Rodriguez (2011); Mattheus et al. (2007)	Airborne images, Cores, Well cuttings, Shallow seismics	38	LGC
38	Pilong Formation, South China Sea, Sunda Shelf	Alqahtani et al. (2015)	Cores, 3D seismics, Shallow seismics	1	LGC
39	Late Quaternary of Manfredonia	Maselli andTrincardi (2013); Maselli et al. (2014)	Cores, Shallow seismics	1	LGC

	Gulf, Adriatic Sea				
42	Lower Tagus Valley, Portugal	Vis et al. (2008); Vis and Kasse (2009)	Cores	1	LGC
44	Rio Grande do Sul, Atlantic coast, Brazil	Weschenfelder et al. (2014)	Cores, Shallow seismics	2	LGC
48	New Jersey shelf, USA	Nordfjord et al. (2005); Nordfjord et al. (2006)	Cores, Shallow seismics	2	LGC
49	Hervey Bay, Queensland, Australia	Payenberg et al. (2006)	Shallow seismics, Bathymetric profile	1	LGC
51	Gulf of Lion, France	Labaune et al.(2005); Labaune et al.(2010); Tesson et al.(2011)	Cores, Shallow seismics	1	LGC
				5	Pre-LGC
59	Bay of Biscay, France	Weber et al.(2004)	Cores, Shallow seismics	3	LGC
60	Bay of Biscay, France	Proust et al. (2010)	Cores, Shallow seismics	4	LGC
61	Bay of Biscay, France	Chaumillonand Weber (2006)	Cores, Shallow seismics	1	LGC
62	Bay of Biscay, France	Menier et al. (2006)	Cores, Shallow seismics	5	LGC
63	Gulf of Lion, France	Tesson et al. (2015)	Cores, Shallow seismics	3	LGC
65	Late Quaternary of Moreton Bay, Queensland, Australia	Lockhart et al. (1996)	Cores, Shallow seismics	4	LGC
67	Pleistocene of Pattani Basin, South China Sea, Gulf of Thailand	Reijenstein et al. (2011)	Well cuttings, 3D seismics, Shallow seismics	2	Pre-LGC
68	Pilong Formation, South China Sea, Gulf of Thailand	Miall (2002)	3D seismics	1	Pre-LGC
69	Pleistocene of southern Java Sea	Posamentier (2001)	Cores, 3D seismics, Shallow seismics	1	LGC
70	Gironde incised valley, France	Allen and Posamentier (1993); Lericolais et al. (2001)	Cores, Shallow seismics	1	LGC
71	Mekong incised valley, Vietnam	Tjallingii et al. (2010)	Cores, Shallow seismics	1	LGC
72	Late Quaternary of Tuscany, Italy	Amorosi et al. (2013); Rossi et al. (2017)	Cores	3	LGC
73	Ombrone incised valley, Italy	Bellotti et al. (2004); Breda et al.(2016)	Cores	1	LGC
74	Volturno incised valley, Italy	Amorosi et al. (2012)	Cores	1	LGC
75	Biferno incised valleys, Italy	Amorosi et al. (2016)	Cores	1	LGC
				2	Pre-

					LGC
76	Tiber Delta, Italy	Milli et al. (2013); Milli et al. (2016)	Cores	1	LGC
77	Metaponto coastal plain, Italy	Tropeano et al. (2013)	Cores, Shallow seismics	3	LGC
78	Assu incised valley, Brazil	Gomes et al. (2016)	Shallow seismics	1	LGC
79	Apodi-Mossoró incised valley, Brazil	Vital et al. (2010)	Shallow seismics	1	LGC
80	South Sea of Korea	Lee et al. (2017)	Cores, Shallow seismics	3	LGC
81	KwaZulu-Natal shelf, South Africa	Green (2009); Benallack et al. (2016)	Cores, Shallow seismics	5	LGC
82	Gulf of Papua, Papua New Guinea	Crockett et al. (2008); Daniell (2008)	Cores, Shallow seismics, Bathymetric profile	3	LGC
83	East China Sea	Li et al. (2002); Li et al. (2006); Wellner and Bartek (2003); Zhang and Li (1996); Zhang et al.(2017)	Cores, Shallow seismics	4	LGC
84	Pearl River incised valleys, South China Sea	Li et al. (2006)	Cores	1	LGC
85	Kanto Plain incised valleys, Japan	Ishihara and Sugai (2017); Ishihara et al. (2012)	Cores	3	LGC
86	Pearl River incised valleys, South China Sea	Zhuo et al. (2015)	Cores, Shallow seismics	5	LGC
87	Mahakam Delta, Indonesia	Sydow (1996); Roberts and Sydow (2003); Crumeyrolle and Renaud (2003)	Cores, 2D seismics, 3D seismics, Shallow seismics	2	LGC
92	KwaZulu-Natal shelf, South Africa	Green and Garlick (2011)	Shallow seismics	6	LGC
93	Maputo Bay, Mozambique	Green et al. (2015)	Cores, Shallow seismics	3	LGC
94	Cameroon shelf	Ngueutchoua and Giresse (2010)	Cores, Shallow seismics	2	LGC
95	Kosi Bay, South Africa	Cooper et al.(2012)	Cores, Shallow seismics	1	LGC
98	Oregon-Washington shelf, USA	Twichell et al. (2010)	Cores, Shallow seismics, Bathymetric profile	2	LGC
99	Virginia shelf, USA	Colman and Mixon (1988); Colman et al. (1990); Foyle and Oertel (1992); Foyle and Oertel (1997); Oertel and Foyle (1995); Shideler et al. (1984)	Cores, Shallow seismics	1	LGC
				3	Pre-LGC
100	Parnaíba incised valleys, Brazil	Aquino da Silva et al. (2016)	Shallow seismics	5	LGC
101	Western	Karisiddaiah et al. (2002)	Shallow seismics,	1	LGC

	continental margin of India		Bathymetric profile		
103	Chukchi shelf, Alaska, USA	Hill et al. (2007); Hill and Driscoll (2008); Stockmaster (2017)	Cores, Shallow seismics	3	LGC
				3	Pre-LGC
104	Santa Catarina coast, Brazil	Cooper et al. (2016)	Cores, Shallow seismics	1	LGC
109	Gulf of Cádiz shelf, Iberian peninsula	Lobo et al. (2001); Gonzalez et al. (2004); Lobo et al. (2018)	Shallow seismics, Surface sediment samples	2	LGC

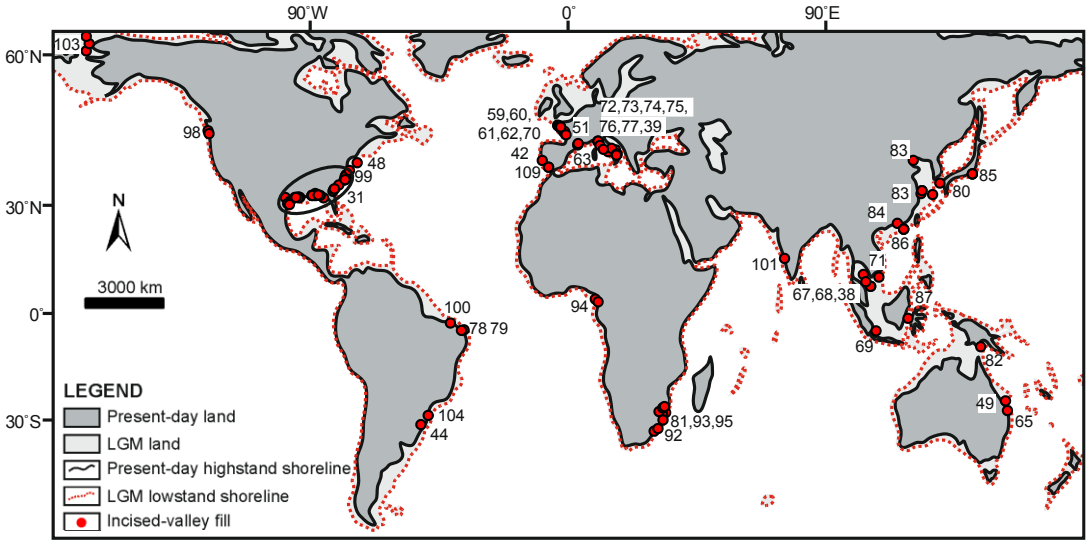

Fig. 3.1. *Location of studied late-Quaternary incised-valley fills. The numbers on the map correspond to the IDs in Table 3.1. Base map modified from Ray and Adams (2011).*

3.4.1 Incised-valley-fill dimensions

In this study, an incised valley is defined as a fluvially eroded, elongate topographic low that is typically larger than a single channel and is generally associated with the juxtaposition of fluvial or estuarine strata on marine deposits and subaerial exposure on interfluves (Van Wagoner et al., 1990; Boyd et al., 2006; Blum et al., 2013). In the original sources, some aggradational channel belts or even channel fills might have been misinterpreted as incised-valley fills. This study avoids inclusion of channel belts or channel fills representing river propagation on the shelf or on shelf-edge deltas at lowstand (Fig. 3.2C). However, a small number of cases (e.g., Posamentier, 2001; Zhuo et al., 2015; Aquino da Silva et al., 2016), where ambiguity as to the classification of the described successions remains, have been included in the database. Incised-valley geometries vary along dip (Strong and Paola, 2008; Martin et al., 2011; Phillips, 2011). Thus, to enable meaningful comparisons, measurements must be made at the same respective location along

the valley axis, to ensure a similar duration of subaerial exposure and record of fluvial and marine processes. In this work valley fills have been classified with respect to the position where their geometry has been characterized, i.e., beneath the present-day coastal plain, on the inner shelf or on the outer shelf. Here, the distinction between inner and outer shelf is made on bathymetry, rather than process regime: the term 'inner shelf' refers to the part of the shelf that extends from the present-day shoreline to the 25 m isobath, whereas the term 'outer shelf' refers to the part of the shelf that extends from the 25 m isobath to the shelf break. Coastal-plain valley fills and inner-shelf valley fills are grouped when analysing the relationships between coastal-plain gradient or coastal-prism convexity versus valley-fill dimensions; inner and outer-shelf valley fills are instead grouped as cross-shelf valleys to assess the relationships between shelf-break depth, shelf width, or shelf gradient versus valley-fill dimensions. This was done to account for the positions where the geometry of incised valleys is expected to be more significantly affected by said controls, as the highstand coastal-prism convexity should control the geometry of valleys carved on the coastal prism, whereas the shelf physiography is predicted to control particularly, although not exclusively, the development of cross-shelf valleys. Only valley fills that represent the products of a single cycle of incision and fill are considered in the subsequent analyses. Compound valley fills that record multiple episodes of incisions and fills, associated with different eustatic cycles, and that thus possess a highly time-transgressive basal surface composed of several amalgamated unconformities, have not been included in this study (cf. Korus et al., 2008). It is also desirable to compare incised-valley fills formed during the same sea-level cycle to account for the effects of the magnitude in sea-level fall on valley dimensions. Here, late-Quaternary incised-valley fills formed during different sea-level cycles are compared, but those associated with the last glacio-eustatic cycle are differentiated and represent the majority of studied examples (135 of 151 valley fills studied; 89%).

The surfaces that should be taken as the boundaries of incised-valley fills have been the subject of debate (Catuneanu et al., 2009). Some authors consider the base of incised-valley fills to represent part of the subaerial unconformity that form sequence boundaries (cf. Helland-Hansen and Martinsen, 1996). In this thinking, the base of an incised-valley fill is placed at the base of the lowstand systems tract, meaning that older falling-stage deposits are not considered part of the fill of an incised valley. In this perspective, the boundaries of incised-valley fills associated with the last glacial cycle would have developed from the Marine Isotope Stage 2 (MIS 2). In contrast, other workers have assigned deposits accumulated during the falling stage to the fill of the incised valleys (e.g., Posamentier et al., 1992; Kolla et al., 1995; Morton and Suter, 1996), such that all of the MIS 4 and younger deposits

would still be contained in the incised-valley fills of the last glacial cycle. Of the 135 studied incised-valley fills related to the last glacial cycle considered herein, 13 include deposits of the falling-stage systems tract, 40 exclude falling-stage deposits, whereas 82 could not be differentiated. Considering units that differ in this way will affect any comparison of their cross-sectional area; instead, comparisons of their thickness and width may not be affected, given the position at which falling-stage deposits are expected to occur (cf. Blum et al., 2013).

Where possible, incised-valley fills are classified on their drainage order (90 of 151 valley fills; 60%), i.e., they are differentiated as trunk valleys that reached the lowstand shoreline versus tributary valleys of variable orders; valley fills known to be the expression of third- or higher-order tributary valleys have not been considered.

Incised-valley-fill dimensions (Table 3.2) were obtained from the original sources, either derived from the text or measured directly on figures using image-analysis software (ImageJ; Schneider et al., 2012). The morphometric parameters that describe the dimensions of incised-valley fills are represented in Fig. 3.2.2A. Valley-fill thicknesses are measured where the body is thickest; in cases for which it is not known whether the thickness is measured relative to the thickest portion of the fill (e.g., in 1D well log sample or core sample), the thickness is reported as 'apparent'. For underfilled valleys, values of 'thickness' include the depth of the relic depressions relative to the valley flanks. Valley-fill widths are measured along strike-oriented transects as the distance between the valley walls. 'Apparent' widths are recorded for measurements that are not perpendicular to the valley-fill axis. Thickness and width measurements are classified as 'partial' or 'unlimited' (*sensu* Geehan and Underwood, 1993; Fig. 3.2B) for cases where the position of pinch-out of a valley-fill is unknown at one or both ends (e.g., due to outcrop termination), respectively. When derived from borehole correlations, width measurements are recorded as 'correlated'; for purposes of data analysis and presentation, 'unlimited' and 'correlated' measures are not differentiated. Valley-fill cross-sectional areas are measured as vertical cross-sections across the valley in an orientation perpendicular to its axis. The area is measured as the vertical cross-sectional area subtended by the base and top of the valley fill or the elevation of interfluves for underfilled valleys. Only maximum values of valley-fill thickness, width and cross-sectional area are used in the statistical analysis: apparent and partial or unlimited observations have been discarded. For cases where the 3D geometry of valley fills is well constrained, usually for high-resolution seismic data, the largest values of maximum valley-fill thickness, width and cross-sectional area along the valley reach are chosen. In cases where the entire 3D geometry of a valley fill is not known and

its downdip variability is not constrained, the largest values of all parameters within the studied sample are recorded, and the observations are classified as located on the shelf or at the highstand coastal prism.

Table 3.2. *Parameters that describe the dimensions of incised-valley fills. T: incised-valley-fill thickness; W: incised-valley-fill width; A: incised-valley-fill cross-sectional area. IVF denotes incised-valley fill.*

Parameter	Definition
T (m)	The thickness from the deepest part of the valley axis to the top of the valley fill or the elevation of interfluves for underfilled valleys.
W (m)	Horizontal distance between the valley walls, measured perpendicular to the valley axis.
A (m^2)	The vertical cross-sectional area subtended by base and top of the valley fill or the elevation of interfluves for underfilled valleys, measured in an orientation perpendicular to the valley axis.

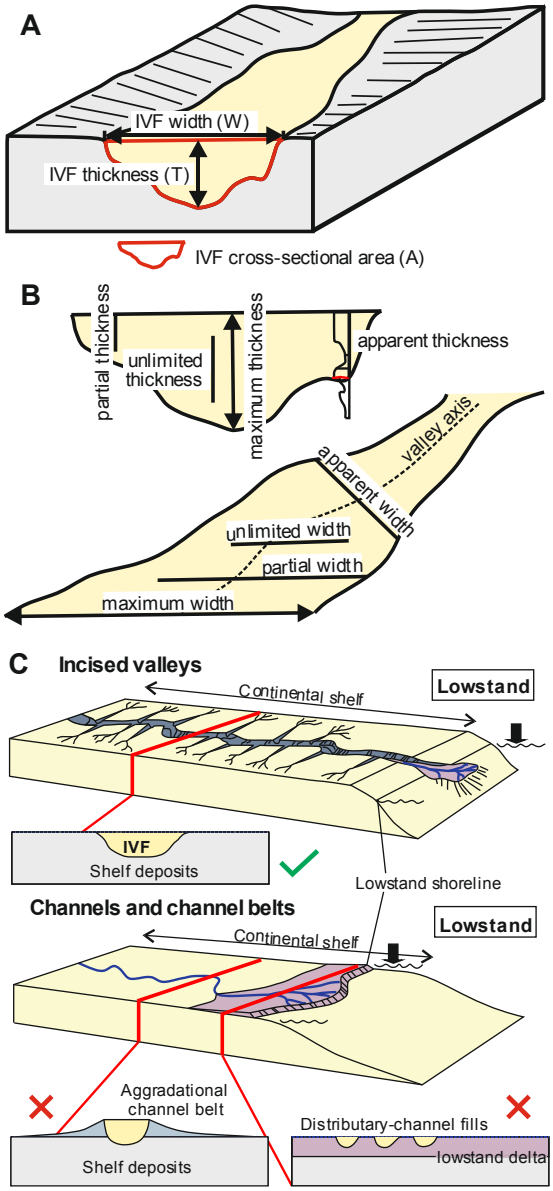

Fig. 3.2. *(A) Incised-valley-fill dimensions (incised-valley-fill thickness, width and cross-sectional area) measured in our analysis. (B) Classification of incised-valley-fill thickness and width by type of observation, i.e., as 'maximum', 'apparent', 'partial' and 'unlimited' (see text). (C) Diagram illustrating channel belts associated with river propagation on the shelf at lowstand and distributary channels associated with lowstand deltas, neither of which are included in this study.*

3.4.2 Quantification of basin physiography

In this study, the present-day physiography of the shelf and subaerial nearshore has been taken as a proxy for the physiography of the continental shelf and nearshore during the Last Interglacial (LI) highstand (Fig. 3.3). However, this assumption carries significant uncertainty due to potential differences in basin physiography between the present and the LI, likely arising from spatial variations in

isostatic adjustment, spatial variations in post-glacial shelf and shelf-break accretion, differences in process regime, variable styles of fluvial and shoreline responses expected in different climatic and tectonic settings, and because of autogenic dynamics. Present-day lower-coastal-plain gradients (Fig. 3.3) have been measured perpendicular to the orientation of the present-day shoreline along a 10-km transect landward of the shore, utilizing digital elevation data from Becker et al. (2009). Gradients have also been calculated for the tract of subaqueous nearshore that extends from the shoreline to 25-m isobath, as representative values of inner-shelf gradients (Fig. 3.3), using digital bathymetric data by Becker et al. (2009). The difference in gradient between present-day lower coastal plains and inner shelves is taken as a measure of the convexity of the present-day coastal prism (Fig. 3.3; Table 3.3). The shelf-break depth is measured at the shelf-break location mapped by Harris et al. (2014), using digital bathymetric data by Becker et al. (2009). The shelf width is measured as the distance from the present-day shoreline to the shelf break, as mapped by Harris et al. (2014). For cases in which the shoreline is irregular and does not mirror the orientation of the shelf break, the length along the valley axis from the present-day shoreline to the shelf break is recorded as an additional attribute.

Table 3.3. *Parameters used to describe the settings of the studied incised-valley fills. CPG10: lower-coastal-plain gradient; ISG25: inner-shelf gradient; CPC: coastal-prism convexity; SBD: shelf-break depth; SW: shelf width; SDL: the length from the shoreline to the shelf break; SG: shelf gradient; L: latitude; DBA: drainage-basin area.*

Parameter	Definition
CPG10 (°)	The mean gradient measured perpendicular to the shoreline along a 10-km transect landward of the present-day shoreline, in degrees.
ISG25 (°)	The mean gradient measured from the present-day shoreline to the 25-m isobath in an offshore direction, in degrees.
CPC (°)	The difference in gradient between present-day lower coastal plains and inner shelves, in degrees.
SBD (m)	Depth of the shelf break.
SW (km)	The horizontal distance between the present-day shoreline and the shelf break.
SDL (km)	The length along the valley axis from the present-day shoreline to the shelf break.

SG (°)	The mean gradient of the shelf between the present-day shoreline and the shelf break, in degrees.
L (°)	The absolute value of the latitude of the location where the incised-valley fill has been measured.
DBA (km^2)	Area of the drainage-basin catchments feeding the incised valley at lowstand, landward of the location where the incised-valley fill has been measured.

3.4.3 Drainage-basin size

The drainage-basin size has been determined based on the catchment area landward of the location where the incised-valley-fill geometry was measured. For valley systems whose drainage networks during the Last Glacial Maximum (LGM) have been reconstructed and presented in the scientific literature, drainage areas were measured at the location where the incised-valley fills were characterized. In other cases, the river systems that contributed to the lowstand drainage network of incised valleys now buried under coastal plains can be reconstructed confidently; in these cases estimations based on catchment areas of present-day rivers have been considered as the sum of all different drainage basins that are inferred to have amalgamated at lowstand, as shown in Fig. 3.4.

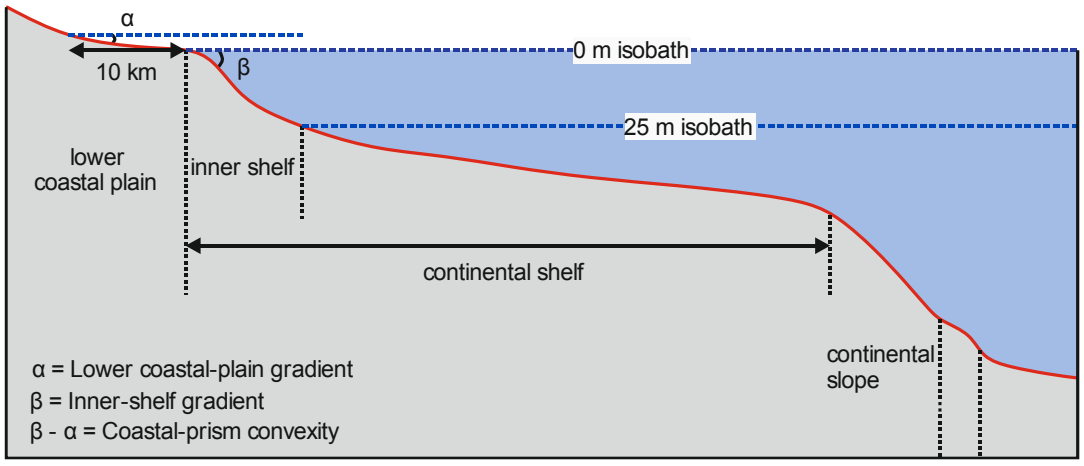

Fig. 3.3. *Definition sketch of the physiography of the depositional profile over which incised valleys develop.*

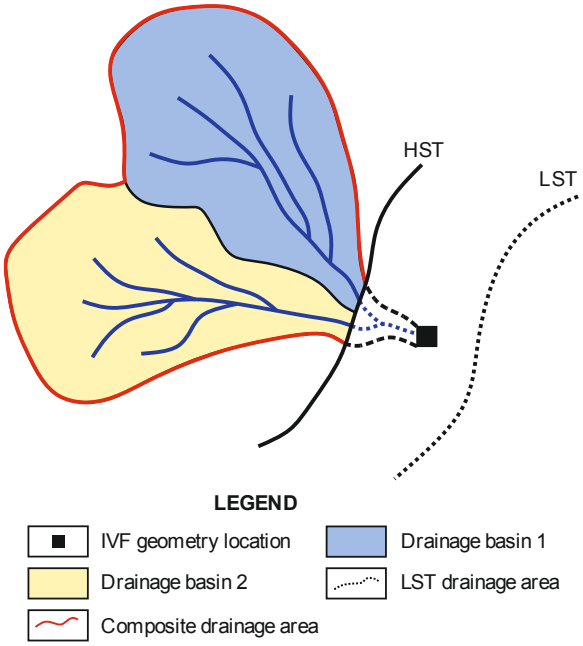

Fig. 3.4. *Schematic diagram illustrating the measurement of contributing drainage-basin area corresponding to each incised-valley fill. HST denotes the highstand coastal shoreline (present-day shoreline) and LST denotes the lowstand shoreline (e.g., LGM shoreline).*

3.4.4 LGM catchment vegetation

The global distribution of dominant vegetation types during the LGM has been mapped by Ray and Adams (2011), based on plant-fossil data and proxy zoological and sedimentologic data. Based on the map by Ray and Adams (2011), the proportionally most prevalent type of vegetation in the catchment area was recorded for each incised-valley fill. Vegetation types were recorded in terms of two alternative schemes (i.e., one including classes: 'forest', 'grassland or woodland', 'desert'; the other including classes: 'tropical or subtropical', 'temperate', 'polar or subpolar').

3.4.5 Statistical analyses

Statistical analyses have been performed to determine relationships between variables and to test hypotheses relating to differences in means across populations. For pairs of continuous variables, Pearson or Spearman correlation coefficients (denoted with R and r hereafter) are respectively used to quantify linear and monotonic relationships, whose statistical significance is expressed as p-values (p hereafter). The statistical significance of differences in the mean of variables across groups is determined with a two-sample t-test when dealing with two sets of

observations, and with one-way analysis of variance (ANOVA) when dealing with three or more sets of observations. Resulting test statistics (*t* for t-tests, *F* for ANOVA) are considered jointly with the number of degrees of freedom (*df* hereafter) to determine the statistical significance of differences across groups, expressed as p-values (*p*). All statistical analyses were performed in Minitab 17.

3.5 Results and interpretations

3.5.1 Continental-margin type

Observations

The studied late-Quaternary valley fills were classified as hosted on passive, active, and transform margins. Valley fills from transform margins and passive margins are considered together in the subsequent analyses. A comparison has been made of incised-valley fills developed on passive and active continental margins. The thickness, width and cross-sectional area (Fig. 3.5A-C) of incised-valley fills associated with active margins are, on average, larger than those along passive margins, and the difference is important for values of mean valley-fill thickness (mean(T) = 50.1 versus 28.2 m; mean(W) = 7,099 versus 3,862 m; mean(A) = 200,545 versus 73,200 m^2, respectively). Two-sample t-tests confirm that means in valley-fill morphometric parameters are significantly different in the two settings (t-value= 4.53, p-value < 0.001, df = 16, for T; t-value= 2.40, p-value= 0.030, df = 15, for W; t-value= 2.90, p-value= 0.010, df = 18, for A). Distributions in drainage area for the two margin types (Fig. 3.5D) show that drainage-basin areas associated with passive margins are larger, on average, than those associated with active margins (mean $DBA_{passive}$ = 60,672 m^2, mean DBA_{active} = 17,012 km^2, 2-sample t-test: t-value= -2.57, p-value= 0.012, df = 76).

Interpretations

Tectonics can significantly influence fluvial incision through a first-order control on basin physiography (Posamentier and Allen, 1999). Tectonically active margins are commonly characterized by the formation of narrow, high-gradient shelves, which favour deep fluvial incision (Schumm and Brakenridge, 1987; Leckie, 1994; Posamentier and Allen, 1999). In contrast, passive margins are characterized by the development of wide, low-gradient shelves, in part because such margins are generally associated with larger drainage-basin areas (Blum et al., 2013), as shown in Fig. 3.5D, and thus lower-gradient shelves (see below); this in turn is reflected in shallower fluvial incision for base-level falls of given magnitude. Distributions of valley-fill thickness for these two margin types (Fig. 3.5A) support this expectation.

In addition, local tectonic uplift might be experienced by shelves on active margins (Posamentier and Allen, 1999; Ishihara and Sugai, 2017), which would induce fluvial incision (Posamentier and Allen, 1999; Holbrook and Schumm, 1999; Holbrook et al., 2006; Tropeano et al., 2013; Ishihara et al., 2011, 2012; Ishihara and Sugai, 2017). For example, the Metaponto coastal plain in Italy (case study 77 in Table 3.1) has been experiencing regional uplift since the Middle Pleistocene (Doglioni et al., 1996; Patacca and Scandone, 2001), at rates varying from 0.3 to 0.9 mm/yr as estimated from dated stranded marine terraces (Cilumbriello et al., 2008, 2010; Caputo et al., 2010; Tropeano et al., 2013). Three incised-valley fills developed beneath the Metaponto coastal plain are characterized by larger-than-average thickness, despite being associated with smaller-than-average drainage areas, as illustrated in Fig. 3.5A-C.

Incised-valley widening is partly driven by the lateral migration of fluvial channel belts (Martin et al., 2011). Previous work based on experiments, numerical modelling and field studies (Strong and Paola, 2006, 2008; Martin et al., 2011; Blum et al., 2013) have shown that lateral channel migration and channel-belt deposition are closely concomitant with valley incision unless the valley sidewalls are resistant to erosion or the system is starved of sediments, implying that valley widening generally follows valley incision temporally during relative sea-level fall. The examples associated with active margins studied here are all incised into unconsolidated sand-rich coastal or shelf deposits, such that valley-fill width is expected to be scaled with valley-fill thickness.

Furthermore, tectonics also indirectly affects the morphology and behaviour of fluvial systems through orographic control on climate. Regions undergoing rapid uplift are typically associated with high relief, favouring orographic precipitation (Joeckel, 1999; Ruddiman, 2013), which in turn controls water discharge. High elevation river basins draining active margins are characterized by larger runoff per basin area (Milliman and Syvitski, 1992). In addition, tectonically active systems are generally associated with smaller catchments than passive ones (Fig. 3.5D), such that storms are more likely to affect the entire drainage basin and floods to propagate through the entire channel network (Sømme et al., 2009a). Thus, tectonically active systems associated with small drainage areas ($<10^4$ km^2) are more prone to large differences between flood and base-flow discharge (2 to 3 orders of magnitude; Sømme et al., 2009a). Additionally, active margins tend to have steep gradients throughout the river network (Flint, 1974; Sømme et al., 2009a; Blum et al., 2013), which are expected to control stream power in a way that would promote fluvial incision (Schumm et al., 1984; Paola et al., 1992; Blum et al., 2013) and lateral migration of river channels (Hooke, 1979, 1980; Nanson and

Hickin, 1983; Lawler et al., 1999; Richard et al., 2005). Furthermore, active margins are commonly subject to hill-slope destabilization, partly because of seismic triggering (Jain and Tandon, 2003; Wilson et al., 2007). Rivers associated with active margins tend to have greater specific sediment yield and carry a higher proportion of bedload than those associated with passive margins (Milliman and Syvitski, 1992), which in turn favour channel lateral migration and thus valley widening (Dietrich and Whiting, 1989; Sheets at al., 2002; Strong and Paola, 2006, 2008; Peakall et al., 2007; Braudrick et al., 2009; Martin et al., 2011; Blum et al., 2013). Peak water discharge and rates of sediment flux might have been particularly high for incised valleys now infilled in the Kanto plain (Japan) and in Indonesia (case study 85 and 87 in Table 3.1, respectively), as these areas were subject to tropical monsoonal climate during the LGM (Crowley and North 1991; Broecker 1995; Adams and Faure, 1997; Ray and Adams, 2011).

As a caveat to these results, it must be noted that the distributions of drainage areas for the incised-valley fills considered in this work do not cover the full spectrum of catchment sizes documented for modern rivers (cf. Blum et al. 2013); in particular, the distribution of drainage areas for valley systems on passive margins considered in this work does not encompass those that would correspond with the world's largest river systems. Considering the highly skewed nature of distributions of drainage areas (Fig. 3.5D), the inclusion of very large valley systems might significantly affect values of maximum size, but less significantly the mean values for which the statistical significance was tested. Notwithstanding, although the data suggest that the type of continental margin is a good predictor of incised-valley fill geometry, any conjecture on the effective role of specific controlling factors needs to be substantiated with more data.

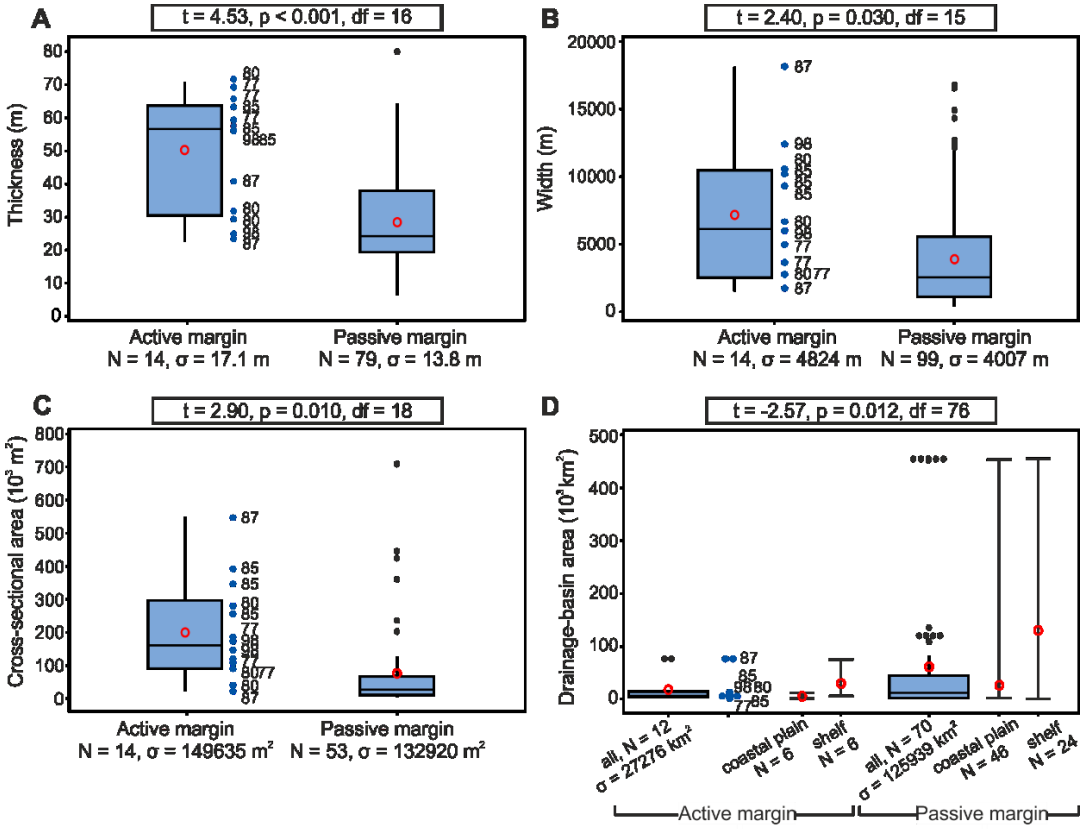

Fig. 3.5. *Box-plots that present distributions in: (A) late-Quaternary incised-valley-fill thickness, (B) width, (C) cross-sectional area, and (D) drainage-basin size, for active and passive continental margins. Individual values are also shown next to the boxplot for active margins and the numerical labels refer to IDs in Table 3.1. In D, mean and range plots are illustrated near each boxplot for examples hosted on the shelf and coastal plains, respectively. For each boxplot, boxes represent interquartile ranges, red open circles represent mean values, horizontal bars within the boxes represent median values, and black dots represent outliers (values that are more than 1.5 times the interquartile range). 'N' denotes the number of readings and 'σ' denotes the standard deviation. The results of 2-sample t-test (t-value, p-value and df) are reported in respective boxes. 'df' denotes the degrees of freedom.*

3.5.2 Basin physiography

3.5.2.1 Shelf-break depth

Observations

The maximum sea-level lowstand during the LGM was 120 to 130 m below that of present-day levels (Fairbanks, 1989; Yokoyama et al., 2000; Lambeck and Chappell, 2001; Peltier and Fairbanks, 2006; Simms et al., 2007b). However, the magnitude of fall varied geographically and across estimates made by different

authors. In the following statistical analysis, to assess distributions in valley-fill dimensions for shelves that were completely or partially exposed at the LGM, different values of shelf-break depth were considered (120 m, 125 m and 130 m). Similar results were obtained for the three different depths; all results are therefore only presented for the 120-m shelf-break depth threshold. For the LGC examples, incised-valley fills hosted on shelves with shelf-break depth larger than 120 m display greater thickness, width and cross-sectional area, on average (Fig. 3.6A-C), than those with shelf break shallower than 120 m (mean(T) = 39.1 m versus 27.5 m; mean(W) = 10,519 m versus 4,004 m; mean(A) = 202,033 m^2 versus 78,538 m^2). Two-sample t-tests for valley-fill dimensions in these two scenarios indicate significant differences between the means of these two populations (t-value = -3.30, p-value = 0.001, df = 103, for T; t-value = -2.86, p-value = 0.006, df = 56, for W; t-value = -2.08, p-value = 0.045, df = 37, for A). Valley fills associated with shelves with deeper shelf breaks tend to have larger drainage-basin areas (mean = 216,131 m versus 27,698 m; 2-sample t-test: t-value = -2.66, p-value = 0.011, df = 42) (Fig. 3.6D).

For cross-shelf valley fills hosted on shelves with shelf break shallower than 120 m (Fig. 3.7A-C), valley-fill thickness is negatively correlated with shelf-break depth (r = -0.427, p-value = 0.033); no correlation is seen between valley-fill width or cross-sectional area and shelf-break depth (r(W) = 0.085, p-value = 0.693; r(A) = -0.110, p-value = 0.616). For cross-shelf valley fills hosted on shelves with shelf break deeper than 120 m (Fig. 3.7A-C), a weak correlation is seen between valley-fill width and shelf-break depth (r = 0.335, p-value = 0.032), whereas there is very weak or no correlation between valley-fill thickness or cross-sectional area and shelf-break depth (r(T) = 0.201, p-value = 0.208; r(A) = 0.057, p-value = 0.792).

Interpretations

Previous work based on conceptual models has proposed (Talling, 1998; Posamentier and Allen, 1999; Posamentier, 2001; Törnqvist et al., 2006) that relative sea-level falls that are larger in magnitude than the depth of the shelf break, by resulting in full exposure of the shelf, will drive the formation of incised valleys cutting through the shelf, whereas relative sea-level falls of magnitude lower than the shelf-break depth are expected to lead to the formation of valleys that are mostly confined around the highstand coastal prism. Fluvial systems on shallower shelves are expected to undergo a greater vertical river-profile adjustment, resulting in greater valley incision. However, the data do not fully support this view, as shelves with breaks deeper than 120 m tend to contain larger incised-valley fills. This could be explained by the fact that the studied shelves with shelf breaks that

are deeper than 120 m are primarily linked to larger drainage-basin areas, compared to those with shallower shelf breaks (Fig. 3.6D).

The correlation between valley-fill thickness and shelf-break depth for cross-shelf valley fills hosted on shelves with shelf break shallower than 120 m (Fig. 3.7A) might indicate a causal link between magnitude of exposure, depth of incision, and resulting valley-fill thickness. However, shelves with deeper shelf breaks tend to have steeper shelf gradients on average, which results in larger differences between the shelf gradient and the fluvial equilibrium profile and therefore should tend to drive deeper fluvial incision for a given relative sea-level fall (Schumm and Brakenridge, 1987; Leckie, 1994; Posamentier and Allen, 1999).

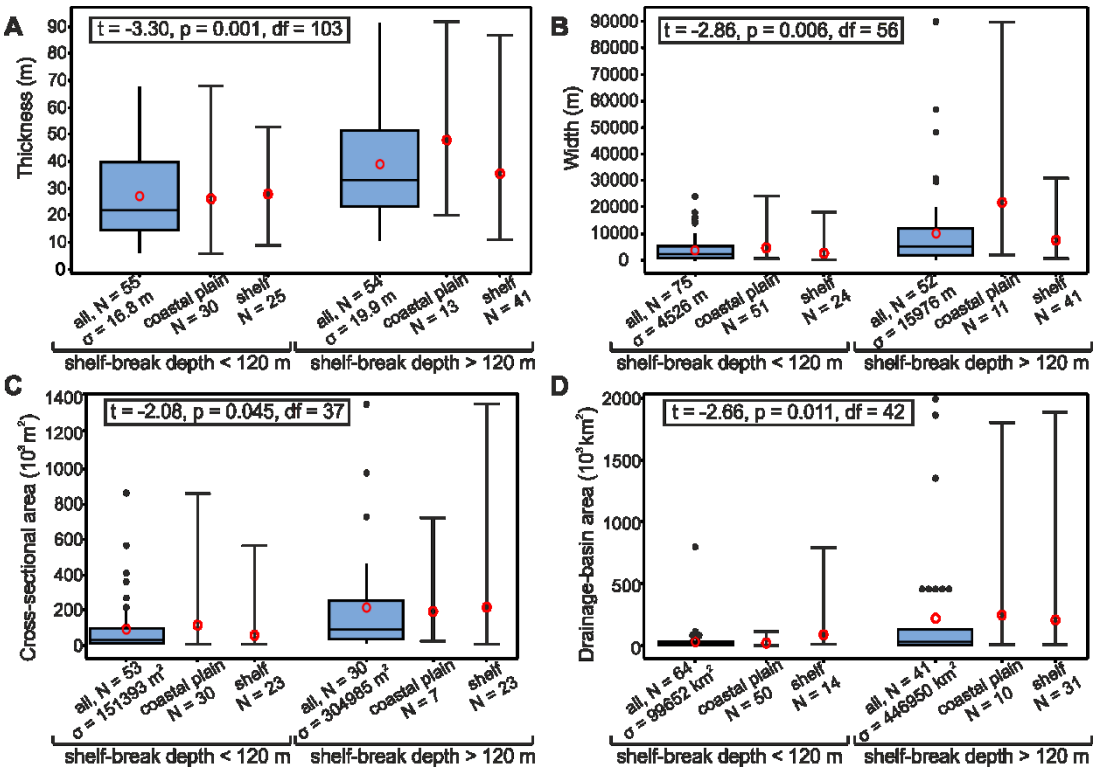

Fig. 3.6. *Box plots and mean/range plots of: (A) LGC incised-valley-fill thickness; (B) width; (C) cross-sectional area; and (D) drainage-basin area distributions for different shelf-break depths, divided by 120 m, which is the magnitude of the fall in eustatic sea-level associated with LGM. Mean and range plots are illustrated near each boxplot for examples hosted on the shelf and coastal plains, respectively. For each boxplot, boxes represent interquartile ranges, red open circles represent mean values, horizontal bars within the boxes represent median values, and black dots represent outliers (values that are more than 1.5 times the interquartile range). For each mean and range plot, red open circles represent mean values and horizontal bars represent the minimum or maximum of all the data. 'N' denotes the number of readings. 'σ' denotes the standard deviation. The results of 2-sample t-test (t-value, p-value and df) are reported in respective boxes. 'df' denotes the degrees of freedom.*

3.5.2.2 Shelf width

Observations

Positive correlations are seen between the width and cross-sectional area of cross-shelf incised-valley fills and the width of the shelf (r(W) = 0.528, p-value < 0.001; r(A) = 0.503, p-value = 0.002) (Fig. 3.8B and C). No apparent correlation is seen between valley-fill thickness and shelf width (R = 0.078, p-value= 0.593) (Fig. 3.8A).

Interpretations

Positive relations between the width or cross-sectional area of cross-shelf incised-valley fills versus the width of the shelf (Fig. 3.8) do not indicate a causal link between shelf width and valley dimensions. Large fluvial basins are generally associated with wider shelves through a control on sediment input and shelf progradation (Burgess and Streel, 2008; Blum and Hattier-Womack, 2009; Olariu and Steel, 2009; Helland-Hansen et al., 2012; Blum et al., 2013). The results might indicate that shelf width and incised-valley-fill dimensions co-vary in relation to a common control exerted by the size of drainage areas.

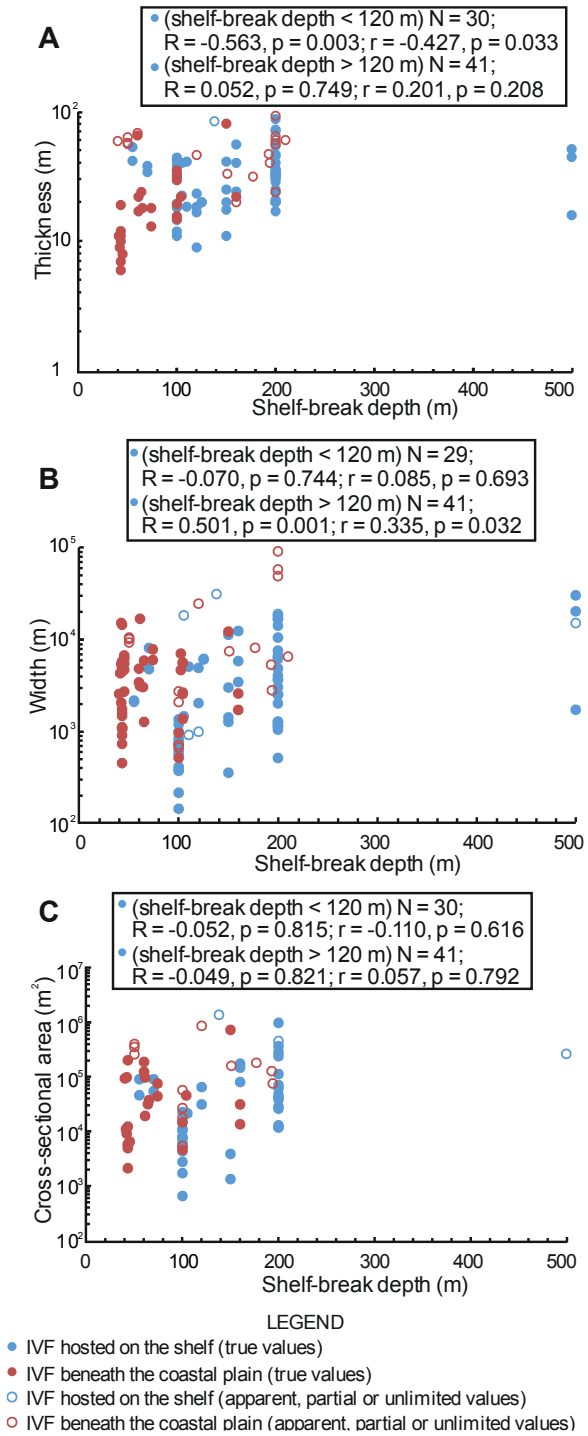

Fig. 3.7. *Plots of: (A) LGC incised-valley-fill thickness; (B) width; and (C) cross-sectional area versus shelf-break depth. For each pair of variables, correlation coefficients and p-values are included in respective boxes for cross-shelf incised-valley fills, and separately reported for shelves with shelf break shallower than 120 m and deeper than 120 m. 'N' denotes the number of readings, 'R' denotes Pearson's R, and 'r' denotes Spearman's rho.*

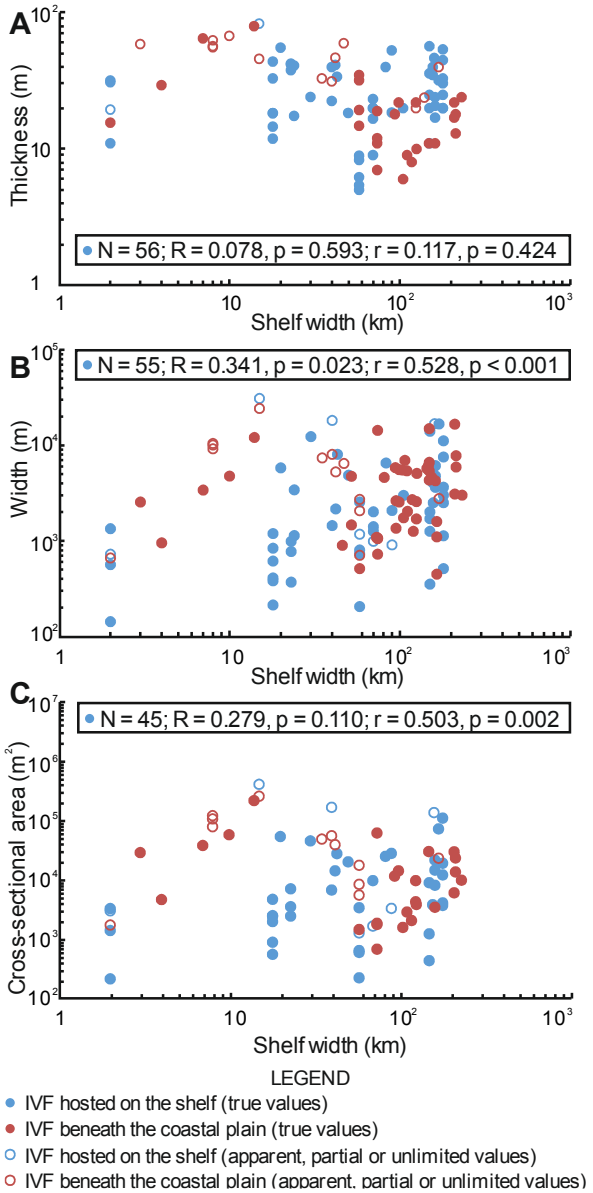

Fig. 3.8. *Plots of: (A) cross-shelf incised-valley-fill thickness; (B) width; and (C) cross-sectional area versus shelf width. For each pair of variables, the correlation coefficients of determination and p-values for cross-shelf valley fills are reported in respective boxes. 'N' denotes the number of readings, 'R' denotes Pearson's R, and 'r' denotes Spearman's rho.*

3.5.2.3 Coastal-plain gradient

Observations

Negative correlations are seen between the width and cross-sectional area of incised-valley fills recognized beneath present-day coastal plains and on the inner shelf versus associated present-day lower coastal-plain gradients (r(W) = -0.452, p-value < 0.001; r(A) = -0.433, p-value < 0.001) (Fig. 3.9B and C). No apparent

correlation is seen between valley-fill thickness and lower coastal-plain gradients (r(T) = -0.198, p-value = 0.064) (Fig. 3.9A). A corresponding negative relationship is seen between drainage-basin area versus coastal-plain gradients (r =-0.388, p-value < 0.001) (Fig. 3.9D).

Interpretations

Negative correlations between the width or cross-sectional area of valley fills versus lower-coastal-plain gradient (Fig. 3.9) are unlikely to indicate a causal link between coastal-plain gradient and valley dimensions. Rather, they likely reflect the fact that smaller basins feeding smaller rivers tend to be associated with higher gradients at the river mouths, and vice versa (Flint, 1974; Blum et al., 2013), as is also evident in Fig. 3.9D.

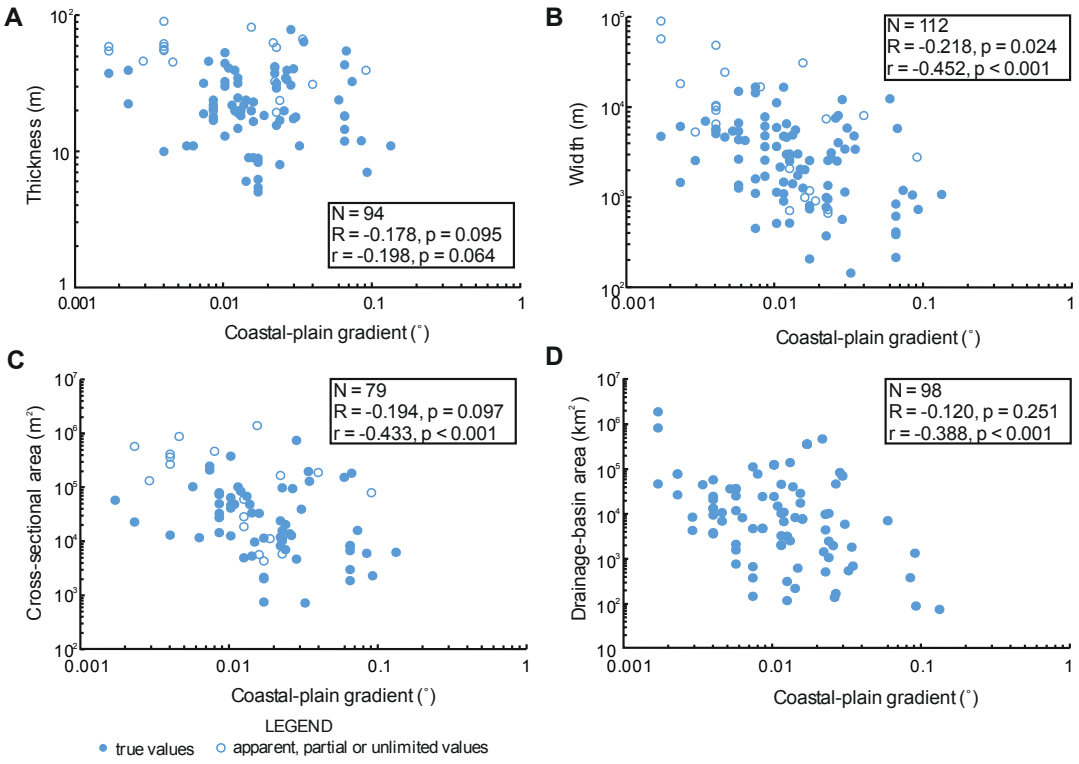

Fig. 3.9. *Plots of: (A) coastal-plain and inner-shelf incised-valley-fill thickness; (B) width; (C) cross-sectional area; and (D) drainage-basin area versus lower coastal-plain gradient. For each pair of variables, the correlation coefficients of determination and p-values are reported in respective boxes. 'N' denotes the number of readings, 'R' denotes Pearson's R, and 'r' denotes Spearman's rho.*

3.5.2.4 Shelf gradient

Observations

For LGC incised-valley fills hosted on the shelf, values of thickness, width and cross-sectional area all tend to decrease with the average shelf gradient ($r(T) = -0.255$, p-value = 0.043; $r(W) = -0.478$, p-value < 0.001; $r(A) = -0.486$, p-value = 0.002) (Fig. 3.10A-C). A corresponding negative relationship is seen between drainage-basin area and shelf-gradient (Fig. 3.10D). For incised-valley fills measured beneath the coastal plains (Fig. 3.10A-D), valley-fill thickness and cross-sectional area are positively correlated with the average shelf gradient ($r(T) = 0.582$, p-value < 0.001; $r(A) = 0.401$, p-value = 0.014); there is very weak or no correlation between valley-fill width or drainage-basin area and the average shelf gradient ($r(W) = -0.004$, p-value = 0.974; $r(DBA) = -0.139$, p-value = 0.289).

Interpretations

These relations may not indicate a causal link between shelf gradient and cross-shelf valley-fill dimensions. Rather, these results might arise because larger fluvial systems associated with larger drainage basins tend to be associated with shelves with lower gradients, as is also indicated in Fig. 3.10D. This might be explained by the fact that the gradient of shelves that occur offshore of river-dominated coasts is in part determined by the profile of the rivers traversing it at lowstand, and larger fluvial systems are associated with lower channel gradients (Wood et al., 1993; Burgess and Streel, 2008; Sømme et al., 2009a, b; Blum and Hattier-Womack, 2009; Olariu and Steel, 2009; Helland-Hansen et al., 2012; Blum et al., 2013).

Positive correlations between coastal-plain valley-fill thickness and shelf gradient (Fig. 3.10A and C) might be attributed to variations in the difference between the gradient of the shelf and the river equilibrium profile (Schumm and Brakenridge, 1987; Leckie, 1994; Posamentier and Allen, 1999).

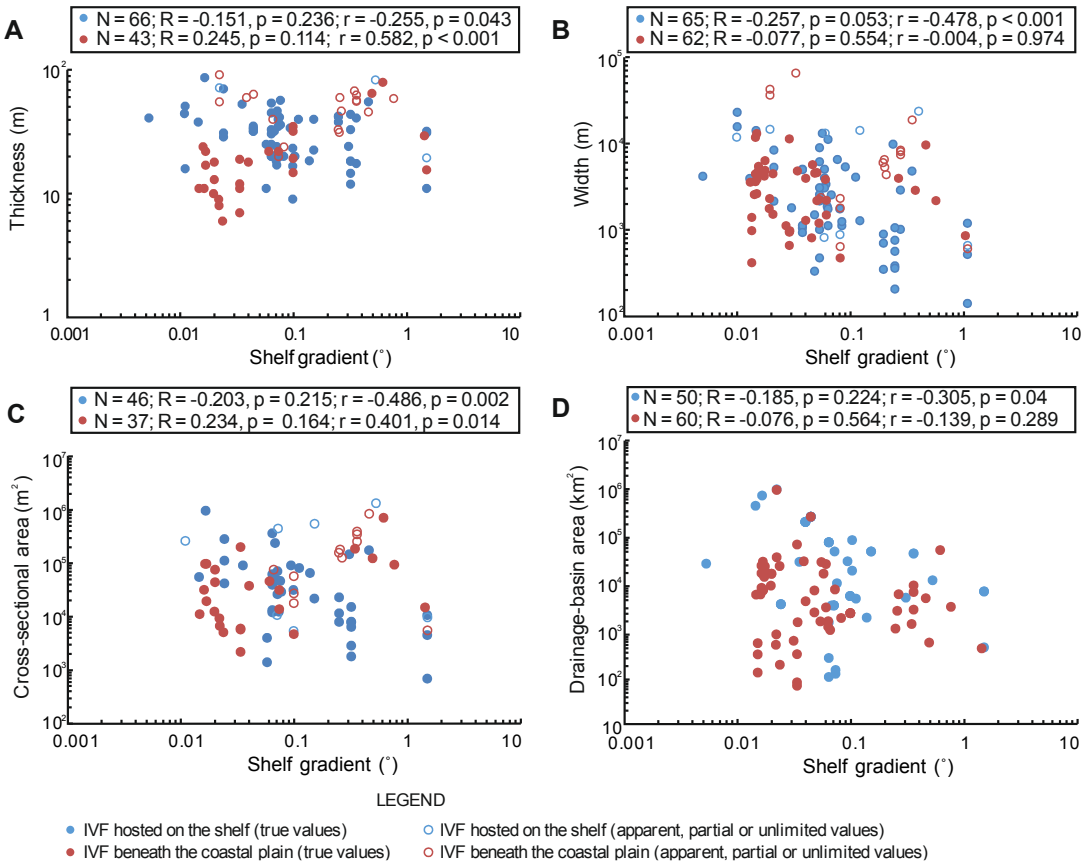

Fig. 3.10. *Plots of: (A) incised-valley-fill thickness; (B) width; (C) cross-sectional area; and (D) drainage-basin area versus shelf gradient. For each pair of variables, the correlation coefficients of determination and p-values for cross-shelf incised-valley fills and valley fills developed beneath the coastal plain are reported in respective boxes. 'N' denotes the number of readings, 'R' denotes Pearson's R, and 'r' denotes Spearman's rho.*

3.5.2.5 Coastal-prism convexity

Observations

In this work, the difference in gradient between present-day lower coastal plains and inner shelves is used as a measure of the convexity of the coastal prism. In order to analyse the relations between coastal-prism convexity and valley-fill dimensions, examples associated with inner shelves that are gentler than the associated lower coastal plains were excluded in this analysis. Fig. 3.11A-C illustrate that for inner shelves that are steeper than the associated lower coastal plains (127 of 135 valley fills; 94%), moderate negative correlations are seen between incised-valley-fill width and cross-sectional area versus the difference in gradient between present-day inner shelf and coastal plain (r(W) = -0.413, p-value

< 0.001; r(A) = -0.255, p-value = 0.034); no correlation is observed between valley-fill thickness and the same gradient difference (r(T) = 0.081, p-value = 0.463).

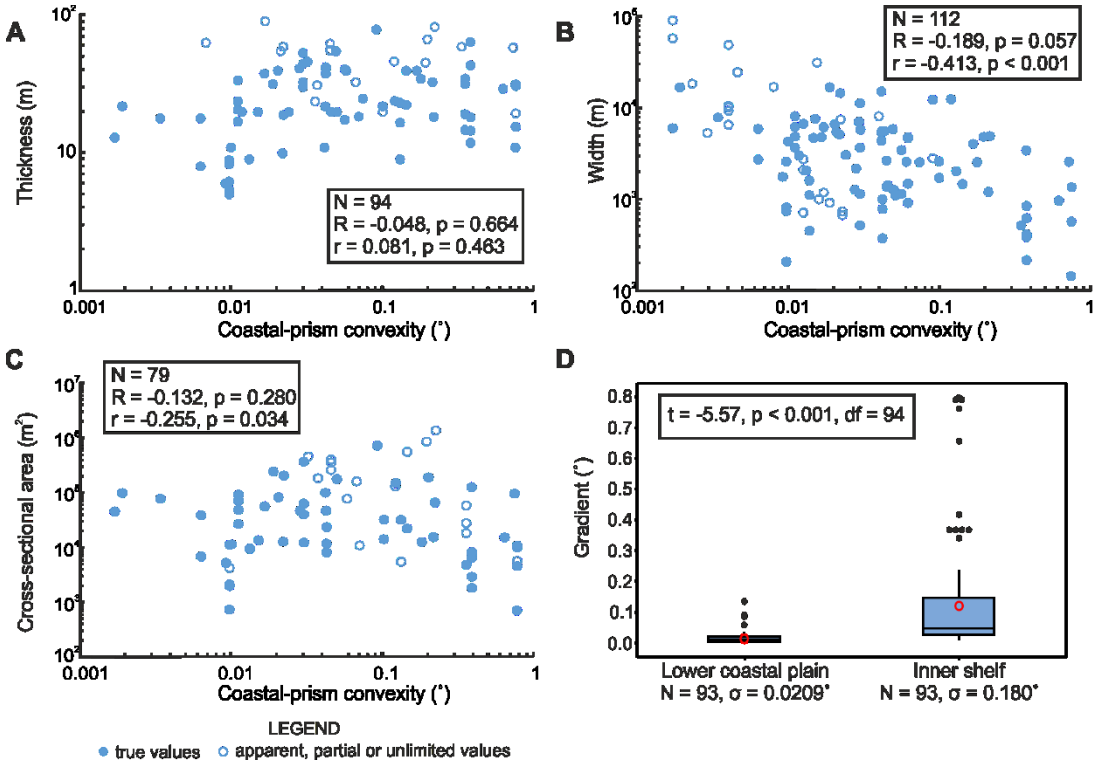

Fig. 3.11. *Plots of: (A) coastal-plain and inner-shelf incised-valley-fill thickness; (B) width and (C) cross-sectional area versus coastal-prism convexity. For each pair of variables, the correlation coefficients of determination and p-values are reported in respective boxes. 'N' denotes the number of readings, 'R' denotes Pearson's R, and 'r' denotes Spearman's rho. (D) Box plots of gradient distributions for lower coastal plains and inner shelves. For each boxplot, boxes represent interquartile ranges, red open circles represent mean values, horizontal bars within the boxes represent median values, and black dots represent outliers (values that are more than 1.5 times the interquartile range). 'N' denotes the number of readings and 'σ' denotes the standard deviation. The results of 2-sample t-test (t-value, p-value and df) are reported in respective boxes. 'df' denotes the degrees of freedom.*

Interpretations

The correlations between the difference in gradients and both valley-fill width and cross-sectional area may not indicate a causal link. Inner-shelf gradients vary from 0.0117° to 0.7957° (mean ISG25 = 0.121°, StDev = 0.180°), which is nearly an order of magnitude larger than the typical gradient of coastal plains (range 0.0017° to 0.0934°, mean CPG10 = 0.0169°, StDev = 0.0209°) (Fig. 3.11D); the difference

in these two gradients might therefore approximate the inner-shelf gradient, and any correlations with the estimated coastal-prism convexity might then merely reflect correlations between shelf gradient and valley-fill width or cross-sectional area (see above).

Some conceptual models (Talling, 1998; Posamentier and Allen, 1999; Posamentier, 2001; Törnqvist et al., 2006) envisage that if the sea level does not fall beyond the shelf break, fully exposing the shelf, magnitude and location of valley incision should primarily be determined by the coastal-prism convexity. However, observations summarised in Fig. 3.11A contradict this hypothesis. This discrepancy might be due to the influence of overriding factors, or to the fact that the estimates of convexity for present-day costal prisms do not approximate the convexity of the coastal prisms established during the last interglacial.

3.5.3 Drainage-basin characteristics

3.5.3.1 Drainage-basin size

Observations

Incised-valley-fill thickness, width and cross-sectional area all correlate directly with drainage-basin size ($r(T) = 0.348$, p-value = 0.001; $r(W) = 0.402$, p-value < 0.001; $r(A) = 0.429$, p-value < 0.001) (Fig. 3.12A-C). For valley fills along passive margins, correlation between valley-fill cross-sectional area and drainage-basin size is stronger ($r = 0.706$, p-value < 0.001) (Fig. 3.12C).

Interpretations

Based on statistical analysis of incised valleys from the northern Gulf of Mexico and the mid-Atlantic US margin, Mattheus et al. (2007), Mattheus and Rodriguez (2011) and Phillips (2011) have demonstrated that valley dimensions at comparable locations along valley axis (at the MIS5e shoreline or near the head of the present-day deltaic plain) are strongly correlated to the drainage-basin area, and that for passive continental margins, where the gradient of coastal plains and shelves does not vary significantly, upstream controls such as discharge should play a primary role in determining valley-fill shape and size. Our observations (Fig. 3.12) support the role of drainage-basin area as important control on incised-valley-fill dimensions, especially for valley fills developed along passive margins. Previous studies (Schumm et al., 1984; Van Heijst and Postma, 2001; Loget and Van Den Driessche, 2009) showed that rates of propagation of retreating knickpoints depend on water discharge and substrate lithology. Paola et al. (1992) demonstrate that the equilibrium time (T_{eq}) for fluvial systems to attain their graded profiles is influenced

by the basin length (L) and the sediment-transport coefficient (v), which is determined by discharge, substrate lithology and relief, as expressed by the equation $Teq = L^2/v$. This suggests that higher water discharge should result in shorter equilibrium time (cf. Thorne, 1994), so that the recorded fluvial incision associated with high water discharge would be closer to the equilibrium profile. Blum et al. (2013) argue that for most fluvial systems Teq is within Milankovitch time scales, and that most rivers are not usually in equilibrium within their backwater lengths (Muto and Swenson, 2005). This view thus implies that for most of the late-Quaternary valley fills studied here, which formed in response to high-frequency sea-level change (Miller et al., 2005; Blum and Hattier-Womack, 2009; Blum et al., 2013), the equilibrium profile was not reached at lowstand (Strong and Paola, 2008). Under this assumption, the amount of valley incision recorded as valley-fill thickness must have been influenced by water discharge to varying degrees. Furthermore, water discharge and drainage-basin area correlate to maximum bankfull depths, which partly account for the depth of incision (Fielding and Crane, 1987; Bridge and Mackey, 1993; Shanley, 2004; Gibling, 2006; Fielding et al., 2006; Syvitski and Milliman, 2007; Blum et al., 2013). Additionally, river lateral migration rates are strongly dependent on water discharge and sediment yield (Hooke, 1979, 1980; Nanson and Hickin, 1983; Lawler et al., 1999; Richard et al., 2005), implying that drainage-basin area should play a significant role in controlling incised-valley-fill width and cross-sectional area.

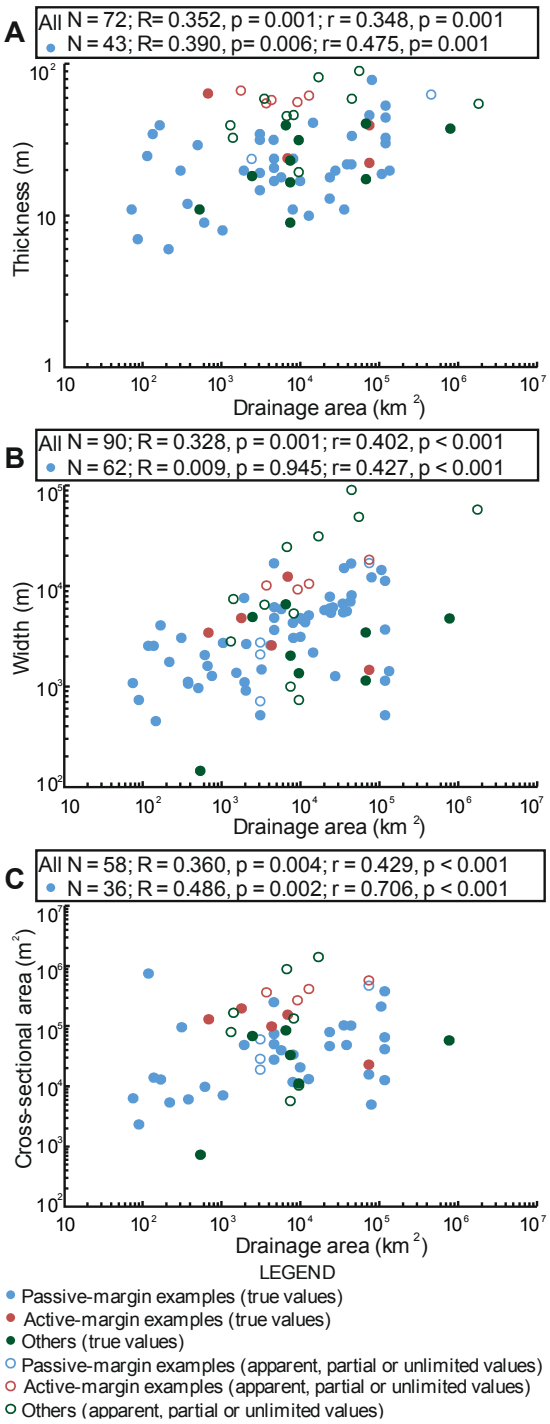

Fig. 3.12. *Plots of: (A) incised-valley-fill thickness; (B) width; and (C) cross-sectional area versus drainage-basin area. For each pair of variables, the correlation coefficients of determination and p-values are reported in respective boxes. 'N' denotes the number of readings, 'R' denotes Pearson's R, and 'r' denotes Spearman's rho.*

3.5.3.2 LGM catchment vegetation

Observations

Valley fills associated with catchments that are inferred to have mainly been covered by forests are, on average, considerably thinner than those with catchments covered by deserts or grasslands/woodlands (mean T = 23.74 m, 35.05 m, 34.15 m; one-way ANOVA: $F(2, 127) = 3.59$, p-value = 0.03) (Fig. 3.13A); mean valley-fill width and cross-sectional area do not vary significantly over these three catchment vegetation types (one-way ANOVA: $F(2, 147) = 3.86$, p-value =0.134 for W; $F(2, 93) = 0.25$, p-value = 0.779 for A) (Fig. 3.13B and C). The thickness of valley fills with catchments covered mainly by tropical/subtropical vegetation types is on average significantly smaller than that with catchments covered by temperate or polar/subpolar vegetation (one-way ANOVA: $F(2, 127) = 4.09$, p-value = 0.019, mean value = 24.33 m, 34.38 m, 36.13 m) (Fig. 3.13D). The means for valley-fill width and cross-sectional area are in agreement with this relationship (one-way ANOVA: $F(2, 147) = 7.39$, p-value =0.001 for W; $F(2, 93) = 3.93$, p-value = 0.023 for A) (Fig. 3.13E and F).

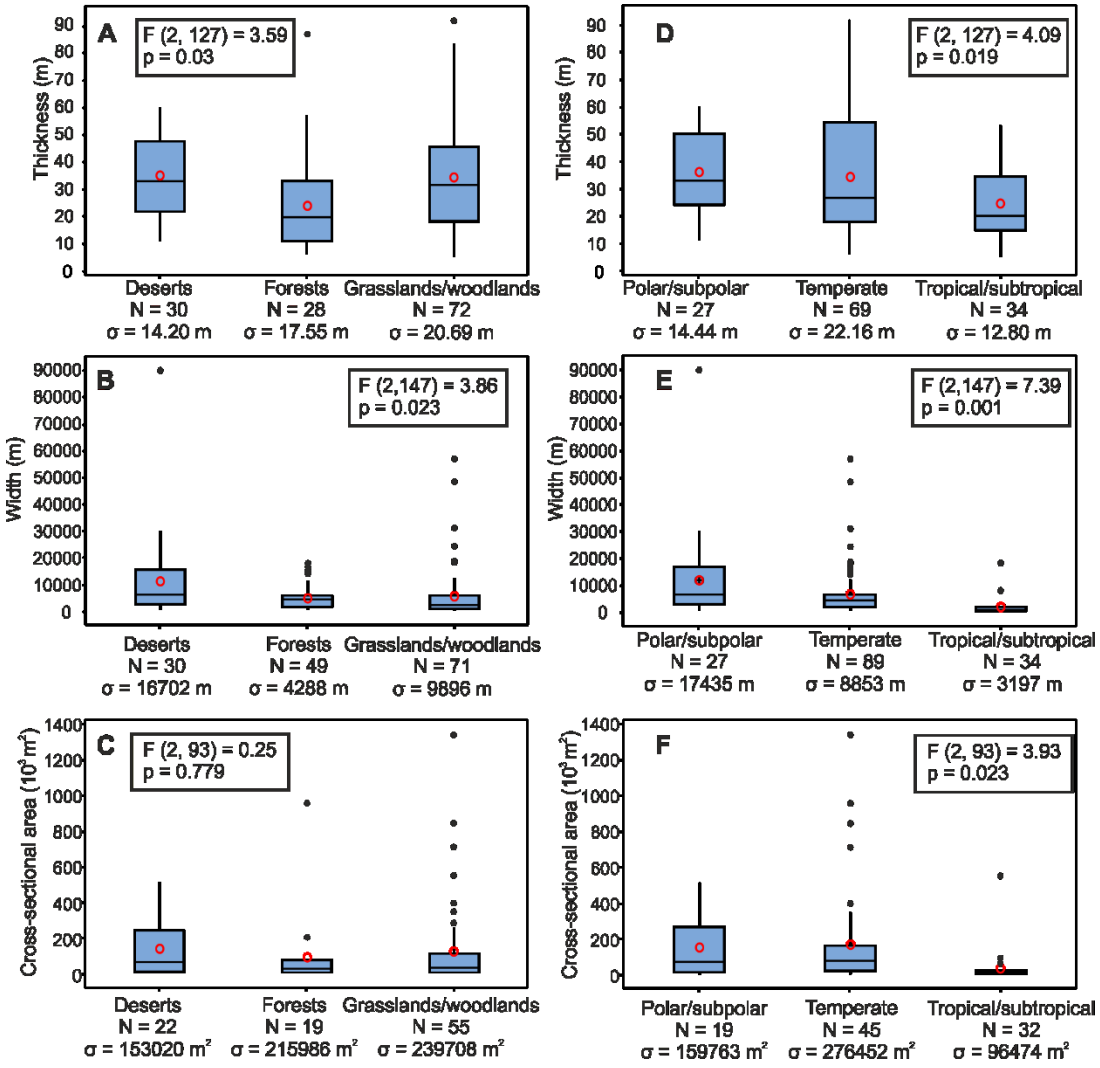

Fig. 3.13. *Box plots of: (A) incised-valley-fill thickness; (B) width and (C) cross-sectional area distributions for different LGM catchment vegetation types ('forest', 'grassland or woodland', 'desert').Box plots of: (D) incised-valley-fill thickness; (E) width and (F) cross-sectional area distributions for different LGM catchment vegetation types ('tropical or subtropical', 'temperate', 'polar or subpolar'). For each boxplot, boxes represent interquartile ranges, red open circles represent mean values, horizontal bars within the boxes represent median values, and black dots represent outliers (values that are more than 1.5 times the interquartile range). 'N' denotes the number of readings. 'σ' denotes the standard deviation. The results of one-way ANOVA (F-value, p-value) are reported in respective boxes. The content bracketed in F-value are degrees of freedom between and within groups respectively.*

Interpretations

Empirical analyses of modern river systems together with computer simulations (e.g., Vandenberghe, 2003; Latrubesse et al., 2011; Wohl et al., 2012) show that vegetation cover can influence the discharge of sediments and water by modulating evapotranspiration and runoff characteristics on the land surface, which in turn determine the degree and rates of fluvial incision and river migration (Hickin and Nanson, 1975, 1984; Blum and Törnqvist, 2000; Cecil et al., 2003; Blum et al., 2013). Drainage basins dominantly covered by tropical or subtropical vegetation types tend to have much more well-developed deep rooting systems and higher density of vegetation cover compared with their counterparts covered by other vegetation patterns; this typically causes stronger evapotranspiration and/or rainfall interception, resulting in stronger buffering of the surface runoff in the catchments and leading to decreased water discharge and decreased sediment supply to fluvial systems (Millar, 2000; Huisink, 2000; Huisink et al., 2002; Vandenberghe, 2003; Blum and Törnqvist, 2000; Blum et al., 2013), which in turn attenuates rates of fluvial incision and lateral migration. Our observations (Fig. 3.13D-F) might reflect these factors, and reveal that the inferred dominant vegetation type in the catchments of incised-valley fills during the LGM could have exerted a control on valley-fill thickness, width and cross-sectional area. However, these results only offer partial insight into the role of vegetation as a control on the geometry of incised-valley fills, given that the type and density of vegetation cover changed over the period of incised-valley formation and infill, especially at the apex of the coastal prism where the valleys experienced the longest sculpting by fluvial and marine processes (Mattheus and Rodriguez, 2011).

3.5.4 Latitude

Observations

Based on the global isotherms derived from atmospheric general circulation model reconstructions (Crowley and North 1991; Broecker 1995), inferred vegetation types (Adams and Faure, 1997; Ray and Adams, 2011), and other palaeotemperature estimates derived from sedimentological and zoological data (Adams and Faure, 1997; Ray and Adams, 2011), for the LGM, tropical zones are constrained to have been positioned between the Equator and 22° latitude, temperate zones to have lied between 22° to 50° latitude, and polar zones largely covered by ice sheets or polar and alpine deserts to have occurred above 50° latitude in both the northern and southern hemispheres. Based on the location where the incised-valley fills were measured, the LGC examples were classified in terms of these latitudinal

belts. No significant difference is identified for means in valley-fill thickness and cross-sectional area across these latitudinal belts (one-way ANOVA: F(2, 111) = 0.15, p-value=0.862 for T; F(2, 85) = 0.29, p-value= 0.747 for A) (Fig. 3.14A and C). Incised-valley fills developed in the 22° to 50° latitudinal belt tend to be wider on average than those at lower latitudes (one-way ANOVA: F(2, 129) = 3.39, p-value=0.037, mean = 6496.3 versus 4314.6 m) (Fig. 3.14B), even though incised valleys developed at latitudes from 0° to 22° are associated with drainage basins that are on average larger than their counterparts in the 22° to 50° range (2-sample t-test: t-value = 3.84, p-value = 0.001, df = 25) (Fig. 3.14D). For valley-fills developed between 0° and 22° latitude, valley-fill thickness tend to increase with latitude (r = 0.421, p-value = 0.040); no correlation is seen instead between valley-fill width or cross-sectional area and latitude (r(W) = 0.107, p-value = 0.626; r(A) = 0.252, p-value = 0.406) (Fig. 3.14E-G). The correlation between drainage-basin area and latitude is consistent with that for valley-fill thickness (r = 0.617, p-value = 0.004) (Fig. 3.14H). For valley-fills developed between 22° and 50° latitude, valley-fill thickness, width and cross-sectional area show weak or modest positive correlation with latitude (r(T) = 0.204, p-value = 0.058; r(W) = 0.417, p-value < 0.001; r(A) = 0.416, p-value < 0.001) (Fig. 3.14E-G).

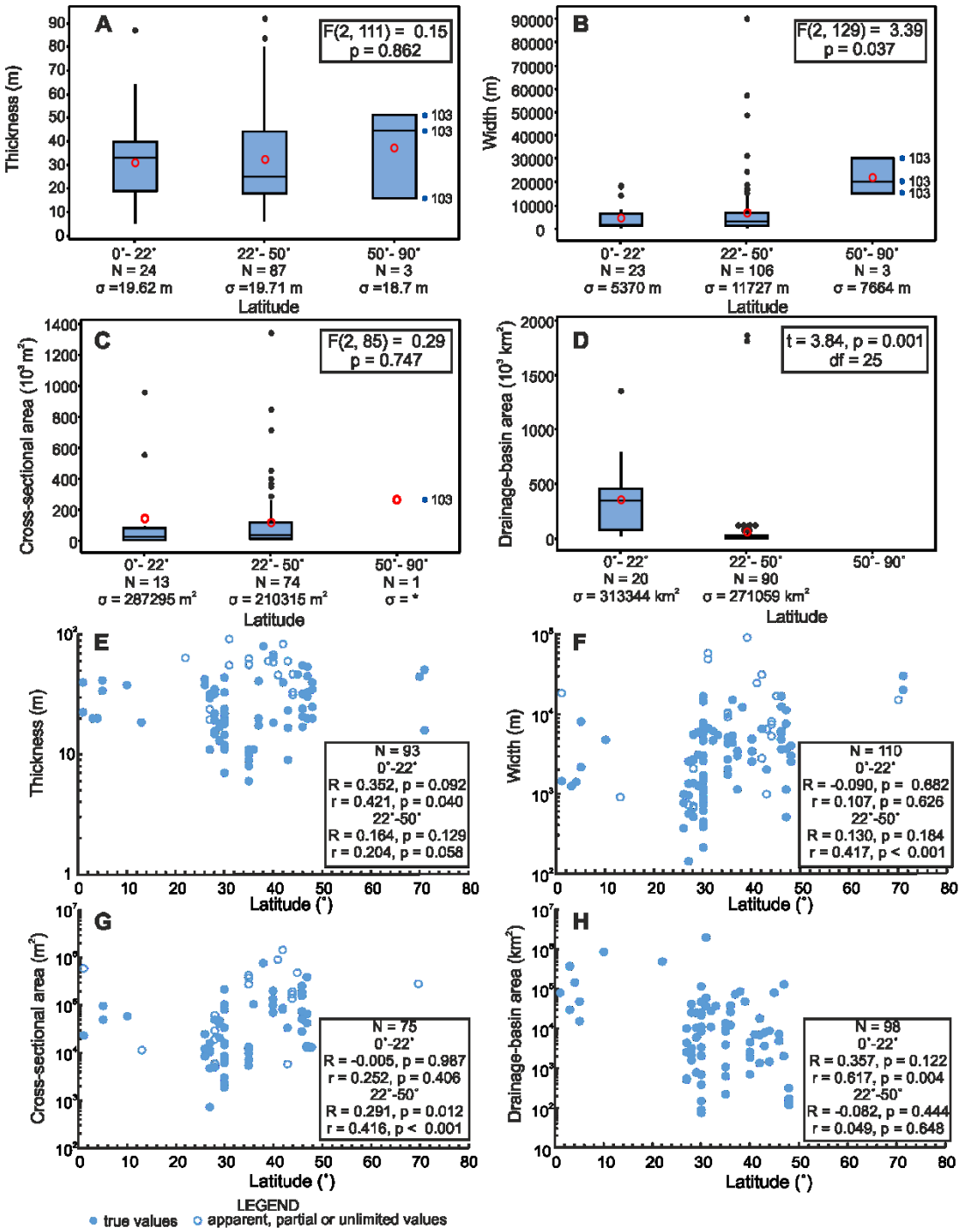
A
F(2, 111) = 0.15
p = 0.862
Thickness (m)
0°- 22°
N = 24
σ =19.62 m
22°- 50°
N = 87
σ =19.71 m
50°- 90°
N = 3
σ =18.7 m
Latitude
B
F(2, 129) = 3.39
p = 0.037
Width (m)
0°- 22°
N = 23
σ = 5370 m
22°- 50°
N = 106
σ = 11727 m
50°- 90°
N = 3
σ = 7664 m
Latitude
C
F(2, 85) = 0.29
p = 0.747
Cross-sectional area (10³ m²)
0°- 22°
N = 13
σ = 287295 m²
22°- 50°
N = 74
σ = 210315 m²
50°- 90°
N = 1
σ = *
Latitude
D
t = 3.84, p = 0.001
df = 25
Drainage-basin area (10³ km²)
0°- 22°
N = 20
σ = 313344 km²
22°- 50°
N = 90
σ = 271059 km²
50°- 90°
Latitude
E
Thickness (m)
N = 93
0°-22°
R = 0.352, p = 0.092
r = 0.421, p = 0.040
22°-50°
R = 0.164, p = 0.129
r = 0.204, p = 0.058
Latitude (°)
F
Width (m)
N = 110
0°-22°
R = -0.090, p = 0.682
r = 0.107, p = 0.626
22°-50°
R = 0.130, p = 0.184
r = 0.417, p < 0.001
Latitude (°)
G
Cross-sectional area (m²)
N = 75
0°-22°
R = -0.005, p = 0.987
r = 0.252, p = 0.406
22°-50°
R = 0.291, p = 0.012
r = 0.416, p < 0.001
Latitude (°)
H
Drainage-basin area (km²)
N = 98
0°-22°
R = 0.357, p = 0.122
r = 0.617, p = 0.004
22°-50°
R = -0.082, p = 0.444
r = 0.049, p = 0.648
Latitude (°)
LEGEND
true values
apparent, partial or unlimited values

Fig. 3.14. *Box plots of: (A) incised-valley-fill thickness; (B) width; (C) cross-sectional area; and (D) drainage-basin size distributions for different latitudinal belts. For each boxplot, boxes represent interquartile ranges, red open circles represent mean values, horizontal bars within the boxes represent median values, and black dots represent outliers (values that are more than 1.5 times the interquartile range). 'N' denotes the number of readings. 'σ' denotes the standard deviation. The results of one-way ANOVA (F-value, p-value) are reported in respective boxes. The content bracketed in F-value are degrees of freedom between and within groups respectively. Plots of: (E) incised-valley-fill thickness; (F) width; (G) cross-sectional area and (H) drainage-basin size versus latitude. For each pair of variables, the correlation coefficients of determination and p-values are reported in respective boxes. 'N' denotes the number of readings, 'R' denotes Pearson's R, and 'r' denotes Spearman's rho.*

Interpretations

Through direct climatic forcing (e.g., temperature and peak precipitation), climate-derived forcing (e.g., presence of permafrost) and partially climate-dependent forcing (e.g., vegetation type), climate acts to influence the behaviour of fluvial systems (Blum and Törnqvist, 2000; Bogaart et al., 2003a, b; Vandenberghe, 2003). Compared with temperate zones, the tropical zones are typically characterized by more intense rainfalls and stronger weathering, which could have resulted in larger rates of delivery of water and sediment, enhancing rates of fluvial incision and river migration (Stallard et al., 1983; Milliman, 1995; Gupta, 2007; Goldsmith et al., 2008; Lloret, et al., 2011; Wohl et al., 2012). However, the distributions of incised-valley-fill dimensions for tropical zones and temperate zones (Fig. 3.14A-C) do not support this assumption. This might be due to the interplay of multiple climate-driven factors such as vegetation and precipitation, which have counteracting effects on water discharge and sediment supply and flux. Polar zones are dominated by ice caps or polar and alpine deserts: here, the size of fluvial catchments is limited as a result, but paraglacial and periglacial processes operate. Three of the studied incised-valley fills are located on the Alaskan Chukchi shelf (case study 103 in Table 3.1; Hill et al., 2007; Hill and Driscoll, 2008; Stockmaster, 2017), which, at the LGM, was a non-glaciated polar desert (Adams and Faure, 1997; Dyke, 2004; Ray and Adams, 2011). The large scale of these valley fills (Fig. 3.14A-C) might be attributed to enhanced fluvial incision and lateral migration (Kasse, 1997; Bogaart et al., 2003c; Vandenberghe, 2003), possibly due to periodic meltwater and sediment discharge from the Cordilleran Ice Sheet (Dyke, 2004) and in periglacial rivers (Woo and Winter, 1993; Vandenberghe, 2003), and to the

occurrence of permafrost through its role in increasing surface runoff by lowering soil permeability (Church, 1983; Woo, 1986; Vandenberghe, 2003). Our observations (Fig.14A-C, E-G) indicate that during the LGM regional variations in incised-valley geometry might have been controlled by climate, in some contexts.

3.5.5 Substratum

Observations

The studied incised-valley fills were classified as either completely hosted in substrates made of unconsolidated sediments ('sedimentary cover'), or in substrates that are partly lithified or that might include basement rocks ('bedrock and sedimentary cover'). Incised-valley fills that are partially hosted in bedrock and sedimentary cover are thicker and wider on average than those hosted in sedimentary cover only (mean thickness = 40.0 m, 30.5 m; mean width = 11,822 m, 4,628 m), with the latter class varying from 15 m to 100 m in thickness and 500 m to 100,000 m in width (Fig. 3.15A-C). Mean valley-fill thickness and width are significantly different between these two populations (2-sample t-test: t-value = 2.24, p-value = 0.030, df = 43 for T and t-value = 2.31, p-value = 0.028, df = 33 for W) (Fig. 3.15B and C).

Interpretations

Substrate types play a significant role on fluvial incision rates (Van Heijst and Postma, 2001; Loget and Van Den Driessche, 2009; Gibling, 2006; Blum et al., 2013) and on the degree to which incision can progress to a graded profile in response to base-level lowering (Paola et al., 1992). Van Heijst and Postma (2001) and Loget and Van Den Driessche (2009) show that knickpoint-migration rates in alluvial settings are significantly larger than those in bedrock settings, corresponding to 1 to 20 m/yr and 0.001 to 0.1 m/yr, respectively. This would imply that valleys that are hosted in sedimentary cover are expected to be deeper than bedrock valley, any time before equilibrium is reached. In addition, the decreased erodibility of bedrock valley walls should result in narrower valley width. Results (Fig. 3.15) contrast with these expectations: this might be due to the fact that larger fluvial systems are more likely to scour to the depth of lithified strata. In this sense, results would still not suggest that substrate lithology is a dominant control on valley-fill dimensions.

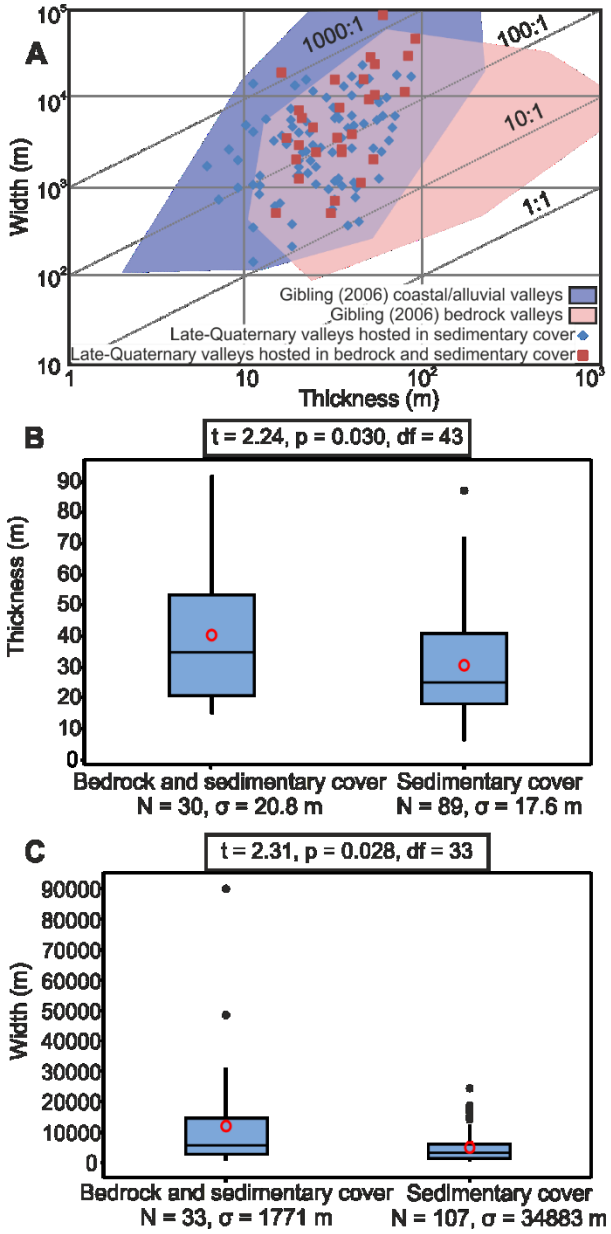

Fig. 3.15. *(A) Scales of late-Quaternary valley fills hosted in bedrock and sedimentary cover and valley fills hosted in sedimentary cover versus incised-valley fills interpreted from ancient successions in the published literature. Ancient valley fills are adapted from Gibling (2006). Box plots of: (B) late-Quaternary incised-valley-fill thickness; and (C) width distributions for different substrate types. For each boxplot, boxes represent interquartile ranges, red open circles represent mean values, horizontal bars within the boxes represent median values, and black dots represent outliers (values that are more than 1.5 times the interquartile range). 'N' denotes the number of readings. 'σ' denotes the standard deviation. The results of 2-sample t-test (t-value, p-value and df) are reported in respective boxes. 'df' denotes the degrees of freedom between groups.*

3.6 Discussion

3.6.1 Controls on the dimensions of incised-valley systems and implications for sequence stratigraphic models

Previous workers have argued that the dimensions of near-shore incised valley systems are primarily a function of the magnitude and rate of relative base-level fall, basin physiography (gradients and convexity along the depositional profile and shelf-break depth), contributing drainage-basin size, climate, substrate characteristics and tectonics (Schumm, 1993; Talling, 1998; Posamentier and Allen, 1999; Blum and Törnqvist, 2000; Posamentier, 2001; Van Heijst and Postma, 2001; Gibling 2006; Strong and Paola, 2006, 2008; Loget and Van Den Driessche, 2009; Martin et al., 2011; Blum et al., 2013). Process-based studies argue that along continental margins, for a given relative sea-level fall, the physiography of the basin determines the largest vertical adjustment of a river system through valley incision (Talling, 1998; Posamentier and Allen, 1999; Posamentier, 2001; Törnqvist et al., 2006), whereas water discharge and substrate characteristics dominantly influence the degree to which, and rate at which, fluvial systems approach their equilibrium profile (Schumm et al., 1984; Paola et al., 1992; Van Heijst and Postma, 2001; Loget and Van Den Driessche, 2009; Loget and Van Den Driessche, 2009).

Our results (Fig. 3.5A-C) indicate that incised-valley systems and their fills developed along active continental margins are thicker and wider, on average, than those along passive continental margins, suggesting that the tectonic context of a continental margin plays a key role – at least indirectly – in determining the geometry of near-shore incised-valley systems. Through its effects on relative sea-level change, distinct characteristics of basin physiography, climate, water discharge and sediment delivery rates, the tectonic setting appears to control the magnitude of valley incision and widening (Posamentier and Allen, 1999; Jain and Tandon, 2003; Ishihara et al., 2011, 2012; Wohl et al., 2012; Tropeano et al., 2013; Vandenberghe, 2003; Ishihara and Sugai, 2017).

Mattheus et al. (2007), Mattheus and Rodriguez (2011) and Phillips (2011) claimed that valley-fill dimensions are primarily controlled by factors that act upstream, in particular by drainage-basin area, which serves as a proxy for water discharge and sediment yield. These authors report that valley-fill dimensions are less influenced by factors such as shelf-break depth, or coastal-plain and shelf gradients. Climate is also known to exert an important control on valley-fill dimensions, especially through modulation of temperature, peak precipitation, vegetation and permafrost in drainage-basin areas, which in turn dictates water discharge, rates of sediment supply and bank stability (Blum et al., 1994; Blum and Törnqvist, 2000;

Vandenberghe, 2003; Bogaart et al., 2003a, b; Blum et al., 2013). The results (Fig. 3.12 and Fig. 3.13D-F) support the dominant role of drainage-basin characteristics in dictating incised-valley-fill dimensions, especially for passive continental margins, and highlight likely controls by the size and dominant vegetation type of catchment areas.

The physiography of the depositional profile over which incised valleys develop also plays a role in valley incision and widening (Summerfield, 1985; Talling, 1998; Posamentier and Allen, 1999; Posamentier, 2001; Blum and Törnqvist, 2000; Törnqvist et al., 2006; Blum et al., 2013). Along continental margins, valley incision tends to begin forming where a convex-up topography is exposed during relative sea-level fall (Summerfield, 1985; Talling, 1998; Blum and Törnqvist, 2000; Blum et al., 2013), which most commonly occurs at either the highstand coastline or at the shelf-slope break. Conceptual models (Talling, 1998; Posamentier and Allen, 1999; Posamentier, 2001; Törnqvist et al., 2006) highlight that when a sea-level fall causes exposure of the entire shelf, incised valleys will form across the whole shelf; on the contrary, when the shelf is only partially exposed by sea-level fall, incised valleys will only be limited to the region of the coastal prism. Additionally, it is embedded in sequence-stratigraphic thinking (Posamentier and Allen, 1999) that the magnitude of incision associated with sequence boundaries is linked to the degree of exposure of the continental shelf. Contrary to this notion, it is observed that valley-fill dimensions for systems with shelf breaks that are shallower than 120 m tend to be smaller, on average, than systems on shelves that are deeper than 120 m (Fig. 3.6A-C). Nonetheless, the negative correlation between valley-fill thickness and shelf-break depth for cross-shelf valley fills hosted on shelves with shelf break shallower than 120 m (Fig. 3.7A) might indicate the expected causal link between magnitude of exposure, incision, and resulting valley-fill thickness, implying that the shelf-break depth plays a role in controlling valley-fill dimensions. Study on the relationships between shelf width, shelf gradient and cross-shelf valley dimensions (Fig. 3.8 and 3.10) might not indicate a causal link between these factors and cross-shelf valley dimensions. Rather, this might indicate shelf width, shelf gradient and cross-shelf valley dimensions co-vary in relation to a common control exerted by the size of drainage areas. The positive correlations between coastal-plain valley dimensions and shelf gradient (Fig. 3.10A and C) might be attributed to the fact that coastal-plain valley fills with steeper shelf gradient have a larger difference between shelf gradient and the original river equilibrium profile, which could lead to deeper fluvial incision for a given relative sea-level fall (Schumm and Brakenridge, 1987; Leckie, 1994; Posamentier and Allen, 1999). In addition, based on observations of present-day gradient profiles along passive margins and margins associated with foreland basins, Talling (1998) highlights that

if the sea level remains above the shelf break, valley incision will be governed primarily by the geometry of the coastal prism and valley incision depth will tend to increase with the coastal-prism convexity. Our analysis of relationships between valley-fill dimensions and coastal-prism convexity (Fig. 3.11) challenges this widely held view and this might be due to the influence of overriding factors, or to the fact that the estimates of convexity for present-day costal prisms do not approximate the convexity of the coastal prisms established during the last interglacial.

In summary, the type of continental margin (active versus passive) appears to be a meaningful predictor of the geometry of incised-valley fills, presumably in relation to characteristics of basin physiography, climate, water discharge and sediment delivery (Fig. 3.16). In addition, our findings indicate that upstream controls (drainage-basin area) appear to be potentially more important than the characteristics of the receiving basin (e.g., coastal-prism convexity, shelf-break depth and substrate lithology) in determining rates and amounts of valley incision and widening, especially for passive continental margins.

3.6.2 Implications for source-to-sink studies and applied significance

The major components of source-to-sink systems – continent, shelf, slope and basin floor segments – are considered to be genetically related in analytical approaches that use mass-balance theory (Sømme et al., 2009a). Based on modern and late-Quaternary fluvial systems from different tectonic and climatic settings, recent work on source-to-sink systems (Anderson et al., 2004, 2016; Syvitski and Milliman, 2007; ; Sømme et al., 2009a,b; Blum et al., 2013; Xu et al., 2016; Sweet and Blum, 2016) has demonstrated scaling relationships between the scale of drainage-basin area, water discharge, river-driven sediment flux, channel-belt dimensions, and the corresponding scale of other distal components of sediment-dispersal systems (e.g. submarine canyons and basin-floor fans). Incised-valley systems play a key role in transferring sediments from hinterland regions to deep-marine environments, especially during lowstands (Posamentier and Allen, 1999; Blum and Törnqvist, 2000; Blum et al., 2013). The positive correlation between incised-valley-fill dimensions and contributing drainage-basin area (Fig. 3.12) documented here is important for source-to-sink analysis because it provides a scaling relationship for incised-valley fills. The scale of incised-valley fills could be used to estimate the scales of their contributing drainage-basin areas and palaeodischarge, and also to predict scales of downdip coarse-grained lowstand deltas or basin-floor fans. Moreover, linking the scale of incised-valley fills to characteristics of catchments and shelves allows for the development of semi-

quantitative guidelines that could be used to predict the size, location and timing of accumulation of potential hydrocarbon reservoirs. Incised-valley fills form important hydrocarbon reservoirs, typically characterized by coarser-grained fluvial deposits at their base and finer-grained estuarine and marine deposits at the top (Wright and Marriott, 1993; Shanley and McCabe, 1994; Zaitlin et al., 1994; Blum et al., 2013). However, as noted above, incised-valley-fill dimensions are influenced by a wide variety of geological controls and hence care should be taken for the exploration of incised-valley plays in different tectonic, physiographic and climatic settings. Notably, our results indicate that incised-valley fills along active continental margins can be thicker and wider than their counterparts along passive continental margins, highlighting the potential of the fills of incised valleys along active margins as exploration targets.

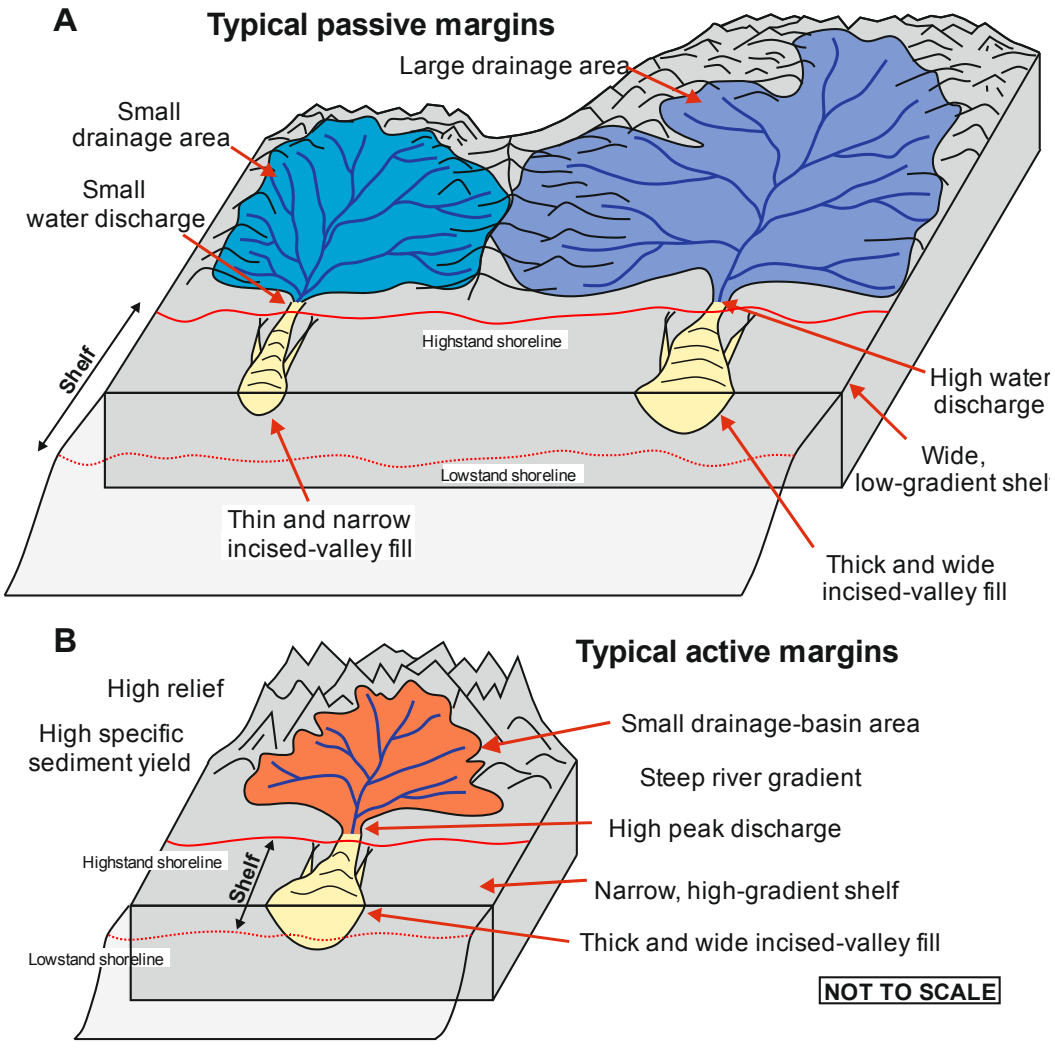

Fig. 3.16. *Schematic diagrams of different incised-valley-fill dimensions corresponding to passive margins (A) and active margins (B). Along passive margins (A), the scale of incised-valley fills associated with large and small drainage-basin area respectively are compared.*

3.7 Conclusions

A database-driven statistical analysis of 151 late-Quaternary incised-valley fills, which is the largest study of this type undertaken so far, has been performed with the aim to investigate controlling factors on the geometry of incised-valley fills.

Results of this analysis have been interpreted on the basis of some assumptions. The thickness of incised-valley fills is thought to be controlled by the degree of shelf or coastal plain incision – itself dictated, at any one location, by the vertical shifts in equilibrium profile driven by changes in base level, water discharge and sediment supply, and by the degree to which that profile is approximated in relation to knickpoint-retreat rates, together with potential truncation by ravinement processes. The width of the valley fills is determined by the rate of lateral migration of channel belts hosted within them, which again scales to water discharge and sediment supply, and by valley-wall erodibility. The main findings can be summarized as follows:

(i) Incised-valley fills developed along active margins are shown to be thicker and wider, on average, than those along passive margins. This indicates that the tectonic setting of continental margins appears to control the geometry of incised-valley fills, likely through its effects on relative sea-level change, and in relation to distinct characteristics of basin physiography, climate, water discharge and modes of sediment delivery.

(ii) Valley-fill geometry is found to be positively correlated with the associated drainage-basin size, confirming the important role of drainage-basin area, a proxy of water discharge, in dictating valley-fill dimensions. This is especially true for incised-valley fills hosted on passive continental margins.

(iii) Climate is also inferred to exert potential controls on valley-fill dimensions, especially through modulation of temperature, peak precipitation, vegetation and permafrost in drainage-basin areas, which in turn dictates water discharge, rates of sediment supply and valley-margin stability.

(iv) Shelves with breaks currently deeper than 120 m contain thicker and wider incised-valley fills, on average, than shelves with breaks shallower than 120 m. This observation is at odds with the view that the magnitude of incision associated with sequence boundaries is linked to the degree of exposure of the continental shelf. This could be explained by the fact that the studied shelves with shelf breaks that are deeper than 120 m are primarily linked to larger drainage-basin areas, compared to those with shallower shelf breaks. Yet, negative correlation between valley-fill thickness and shelf-break depth for cross-shelf valley fills hosted on shelves whose margin is shallower than 120 m might indicate that shallow shelves record a causal link between magnitude of exposure, incision, and resulting valley-fill thickness.

(v) The lack of correlation between valley-fill thickness and present-day coastal-prism convexity challenges the idea that, especially if the sea level does not fall beyond the shelf break, the magnitude and location of valley incision should primarily be determined by the coastal-prism convexity. This discrepancy might alternatively be due to the influence of overriding factors (e.g., the size of drainage areas), or to the fact that present-day costal prisms do not approximate the form of coastal prisms established during the LI.

To some degree, these results challenge paradigms embedded in sequence stratigraphic thinking, and have significant implications for analysis and improved understanding of source-to-sink sediment route ways and for attempting semi-quantitative predictions of the occurrence and characteristics of hydrocarbon reservoirs. It is only through the analysis of very large composite datasets that describe the attributes of a large number of example systems that insight can be gained to demonstrably show the relative roles of many different controls which interact to determine the geometry of incised valley systems. This study accomplishes this via a novel database-driven approach.

4 Quantitative analysis of the stratigraphic architecture of incised-valley fills: a global comparison of Quaternary systems

4.1 Summary

Facies models of the internal fills of incised valleys developed in shelf and coastal settings during cycles of relative sea-level change are largely conceptual, descriptive and qualitative in form; moreover, they are commonly bespoke to individual examples. Here, a database-driven quantitative statistical analysis of 87 late-Quaternary incised-valley fills (IVFs) has been undertaken to assess the general validity and predictive value of classical facies models for IVFs, and to investigate the relative importance of possible controls on their stratigraphic organization. Based on datasets from the published literature stored in a sedimentological database, the geometry and proportion of systems tracts, and of architectural elements of different hierarchies within IVFs are quantified. These variables were analysed to assess how they vary in relation to parameters that represent potential controlling factors: relative sea-level stage, continental-margin type, drainage-basin area, valley geometry, basin physiography and shoreline hydrodynamics.

The stratigraphic organization of the studied coastal-plain IVFs is generally consistent with that represented in facies models, the primary control being the rate and magnitude of relative sea-level change. However, results from this study demonstrate significant variability in the stratigraphic architectures of IVFs, which is not accounted for by existing models. Variations in the facies architecture of coastal-plain and cross-shelf valley fills can be attributed to controls other than sea level, and expressed in relationships with continental-margin type, basin physiography, catchment area, river-system size and shoreline hydrodynamics. The following primary findings arise from this research. (i) Compared to their counterparts on passive margins, coastal-plain IVFs hosted on active margins contain, on average, a higher proportion of fluvial deposits and a lower proportion of central-basin estuarine deposits; estuarine deposits tend however to be thicker. This suggests a control on IVF stratigraphic architecture exerted by distinct characteristics of the tectonic setting of the host continental margins, notably basin

physiography, rates and mode of sediment supply, and nature of sediment load. (ii) The thickness and proportion of lowstand systems tract are positively correlated with coastal-plain IVF dimensions, likely reflecting the role of drainage-basin area in dictating the scale of the fluvial systems that carved and infilled the valleys. (iii) Positive correlations are observed between the thickness of fluvial deposits, bayhead-delta deposits and central-basin estuarine deposits, versus coastal-plain IVF dimensions and valley catchment area. This suggests a control exerted by the river-system scale on sediment-supply rates and on the accommodation determined by valley size. (iv) Positive correlations between the thickness and proportion of barrier-complex deposits within cross-shelf IVFs versus mean shelf gradient indicate that the geometry of the shelf might control the establishment and preservation of barrier-island environments in incised valleys located on the shelf. (v) Correlations between the width of coastal-plain IVFs and present-day mean tidal range at the shoreline indicate that tidal dynamics may contribute to the widening of the incised valleys. Positive correlation is observed between the proportion of tide-dominated elements in highstand IVF deposits and IVF width, suggesting possible effects of interplays between hydrodynamic conditions and the geometry of incised valleys on their infills.

This study highlights the complexity of the internal fills of incised valleys, which must be considered when attempting the application of facies models of IVFs to rock-record interpretations or as predictive tools in subsurface studies.

4.2 Introduction

Incised valleys are fluvially eroded, elongate palaeotopographic lows developed in shelf and coastal settings during episodes of relative sea-level fall, and subsequently inundated, infilled and reworked by fluvial, coastal and marine processes during sea-level rise (Posamentier and Allen, 1999; Zaitlin et al, 1994; Blum et al., 2013). The fills of incised valleys represent critical stratigraphic archives of environmental change in coastal regions, in response to changes in sea level and climate. They are especially important in this regard as adjacent shelf areas commonly store a less complete sedimentary record because of physical reworking and/or sediment starvation (Boyd et al., 2006; Simms et al., 2010; Mattheus and Rodriguez, 2011). For this reason, the fills of incised valleys have also been the subject of detailed sequence stratigraphic analyses (e.g., Lin et al., 2005; Dalrymple, 2006; Chaumillon et al., 2010). Additionally, valley infills are important hydrocarbon reservoir targets and they also serve as reference for exploration of downdip deep-marine sands (Dalrymple et al. 1994; Shanley and McCabe, 1994;

Zaitlin et al., 1994; Blum et al., 2013). Therefore, predictions of the internal sedimentary architecture of valley infills are desirable in subsurface characterization and hydrocarbon exploration workflows (e.g., Hampson et al., 1999; Stephen and Dalrymple, 2002; Bowen and Weimer, 2003; Salem et al., 2005). Furthermore, in many present-day settings, estuaries and rias that commonly develop at the mouths of incised valleys during sea-level rise, accommodate large and dense human populations and constitute fragile coastal settings of primary economic and ecological importance (Kennish, 1991; Chaumillon et al., 2010; Zhang et al., 2014; Marlianingrum et al., 2019).

Given the scientific, economic and ecological importance of incised-valley fills (IVFs), extensive research has been undertaken to characterise their stratigraphic organization (e.g., Roy, 1984; Dalrymple et al., 1992; Allen and Posamentier, 1993, 1994b; Zaitlin et al., 1994; Boyd et al., 2006; Blum et al., 2013). Widely adopted models of coastal-plain incised-valley development and infill (Dalrymple et al., 1992; Allen and Posamentier, 1994b; Zaitlin et al., 1994) typically envisage three segments: (i) a proximal landward segment mostly occupied by fluvial systems throughout its depositional history; (ii) a medial segment recording a drowned-valley estuarine complex that existed around the time of maximum transgression, overlying a lowstand to transgressive succession of fluvial and estuarine deposits; and (iii) a seaward segment typically comprising basal fluvial deposits overlain by estuarine deposits and capped by fully marine deposits. Considerable prior research has focussed on the analysis of individual case-study examples whereby comparisons are made between the internal fills of individual incised valleys and the general stratigraphic organization of incised-valley fills depicted by the above-mentioned “classical” models. Individual examples have been considered in detail to document and decipher the relative importance of distinct controlling factors responsible for sedimentological complexity, notably sea level, tectonics, sediment supply, antecedent topography and hydrodynamics. As such, the great majority of current models with which to account for the internal fills of incised valleys are either bespoke to individual case-study examples, else are largely conceptual, descriptive and qualitative in form.

In this study, a database-driven approach has been taken, the aim being to quantitatively document and account for the wide variability in facies architecture present across a large number of globally distributed incised-valley fills. This approach seeks to assess the general validity of classical facies models that remain widely employed as predictive tools, and to investigate the relative importance of possible controls on the stratigraphic organization of incised-valley fills quantitatively. This work is based on a synthesis of 87 late-Quaternary incised-

valley fills from the published literature, the majority of which formed during the last glacio-eustatic cycle. The incised-valley fills considered in this work only comprise of valley systems carved in response to relative sea-level falls and infilled by alluvial, transitional (i.e., paralic) and shallow-marine strata in shelf and coastal-plain settings (Van Wagoner et al., 1990; Boyd et al., 2006; Blum et al., 2013); inland alluvial valleys are not considered. The studied examples are representative of different climatic, hydrodynamic and tectonic settings, and are distributed globally. By restricting the scope of investigation to late-Quaternary examples, the principal controlling factors that govern valley-fill characteristics – such as the rate and magnitude of sea-level change, sediment supply, antecedent topography, hydrodynamics and tectonics – can be constrained closely. This is made possible by the widespread availability of large amounts of published data (e.g., shallow seismic, core logs, dating methods) describing the late-Quaternary stratigraphic record.

Specific objectives of this work are as follows: (i) to undertake a comprehensive quantitative analysis of the geometry, spatial relationships, stacking patterns, and lithological heterogeneity of deposits that form the infill of late-Quaternary incised valleys documented in the published literature; (ii) to illustrate the variability in sedimentary architectures seen in the studied incised-valley fills with respect to facies models; (iii) to evaluate the relative roles of possible controls in determining the internal fills of incised valleys; and (iv) to present implications of the results for sequence-stratigraphic models and for subsurface-reservoir prediction and characterization.

4.3 Methods

A database approach based on the synthesis of data from 87 late-Quaternary incised-valley fills is utilized. Data on the sedimentology of these incised-valley fills are included in a relational database, the Shallow-Marine Architecture Knowledge Store (SMAKS; Colombera et al., 2016). SMAKS stores data on the sedimentary architecture and geomorphic organization of shallow-marine and paralic siliciclastic depositional systems; it includes quantitative and qualitative data on geological entities of different types (e.g., facies, architectural elements), and on their associated depositional systems, themselves classified on multiple parameters (e.g., shelf width, delta catchment area) and metadata (e.g., data types, data sources).

Of the 87 late-Quaternary incised-valley fills considered in this study, 85 developed during the last glacial–interglacial cycle (LGC); two are of pre-LGC age. The primary data have been derived from 77 published literature sources. A detailed account of the case studies included in this work, their associated bibliographic references and the types of data used in each is reported in Table 4.1; the location of the studied incised-valley fills is shown in Fig. 4.1. Here, an individual case study refers to either a group of genetically related incised-valley fills (occurring on the same continental shelf or coastal plain) or to a single incised-valley fill. This work does not cover all incised-valley fills documented in the scientific literature. The chosen IVFs were selected based on the availability of data that were suited to the scopes of this study. Importantly, only valley fills that represent single cycles of incision and fill are included in the database; compound valley fills that represent multiple episodes of incisions and fills, associated with different eustatic cycles were excluded (cf. Korus et al., 2008). IVFs from present-day high-latitude regions, which are likely to have recorded periglacial and paraglacial processes, were also not included. Yet, the database was compiled trying to avoid geographical bias and attempting to make the comparative study as global and wide-reaching as possible. For the studied examples, investigations of the internal fills of valleys developed in coastal-plain settings are generally based on several 1D cores and/or 1D well logs. By contrast, studies based on cross-shelf valley fills tend to be based on 2D or 3D high-resolution seismic data, in some cases calibrated by cores.

The relative importance of different controls on the internal fills of incised valleys has been interpreted from (i) comparison of descriptive statistics and associated statistical tests, and (ii) determination of correlation between variables. In this work, the database output comprises the following: (i) estimations of the absolute proportion of systems tracts within incised-valley fills, computed as systems tract-to-valley-fill thickness ratio; (ii) the relative proportion of architectural elements preserved in different systems tracts within valley fills; (iii) the relative proportion of architectural elements within valley fills; and (iv) the geometry of these sedimentary bodies.

Table 4.1. *Case studies on late-Quaternary incised-valley fills stored in the Shallow-Marine Architecture Knowledge Store (SMAKS) database. For each case study, the table reports published literature sources, data types, and the age of formation as being either of last glacial–interglacial cycle (LGC) or pre-LGC. Case-study identification numbers (ID) relate to those coded in the SMAKS database (Colombera et al., 2016) and are referred to in following figures. N = number of incised-valley-fill elements developed for each case study, distinguished as LGC or pre-LGC.*

ID	Case study	Data source	Data types	N	Age
31	Composite database, Gulf of Mexico and Atlantic Ocean, USA	Mattheus et al. (2007); Rodriguez et al. (2008); Mattheus and Rodriguez (2011); Mattheus and Rodriguez (2014)	Airborne images, Shallow seismics, Well cuttings, Cores	3	LGC
38	Pilong Formation, South China Sea, Sunda Shelf	Alqahtani et al. (2015)	Cores, 3D seismics, Shallow seismics	1	LGC
39	Late Quaternary of Manfredonia Gulf, Adriatic Sea	Maselli and Trincardi (2013); Maselli et al. (2014)	Cores, Shallow seismics	1	LGC
48	New Jersey shelf, Atlantic Ocean	Nordfjord et al. (2005); Nordfjord et al. (2006)	Cores, Shallow seismics	2	LGC
49	Hervey Bay, Queensland, Australia	Payenberg et al. (2006)	Shallow seismics, Bathymetric profile	1	LGC
59	Bay of Biscay, France	Weber et al. (2004); Chaumillon and Weber (2006); Chaumillon et al. (2008)	Cores, Shallow seismics	3	LGC
60	Bay of Biscay, France	Chaumillon et al. (2008); Proust et al. (2010)	Cores, Shallow seismics	1	Pre-LGC
61	Bay of Biscay, France	Chaumillon and Weber (2006); Chaumillon et al. (2008)	Cores, Shallow seismics	1	LGC
62	Bay of Biscay, France	Proust et al. (2001); Menier (2004); Menier et al. (2006); Chaumillon et al. (2008); Menier et al. (2010)	Cores, Shallow seismics	3	LGC
67	Pleistocene of Pattani Basin, South China Sea, Gulf of Thailand	Reijenstein et al. (2011)	Well cuttings, 3D seismics, Shallow seismics	2	LGC
69	Pleistocene of southern Java Sea	Posamentier (2001)	Cores, 3D seismics, Shallow seismics	1	LGC
70	Gironde incised valley, France	Allen and Posamentier (1993); Allen and Posamentier (1994a and 1994b); Lericolais et al. (2001); Féniès et al. (2010)	Cores	1	LGC
72	Late	Amorosi et al. (2008); Amorosi et	Cores	3	LGC

	Quaternary of Tuscany, Italy	al. (2013); Rossi et al. (2017)		1	Pre-LGC
73	Ombrone incised valley, Italy	Bellotti et al. (2004); Breda et al. (2016)	Cores	1	LGC
74	Volturno incised valley, Italy	Amorosi et al. (2012)	Cores	1	LGC
75	Biferno incised valleys, Italy	Amorosi et al. (2016)	Cores	1	LGC
76	Tiber Delta, Italy	Milli et al. (2013); Milli et al. (2016)	Cores	1	LGC
77	Metaponto coastal plain, Italy	Cilumbriello et al. (2010); Grippa et al. (2011); Tropeano et al. (2013)	Cores, Shallow seismics	2	LGC
81	KwaZulu-Natal shelf, South Africa	Green (2009); Benallack et al. (2016)	Cores, Shallow seismics	1	LGC
83	East China Sea, China	Zhang and Li (1996); Li and Wang (1998); Li et al. (2002); Wellner and Bartek (2003); Lin et al. (2005); Li et al. (2006); Zhang et al. (2014); Zhang et al. (2017)	Cores	4	LGC
85	Kanto Plain incised valleys, Japan	Ishihara et al. (2012); Tanabe et al. (2015); Ishihara and Sugai (2017)	Cores	3	LGC
92	KwaZulu-Natal shelf, South Africa	Green and Garlick (2011); Green et al. (2013a); Green et al. (2013b)	Shallow seismics	3	LGC
93	Maputo Bay, Mozambique	Green et al. (2015)	Cores, Shallow seismics	3	LGC
125	Pakarae incised valley, New Zealand	Wilson et al. (2007)	Outcrop, Cores	1	LGC
126	Isumi incised valley, Japan	Sakai et al. (2006)	Outcrop, Cores	1	LGC
127	Bay of Biscay, France	Féniès and Lericolais (2005); Chaumillon et al. (2008); Allard et al. (2009); Féniès et al. (2010)	Cores, Shallow seismics	1	LGC
132	Manawatu incised valley, New Zealand	Clement et al. (2017); Clement and Fuller (2018)	Cores, Wireline logs	1	LGC
134	Weiti incised valley, New Zealand	Heap and Nichol (1997)	Cores	1	LGC
135	Burrill Lake incised valley, New South Wales, Australia	Sloss et al. (2006)	Cores, Shallow seismics	2	LGC
136	Lake Illawarra incised valley, New South Wales, Australia	Sloss et al. (2005)	Cores, Shallow seismics	5	LGC
137	Lake Conjola incised valley, New South Wales, Australia	Sloss et al. (2010)	Cores	4	LGC

138	North Carolina coastal-plain incised valleys, North Carolina, USA	Mattheus and Rodriguez (2014)	Cores, Shallow seismics	2	LGC
139	Lavaca incised valley, Texas, USA	Wilkinson and Byrne (1977)	Cores	1	LGC
140	Calcasieu incised valley, Louisiana, USA	Nichol et al. (1996)	Well cuttings, Shallow seismics	1	LGC
141	Late Quaternary of Gulf of Mexico, USA	Greene et al. (2007)	Cores, Shallow seismics	13	LGC
142	Nueces incised valley, Texas, USA	Simms (2005); Simms et al. (2006)	Cores, Shallow seismics	1	LGC
143	Sabine-Neches incised-valley system, USA	Anderson et al. (1991)	Cores, Shallow seismics	1	LGC
144	Trinity-San Jacinto incised-valley system, Texas, USA	Smyth (1991); Rodriguez et al. (2005)	Cores, Shallow seismics	2	LGC
146	Baffin Bay incised valley, Texas, USA	Simms et al. (2010)	Cores, Shallow seismics	2	LGC
147	Kushiro Plain incised valley, Japan	Takashimizu et al. (2016)	Cores	1	LGC
148	Echigo Plain, Japan	Tanabe et al. (2013)	Cores	1	LGC
149	Song Hong delta system, Vietnam	Tanabe et al. (2006)	Cores	1	LGC
158	Song Hong (Red River) incised valley, Gulf of Tonkin, Vietnam	Wetzel et al. (2017)	Cores, Shallow seismics, Bathymetric profile	1	LGC

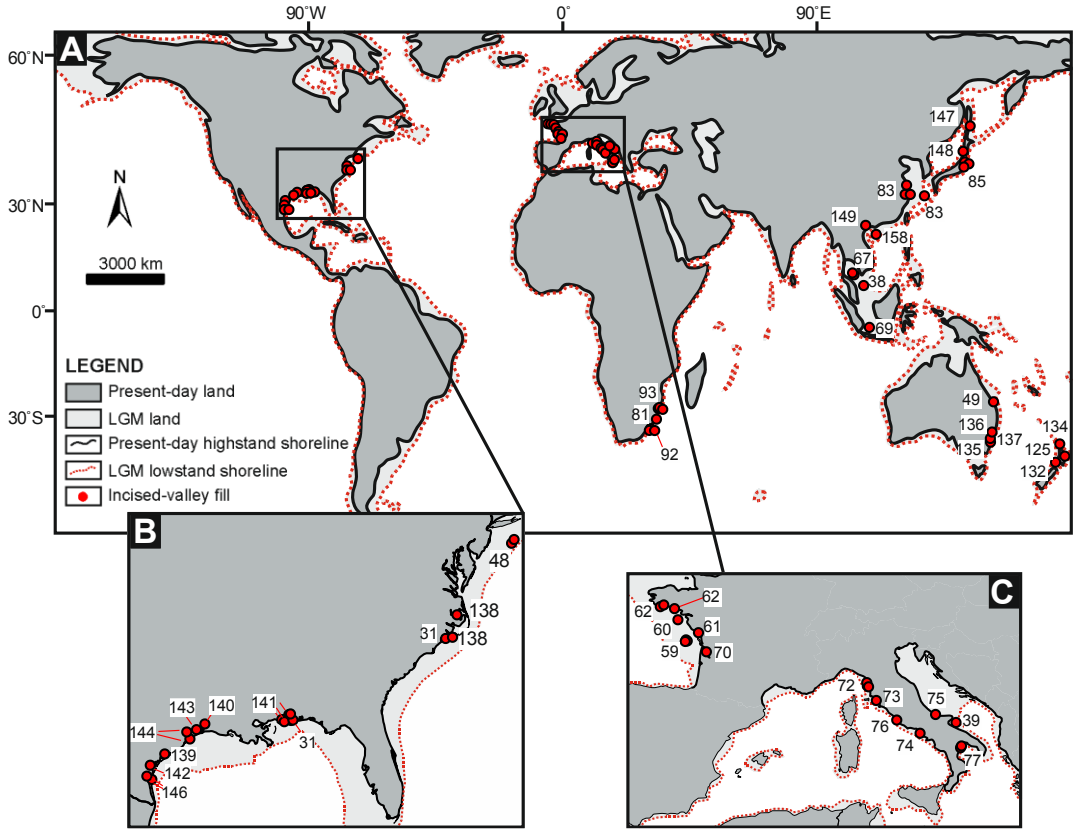

Fig. 4.1. *(A) Geographic location of late-Quaternary incised-valley fills considered in this work, with inset maps for North America (B), and southern Europe (C). The numbers on the map correspond to the IDs in Table 4.1. Base map modified from Ray and Adams (2001).*

4.3.1 Scope of investigation

Large variations in IVF architecture and geometry exist along the dip profile of incised-valley systems (Dalrymple et al., 1992; Zaitlin et al., 1994; Chaumillon et al., 2010; Blum et al., 2013; Strong and Paola, 2008; Martin et al., 2011; Phillips, 2011). Thus, to enable meaningful comparisons, measurements should ideally be made at the same respective location along the valley axis. However, the use of data from the published literature imposes some limitations to our ability to refer observations from different IVFs to a common reference system. In this work, observations are broadly categorized based on the position where the measurements were made, by classifying the studied valley fills depending on whether they now occur beneath present-day coastal plains or on continental shelves (N = 61 and 27, respectively). For incised-valley fills that sit beneath modern coastal plains, the analyses have focussed on relationships between the proportion and geometry of architectural elements that compose them versus continental-margin type, catchment and river-system size, basin physiography and descriptors of present-day hydrodynamics.

For cross-shelf valleys, relationships between shelf gradient versus the proportion and geometry of certain architectural element types are specifically investigated in detail.

In the analysis of properties relating to systems tracts and elements in incised-valley fills, only lowstand (LST), transgressive (TST) and highstand (HST) systems tracts are considered; falling-stage systems tracts (FSST) are discarded for this purpose, even where they are reported as part of the incised-valley fill (N = 3). This was done to conform to sequence stratigraphic models (cf. Helland-Hansen and Martinsen, 1996) that place the sequence boundary at the base of the LST. However, there are several cases where the deposits contained in the infill of the IVFs have not been assigned to systems tract, and it is possible that some of those deposits actually record deposition during falling stage; if these deposits were reported as contained in the IVF, they are considered in this study.

4.3.2 Architectural-element classifications

In the SMAKS database, architectural elements within valley fills are classified in terms of two alternative schemes (Table 4.2). Scheme 1 (Fig. 4.2A) classifies the elements on their interpreted (sub-) environment of deposition. Based on the interpretations given in the original work, architectural elements within valley fills are classified as fluvial deposits, non-bay delta, bayhead delta, estuarine bay/lagoon, barrier complex, tidal sand-bar complex, tidal-flat/-channel deposits, nearshore deposits and open-shelf deposits. The non-bay delta environment is defined as a deltaic system that is not fully contained within the confines of the embayment resulting from valley topography (Fig. 4.2B); only the parts of non-bay delta deposits that infill the incised valleys are considered in the analyses. The barrier complex sub-environment is defined as the preserved product of a dynamic set of barrier-island environments formed by wave and tidal action, such as tidal inlets, washovers, and flood-tidal deltas; this class includes both spits and barriers (Dalrymple et al. 1992; Zaitlin et al. 1994; Masselink and Hughes 2003). In Scheme 2 architectural elements are classified according to the dominant process regime they record, as interpreted in the original source work; in-valley architectural elements are classified as fluvial-, wave- or tide-dominated deposits. In some cases, certain deposits (e.g., worm-tube reef, prograding wedge) cannot be classified according to these schemes. However, the schemes (Table 4.2) encompass the fundamental architectural-element types associated with incised-valley fills and can be applied in parallel. For scopes of analysis and establishment of an audit trail, the classes of deposits and nomenclatures adopted in the primary

data sources are also recorded, though these are not used in the presentation of the results.

Table 4.2. *Schemes adopted for the classification of architectural elements within incised-valley fills.*

Scheme 1	fluvial deposits	Fluvial channel and floodplain deposits.
	non-bay delta	A deltaic system that is not fully contained within the confines of the embayment resulting from valley topography. Its delta top sits at higher elevation than the valley interfluves, which are locally buried by the delta, and it infills some relict valley topography during late TST or HST.
	bayhead delta	Delta at the head of an estuarine bay or lagoon into which a river discharges.
	estuarine bay/lagoon	The transition zone between the riverine and the marine environment, where fresh and salt water mix (cf. Allen, 1991), dominated by clay flocculation. It corresponds to 'central basin' environment of Dalrymple et al. (1992).
	barrier complex	Preserved product of a dynamic set of contiguous environments related to barriers or spits (sandy islands above high tide, parallel to the shore, and separated from the coastal plain by a lagoon or bay), such as tidal inlets, washovers, flood-tidal deltas (Dalrymple et al., 1992; Zaitlin et al., 1994; Masselink and Hughes, 2003).
	tidal sand-bar complex	Preserved product of the evolution of a field of tidal bars (Olariu et al., 2012), which are commonly formed within a tide-dominated estuary (e.g., Dalrymple and Zaitlin, 1994; Fenies and Tastet, 1998; Dalrymple et al., 2003) or on the open shelf (e.g., Houbolt, 1968; Berné et al., 2002).
	tidal flat and tidal channel	Preserved product of deposition in areas of low relief that are alternately exposed and inundated by astronomical tides (cf. Schwartz, 2005), traversed by tidal channels.
	nearshore	Bathymetric tract comprised between mean fairweather wave base and mean high water. It includes ‘shoreface’ and ‘foreshore’ environments of Reading and Collinson (1996).
	open shelf deposits	Bathymetric tract comprised below the mean fairweather wave base, down to the shelf break. It includes 'offshore transition' and 'offshore' environments of Reading and Collinson (1996).
Scheme 2	fluvial	Products of deposition dominated by river currents.
	wave	Products of deposition dominated by wave action.
	tide	Products of deposition dominated by tidal currents.

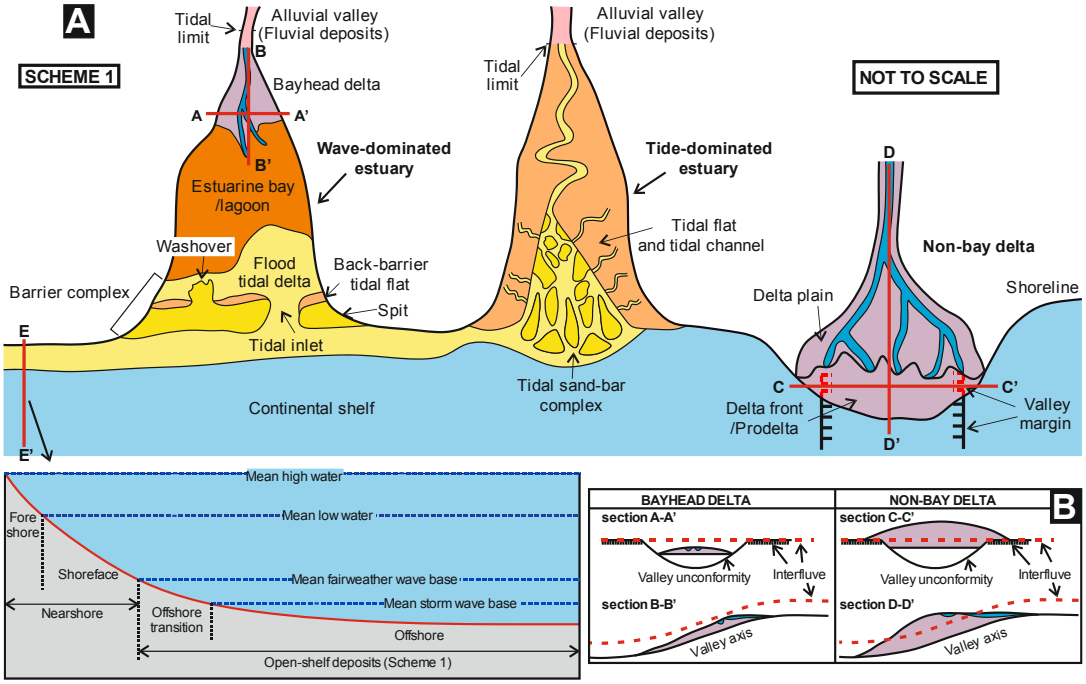

Fig. 4.2. *Definition sketch (A) illustrating the classification of in-valley architectural elements by (sub-)environment of deposition used in this work. Modified from Dalrymple et al. (1992). Inset sketch B depicts idealized sections illustrating the difference between bayhead delta and non-bay delta architectural elements, as defined in this work, and as would be seen along strike and dip orientations. Non-bay deltas are defined as deltaic systems that are not fully contained within the confines of the embayment resulting from valley topography; their delta top sits at higher elevation than the valley interfluves, and they infill some relict valley topography during late TST or HST.*

4.3.3 Architectural-element geometry and proportion

In SMAKS, incised-valley fills are themselves recorded as higher-order architectural elements, which act as parent elements to those that form their infills, i.e., their hierarchal containment is tracked (Colombera et al., 2016). The measurement of their geometry (Fig. 4.3A) follows the approach used by Wang et al. (2019). Incised-valley-fill thickness is defined as the vertical distance between the valley bottom, where deepest, and the top of the valley fill or (for underfilled valleys) the elevation of the interfluves at the valley margins. The term ‘thickness’ is also used to describe the total vertical extent of underfilled valleys because this parameter is always analysed jointly with the thickness of filled valleys. The valley-fill width is defined as the horizontal distance between the valley walls, measured perpendicularly to the valley axis. The valley-fill cross-sectional area is defined as the vertical cross-sectional area subtended by the valley base and either the top of

the valley fill or the elevation of interfluves (for underfilled valleys), measured in an orientation perpendicular to the valley axis. The only geometrical parameter analysed in this study for in-valley architectural elements is the thickness. Where the 3D geometry of a certain element is well-constrained (e.g., in high-resolution seismic data), the largest value of thickness of the element along the valley reach is taken, otherwise the largest value of thickness in the studied sample is recorded. Where it is unknown whether the maximum element thickness is observed (e.g., in a 1D core or well-log sample), the thickness is reported as 'apparent'. Where the base or top of a certain element, or both, are not seen, the thickness is reported as 'partial' or 'unlimited' (*sensu* Geehan and Underwood, 1993; Fig. 4.3B), respectively. In statistical analyses of architectural-element thicknesses, only maximum values are used: apparent, partial and unlimited observations are only used for computing element proportions. However, even for this purpose the use of incomplete thicknesses can introduce error to the estimations, since certain deposits might preferentially occur at lower stratigraphic levels, which are commonly undersampled.

Based on their position, architectural elements that form the incised-valley fills are classified as located beneath present-day coastal plains or on shelves. The relative proportion of architectural elements preserved in different systems tracts within valley fills has been computed based on the sum of their thickness in each systems tracts (Fig. 4.3D). Similarly, the relative proportion of architectural elements within valley fills has been computed based on the sum of their thickness within valley fills (Fig. 4.3D). For overfilled IVFs, only the parts of architectural elements or systems tracts that are contained within the incised valleys are considered in the analyses (Fig. 4.3C). Element proportions have been computed accounting for the fact that in-valley architectural elements can themselves be nested hierarchically. For example, flood-tidal-delta deposits may be encapsulated in a barrier-complex element, or delta-plain deposits may form parts of a non-bay delta (Fig. 4.2A). Therefore, elements at different hierarchal levels can be selectively included or excluded depending on whether they are classified according to schemes of interest for the scopes of a particular analysis.

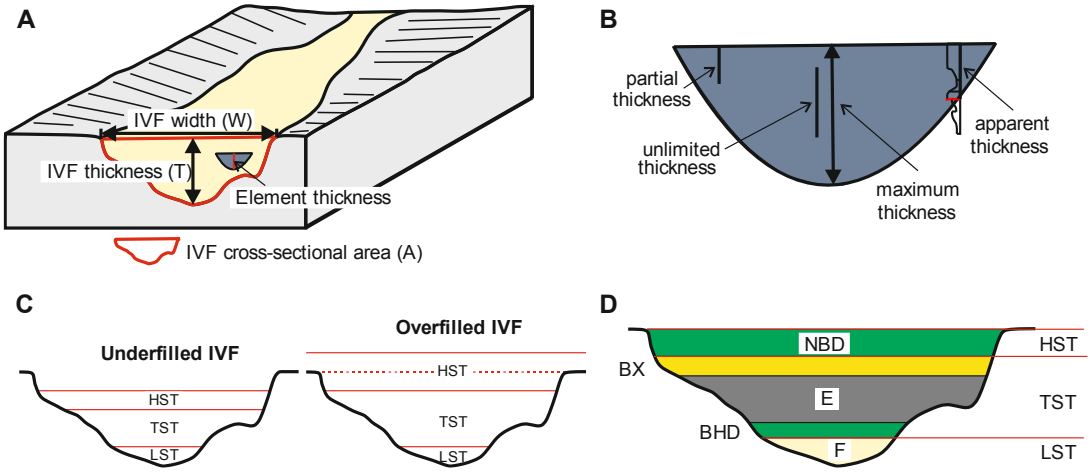

Fig. 4.3. *(A) Incised-valley-fill dimensions (thickness, width and cross-sectional area) and in-valley architectural element thickness measured in the analysis herein. (B) Classification of in-valley architectural element thickness by type of observation, i.e., as 'maximum', 'apparent', 'partial' and 'unlimited' (see text). (C) Schematic diagrams illustrating the internal fills for underfilled and overfilled incised valleys (Simms et al., 2006). (D) Diagram illustrating the containment of systems tracts in valley fills, of architectural elements in different systems tracts and of architectural elements in valley fills. For presentation purposes, architectural elements are only shown as classified on Scheme 1; the same elements can also be classified according to Scheme 2. F = fluvial deposits; BHD = bayhead delta; E = estuarine bay/lagoon deposits; BX = barrier complex; NBD = non-bay delta.*

4.3.4 Attributes on geological boundary conditions

In this work, the datasets are filtered on attributes that describe the continental-margin type, drainage-basin area, incised-valley-fill dimensions, basin physiography and shoreline hydrodynamics. The incised-valley fills are classified on the type of continental margin on which they are hosted. The drainage-basin area is defined as the area of the catchments that fed the incised valley at lowstand, landward of the location where the incised-valley-fill geometry was measured (see Wang et al., 2019, for details).

4.3.4.1 Basin physiography

According to the morphometric definitions and map of global distribution of enclosed and semi-enclosed seas by Healy and Harada (1991a), the coastal-plain IVFs were classified as located along coastlines that either face enclosed/semi-enclosed seas (N = 23) or open oceans (N = 26). An enclosed or semi-enclosed sea is defined as a sea that is surrounded by land and that is connected with an ocean or another sea by one or more entrances. For practical purposes, this term is

restricted to features identifiable on a world map of scale 1:15M to 1:25M. In agreement with Healy and Harada (1991a), certain gulf regions, including the Gulf of Mexico and the Gulf of Thailand, were classified as enclosed or semi-enclosed seas, whereas others, such as the Bay of Biscay, were classified as open-ocean settings.

The present-day shelf physiography is used as a proxy for the physiography of the shelf through the evolution of the valley fills (cf. Wang et al. 2019). Data on shelf width and shelf-break depth are based on the map by Harris et al. (2014) and the digital bathymetric data from Becker et al. (2009). The shelf gradient was calculated as the mean gradient of the shelf between the present-day shoreline and the shelf break. The database also records whether cross-shelf incised-valley fills are characterized on the inner or on the outer shelf. The distinction between inner and outer shelf being made on bathymetry rather than on process regime: the boundary between inner and outer shelf is arbitrarily placed at the 25-m isobath (cf. Wang et al., 2019).

4.3.4.2 Present-day shoreline hydrodynamics

Mean tidal range and mean wave height at present-day shorelines have been recorded for incised-valley systems beneath modern coastal plains, utilizing digital data from NOAA (2019) and METOCEAN (2019). Values of mean tidal range and mean wave height may not be representative of those at the position where the geometry and architecture of the IVFs were characterized. The duration of tide and wave measurements varies depending on location. Based on records of mean tidal range and mean wave height at the shoreline, the present-day hydrodynamic regime of the coasts (Fig. 4.4) was classified as tide-dominated, mixed-energy tide-dominated, mixed-energy wave-dominated, or wave-dominated, according to the classification of Davis and Hayes (1984). Because hydrodynamic conditions will vary significantly through a cycle of relative sea-level change (Nordfjord et al., 2006; Yoshida et al., 2005), this classification is only applied to deposits accumulated during the present-day highstand and incorporated in the HST of the incised-valley fills.

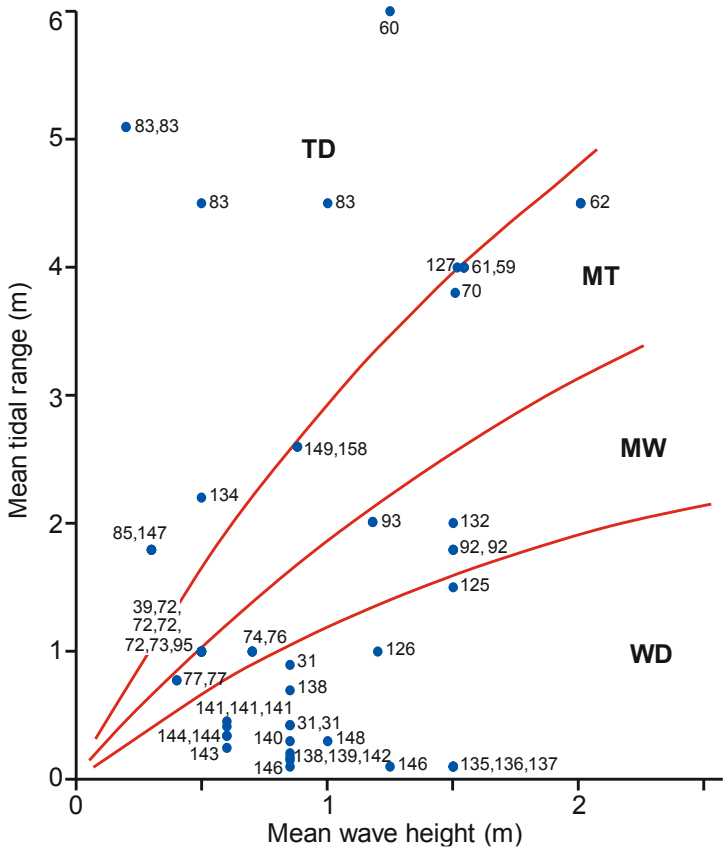

Fig. 4.4. *Plot of mean tidal range versus mean wave height for the present-day shorelines of the studied coastal-plain valleys (cf. Davis and Hayes, 1984). WD = wave-dominated; MW = mixed-energy wave-dominated; MT = mixed-energy tide-dominated; TD = tide-dominated. The numerical labels next to the spots refer to IDs in Table 4.1. Data from NOAA (2019) and METOCEAN (2019).*

4.3.5 Statistical analyses

Statistical analyses of database outputs have been performed in Minitab 18 and R (version 3.6.1) (R Core Team, 2019). Statistical analyses have been undertaken to determine relationships between continuous variables and to test hypotheses relating to differences in means or distributions of variables across groups. To quantify linear and monotonic relationships between pairs of continuous variables, Pearson or Spearman correlation coefficients (R and r hereafter) are used respectively; their statistical significance is expressed as P-values (P hereafter). To determine the statistical significance of differences in means across populations, a two-sample t-test is used when comparing two sets of observations, whereas one-way analysis of variance (ANOVA) is used when comparing three or more sets of observations. Normality and homoscedasticity of the data were checked before performing these tests, and any variable transformation was applied where needed. The statistical significance of differences across groups, expressed as P-values (P),

are determined by resulting test statistics (t for t-tests, F for ANOVA) and the number of degrees of freedom (df hereafter). For distributions that are highly skewed and zero-inflated, such as distributions of architectural-element proportions, nonparametric tests are used: the Wilcoxon rank-sum test is used when comparing two sets of observations, whereas the Kruskal-Wallis test is used when dealing with three or more groups. The statistical significance of differences in the distributions across groups is expressed by P-values. P-values are compared with significance levels (α hereafter) that equal 0.05 or 0.1, to determine whether the null hypothesis is rejected.

Additionally, principal component analysis and hierarchical cluster analysis of the variables, were performed on 30 coastal-plain IVFs for which it was possible to constrain the following eight variables: shelf width, shelf-break depth, IVF thickness, IVF width, drainage area, mean wave height, mean tidal range and proportion of fluvial deposits in the valley fills. These multivariate analyses were undertaken for scopes of dimensionality reduction and identification of redundancy across variables. Details, results and discussion of the multivariate analyses are only included in the Supplementary Information.

Further explanation of the statistical methods used can be found in Davis et al. (2002).

4.3.6 Limitations

Some limitations to the current study that are worth highlighting before any results are presented can be summarized as follows.

1. Potential bias exists because of the difficulty in recognizing bounding surfaces in 1D datasets. For example, the thickness and proportion of lowstand fluvial deposits might be over- or underestimated due to the difficulty in recognizing the boundary between lowstand and falling-stage (or older) alluvial units. This type of bias is a significant source of uncertainty in the assessment of variability in the proportion of systems tract or elements for coastal-plain IVFs (section 3.1.1). Additionally, this type of bias might also arise when assessing the difference between the internal fills of coastal-plain incised valleys and cross-shelf incised valleys (section 3.1.2) as the recognition of sequence boundaries relies on different techniques of investigation in onshore versus offshore settings. In seismic sections, where sequence boundaries may be readily apparent, lowstand fluvial deposits tend to be identified more easily, whereas in 1D datasets based on cores or well logs the thickness of lowstand fluvial deposits may be over- or underestimated due to their amalgamation with alluvial deposits of the falling stage or of previous cycles.

2. Relationships between direction and magnitude in relative sea-level rise and fall and characteristics of IVF architecture could not be examined in detail. Spatial and temporal variability in sea-level fluctuations are known to exert a control on IVF architecture (Thomas and Anderson, 1994; Nichol et al., 1996; Rodriguez et al., 1999; Hori et al., 2002), and it is therefore likely that some variability in the data presented in this work is related to the temporal change in the rate of post-LGM sea-level rise and fall and to geographic variations of sea level. Additionally, the valley reaches studied in the original data sources might have been filled under different sea-level conditions depending on their positions relative to the present-day shoreline. A binary distinction between coastal-plain IVFs and cross-shelf IVFs is therefore necessarily simplistic.

3. Characteristics relating to the shape of incised valleys and to their variations in shape along their dip extent were not examined. Previous work (Heap and Nichol, 1997; Rodriguez et al., 2005; Rodriguez et al., 2008) has shown that the shape of incised valleys acts as a controlling factor on IVF architecture; for example, the progressive inundation of terraces in terraced IVFs can result in step-wise changes in accommodation space and in variations of hydrodynamic processes, which can influence the valley-fill architecture. It is desirable to attempt further analysis with additional metrics of valley-shape variability along dip to consider its potential control on stratigraphic architectures.

4. Factors relating to the morphology of the bedrock that might be exposed along the base of incised valleys and to its potential control on hydrodynamics and resultant sedimentation were not examined.

4.4 Results

4.4.1 Valley-fill stratigraphic organization and sea-level control

The sedimentary architecture of incised-valley fills that sit beneath present-day coastal plains and of those that occur on continental shelves are expected to differ, particularly with respect to the extent to which the different systems tracts are preserved in the valley fill, and in the abundance of architectural-element types and its variation through systems tracts (Dalrymple et al., 1992; Allen and Posamentier, 1993, 1994b; Zaitlin et al., 1994; Blum et al., 2013). To assess the significance of these differences, the stratigraphic architecture of coastal-plain (N = 20) and cross-shelf incised-valley fills (N = 18) is considered separately.

4.4.1.1 Coastal-plain incised valleys

The ratio between the thickness of deposits belonging to a certain systems tract in the valley fill and the thickness of the valley fill itself ('systems tract-to-valley-fill thickness ratio', or simply 'thickness ratio', hereafter) is taken as an estimation of the proportion of the systems tract in the incised-valley fill. The mean thickness ratio (avgTR) of TSTs in incised-valley fills is significantly higher than that of LSTs or HSTs ($avgTR_{LST}$ = 0.18; $avgTR_{TST}$ = 0.62; $avgTR_{HST}$ = 0.20; one-way ANOVA: F(2,57) = 52.42, P-value < 0.001; Fig. 4.5A). Likewise, the thickness of TSTs within incised-valley fills is, on average, significantly larger than that of LST or HST ($avgT_{LST}$ = 11.8 m; $avgT_{TST}$ = 34.6 m; $avgT_{HST}$ = 11.7 m; one-way ANOVA: F(2,57) = 26.02, P-value < 0.001; Fig. 4.5B).

For architectural elements accumulated during lowstand times, and which form LSTs in incised-valley fills, fluvial deposits are the most abundant (mean proportion: avgP = 0.98, σ = 0.06; Fig. 4.5C). In TST valley-fill deposits, estuarine bay/lagoon (avgP = 0.51, σ [standard deviation] = 0.25) deposits are the most abundant type of elements, whereas the second most abundant is represented by fluvial deposits (avgP = 0.20, σ = 0.23). For architectural elements accumulated during highstand times, and which form HSTs, the type with the largest average proportion is represented by non-bay deltas, i.e., deltaic systems that are not fully contained within the confines of the embayment resulting from valley topography, (avgP = 0.29, σ = 0.41); the second most abundant type on average is represented by estuarine bay/lagoon elements (avgP = 0.25, σ = 0.34).

For architectural elements across systems tracts, the mean proportion of fluvial deposits within LST is higher than that within TST or HST ($avgP_{LST}$ = 0.98, σ = 0.06; $avgP_{TST}$ = 0.2, σ = 0.23; $avgP_{HST}$ = 0.06, σ = 0.12; Fig. 4.5C). The mean proportion of estuarine bay/lagoon elements within TST is higher than that within LST or HST ($avgP_{LST}$ = 0.00, σ = 0.00; $avgP_{TST}$ = 0.51, σ = 0.25; $avgP_{HST}$ = 0.25, σ = 0.34). When bayhead-delta and non-bay delta units are considered jointly, the mean proportion of these deltaic deposits within HSTs is higher than that within LSTs or TSTs ($avgP_{LST}$ = 0.00, σ = 0.00; $avgP_{TST}$ = 0.09, σ = 0.18; $avgP_{HST}$ = 0.39, σ = 0.38). Differences in the distributions of proportion of fluvial, estuarine bay/lagoon, and deltaic elements across different types of systems tracts are significant at α of 0.05, based on Kruskal-Wallis test (H = 34.69, P-value < 0.001 for fluvial; H = 24.85, P-value < 0.001 for estuarine bay/lagoon elements; H = 13, P-value = 0.002 for deltaic elements).

The thickness of fluvial deposits within TSTs is higher on average than that within LSTs or HSTs ($avgT_{LST}$ = 8.44 m, σ= 7.58 m; $avgT_{TST}$ = 13.12 m, σ= 6.75 m; $avgT_{HST}$ = 6.4 m, σ= 2.29 m; Fig. 4.5D). Differences in the distributions of thickness

of fluvial deposits across systems tracts are significant at α of 0.1 (one-way ANOVA: F(2,50) = 3.09, P-value = 0.055). Differences in the thickness distributions of bayhead delta, estuarine bay/lagoon and barrier-complex elements between TST and HST are not significant, based on two-sample t-tests (t-value = -0.84, P-value = 0.422, df = 10, for bayhead delta; t-value = -1.5, P-value = 0.157, df = 14, for estuarine bay/lagoon; t-value = -0.21, P-value = 0.841, df = 4, for barrier complex).

No significant difference exists between the thickness distributions for incised-valley fills that contain HST deposits compared to those that were overfilled and/or ravined during transgressions and do not contain HST deposits (mean value = 54.2 m versus 50.9 m; σ = 16.2 m versus 24.2 m; two-sample t-test: t-value = 0.28, P-value = 0.788, df = 5).

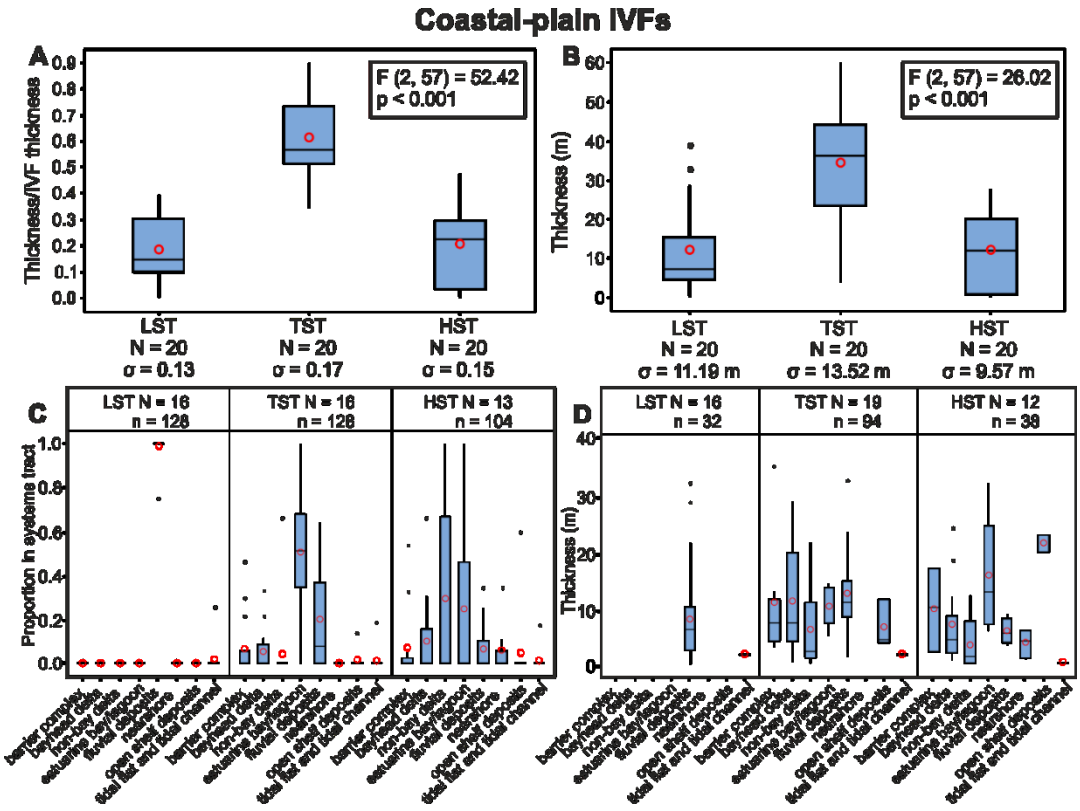

Fig. 4.5. *Box plots that present distributions in: (A) systems-tract-to-valley-fill thickness ratio and (B) thickness of different systems tracts preserved in coastal-plain incised-valley fills; (C) proportion and (D) thickness of architectural elements belonging to each type of systems tract in coastal-plain valley fills. For each box plot, boxes represent interquartile ranges, red open circles represent mean values, horizontal bars within the boxes represent median values and black dots represent outliers (values that are more than 1.5 times the interquartile range). 'N' denotes the number of incised-valley fills and associated systems tract, 'n' denotes the number of architectural elements in each systems tract and 'σ' denotes the standard deviation. The results of one-way ANOVA are reported in boxes in parts A and B, as: F-value (degrees of freedom between and within groups in brackets), P-value.*

4.4.1.2 Cross-shelf incised valleys

For systems tracts within incised-valley fills, the mean systems-tract-to-valley-fill thickness ratio of LSTs or TSTs is significantly higher than that of HSTs ($avgTR_{LST}$ = 0.36; $avgTR_{TST}$ = 0.55; $avgTR_{HST}$ = 0.08; one-way ANOVA: F(2,51) = 24.34, P-value < 0.001; Fig. 4.6A). The thickness ratio of LST deposits within cross-shelf valley fills is, on average, higher than that within coastal-plain valley fills ($avgTR_{shelf}$ = 0.36; $avgTR_{coastal\text{-}plain}$ = 0.18; Figs. 5A and 6A).

Likewise, the thickness of LSTs or TSTs within incised-valley fills is, on average, significantly larger than that of HST ($avgT_{LST}$ = 13.71 m; $avgT_{TST}$ = 18.95 m; $avgT_{HST}$ = 3.24 m; one-way ANOVA: F(2,51) = 11.53, P-value < 0.001; Fig. 4.6B).

For architectural elements accumulated during lowstand and that form LSTs in incised-valley fills, fluvial deposits are in almost all cases the only type of deposit (Fig. 4.6C). For architectural elements accumulated during TST, estuarine-bay/lagoon deposits (avgP = 0.35, σ = 0.40) are the ones with highest average proportion, followed by barrier-complex deposits (avgP = 0.21, σ = 0.32), and tidal-flat and tidal-channel elements (avgP = 0.10, σ = 0.18). For architectural elements accumulated during highstand and that form HSTs, the most abundant element type is open-shelf deposits (avgP = 0.7, σ = 0.48).

The mean proportion of fluvial deposits within LST is higher than that within TST or HST ($avgP_{LST}$ = 1, σ = 0; $avgP_{TST}$ = 0.07, σ = 0.25; $avgP_{HST}$ = 0, σ = 0; Fig. 4.6C). The mean proportion of estuarine bay/lagoon deposits within TST is higher than that within LST or HST ($avgP_{LST}$ = 0, σ = 0; $avgP_{TST}$ = 0.35, σ = 0.40; $avgP_{HST}$ = 0.1, σ = 0.32). The mean proportion of open-shelf deposits within HST is higher than that within LST or TST ($avgP_{LST}$ = 0, σ = 0; $avgP_{TST}$ = 0.08, σ = 0.24; $avgP_{HST}$ = 0.7, σ = 0.48). Differences in the distributions of proportion of fluvial, estuarine bay/lagoon, and open-shelf deposits across different systems tracts in valley fills are statistically significant at α of 0.05, based on Kruskal-Wallis test (H = 35.92, P-value < 0.001 for fluvial deposits; H = 12.44, P-value = 0.002 for estuarine bay/lagoon; H = 17.17, P-value < 0.001 for open-shelf deposits).

The average thickness of fluvial deposits, i.e., of stratigraphic packages that might variably include fluvial channel and floodplain deposits, is not significantly different between LST and TST ($avgT_{LST}$ = 15.3 m [σ = 11.7 m], $avgT_{TST}$ = 15.8 m [σ = 1.63 m]; two-sample t-test: t-value = -0.19, P-value = 0.854, df = 15; Fig. 4.6D). The average thickness of open-shelf deposits is smaller in HST than in TST intervals ($avgT_{HST}$ = 3.7 m [σ = 1.68 m], $avgT_{TST}$ = 12.7 m [σ = 11.6 m]); however, these differences are not statistically significant (two-sample t-test: t-value = -1.55, P-value = 0.218, df = 3).

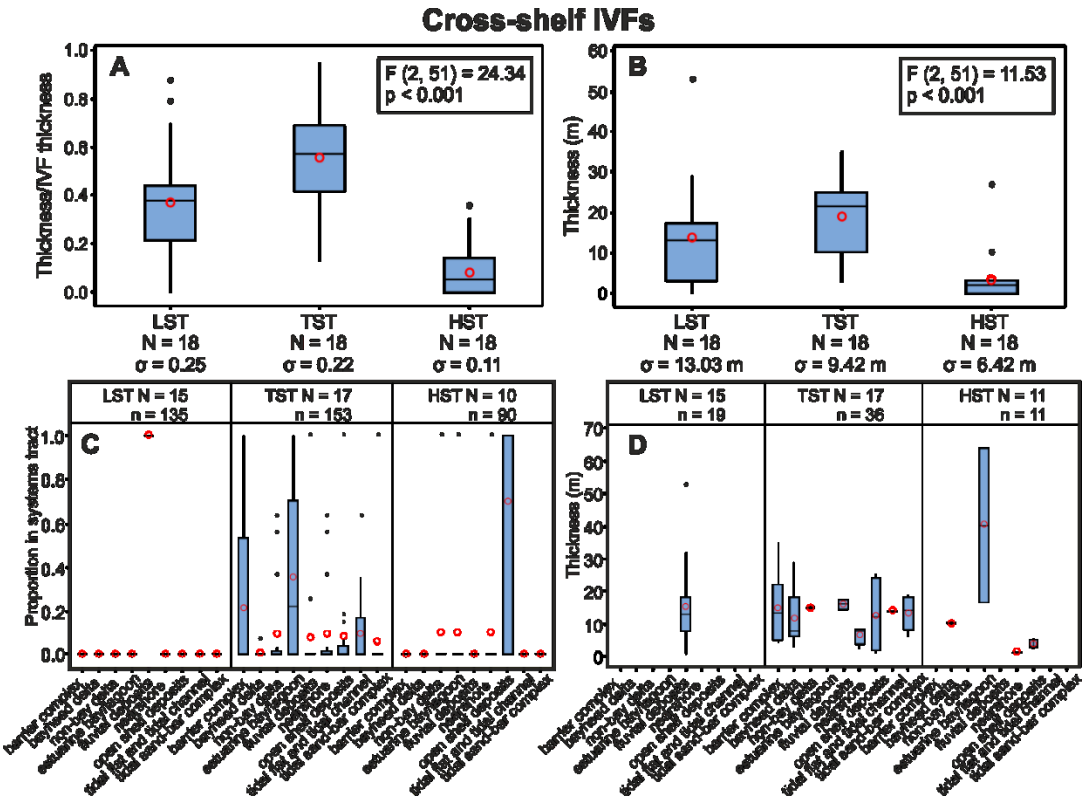

Fig. 4.6. *Box plots that present distributions in: (A) thickness ratio and (B) thickness of different systems tracts preserved in cross-shelf incised-valley fills; (C) proportion and (D) thickness of architectural elements belonging to types of systems tract in cross-shelf valley fills. For each box plot, boxes represent interquartile ranges, red open circles represent mean values, horizontal bars within the boxes represent median values and black dots represent outliers (values that are more than 1.5 times the interquartile range). 'N' denotes the number of incised-valley fills and associated systems tract, 'n' denotes the number of architectural elements in each systems tract and 'σ' denotes the standard deviation. The results of one-way ANOVA are reported in boxes in parts A and B, as: F-value (degrees of freedom between and within groups in brackets), P-value.*

4.4.2 Continental-margin type

The mean and median proportions of fluvial deposits within incised-valley fills developed along tectonically active margins are higher than those for valley fills along passive margins (Fig. 4.7A). A 17% difference in mean proportion of fluvial deposits is seen between active margins and passive margins, for which differences in the distributions are statistically significant at α of 0.05, based on Wilcoxon rank-sum tests (W = 242, P-value = 0.007). For incised-valley fills developed along tectonically active margins, the mean proportions of bayhead delta or estuarine bay/lagoon elements appear to be lower than those for valley fills along

passive margins. However, differences in the distributions of the proportions of these two types of elements within incised-valley fills across margin types are not statistically significant, based on Wilcoxon rank-sum tests (W = 154, P-value = 0.721 for bayhead delta; W = 146, P-value = 0.554 for estuarine bay/lagoon deposits).

Differences in means of the thickness of fluvial, bayhead-delta and barrier-complex elements within valley fills across these two settings are not statistically significant, based on two-sample t-tests (t-value = 1.04, P-value = 0.307, df = 37, for fluvial deposits; t-value = -1.16, P-value = 0.265, df = 15, for bayhead delta; t-value = 0.71, P-value = 0.486, df = 19, for barrier complex; Fig. 4.7B). The thickness of estuarine bay/lagoon elements within valley fills along active margins is, on average, larger than that within valley fills along passive margins ($avgT_{active}$ = 11.7 m, $avgT_{passive}$ = 6.5 m; two-sample t-test: t-value = 2.76, P-value = 0.01, df = 29).

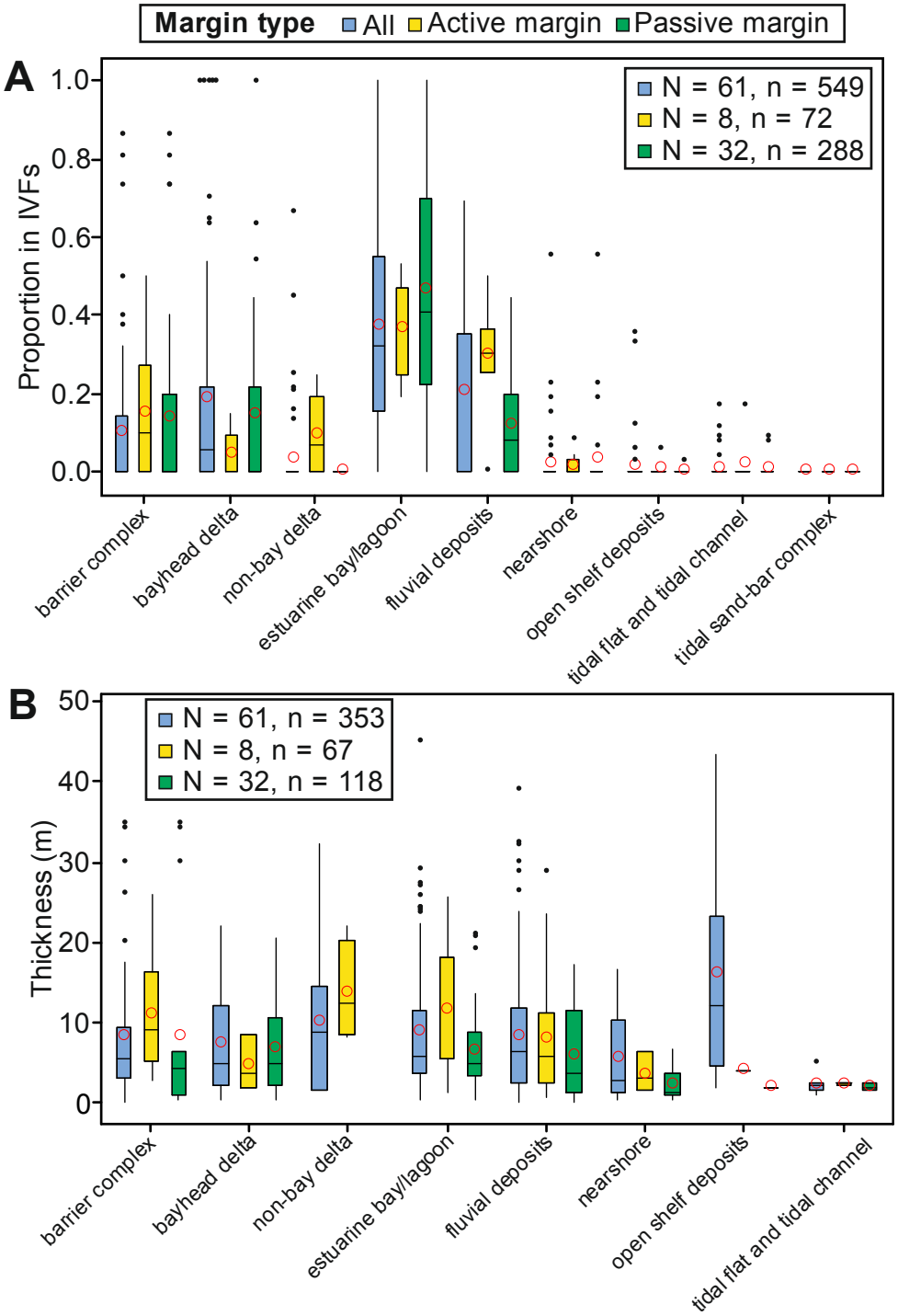

Fig. 4.7. *Box plots that present distributions in: (A) proportion and (B) thickness of different architectural-element types within coastal-plain incised-valley fills; data are presented for all the examples, and separately for active and passive continental margins. For each box plot, boxes represent interquartile ranges, red open circles represent mean values, horizontal bars within the boxes represent median values and black dots represent outliers (values that are more than 1.5 times the interquartile range). 'N' denotes the number of incised-valley fills associated with each margin type and 'n' denotes the number of corresponding in-valley architectural elements.*

4.4.3 Catchment and basin physiography

4.4.3.1 Record of systems tracts in incised-valley fills and river-system size

For systems tracts in incised-valley fills, positive correlations are seen between the thickness of LST deposits versus incised-valley-fill thickness, width and cross-sectional area (Fig. 4.8A to C; Table 4.3). Positive correlations are also seen between the thickness of TST deposits versus incised-valley-fill thickness and valley drainage-basin area (Fig. 4.8A and 8D; Table 4.3). A modest positive relationship is seen between HST thickness and incised-valley-fill thickness (Fig. 4.8A; Table 4.3).

Positive correlations are seen between the LST-to-valley-fill thickness ratio and incised-valley-fill thickness or cross-sectional area (Fig. 4.8E and 8G; Table 4.3). No apparent correlations are seen between thickness ratios of TSTs or HSTs versus incised-valley-fill dimensions or drainage-basin areas (Fig. 4.8E to H; Table 4.3).

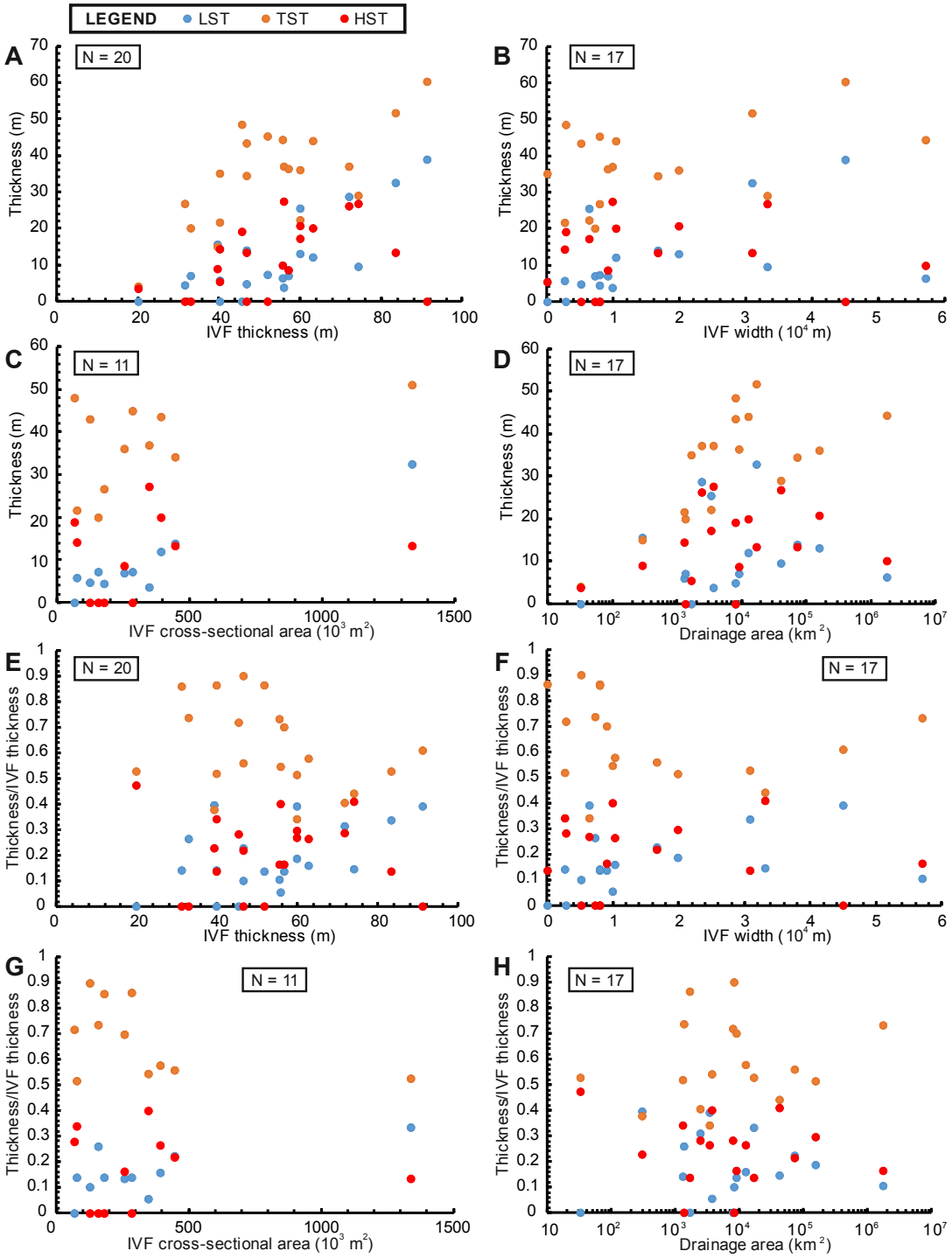

Fig. 4.8. *Cross-plots of the thickness of systems tracts within coastal-plain incised-valley fills versus IVF thickness (A), width (B), cross-sectional area (C) and drainage-basin area (D). Cross-plots of the thickness ratio of systems tracts within coastal-plain incised-valley fills versus IVF thickness (E), width (F), cross-sectional area (G) and drainage-basin area (H). For each pair of variables, the correlation coefficients and P-values are reported in Table 4.3. 'N' denotes the number of incised-valley fills.*

Table 4.3. *Correlation coefficients and P-values reported for the relationship between the thickness or thickness ratio of systems tracts within coastal-plain incised-valley fills versus IVF thickness, IVF width, IVF cross-sectional area and drainage area. 'N' denotes the number of readings, 'R' denotes Pearson's R, and 'r' denotes Spearman's rho.*

Parameters	Systems tract	IVF thickness	IVF width	IVF cross-sectional area	Drainage area
Thickness	LST	N = 20; R = 0.774, p < 0.001; r = 0.666, p = 0.001	N = 17; R = 0.498, p = 0.042; r = 0.596, p = 0.012	N = 11; R = 0.958, p < 0.001; r = 0.727, p = 0.011	N = 17; R = -0.111, p = 0.671; r = 0.258, p = 0.317
	TST	N = 20; R = 0.700, p = 0.001; r = 0.611, p = 0.004	N = 17; R = 0.456, p = 0.065; r = 0.380, p = 0.133	N = 11; R = 0.490, p = 0.126; r = 0.291, p = 0.385	N = 17; R = 0.243, p = 0.347; r = 0.613, p = 0.009
	HST	N = 20; R = 0.391, p = 0.089; r = 0.450, p = 0.047	N = 17; R = 0.050, p = 0.849; r = 0.191, p = 0.463	N = 11; R = 0.204, p = 0.547; r = 0.191, p = 0.574	N = 17; R = -0.086, p = 0.744; r = 0.336, p = 0.187
Thickness ratio	LST	N = 20; R = 0.498, p = 0.026; r = 0.411, p = 0.071	N = 17; R = 0.345, p = 0.175; r = 0.441, p = 0.076	N = 11; R = 0.690, p = 0.019; r = 0.536, p = 0.089	N = 17; R = -0.132, p = 0.612; r = 0.147, p = 0.572
	TST	N = 20; R = -0.329, p = 0.157; r = -0.30, p = 0.169	N = 17; R = -0.226, p = 0.384; r = -0.350, p = 0.168	N = 11; R = -0.454, p = 0.160; r = -0.364, p = 0.272	N = 17; R = 0.213, p = 0.412; r = 0.111, p = 0.672
	HST	N = 20; R = -0.055, p = 0.819; r = 0.086, p = 0.717	N = 17; R = -0.025, p = 0.925; r = 0.104, p = 0.691	N = 11; R = 0.011, p = 0.973; r = 0.014, p = 0.968	N = 17; R = -0.133, p = 0.610; r = -0.099, p = 0.706

4.4.3.2 Architectural elements and river-system size

Relationships between river-system size and the proportion and thickness of architectural elements within valley fills have been investigated, by considering classifications of the elements by sub-environment of deposition (Fig. 4.9; Table 4.4) and according to their process regime (Fig. 4.10; Table 4.5). In these analyses, the size of the valley systems are considered in terms of incised-valley-fill thickness, width, and drainage area (Fig. 4.9 and 10; Tables 4 and 5).

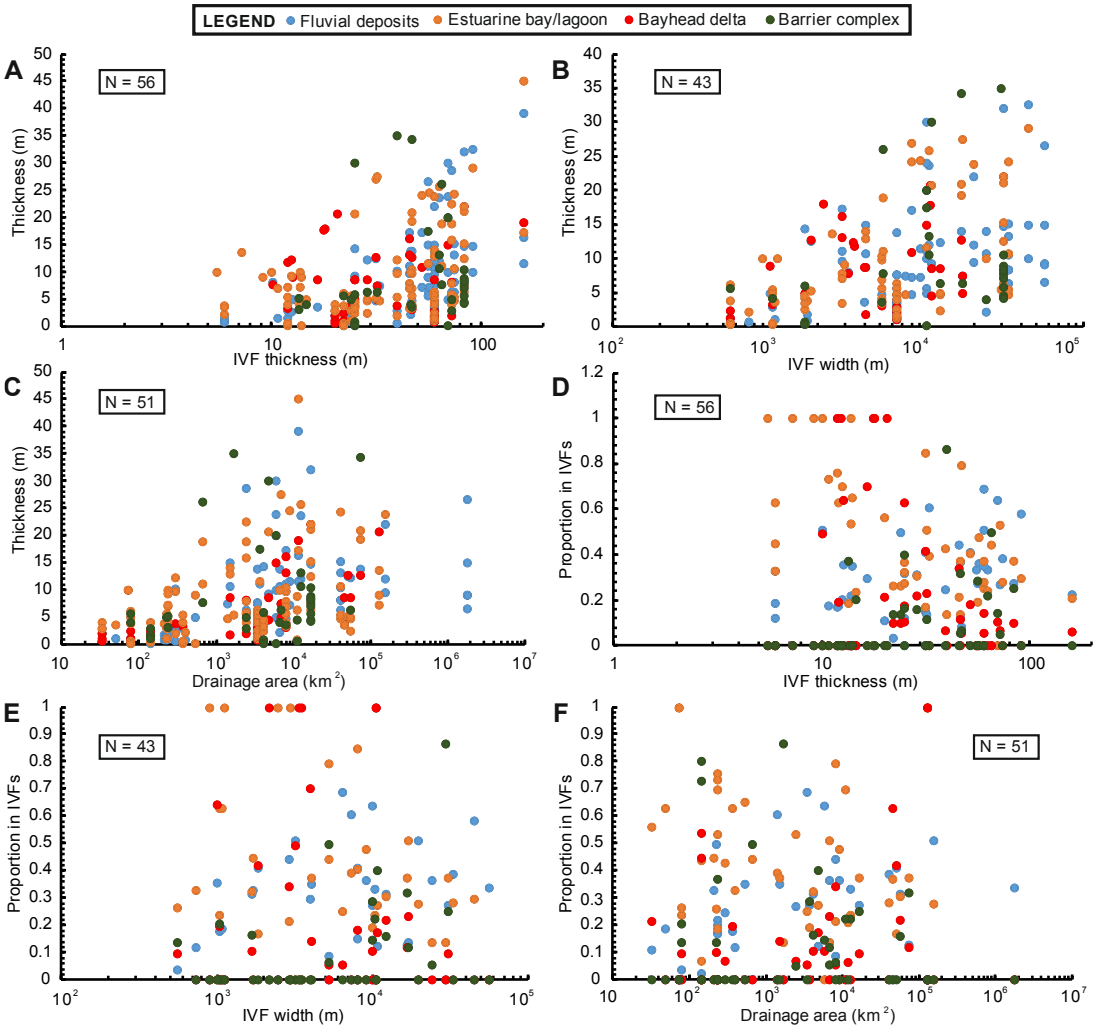

Fig. 4.9. *Cross-plots of thickness of architectural elements within coastal-plain incised-valley fills versus IVF thickness (A), width (B) and drainage-basin area (C). Cross-plots of proportion of architectural elements within coastal-plain incised-valley fills versus IVF thickness (D), width (E) and drainage-basin area (F). Architectural elements are classified on their sub-environment of deposition. For each pair of variables, the correlation coefficients and P-values are reported in respective cell in Table 4.4. 'N' denotes the number of incised-valley fills.*

Table 4.4. *Correlation coefficients and P-values reported for the relationship between the thickness or proportion of fluvial deposits, estuarine bay/lagoon, bayhead delta and barrier complex elements within IVFs versus IVF thickness, IVF width and drainage area. 'N' denotes the number of readings, 'R' denotes Pearson's R, and 'r' denotes Spearman's rho.*

Parameters	Elements	IVF thickness	IVF width	Drainage area
Thickness	Fluvial deposits	N = 56; R = 0.508, p < 0.001; r = 0.458, p < 0.001	N = 43; R = 0.406, p < 0.001; r = 0.529, p < 0.001	N = 51; R = 0.171, p = 0.090; r = 0.691, p < 0.001
	Estuarine bay/lagoon	N = 56; R = 0.517, p = 0.001; r = 0.420, p < 0.001	N = 43; R = 0.454, p < 0.001; r = 0.524, p < 0.001	N = 51; R = 0.220, p = 0.027; r = 0.351, p < 0.001
	Bayhead delta	N = 56; R = 0.230, p = 0.144; r = 0.017, p = 0.915	N = 43; R = 0.390, p = 0.027; r = 0.225, p = 0.216	N = 51; R = 0.550, p < 0.001; r = 0.782, p < 0.001
	Barrier complex	N = 56; R = 0.047, p = 0.797; r = 0.242, p = 0.175	N = 43; R = 0.112, p = 0.570; r = 0.324, p = 0.093	N = 51; R = 0.314, p = 0.055; r = 0.318, p = 0.052
Proportion	Fluvial deposits	N = 56; R = 0.412, p = 0.002; r = 0.473, p < 0.001	N = 43; R = 0.264, p = 0.088; r = 0.273, p = 0.077	N = 51; R = 0.082, p = 0.570; r = 0.237, p = 0.094
	Estuarine bay/lagoon	N = 56; R = -0.243, p = 0.071; r = -0.24, p = 0.059	N = 43; R = -0.238, p = 0.125; r = -0.191, p = 0.220	N = 51; R = -0.175, p = 0.219; r = -0.113, p = 0.430
	Bayhead delta	N = 56; R = -0.242, p = 0.072; r = 0.014, p = 0.918	N = 43; R = -0.235, p = 0.129; r = -0.103, p = 0.511	N = 51; R = -0.039, p = 0.785; r = 0.126, p = 0.379
	Barrier complex	N = 56; R = 0.399, p = 0.002; r = 0.354, p = 0.007	N = 43; R = 0.335, p = 0.028; r = 0.299, p = 0.051	N = 51; R = 0.082, p = 0.566; r = -0.017, p = 0.907

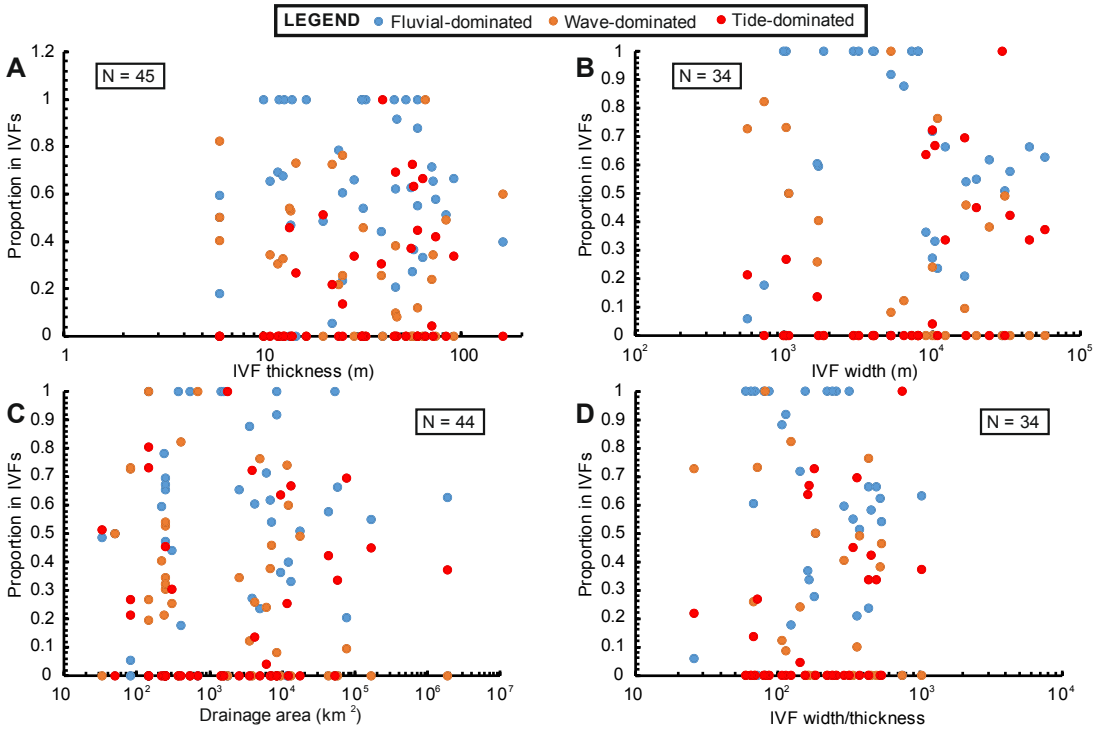

Fig. 4.10. *Cross-plots of proportion of architectural elements (Scheme 2) within coastal-plain incised-valley fills versus IVF thickness (A), width (B), drainage-basin area (C) and width-to-thickness ratio (D). Architectural elements are classified on their dominant process regime. For each pair of variables, the correlation coefficients and P-values are reported in respective cell in Table 4.5. 'N' denotes the number of incised-valley fills.*

Table 4.5. *Correlation coefficients and P-values reported for the relationship between the proportion of fluvial-dominated, wave-dominated and tide-dominated elements within IVFs versus IVF thickness, IVF width and drainage area. 'N' denotes the number of readings, 'R' denotes Pearson's R, and 'r' denotes Spearman's rho.*

Elements	IVF thickness	IVF width	Drainage area	IVF width/thickness
Fluvial-dominated	N = 45; R = -0.081, p = 0.596; r = -0.085, p = 0.58	N = 34; R = -0.146, p = 0.412; r = -0.161, p = 0.362	N = 44; R = 0.062, p = 0.690; r = 0.178, p = 0.247	N = 34; R = -0.165, p = 0.350; r = -0.179, p = 0.310
Wave-dominated	N = 45; R = -0.056, p = 0.715; r = -0.201, p = 0.185	N = 34; R = -0.217, p = 0.218; r = -0.246, p = 0.161	N = 44; R = -0.176, p = 0.252; r = -0.337, p = 0.025	N = 34; R = -0.153, p = 0.389; r = -0.111, p = 0.530
Tide-dominated	N = 45; R = 0.160, p = 0.294; r = 0.293, p = 0.051	N = 34; R = 0.414, p = 0.015; r = 0.457, p = 0.007	N = 44; R = 0.112, p = 0.469; r = 0.129, p = 0.403	N = 34; R = 0.369, p = 0.032; r = 0.271, p = 0.120

4.4.3.3 Process regime, architectural elements and coastal physiography

For coastal-plain IVFs, differences in both present-day processes (mean wave height and mean tidal range at the shoreline) and preserved sedimentary products (proportion of elements recording different process regimes) across enclosed or semi-enclosed sea and open-ocean settings (Fig. 4.11) are investigated. The mean wave height (avgMWH) for the studied open-ocean settings is, on average, higher than that in enclosed or semi-enclosed seas ($avgMWH_{open}$ = 1.077 m, $avgMWH_{enclosed}$ = 0.713 m; two-sample t-test: t-value = -3.14, P-value = 0.004, df = 33; Fig. 4.11A). The mean tidal range (avgTR) in the studied open-ocean settings is, on average, higher than that in enclosed or semi-enclosed seas ($avgTR_{open}$ = 1.48 m, $avgTR_{enclosed}$ = 0.640 m; two-sample t-test: t-value = -2.41, P-value = 0.022, df = 29; Fig. 4.11B).

The mean proportion of wave-dominated elements in IVFs facing enclosed or semi-enclosed seas is marginally lower than that for IVFs associated with open oceans ($avgP_{enclosed}$ = 0.231 vs $avgP_{open}$ = 0.287), though to a level that is not statistically significant (two-sample t-test: t-value = -0.65, P-value = 0.522, df = 45). The proportion of tide-dominated elements in IVFs associated with enclosed or semi-enclosed seas is, on average, significantly lower than that for IVFs associated with open oceans ($avgP_{enclosed}$ = 0.051 vs $avgP_{open}$ = 0.315; two-sample t-test: t-value = -3.87, P-value <0.001, df = 33). The mean proportion of fluvial-dominated elements in IVFs associated with enclosed or semi-enclosed seas is significantly higher than that for IVFs facing open oceans ($avgP_{enclosed}$ = 0.718 vs $avgP_{open}$ = 0.399; two-sample t-test: two-sample t-test: t-value = 3.54, P-value = 0.001, df = 44).

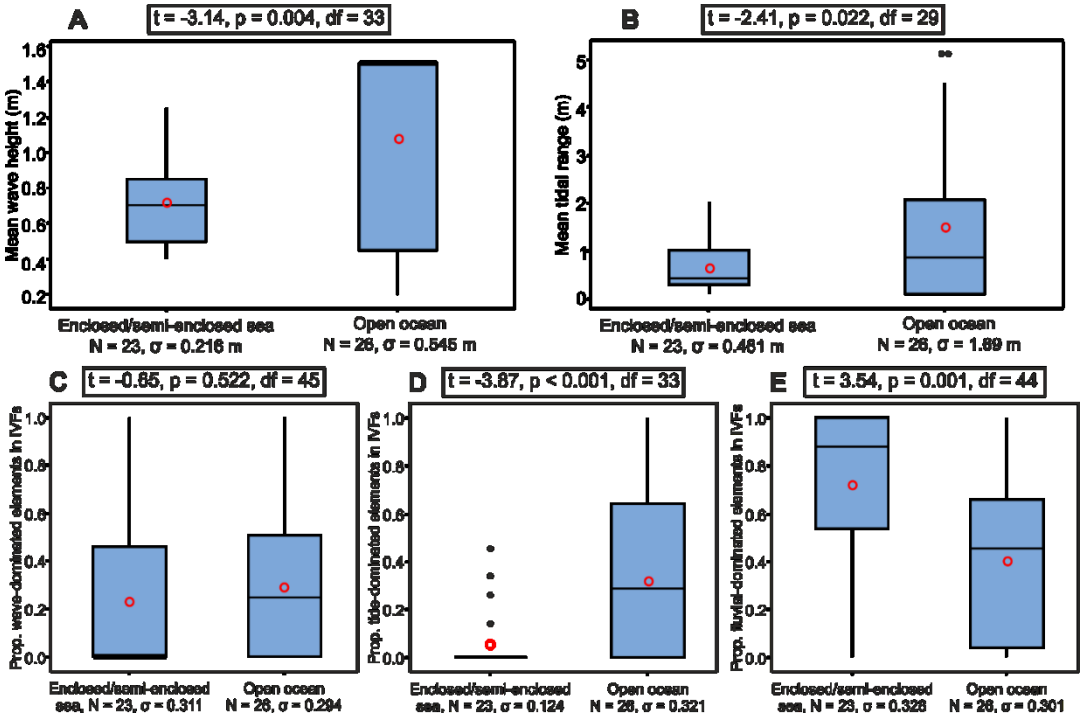

Fig. 4.11. *(A, B) Box-plots of distributions of mean wave height (A) and mean tidal range (B) at the present-day shoreline of the studied coastal-plain incised-valley fills associated with enclosed or semi-enclosed seas and with open oceans. (C-E) Box-plots of distributions of the proportion of architectural elements (Scheme 2; see Table 4.2) in coastal-plain IVFs for enclosed/semi-enclosed seas and open oceans. For each box-plot, boxes represent interquartile ranges, red open circles represent mean values, horizontal bars within the boxes represent median values, and black dots represent outliers (values that are more than 1.5 times the interquartile range). 'N' denotes the number of readings. 'σ' denotes the standard deviation. The results of two-sample t-test (t-value, P-value and degrees of freedom) are reported in boxes.*

4.4.3.4 Process regime, architectural elements and shelf physiography

For coastal-plain IVFs, relationships between shelf physiography (shelf width, shelf-break depth and shelf gradient) and present-day hydrodynamic conditions (Table 4.6) are investigated. A modest positive correlation is noted between mean wave height at the present-day shoreline at the IVF location versus shelf-break depth. Relationships between shelf physiography and the proportion in coastal-plain IVFs of architectural elements classified according to their dominant process regime (Table 4.6) are also investigated. A modest positive correlation is noted between the proportion of wave-dominated elements in IVFs versus the average shelf gradient.

Table 4.6. *Correlation coefficients and P-values reported for the relationship between mean wave height, mean tidal range at present-day shorelines and the proportion of fluvial-dominated, wave-dominated and tide-dominated elements within coastal-plain IVFs versus shelf width, shelf-break depth and shelf gradient (N = 49). 'N' denotes the number of incised-valley fills, 'R' denotes Pearson's R, and 'r' denotes Spearman's rho.*

Quantity	Shelf width	Shelf-break depth	Shelf gradient
Mean wave height	R = 0.093, p = 0.547; r = 0.171, p = 0.267	R = 0.496, p < 0.001; r = 0.430, p = 0.002	R = 0.200, p = 0.168; r = 0.260, p = 0.071
Mean tidal range	R = 0.077, p = 0.617; r = -0.109, p = 0.481	R = 0.260, p = 0.071; r = -0.027, p = 0.853	R = -0.228, p = 0.115; r = -0.233, p = 0.108
Proportion of fluvial-dominated deposits	R = 0.204, p = 0.183; r = 0.176, p = 0.252	R = -0.230, p = 0.111; r = -0.229, p = 0.114	R = -0.140, p = 0.336; r = -0.239, p = 0.097
Proportion of wave-dominated deposits	R = -0.174, p = 0.258; r = -0.099, p = 0.523	R = 0.100, p = 0.493; r = 0.191, p = 0.190	R = 0.346, p = 0.015; r = 0.449, p = 0.001
Proportion of tide-dominated deposits	R = -0.080, p = 0.607; r = -0.024, p = 0.878	R = 0.181, p = 0.214; r = 0.247, p = 0.087	R = -0.195, p = 0.180; r = -0.155, p = 0.288

4.4.3.5 Sub-environments of architectural elements and shelf gradient

For incised-valley fills hosted on the outer shelf, positive correlations are seen between the average shelf gradient and both the thickness and proportion of barrier-complex elements (Fig. 4.12; Table 7).

For incised-valley fills hosted on the shelf, no correlation is noted between the thickness of estuarine bay/lagoon elements versus the average shelf gradient (Fig. 4.12A; Table 7); a modest positive correlation is noted between the proportion of estuarine bay/lagoon elements versus the average shelf gradient (Fig. 4.12B; Table 7).

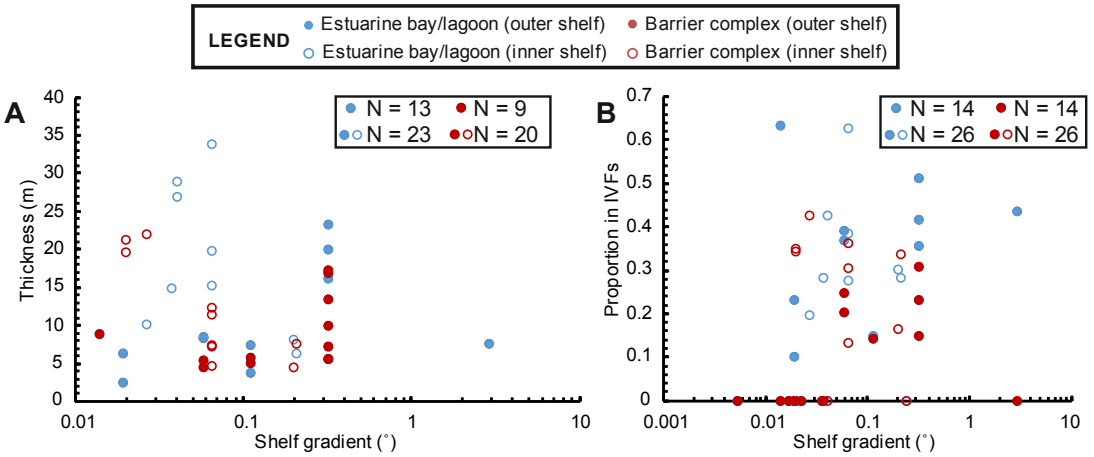

Fig. 4.12. *Plots of thickness (A) and proportion (B) of architectural elements within cross-shelf incised-valley fills versus shelf gradient. For each pair of variables, the correlation coefficients and P-values are reported in respective cell in Table 7. 'N' denotes the number of readings.*

Table 4.7. *Correlation coefficients and P-values reported for the relationship between the thickness or proportion of estuarine bay/lagoon and barrier complex elements within IVFs versus shelf gradient. Note that these two elements are classified into two groups, i.e., those hosted on the outer shelf and those hosted on the inner shelf. 'N' denotes the number of readings, 'R' denotes Pearson's R, and 'r' denotes Spearman's rho.*

Parameters	Elements	Position	Shelf gradient
Thickness	Estuarine bay/lagoon	Outer shelf	N = 13; R= -0.004, p = 0.990; r = 0.531, p = 0.062
		Shelf	N = 23; R= -0.139, p= 0.538; r= 0.122, p= 0.588
	Barrier complex	Outer shelf	N = 9; R= 0.546, p = 0.128; r = 0.741, p = 0.022
		Shelf	N = 20; R= -0.232, p= 0.340; r= -0.226, p= 0.351
Proportion	Estuarine bay/lagoon	Outer shelf	N = 14; R= 0.314, p = 0.274; r = 0.494, p = 0.072
		Shelf	N = 26; R= 0.245, p= 0.228; r= 0.49, p= 0.011
	Barrier complex	Outer shelf	N = 14; R= -0.107, p = 0.715; r = 0.625, p = 0.017
		Shelf	N = 26; R= -0.142, p= 0.487; r= 0.325, p= 0.106

4.4.4 Shoreline hydrodynamics

Previous work based on late-Quaternary incised-valley-fill systems and outcrop studies of ancient successions (e.g., Yoshida et al., 2005; Nordfjord et al., 2006; Tanabe et al., 2006) has demonstrated that hydrodynamic conditions through a relative sea-level cycle change in response to several factors, such as wind regime, coastal bathymetry, shelf-break depth, shelf width, their effect on tidal resonance,

and frictional forces. To investigate the relationships between coastal hydrodynamics and resultant sedimentary record, this work only focuses on deposits accumulated during highstand and incorporated in the HST of incised-valley fills, by considering the present-day hydrodynamic regimes at the respective shorelines. The following observations (Fig. 4.13) are based on a limited dataset (N = 19) and thus any relationships between hydrodynamics and highstand deposits in incised-valley fills needs to be substantiated with more data.

For deposits accumulated during highstand and forming HSTs within coastal-plain incised-valley fills (Fig. 4.13A), the thickness ratio of HSTs in valley fills associated with present-day mixed-energy to fully wave-dominated conditions is smaller on average compared to that of valley fills associated with present-day fully tide-dominated conditions or mixed-energy tide-dominated conditions ($avgTR_{HST\text{-}MW/WD}$ = 0.18; $avgTR_{HST\text{-}TD}$ = 0.26; $avgTR_{HST\text{-}MT}$ = 0.26); differences in mean values of the thickness ratio of HSTs in valley fills across different present-day hydrodynamic regimes are not statistically significant (one-way ANOVA: F(2,16) = 0.52, P-value = 0.602).

For architectural elements accumulated during the highstand and forming HSTs within incised-valley fills, the proportion of tide-dominated elements is on average higher in incised-valley fills associated with present-day tide-dominated conditions (e.g., Palaeo-Arakawa valley, Palaeo-Nakagawa valley, Palaeo-Tokyo valley in Japan; Qiantang valley in China) or mixed-energy tide-dominated conditions (e.g., Gironde estuary in France), compared to valley fills associated with increased dominance of wave processes ($avgP_{TD}$ = 0.73; $avgP_{MT}$ = 0.60; $avgP_{MW/WD}$ = 0;.00 Fig. 4.13B). For example, according to the classification of Davis and Hayes (1984), the Qiantang incised valley (China; case study 83 in Table 4.1), now a drowned-valley estuary, is currently subject to tide-dominated conditions at the modern shoreline. The HST of the valley fills is characterized by a tide-dominated estuary that contains a tidal sand-bar complex. In the HSTs of incised-valley fills associated with present-day mixed-energy to fully wave-dominated conditions, the proportion of wave-dominated elements is on average higher compared to that in valley-fills associated with present-day fully tide-dominated conditions or mixed-energy tide-dominated conditions ($avgP_{MW/WD}$ = 0.86; $avgP_{MT}$ = 0.17; $avgP_{TD}$ = 0.08).

For coastal-plain incised valleys, relationships are also investigated between valley-fill width and present-day hydrodynamic regimes (Fig. 4.14). A positive correlation is seen between incised-valley-fill width versus present-day mean tidal range at the shoreline (r = 0.654, P-value <0.001; Fig. 4.14A). A very weak negative correlation is seen between incised-valley-fill width versus present-day mean wave height at the shoreline (r = -0.256, P-value = 0.111; Fig. 4.14B). The width of valley fills in

tide-dominated or mixed-energy tide-dominated conditions is on average higher than that associated with valley fills in mixed-energy wave-dominated or fully wave-dominated conditions ($avgW_{TD}$ = 27511 m; $avgW_{MT}$ = 22247 m; $avgW_{MW}$ = 10968 m; $avgW_{WD}$ = 4556 m; Fig. 4.14C); differences in mean values of incised-valley-fill width across different present-day hydrodynamic regimes are statistically significant (one-way ANOVA: F(3,29) = 7.24, P-value = 0.001).

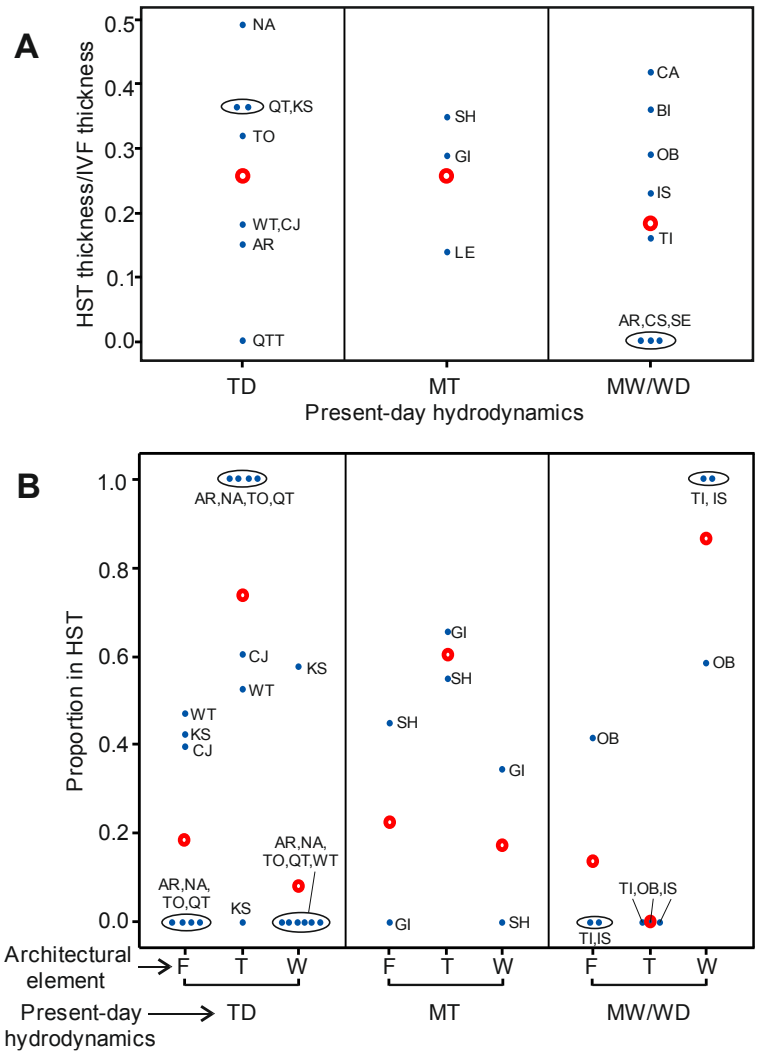

Fig. 4.13. *Individual-value plot of thickness ratios of HSTs in coastal-plain valley fills (A) and of the proportion of architectural elements (Scheme 2; F: fluvial-dominated deposits; T: tide-dominated deposits; W: wave-dominated deposits) in the HST of coastal-plain incised-valley fills (B) for different hydrodynamic regimes at modern shorelines (TD: tide dominated; MT: mixed tide dominated; MW: mixed wave dominated; WD: wave dominated). Red open circles represent mean values. The text label near each individual value denotes the valley fill as follows: GI = Gironde estuary, France; OB = Ombrone valley, Italy; TI = Tiber valley, Italy; AR = Arno valley, Italy; SE = Serchio valley, Italy; CS = Camaiore-Stiava valley, Italy; BI = Biferno upper valley, Italy; LE = Leyre valley, France; CA = Calcasieu valley, USA; CJ = Changjiang valley, China; QT = Qiantang valley, China; QTT = Qiantang-Taihu valley, China; AR = Palaeo-Arakawa valley, Japan; NA = Palaeo-Nakagawa valley, Japan; TO = Palaeo-Tokyo valley, Japan; KS = Kushiro plain valley, Japan; SH = Song Hong valley, Vietnam; IS = Isumi valley, Japan; WT = Weiti valley, New Zealand.*

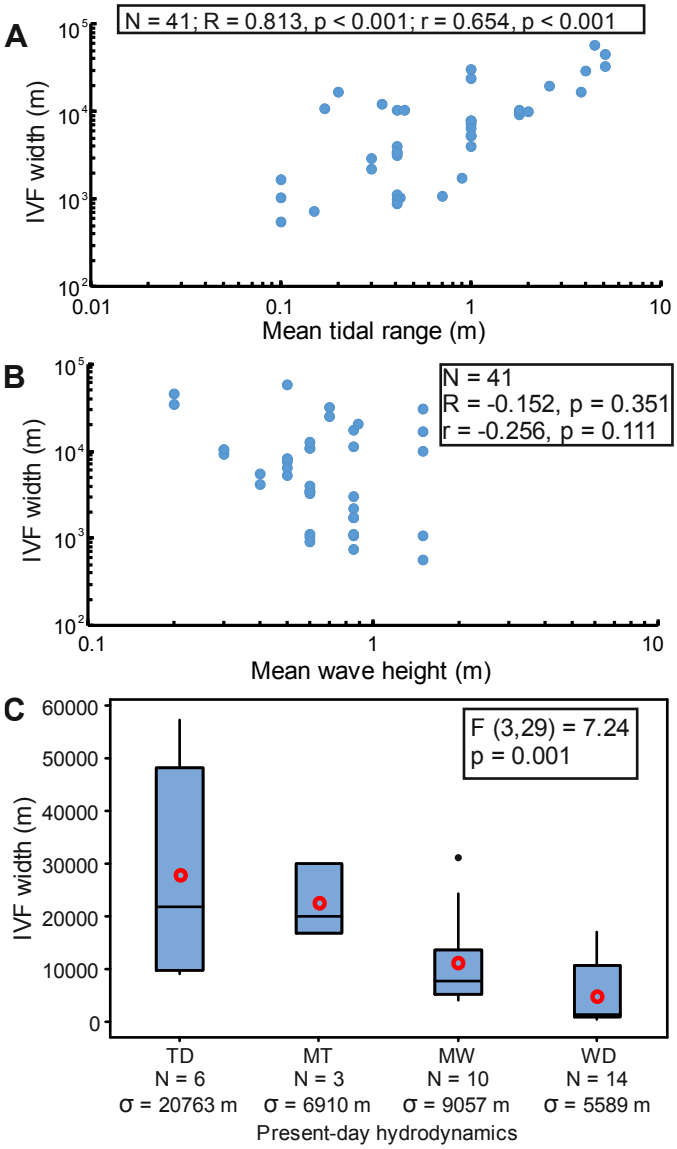

Fig. 4.14. *(A, B) Cross-plots of incised-valley-fill width versus mean tidal range (A) and mean wave height (B) at the modern shoreline. For each pair of variables, the correlation coefficients and P-values are reported in respective boxes. 'N' denotes the number of readings, 'R' denotes Pearson's R, and 'r' denotes Spearman's rho. (C) Box plot of distributions of incised-valley-fill width for different present-day hydrodynamic regimes (TD: tide dominated; MT: mixed tide dominated; MW: mixed wave dominated; WD: wave dominated). For each box plot, boxes represent interquartile ranges, red open circles represent mean values, horizontal bars within the boxes represent median values, and black dots represent outliers (values that are more than 1.5 times the interquartile range). 'N' denotes the number of readings. 'σ' denotes the standard deviation. The results of one-way ANOVA are reported in the box in part C, as: F-value (degrees of freedom between and within groups in brackets), P-value.*

4.5 Discussion

4.5.1 Comparison with previously published models

A comparison of the studied late-Quaternary examples with generic facies models for incised-valley fills (e.g., Dalrymple et al., 1992; Zaitlin et al., 1994) and with a model proposed for the Gironde estuary in France (Allen and Posamentier, 1994b) highlights what aspects of the models are, or are not, supported by observations in late-Quaternary examples.

In both the coastal-plain and cross-shelf incised-valley fills studied in this work, the TST represents the largest part of the fills (Fig. 4.5A and 6A). Coastal-plain valley fills (cf. the 'middle segment' in Zaitlin et al., 1994) are typically characterized by fluvial deposits in LSTs and estuarine bay/lagoon deposits in TSTs, capped by non-bay deltaic deposits or bayhead delta deposits in HSTs (Fig. 4.5). Cross-shelf valley fills (cf. the 'outer segment' in Zaitlin et al., 1994) are typically characterized by fluvial deposits in LSTs and estuarine bay/lagoon deposits in TSTs, capped by condensed open-shelf deposits in HSTs (Fig. 4.5). Observations of stratigraphic organization in the studied late-Quaternary examples support the classical facies models for incised-valley fills as a representative base case (Dalrymple et al., 1992; Zaitlin et al., 1994; Allen and Posamentier, 1994b).

However, the internal fills of valleys incised into modern shelves display significant variability in facies architecture (Fig. 4.15C; cf. Chaumillon et al., 2008) and differ in two ways from the studied coastal-plain valleys and from what is represented in the models.

First, the studied cross-shelf incised-valley fills are characterized by a higher proportion of lowstand deposits, compared to the studied coastal-plain valley fills (Fig. 4.5A and 6A). Specifically, in the palaeo-Chao Praya valleys (Case study 67, Table 4.1; Reijenstein et al., 2011) on the Sunda shelf, LST fluvial deposits make up the largest portion of the valley fills, and are only capped by relatively thin TST estuarine mud deposits. In the Changjiang-Qiangtangjiang incised valley of the East China Sea shelf (Case study 83 in Table 4.1; Wellner and Bartek, 2003), LST fluvial deposits represent the largest part of the valley fills, capped by limited HST tidal-bar complex deposits. Transgression within this valley fill is only recorded by ravinement. These characteristics also contrast with the limited LST fluvial deposits depicted in existing models for the seaward portion of incised-valley fills (Zaitlin et al., 1994; Allen and Posamentier, 1994b). There may be two reasons for this difference. Firstly, some of the valleys in this study are fed by large river systems, with extensive catchments arising from the amalgamation of the drainage areas of rivers that join on the shelf. Thus, these large rivers, which are associated with

large drainage areas and maximum bankfull depths, can generate thicker channel belts, bars and channel fills (Fielding and Crane, 1987; Bridge and Mackey, 1993; Shanley, 2004; Fielding et al., 2006; Gibling, 2006; Blum et al., 2013); this, in turn, can translate to thicker LST fluvial deposits within valley fills. Furthermore, the gradient of shelves that occur offshore of river-dominated coasts is in part determined by the profile of the rivers traversing it at lowstand, and larger fluvial systems are associated with lower channel gradients (Wood et al., 1993; Burgess et al., 2008; Blum and Womack, 2009; Olariu and Steel, 2009; Sømme et al., 2009a and 2009b; Helland-Hansen et al., 2012; Blum et al., 2013). Thus, larger valleys, being fed by larger river systems, are generally associated with lower-gradient shelves on which the shoreline can migrate rapidly in response to transgression. This could cause any high-energy environment (wave and/or tide dominated environment) at the shoreline to rapidly backstep along the path of extant cross-shelf incised valleys, therefore minimizing the impact of potential erosion of fluvial deposits.

Second, compared to the studied coastal-plain examples, the studied cross-shelf incised-valley fills are characterized by a higher proportion of shelf deposits (Fig. 4.5A and 6A). Some incised valleys hosted on the shelf had not yet been filled completely by sediments when the transgressive shoreline backstepped over them, or were excavated again during transgression, leading to the filling of the relict accommodation with open-marine deposits (Simms et al., 2010). Depending on the dominant shelf process responsible for filling the valley, the nature of the infills of these valleys (Fig. 4.15C) can vary, and can include, for instance, the preserved products of shelf dunes (Case study 49 in Table 4.1; Payenberg et al., 2006), of sediment gravity flows (Thieler et al., 2007), or offshore muds (Case study 67 in Table 4.1; Reijenstein et al., 2011). Specifically, the incised-valley fill hosted on the outer shelf in Hervey Bay, on the Pacific coast of Australia (Case study 49 in Table 4.1; Payenberg et al., 2006), is thought to be entirely filled by the deposits of shelf sand dunes, developed under the influence of strong tidal currents prevailing on the modern shelf. This valley fill is distinctively different from the fluvial- to estuarine-filled system presented by the general valley-fill models for the seaward portion of incised valleys (Dalrymple et al., 1992; Zaitlin et al., 1994; Allen and Posamentier, 1994b).

The general stratigraphic organization of the studied incised-valley fills is consistent with what is depicted qualitatively in classical facies models (e.g., Dalrymple et al., 1992; Zaitlin et al., 1994; Allen and Posamentier, 1994b), which reflect the primary control of sea level. However, overall, based on a large composite dataset, this synthesis demonstrates the internal fills of incised valleys are characterized by

significant variability in stratigraphic architectures (Fig. 4.15; cf. Chaumillon et al., 2008; 2010), which is not accounted for by these models. Variations in the facies architecture of coastal-plain and cross-shelf valley fills can be attributed to controls other than relative sea-level change, such as tectonic setting (continental-margin type), basin physiography, catchment area, river-system size and shoreline hydrodynamics. In the following section, these controls are discussed in detail.

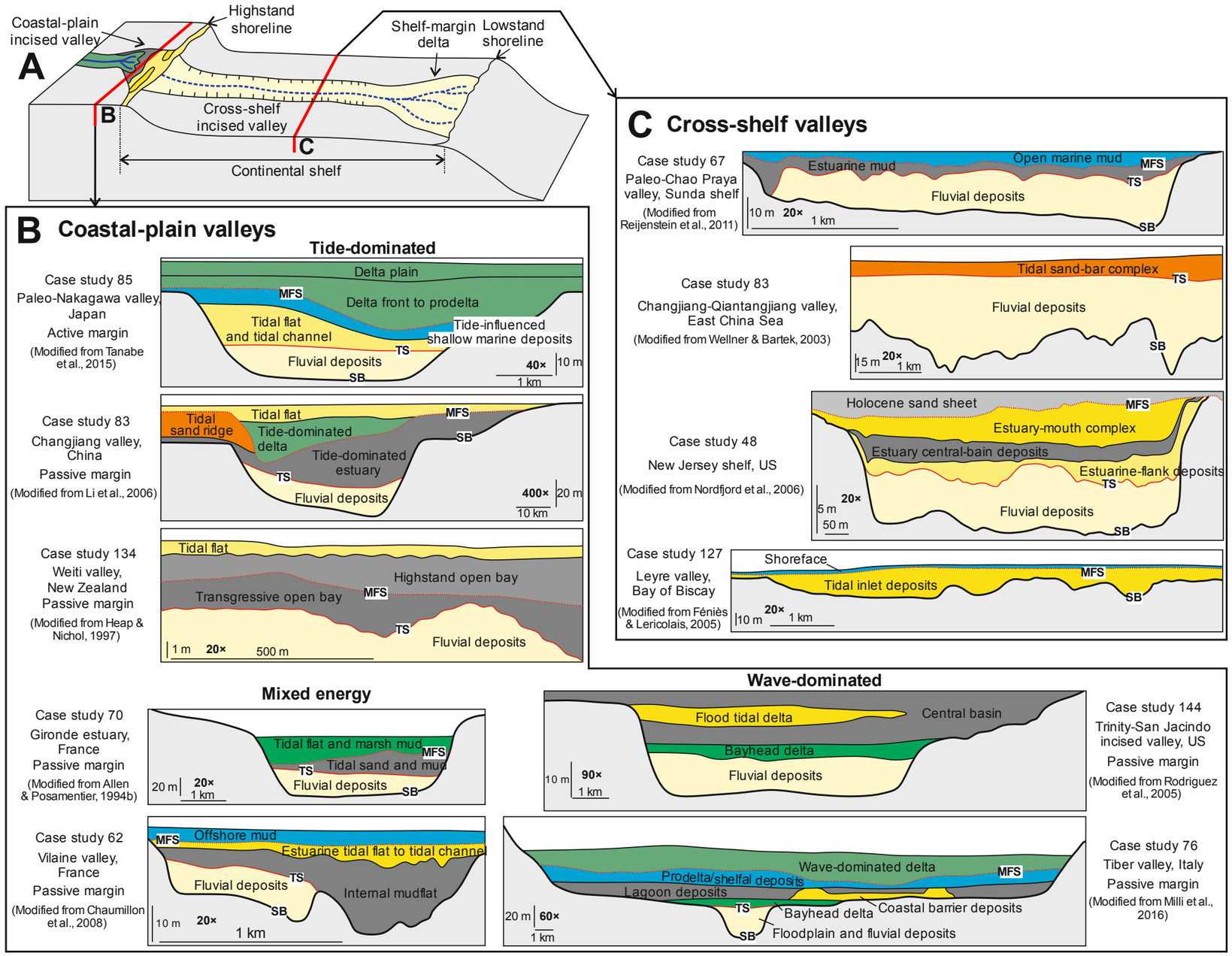

***Fig. 4.15**. Example stratigraphic architectures of incised-valley fills, illustrating the variability observed along strike-oriented cross sections for some of the late-Quaternary coastal-plain (B) and cross-shelf (C) valley fills considered in this work. In (B), the examples for coastal-plain valley fills are grouped by classes of present-day hydrodynamic regimes at the shoreline; continental-margin types are also indicated. Key sequence-stratigraphic bounding surfaces (SB, TS and MFS) are shown for examples for which sequence-stratigraphic interpretations were presented in the original source work. SB denotes the sequence boundary, TS denotes the transgressive surface, and MFS denotes the maximum flooding surface.*

4.5.2 Controls on the internal fills of incised valleys

4.5.2.1 Continental-margin type

Incised-valley systems are likely to record variations in sediment yield, sediment supply, and resulting shoreline progradation rates and rates at which drowned-valley estuaries undergo continentalization (Dalrymple, 2006; Wilson et al., 2007; Clement et al., 2017; Clement and Fuller, 2018), which themselves might be expected to vary characteristically across types of continental margins. The results presented in this study (Fig. 4.7A) indicate that a higher proportion of fluvial deposits and a lower proportion of central-basin estuarine deposits are observed in incised-valley fills hosted on active margins compared to those on passive margins. These observations contrast with the fact that passive margins are typically associated with larger rivers (Syvitski and Milliman, 2007; Sømme et al., 2009a), and are therefore usually associated with (i) higher rates of sediment supply (Syvitski and Milliman, 2007; Blum et al., 2013), which control shoreline progradation rates, and (ii) with larger maximum bankfull depths, which translate to thicker channel belts, bars and channel fills (Fielding and Crane, 1987; Bridge and Mackey, 1993; Shanley, 2004; Fielding et al., 2006; Gibling, 2006; Blum et al., 2013). An explanation of this inconsistency appears elusive. The lower proportion of central-basin deposits within incised-valley fills along active margins could be explained by the nature of sediment load carried by the respective river systems. River systems along passive margins are generally larger than their active-margin counterparts, and tend to carry high suspended-sediment load, which can feed estuaries and be deposited as fluid muds around the turbidity maximum (e.g., Portela et al., 2013; Carlin et al., 2015).

Previous work (Wang et al., 2019) has demonstrated that incised-valley fills along active margins tend to be thicker and wider on average than those along passive margins. This may be seen because active margins are generally associated with higher-gradient shelves, resulting in larger differences between the shelf gradient and the lowstand fluvial equilibrium profile, which in turn favours deeper fluvial incision for a given sea-level fall (Schumm and Brackenridge, 1987; Leckie, 1994; Posamentier and Allen, 1999). Moreover, active margins are generally associated with high specific sediment yield and rivers that drain active margins tend to have a high bedload-to-suspended-load ratio (Milliman and Syvitski, 1992), which promotes more rapid attainment of equilibrium profiles (Dietrich and Whiting, 1989; Sheets et al., 2002; Peakall et al., 2007; Martin et al., 2011; Blum et al., 2013); a tendency to reach equilibrium more easily might therefore result in fluvial incision being deeper, on average, than what is typical for passive-margin valleys. The observation that estuarine bay/lagoon elements are thicker on average in incised-

valley fills along active margins than in those along passive margins (Fig. 4.7B) might arise because valleys along active margins, by being more deeply incised on average, will also tend to host greater accommodation. This might favour the development of thicker estuarine bay/lagoon elements within valley fills on active margins. The results suggest that continental margin types exert an indirect effect on the geometry of estuarine bay/lagoon element within incised-valley fills through a control on valley morphology.

Results from this study suggest that the type of continental margin might be taken as a predictor of the internal fills of incised valleys, likely because of the effects of the tectonic setting on basin physiography, rates and mode of sediment supply, and nature of sediment load. This view is in part supported by the result of principal component analysis (see Supplementary information; text and Fig. 4.17A) applied to a limited dataset of 30 IVFs for which eight variables can be constrained; this analysis indicates that overall the studied IVFs tend to display differences in the studied variables that map onto the type of continental margin on which they are hosted.

4.5.2.2 Shelf physiography

The development of barrier islands that can be stranded on the shelf during TST tend to develop in association with stadials during deglaciation, i.e., in relation with periods of negligible or slow rates of relative sea-level rise known as stillstands or slowstands (e.g., Cooper, 1958; Cooper, 1991; Trincardi et al., 1994; Storms et al., 2008; Salzmann et al., 2013). Preservation of these barrier islands on the shelf during transgression is believed to be facilitated by factors such as rapid sea-level rise after stillstands (e.g., Storms et al., 2008; Salzmann et al., 2013), early cementation of the barrier form (Gardner et al., 2005, 2007; Salzmann et al., 2013; Green et al., 2013a, 2014), and gentle antecedent shelf gradient and reduced wave-energy (Cooper et al., 2016; Storms et al., 2008). Rapid sea-level rise after stillstands is shown to be conducive to the preservation of barrier-island deposits (Belknap and Kraft, 1981; Forbes et al., 1995; Storms et al., 2008; Salzmann et al., 2013). Rapid sea-level rise is typically associated with only limited reworking or breakdown of the barrier form during ensuing transgressive ravinement (Storms et al., 2008; Salzmann et al., 2013; Cooper et al., 2016). Antecedent shelf gradient is also shown to be a control on the preservation of barrier islands (Storms et al., 2008; Salzmann et al., 2013; Pretorius et al., 2016; Green et al., 2018). Cattaneo and Steel (2003) point out that, given the same unit of time of relative sea-level rise, the effects of erosion at the shoreline across high-gradient shelves is much greater than that across low-gradient shelves during ensuing transgressive ravinement,

resulting in severe reworking or breakdown of the barrier systems. This is because the shoreline does not translate over a large distance for the same amount of sea-level rise and erosion is therefore focussed over a shorter profile for the same unit of time (Davis and Clifton, 1987). However, the results of this study (Fig. 4.12) challenge the applicability of this notion to incised-valley systems, as positive correlations are observed between the thickness and proportion of barrier-complex deposits within incised-valley fills versus the average shelf gradient in the last sea-level cycle. Previous work documents that equilibrium in sandy shorelines is attained over timescales of 10^2 to 10^3 years (Cowell and Thom, 1994; Stive and de Vriend, 1995). For a given relative sea-level change, horizontal shoreline shifts increase in magnitude with decreasing shelf gradient. Thus, compared to lower-gradient shelves, any high-energy environment located in the area of the coastline across steeper-gradient shelves will stabilize at a location for longer periods during episodes of negligible or slow rates of relative sea-level rise, potentially promoting accumulation of barrier-complex deposits within cross-shelf valleys (e.g., Posamentier, 2001; Reijenstein et al., 2011; Wetzel et al., 2017). The control by shelf gradient on transgression also plays an indirect role on the erodibility of barrier deposits when accompanied with climate. It has been proposed (Frankel, 1968; Hopley, 1986; Moore, 2001; Vousdoukas et al., 2007; Cawthra and Uken, 2012) that the rates of shoreline cementation in warm tropical or sub-tropical climates can be particularly rapid, occurring on a scale of months to decades. Hence, longer periods of early cementation of the barriers along steeper shelves, prior to barrier overstepping, might make the barrier deposits more resistant to erosion during ensuing transgressive ravinement. Positive correlations between both the thickness and proportion of barrier-complex elements versus the average shelf gradient (Fig. 4.12) support the idea that the shelf gradient plays a role in controlling the establishment and preservation of barrier-complex deposits within incised valleys hosted on the shelf. However, these observations are based on limited data (N = 9 for the thickness of barrier-complex elements and N = 14 for the proportion of barrier-complex elements) and thus any conjecture on the effective role of shelf gradient on the development and preservation of barrier-complex deposits within valley fills needs to be substantiated through further study. Additionally, expected relationship between shelf gradient and characteristics of barrier-complex deposits in incised-valley fills might be masked by overriding factors, such as early cementation controlled by palaeo-climates, or wave and tide energy regimes, or by the fact that the present-day average shelf gradient does not approximate the local shelf gradient established during transgression.

Positive correlations between the proportion of estuarine bay/lagoon elements versus the average shelf gradient (Fig. 4.12B) are attributed to the fact that steeper

shelves could result in larger difference between shelf gradient and the fluvial equilibrium profile and therefore should tend to drive deeper fluvial incision for a given relative sea-level fall (Schumm and Brackenridge, 1987; Leckie, 1994; Posamentier and Allen, 1999; Wang et al., 2019), thereby providing increased accommodation for estuarine bay/lagoon deposits that can be preserved in incised valleys. Thus, the shelf gradient may exert an indirect control on the development and preservation of the geometry of estuarine bay/lagoon deposits within cross-shelf incised valleys through its effects on incised-valley dimensions and the resultant accommodation space.

4.5.2.3 Catchment and river-system size

Positive correlations between the thickness or proportion of LST deposits versus incised-valley-fill dimensions (Fig. 4.8) might reflect how these parameters tend to co-vary in relation to a common control exerted by the size of drainage areas. Previous work (Mattheus et al., 2007; Mattheus and Rodriguez, 2011; Phillips 2011; Wang et al., 2019) has demonstrated that the size of incised valleys shows positive correlation with the size of their drainage basins. Water discharge, which is positively correlated with drainage-basin area (Syvitski and Milliman, 2007), controls the maximum bankfull depth of a river. Hence, river size and the geometry of fluvial deposits (thickness of barforms, channel fills and channel belts) are expected to be scaled to drainage-basin area. Positive scaling relationships between drainage-basin area, water discharge, single-storey channel-belt sand-body thickness (channel-fill or barform thickness), and river size are recognised in studies based on late-Quaternary examples (Blum et al., 2013), compilation of ancient channel-belt scales from published literature (Gibling, 2006) and regional case studies (e.g., Shanley, 2004; Fielding et al., 2006). Thus, these results might reflect the fact that the development of valleys having larger drainage basins and characterized by higher bankfull discharges will tend to be filled by thicker fluvial deposits preserved in LSTs. It needs to be considered, however, that relationships between the thickness and proportion (thickness ratio) of LST deposits in incised-valley fills and the size of the valley catchments – albeit positive – are modest and not statistically significant (Table 4.3).

Sedimentation associated with the TST takes place when accommodation is being created at its fastest rate by relative sea-level rise. Positive correlation between the thickness of TST deposits versus incised-valley-fill thickness (Fig. 4.8A) can be explained by the fact that deeper valleys will be more likely to record the full expression of a TST and to contain maximum flooding surfaces within their confines. However, this interpretation is at odd with the fact that no significant

difference exists between the thickness distributions for incised-valley fills that contain HST deposits compared to those that were overfilled and/or ravined during transgressions and do not contain HST deposits.

Positive correlations between the thickness of fluvial deposits versus incised-valley-fill dimensions (Fig. 4.9A to C) might reflect how these variables are expected to co-vary in relation to a common control exerted by the size of drainage areas. The results suggest that the thickness of fluvial deposits in valley fills might reflect the thickness of channel belts, which is itself controlled by the size of their drainage-basin areas.

Based on studies of the internal fills of modern estuaries in New Zealand (e.g., Heap and Nichol, 1997; Wilson et al., 2007; Abrahim et al., 2008; Kennedy et al., 2008; Clement et al., 2017), it has been proposed that shallower estuaries are more easily backfilled than deeper ones, especially when they are coupled with river systems with high sediment supply, such that the relatively restricted space within valley fills tends to limit the development of deeper central-basin environments (estuarine bay/lagoon deposits), where fine-grained sediments accumulate. Additionally, large river systems associated with low-gradient coastal plains – typical of passive margins – are prone to carrying substantial suspended-sediment load when they reach the sea (Milliman and Syvitski, 1992). These fine-grained sediments can feed estuaries and be deposited as fluid muds around the turbidity maximum (e.g., Portela et al., 2013; Carlin et al., 2015), especially if tidal processes are important (e.g., Dalrymple et al., 2012). Positive relations between the thickness of estuarine bay/lagoon elements versus incised-valley-fill dimensions and drainage-basin area (Fig. 4.9A to C) support these expectations only to a certain degree, as the thickness of the valley may not necessarily be a good proxy for the depth of the estuary during TST or HST. The results suggest that both drainage-basin area and incised-valley geometry could act as factors that control the accumulation of estuarine deposits preserved within incised valleys.

Positive correlations between the thickness of bayhead-delta deposits versus drainage-basin area (Fig. 4.9C) could possibly reflect the fact that more rapidly prograding bayhead deltas associated with larger river systems will have advanced into deeper parts of their estuaries. However, this interpretation carries significant uncertainty as the 3D geometry of bayhead delta deposits is not typically characterized, and packages of bayhead-delta deposits may incorporate vertically amalgamated lobes that cannot be resolved in core.

Overall, the size of drainage areas appears to control the thickness of fluvial deposits, of bayhead-delta deposits and of estuarine bay/lagoon deposits in incised-valley fills (Fig. 4.9A to C) through its effects on water discharge, sediment

supply, the character of sediment load and in-valley accommodation related to incised-valley geometry.

4.5.2.4 Shoreline hydrodynamics

4.5.2.4.1 Control of hydrodynamic conditions on sedimentation

Hydrodynamic conditions at the shoreline control the deposition and preservation potential of sedimentary bodies in estuaries (Tessier et al., 2010a and b; Menier et al, 2010; Proust et al, 2010; Ferrer et al., 2010; Tessier, 2012). Wave-dominated estuaries are typically characterized by a barrier beach and a tidal-inlet complex at their mouth, passing landward into central-basin muds and bayhead delta deposits (Dalrymple et al., 1992; Zaitlin et al., 1994; Ferrer et al., 2010; Tesson et al., 2010). Tide-dominated estuaries are typically characterized by tidal sandbars that grade to mudflats and salt marshes up-estuary (Dalrymple et al., 1992; Zaitlin et al., 1994; Tessier, 2012). In highstand deposits, the observation of higher proportions of tide-dominated elements (e.g., tidal flat and tidal channel, tidal sand-bar complex, tidal inlet and flood tidal delta subenvironment) in valley fills associated with full or mixed-energy tide-dominated conditions than in those with more wave-dominated conditions (Fig. 4.13B) indicates the expected increased dominance of tidal processes on sedimentation. Likewise, higher proportions of wave-dominated elements (e.g., nearshore, barrier complex sub-environments) in valley fills associated with full to mixed-energy wave-dominated conditions than in those with more tide-dominated conditions (Fig. 4.13B) indicate the expected increased dominance of wave processes on sedimentation. The results (Fig. 4.13B) likely reflect the importance of hydrodynamic processes in determining the types of sub-environments recorded as sedimentary bodies in the HST of coastal-plain incised-valley fills.

Based on the synthesis of data from 10 incised valleys that occur along the Mediterranean and Atlantic coasts of France, Chaumillon et al. (2010) argued that within the outer segments of the valley fills (cross-shelf valley fills, in this paper), the HST to TST ratio increases from wave-dominated to tide-dominated settings because of the deeper wave base offshore wave-dominated coasts. Chaumillon et al. (2010) also proposed that in the middle segments of the valley fills (coastal-plain valley fills, in this paper), the thickness of HSTs does not vary significantly across different hydrodynamic regimes, despite differences seen in the types of sub-environments incorporated in the HST of valley fills under different hydrodynamic conditions. Our data (Fig. 4.13A) support the claim made by Chaumillon et al.

(2010) for coastal-plain valley fills, but any interpretation is highly uncertain, as the dataset is limited (N = 19).

4.5.2.4.2 Control of hydrodynamic conditions on IVF geometry

With regards to the relationship between incised-valley-fill width and present-day hydrodynamic regimes, Mattheus and Rodriguez (2011) argued that bay-ravinement, or estuarine shoreline erosion, which is controlled by the imposing energy regime of waves and tides, can lead to the widening of incised valleys. However, our data (Fig. 4.14) do not fully support this idea, as no apparent correlation is seen between incised-valley-fill width versus mean wave height at modern shorelines. This might arise because wave ravinement tends to truncate the topmost part of the interfluves of some incised valleys, where each valley is expected to have been widest (Fig. 4.16A); this fact might counteract the effects of any widening of the incised valleys by wave erosion. This discrepancy might also arise from the fact that the present-day hydrodynamic conditions at the shoreline may not be representative of those that existed during the late TST or due to the influence of other factors such as catchment size, vegetation, substrate and climate.

Positive correlation between incised-valley-fill width versus present-day mean tidal range at the shoreline (Fig. 4.14A) could be explained by the fact that tidal ravinement might drive erosion of valley margins, which promotes the widening of the incised valleys (Fig. 4.16B).

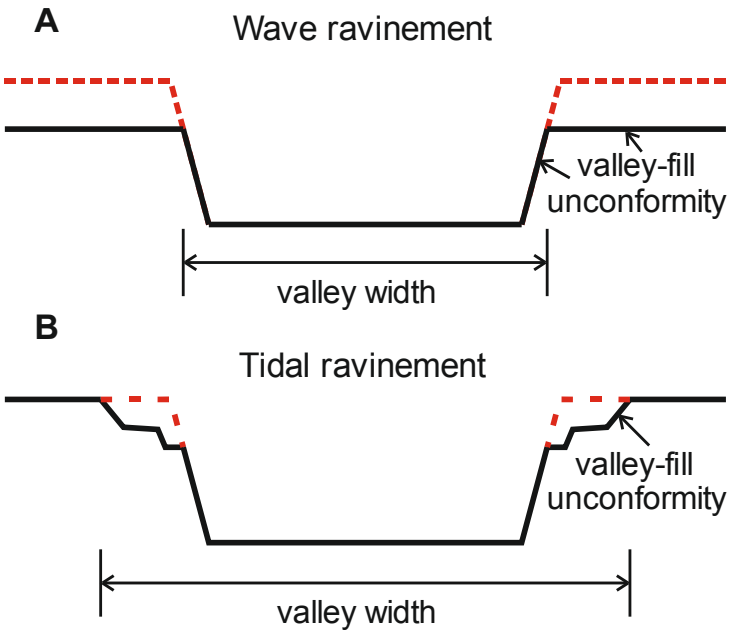

Fig. 4.16. *Schematic diagrams illustrating the evolution of valley width in response to wave ravinement (A) and tidal ravinement (B). Red dashed line denotes the pre-ravinement valley shape.*

4.5.2.4.3 Control of IVF geometry on hydrodynamic conditions

The geometry of incised valleys being flooded has also been recognized as a factor controlling the internal fills of incised valleys through its control on hydrodynamic conditions (Dalrymple et al., 1992; Chaumillon et al., 2010; Nordfjord et al., 2006). The tidal prism at any location is a function of the shape of the drowned-valley estuaries, their geographic orientation, shelf geometry, tidal resonance, which itself is determined by shelf width and shelf depth, and frictional forces (Luketina, 1998; Hume, 2005; Davis et al., 2009). Generally, funnel-shaped valleys tend to enhance the amplification of tidal waves and thus the occurrence of tide-dominated conditions (Dalrymple et al., 1992; Chaumillon et al., 2010; Tessier et al., 2012). Based on observations of seismic data of late-Quaternary incised-valley fills on the New Jersey shelf, Nordfjord et al. (2006) argued that narrower and deeper valleys should promote the development of tide-dominated environments, whereas broader valleys might be, comparatively, more dominated by wave processes. However, our observations (Fig. 4.10) do not support the assumption made by Nordfjord et al. (2006). Positive correlation between incised-valley-fill width and the proportion of tide-dominated elements (Fig. 4.10B) might reflect how these two variables co-vary in response to a common control exerted by the present-day hydrodynamic regime (mean tidal range) at the shoreline (Fig. 4.13B and Fig. 4.14A). This observation (Fig. 4.10B) could also be explained by the fact that wider valleys with gentler

gradient, generally associated with larger rivers, will tend to have larger tidal prism and thus experience stronger tidal currents. Furthermore, for narrow and linear valleys, tidal flow tends to be dampened by friction on the valley margins and tidal-wave energy is dissipated by diffraction. Thus, our observations (Fig. 4.10B) can be seen to support the idea that the influence of valley geometry on tides leaves a distinct sedimentary record; else, they reflect the control of present-day mean tidal range at the shoreline on incised-valley-fill width. However, this interpretation carries uncertainty, as the present-day incised-valley-fill geometry is in part used as a proxy for the valley geometry through time, ignoring temporal variations in valley geometry (cf. Blum and Price, 1998; Rodriguez et al., 2008; Blum et al., 2013).

No or weak correlations are seen between the proportion of wave-dominated elements in IVFs and parameters that describe the IVF geometry. However, detailed descriptors of the planform shape of the valley and of the morphology of the bedrock, which might affect the extent to which an IVF could be exposed to wave action, were not considered in this work.

4.5.2.4.4 Control of basin physiography on hydrodynamic conditions

Other authors (Healy and Werner, 1987; Healy and Harada, 1991b) have proposed that, compared to open-ocean-facing settings, the coasts of enclosed or semi-enclosed seas generally experience lower hydrodynamic energy. This is especially true for coasts characterized by offshore topographic sills that can shelter the shorelines. Enclosed or semi-enclosed seas are generally characterized by more restricted fetch, lower wave heights, and lower tidal range. Our observations (Fig. 4.11) are compatible with the idea that the type of coastal physiography and size of the sea into which a valley discharges could act as controls on the internal fills of coastal-plain incised valleys, since variations in the record of dominant depositional processes are seen in the valley fills that are consistent with differences in hydrodynamic conditions across these settings.

Wave energy at the shoreline depends largely on deep-water wave energy, the water depth of the basin and the frictional attenuation that occurs on the shelf (Reading and Collinson, 1996). This frictional attenuation is determined by the gradient of the sea floor, which itself is a function of the nature and width of the shelf and the rate and type of sediment supply to the nearshore zone. Positive correlations between mean wave height and shelf-break depth and between the proportion of wave-dominated elements in IVFs and the average shelf gradient (Table 4.6) could be explained by the fact that the shorelines of shallower shelves tend to be subject to lower wave energy.

4.6 Conclusions

A database-driven statistical analysis of 87 late-Quaternary incised-valley fills has been undertaken, to assess the general validity of classical facies models that remain widely employed as predictive tools, and investigate the relative importance of different controls on the stratigraphic organization of incised-valley fills. The main findings are summarized as follows.

(i) The general stratigraphic organization of the studied coastal-plain incised-valley fills is consistent with what represented in classical facies models, but significant variability in stratigraphic architectures is seen.

(ii) Compared to the studied coastal-plain valleys, the internal fills of valleys incised into modern shelves are characterized by a higher proportion of lowstand deposits and a higher proportion of open-shelf sediments.

(iii) Compared to valley fills hosted on passive margins, a higher proportion of fluvial deposits, a lower proportion of central-basin estuarine deposits and thicker central-basin estuarine deposits are typically observed in incised-valley fills hosted on active margins; this is interpreted as reflecting a control by the tectonic setting of continental margins on the internal fills of incised valleys, through its effects on basin physiography, rates and mode of sediment supply, and nature of sediment load.

(iv) The thickness or proportion of LST deposits is found to be positively correlated with incised-valley-fill dimensions, likely because of the role of the size of catchment areas and water discharge in dictating the scale of lowstand fluvial systems.

(v) Positive scaling shown by the thickness of fluvial, bayhead-delta, and estuarine bay/lagoon with incised-valley-fill dimensions and valley drainage-basin area suggests that the valley catchment size controls the scale of these deposits, possibly through effects on water discharge, sediment supply, sediment-load type, and incised-valley geometry.

(vi) Positive correlations between the thickness and proportion of barrier-complex deposits within incised-valley fills versus present-day average shelf gradient indicate a possible control by the physiography of the shelf on the establishment and preservation of barrier-island environments within incised valleys.

(vii) The gradient of the shelf may also exert an indirect control on the development and preservation of the geometry of estuarine muds in

cross-shelf valley fills by partly determining depths of incisions and resultant in-valley accommodation.

(viii) Correlations between incised-valley-fill width versus present-day mean tidal range or mean wave height at the shoreline indicate that tidal dynamics at the shoreline may control the widening of the incised valleys. Correlation between the proportion of tide-dominated elements within incised-valley fills and incised-valley-fill width might arise because of reciprocal controls between hydrodynamic conditions and valley geometry.

(ix) Differences in proportion of elements recording different process regimes are seen between valley fills from open-ocean settings and those from enclosed or semi-enclosed seas, which are consistent with differences in hydrodynamic conditions across these settings.

This study is important because it highlights the complexity of the internal sedimentary fills of incised valleys to a level of detail that is not accounted for by the general stratigraphic organization depicted by widely employed traditional facies and sequence-stratigraphic models. This work highlights the role of continental-margin type, drainage-basin area, valley geometry, basin physiography and shoreline hydrodynamics – in addition to the role of relative sea-level stage – in controlling the internal architecture of incised valley fills.

These results can be applied to guide interpretations and attempt predictions of the architecture of ancient paralic successions, in the subsurface and in outcrop. However, all the studied examples are from the late Quaternary, and record relatively high-frequency, high-amplitude changes in sea level: care must therefore be taken when attempting to use these examples as templates for interpreting or predicting the stratigraphic architecture of ancient systems, especially for those developed under greenhouse climates and subject to modest sea-level fluctuations.

4.7 Supplementary information: Multivariate analysis

Several of the variables investigated through bivariate analyses in this work can be interpreted to covary in relation to common controlling factors (e.g., drainage area vs shelf width; cf. Wang et al. 2019). It is therefore desirable to identify variables with similar behaviour, and consider whether all the studied variables can be reduced to a smaller number of interpretable combinations thereof. To attempt a reduction of the dimensionality of the variables and identify their redundancy, two multivariate statistical techniques, principal component analysis (PCA) and

hierarchical cluster analysis (HCA), were performed on coastal-plain IVFs. These analyses involved the following eight variables: shelf width, shelf-break depth, IVF thickness, IVF width, drainage area, mean wave height, mean tidal range and proportion of fluvial deposits in IVFs (Fig. 4.17). Several of the studied variables are intimately associated with the types of continental margin hosting the incised-valley fills (IVFs), and therefore a principal component analysis can also help establish the value of margin types as predictors of characteristics of incised-valley fills and of their geological boundary conditions. However, as the original published datasets vary significantly with respect to the variables that are constrained for each, even selecting a limited number of parameters results in a significant reduction in the number of incised-valley fills that can be employed simultaneously in a multivariate study. Based on the eight selected variables, the dataset employed in the multivariate analyses is limited to 30 IVFs, i.e., only 34% of the 87 examples studied overall.

4.7.1 Methods

Multivariate analyses of database outputs in this section were performed with R (version 3.6.1) (R Core Team, 2019) and Minitab 18.

The principal component analysis (PCA) was performed in R using the built-in function prcomp, and results presented using packages GGBIPLOT (Vu, 2011) and FACTOEXTRA (Kassambara and Mundt, 2017). The original variables were scaled to unit variance. Scores of the first two principal components (PC1 and PC2) for the 30 IVFs are presented in a biplot, together with the loadings of each variable; the contribution of each variable to PC1 and PC2 are presented in bar charts (Fig. 4.17A). In the biplot, the IVFs are colour-coded by continental-margin type.

A correlation matrix of Pearson's correlation coefficients between the variables was represented as a heatmap, produced using the R function cor and plotted using the R package GGPLOT2 (Wickham, 2016). Hierarchical cluster analysis (HCA) of the variables was performed based on these Pearson's correlation coefficients, with complete linkage and correlation coefficient distance, in Minitab 18.

4.7.2 Results

Principal components 1 and 2 (PC1 and PC2) account for 32.8% and 20.9% of the total variance in this dataset, respectively (Fig. 4.17A). The variables that contribute most to PC1 are IVF thickness, mean tidal range, shelf-break depth and IVF width, whereas the variables that contribute most to PC2 are the mean wave height, shelf

width and IVF thickness (Fig. 4.17A). The distribution of the studied examples in the biplot (Fig. 4.17A) indicates that IVFs developed along tectonically passive margins and active margins form two distinct clusters.

The HCA of Pearson's correlation coefficients of the variables (Fig. 4.17B) suggests that the variables that have a relatively more similar behaviour with regards to their relationships with the full set of eight variables are as follows (in this order): the mean tidal range with the IVF width, the mean wave height with the shelf-break depth, and the IVF thickness with the proportion of fluvial deposits in IVFs. However, for the 30 IVFs employed in the PCA and HCA, Pearson's correlation coefficients between variables differ, even markedly in some cases (e.g., mean tidal range vs shelf-break depth, between mean wave height vs shelf width), from the results of bivariate analyses (Fig. 4.17B; Table 4.6).

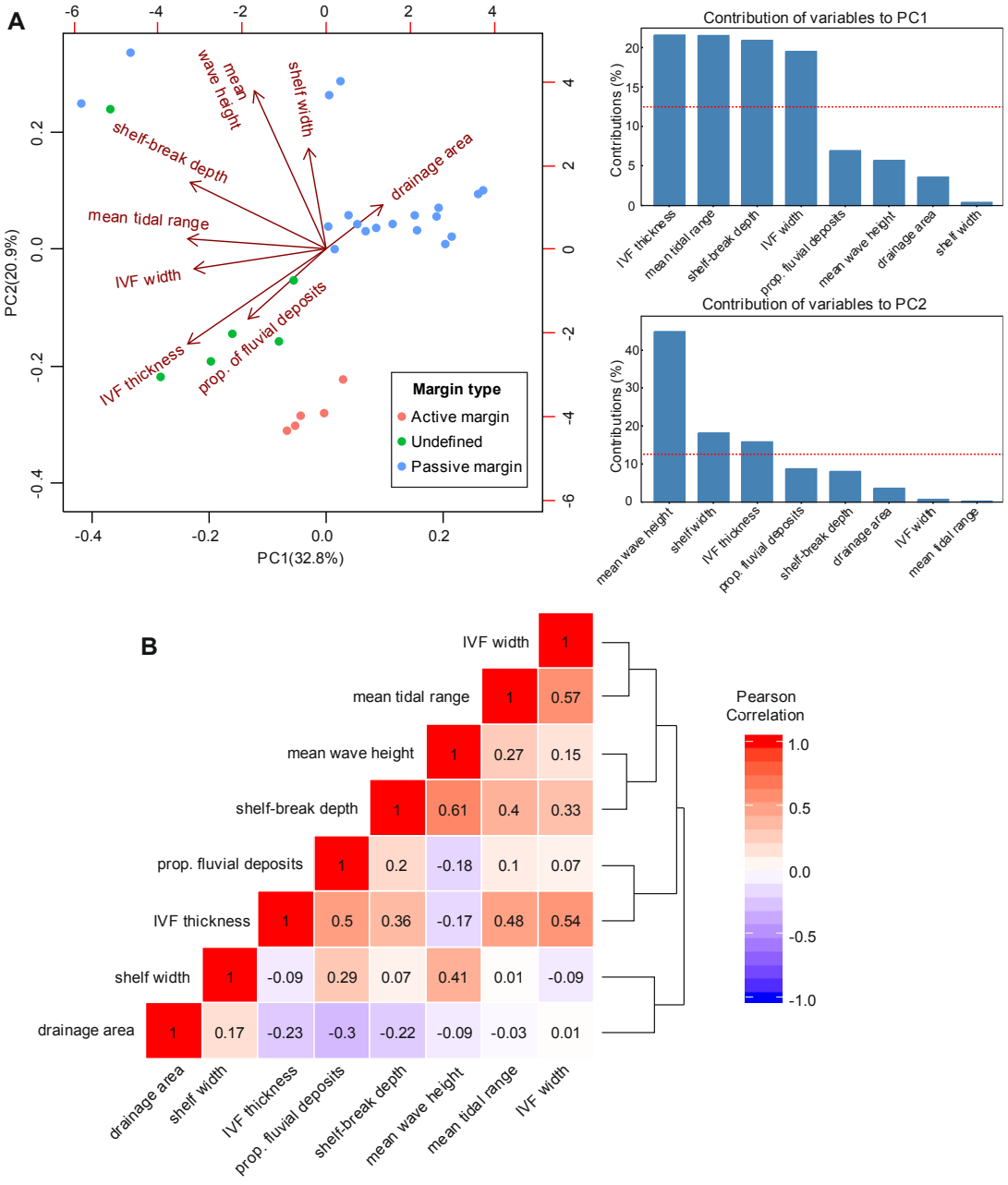

Fig. 4.17. *(A) Biplot of scores of principal components 1 and 2, based on eight variables, for 30 coastal-plain incised valley fills, together with bar charts of the contribution of each variable to PC1 and PC2 respectively. In the biplot, the IVFs are colour-coded by continental-margin type, whereas loadings of the eight variables are presented as arrows. The left and bottom axis labels of the biplot denote the loadings, while the right and top axis labels denote the scores. (B) Correlation matrix heatmap showing Pearson's correlation coefficients between eight variables for 30 coastal-plain IVFs. A dendrogram that summarizes the outcome of a hierarchical cluster analysis is also illustrated on the right-hand side of the heatmap.*

4.7.3 Discussion

The PCA (Fig. 4.17A) indicates that, overall, the studied IVFs tend to display differences in the studied variables that map onto the type of continental margin on which they are hosted. This observation corroborates the idea that the type of continental margins can be taken as a predictor of geological boundary conditions that control the internal fills of incised valleys.

However, the PCA (Fig. 4.17A) only accounts for a limited amount of the total variance in the dataset (53.7%), and the resulting principal components are not readily interpretable in geological terms. Furthermore, some of the correlation coefficients reported in the correlation matrix on which the HCA (Fig. 4.17B) is based, particularly those between mean tidal range and shelf-break depth and between mean wave height and shelf width, differ significantly in magnitude from corresponding coefficients obtained through bivariate analyses of the wider data pool. This discrepancy arises because the multivariate analyses are based on a limited dataset (N = 30). The results of both PCA and HCA should therefore be considered with care.

5 Palaeohydrologic characteristics and palaeogeographic reconstructions of incised-valley-fill systems: Insights from the Namurian successions of the United Kingdom and Ireland

5.1 Summary

Incised-valley fills developed in coastal-plain to continental-shelf regions under icehouse conditions contain sedimentological evidence of the scale of large river systems that existed throughout Earth history and can provide insight into palaeogeographic configurations.

A data synthesis has been undertaken for 18 Namurian (Carboniferous) sandstone-dominated fluvial successions from the United Kingdom and Ireland, interpreted as forming the majority of the infill of cross-shelf incised valleys. The aim is to characterize the palaeohydrology of these ancient river systems and to refine the regional palaeogeographic reconstructions for the basins that hosted them. This is accomplished by quantitative analyses of facies proportions, valley-fill geometry and thickness of dune-scale cross-strata, and with consideration of incised-valley-fill scaling relationships for late-Quaternary systems.

The following main findings arise from this study: (i) the facies organization of the studied valley fills supports the view that their formative palaeorivers were perennial and characterized by relatively low discharge variability, as expected in consideration of the dominantly equatorial humid tropical climate prevailing in the study areas during the Namurian; (ii) observed variations in facies characteristics, including proportions of facies indicative of likely upper- vs. lower-flow-regime conditions and thickness distributions of sets of cross-bedded sandstone, might reflect a control exerted by the size of drainage areas on river hydrology; (iii) integration of the proposed estimations of the size of drainage areas with existing provenance and sedimentological data yields improved understanding of potential source areas, thereby enabling tentative reconstructions of source-to-sink systems, and contributes to the refinement of regional palaeogeographic reconstructions for the Namurian.

The approach illustrated in this work is more widely applicable to the study of palaeohydrologic characteristics and palaeogeographic reconstructions of incised-valley fills globally and through geological time.

5.2 Introduction

Incised valleys are fluvially eroded, elongate palaeotopographic lows that develop in shelf and coastal settings in response to relative sea-level fall, and which tend to be subsequently inundated, infilled and reworked by fluvial, coastal and marine processes during sea-level rise (Posamentier and Allen, 1999; Zaitlin et al, 1994; Blum et al., 2013). Extensive research has been undertaken on both recent and ancient incised-valley-fill successions because of their potential to archive complex sedimentary responses to changes in relative sea level and climate (Boyd et al., 2006; Simms et al., 2010; Mattheus and Rodriguez, 2011), and because of their importance as hosts for natural resources, notably as hydrocarbon reservoirs (Hampson et al., 1999; Stephen and Dalrymple, 2002; Bowen and Weimer, 2003; Salem et al., 2005).

Quaternary incised-valley fills arising as a consequence of icehouse glacio-eustatic cyclicity record incision and infill by trunk rivers that traversed coastal plains extending to continental-shelf margins. The rivers that generated these valleys commonly merged on lowstand shelves, such that their drainage basins amalgamated into alluvial catchments that were, at times, larger than any modern highstand drainage basin. In the rock record, sedimentary bodies interpreted as incised-valley fills and developed primarily under icehouse conditions contain sedimentological evidence of the scale of many large river systems that existed throughout Earth history and can therefore provide insight into palaeogeographic configurations.

In Namurian (late Mississippian [Serpukhovian] to early Pennsylvanian [Bashkirian]) outcropping and subsurface successions of the United Kingdom (UK) and Ireland, thick sandstone-dominated fluvial deposits interpreted as forming the majority of the infill of cross-shelf incised valleys have been well documented. These incised-valley-fill (IVF) successions are interpreted to have developed in response to high-frequency, high-magnitude eustatic sea-level changes in relation to Gondwanan glacial-interglacial episodes (Hampson et al., 1997; Hampson et al., 1999; Davies et al., 1999; Davies, 2008). During the Namurian, a suite of sedimentary basins in the region now occupied by the UK and Ireland existed that was part of a series of linked basins that extended across what is now NW Europe and eastern Canada. The sedimentary infill of these basins occurred at palaeoequatorial latitudes (**Fig. 5.1**), under conditions of overall humid tropical climate (Davies et al., 1999; Davies,

2008). Fifty Namurian, ammonoid-bearing (goniatite) marine bands are identified in successions from this region (**Fig. 5.2**), which provide exceptional stratigraphic resolution (Davies et al., 1999; Davies, 2008; Waters and Condon, 2012). Previous work in Namurian basins of the UK and Ireland (e.g., Bristow and Myers, 1989; Bristow, 1993; Hampson et al., 1999; Ellen et al., 2019) has focused on qualitative analyses of the internal facies architecture of these IVFs, which led these workers to interpret the river systems feeding these IVFs as having low-sinuosity, probably braided, planforms at low-river stage. Provenance studies (e.g., Hallsworth et al., 2000; George, 2001; Hallsworth and Chisholm, 2008; Pointon et al., 2012) are also available for these IVFs, which provide insights regarding the likely source areas and extent of their formative rivers.

However, questions still remain in relation to the palaeohydrology and palaeogeography of these river systems, and such questions can potentially be answered with additional analyses of sedimentological and architectural characteristics of the several examples of IVFs identified in these successions.

In this study, a database-driven synthesis of data from 18 Namurian incised-valley fills from the UK and Ireland has been performed to quantitatively estimate palaeohydrological characteristics of these ancient river systems, and to attempt to refine the regional palaeogeographic reconstructions for the basins that hosted them. Specific objectives of this work are as follows: (i) to decipher palaeohydraulic characteristics from facies proportions and geometry of cross-strata within incised-valley fluvial deposits; (ii) to investigate upstream controls on the facies architecture of incised-valley fluvial deposits; (iii) to illustrate a novel integrated approach to the estimation of the size of drainage areas for deep-time incised-valley fills, based on dune-scale cross-set thickness and incised-valley-fill dimension; (iv) to present how results have implications for regional palaeogeographic reconstructions, when considered in combination with provenance studies and sedimentological data.

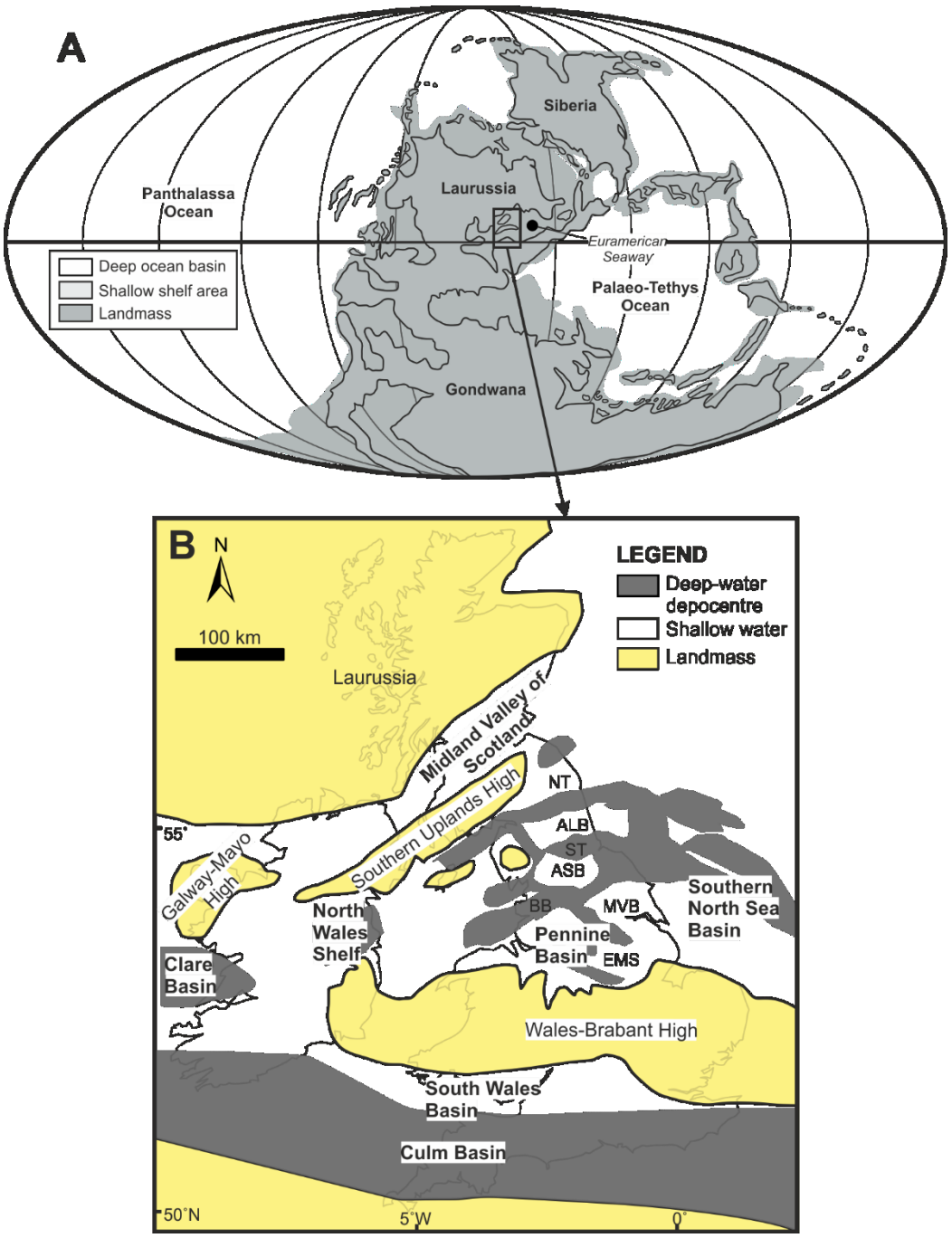

Fig. 5.1. *(A) Global palaeogeographic map for the late Mississippian, with inset map (B) illustrating landmasses, deep-water depocentres and shallow-water areas across the UK and Ireland during the late Mississippian. Note that the extent of Gondwanan ice sheets is not shown in (A). Modified from Davies et al. (2012) and Davies (2008). Selected palaeogeographic and basin names discussed in this paper are shown. ALB = Alston Block; ASB = Askrigg Block; BB = Bowland Basin; EMS = East Midlands Shelf; MVB = Market Weighton Block; ST = Stainmore Trough; NT = Northumberland Trough.*

Chronostratigraphy					Biostratigraphy			IVF age						
Period	Series	Stage	Regional stage	Regional substage	Western European Marine Band: Ammonoid zone	Western European Marine Band: Diagnostic ammonoid	Meso-them	Clare Basin	South Wales Basin	North Wales Shelf	Pennine Basin	East Midlands Shelf	Southern North Sea	Midland Valley of Scotland
Carboniferous	Pennsylvanian	Bashkirian	Namurian	Yeadonian	*Ca. cumbriense* (G_{1b})	*Ca. cumbriense* ($G_{1b}1$)	N11		FRS	AGN	URRP	URRE	LNS	
						Anthracoceras								
					Ca. cancellatum (G_{1a})	*Ca. cancellatum* ($G_{1a}1$)					LRRP			
				Marsdenian	*B. superbilinguis* (R_{2c})	*V. sigma* ($R_{2c}2$)	N10					CGE	LTSS	
						B. superbilinguis ($R_{2c}1$)								
					B. bilinguis (R_{2b})	*B. metabilinguis* ($R_{2b}5$)	N9					ASHP		
						B. eometabilinguis ($R_{2b}4$)								
						B. bilinguis ($R_{2b}3$)					MGP			
						B. bilinguis ($R_{2b}2$)								
						B. bilinguis ($R_{2b}1$)								
					B. gracilis (R_{2a})	*B. gracilis* ($R_{2a}1$)								
				Kinderscoutian	*R. reticulatum* (R_{1c})	- ($R_{1c}5$)	N8							
						R. coreticulatum ($R_{1c}4$)					LKG8			
						R. reticulatum ($R_{1c}3$)					LKG6			
						R. reticulatum ($R_{1c}2$)								
						R. reticulatum ($R_{1c}1$)		KCL						
					R.eoreticulatum (R_{1b})	*R. stubblefieldi* ($R_{1b}3$)	N7	TCL						
						R. nodosum ($R_{1b}2$)								
						R. eoreticulatum ($R_{1b}1$)								
					H. magistrorum (R_{1a})	*R. dubium* ($R_{1a}5$)	N6							
						R. todmordense ($R_{1a}4$)								
						R. subreticulatum ($R_{1a}3$)								
						R. circumplicatile ($R_{1a}2$)								
						H. magistrorum ($R_{1a}1$)								
				Alportian	*V. eostriolatus* (H_{2c})	*Hm. prereticulatus* ($H_{2c}2$)								
						V. eostriolatus ($H_{2c}1$)								
					Ho. undulatum (H_{2b})	*Ho. Undulatum* ($H_{2b}1$)	N5							
					Hd. proteum (H2a)	*Hd. proteum* ($H_{2a}1$)								
				Chokierian	*H. beyrichianum* (H_{1b})	*I. sp nov.* ($H_{1b}2$)	N4							
						H. beyrichianum ($H_{1b}1$ a-b)								
					I. subglobosum (H_{1a})	*I. subglobosum* ($H_{1a}3$)								
						I. subglobosum ($H_{1a}2$)								
						I. subglobosum ($H_{1a}1$)								
	Mississippian	Serpukhovian		Arnsbergian	*N. stellarum* (E_{2c})	*N. nuculum* ($E_{2c}4$)	N3							
						N. nuculum ($E_{2c}3$)								
						N. nuculum ($E_{2c}2$)					LFGP			
						N. stellarum ($E_{2c}1$)								
					Ct. edalensis (E_{2b})	*Ct. nititoides* ($E_{2b}3$)	N2							
						Ct. nitidus ($E_{2b}2$ a-c)								
						Ct. edalensis ($E_{2b}1$ a-c)								
					C. cowlingense (E_{2a})	*E. yatesae* ($E_{2a}3$)	N1							
						Anthracoceras ($E_{2a}2\beta$)								
						C. Gressinghamense ($E_{2a}2\alpha$)					UHEP			MVS
						E. ferrimontanum ($E_{2a}2$)								
						C.cowlingense ($E_{2a}1$ a-c)								
				Pendleian	*C. malhamense* (E_{1c})	- ($E_{1c}2$)								
						C. malhamense ($E_{1c}1$)					BGP			
					C. brandoni (E_{1b})	*T. pseudobilinguis* (E1b2 a-b)								
						C. brandoni ($E_{1b}1$)								
					C. leion (E_{1a})	*C.leion* ($E_{1a}1$ a-c)								

Fig. 5.2. *Schematic stratigraphic columns for selected Namurian basins in the UK and Ireland, illustrating the age of the studied incised-valley fills (IVFs) considered in this work. Modified from Dean et al. (2011), Waters and Condon (2012) and Bijkerk (2014). Abbreviations for ammonoids: B = Bilinguites; Ca = Cancelloceras; C = Cravenoceras; Ct = Cravenoceratoides; E = Eumorphoceras; H = Hodsonites; Hd = Hudsonoceras; Hm = Homoceratoides; Ho = Homoceras; I = Isohomoceras; N = Nuculoceras; R = Reticuloceras; V= Verneulites.*

5.3 Geological setting

In the UK and Ireland, basin evolution during the early Carboniferous between the Wales-Brabant High and Southern Uplands High was strongly influenced by the reactivation of late Caledonian basement structures, resulting in the development of a series of fault-controlled extensional basins and structurally emergent blocks (**Fig. 5.1**). During the Namurian, regional thermal subsidence was dominant in this region and active rifting became less important. To the south of the Wales-Brabant High, the South Wales Basin was affected by the Variscan orogeny and formed one of several E-W-trending foreland basins. The late-Namurian strata relating to the deposition of the Farewell Rock IVF studied in this work were deposited on the cratonic margin of the foredeep zone of this foreland basin (George, 2001).

During the late Mississippian to early Pennsylvanian (Namurian), the studied basins were located at near-equatorial palaeolatitudes, a few degrees north of the equator (**Fig. 5.1**; Scotese and McKerrow, 1990; Blakey, 2016). The prevailing climates were characterized by predominantly humid tropical conditions and short-term seasonally drier intervals, as recorded by the presence of gleysols and peat mires (Davies, 2008; Davies et al., 2012).

The different Namurian basins of the UK and Ireland all display similar infill motifs (Collinson, 1988). The earliest stage of basin fill led to accumulation of mudstones of deep-water origin, which tended to be deposited in the basin depocentres. Overlying deposits typically comprise a turbidite-fronted deltaic succession, which tended to infill the inherited bathymetry of a particular basin or sub-basin. After the inherited bathymetry was infilled, the basin was subsequently filled by a widespread shallow-water deltaic succession. Many thick sandstone-dominated fluvial deposits occurred within turbidite-fronted deltaic or shallow-water deltaic successions and were interpreted as valley fills that cut into marine or coastal deposits during episodes of falling sea level (Hampson et al., 1997; Hampson et al., 1999; Davies et al., 1999; Davies, 2008). These units are the focus of this work.

Global sea-level fluctuations during the Namurian were characterized by high-frequency and high-magnitude sea-level changes, due to the waxing and waning of Gondwanan ice sheets (Maynard and Leeder, 1992; Hampson et al., 1997; Wright and Vanstone, 2001). Fifty continental-scale ammonoid-bearing marine bands, interpreted as maximum flooding surfaces relating to glacio-eustatic sea-level rises (e.g., Maynard, 1992; Church and Gawthorpe, 1994; Martinsen et al., 1995; Hampson et al., 1997; Davies et al., 1999), are identified in Namurian siliciclastic successions in the UK and Ireland (Waters and Condon, 2012; **Fig. 5.2**). The mean periodicity of these marine bands has been estimated at 185 kyr (Holdsworth and

Collinson, 1988; Martinsen et al., 1995), 120 kyr (Maynard and Leeder, 1992), 90 kyr (Collinson, 2005) or 65 kyr based on SHRIMP U–Pb zircon dating (Riley et al., 1995). These values are consistent with fourth-order cyclicity *sensu* Mitchum and Van Wagoner (1991). The magnitude of eustatic sea-level fluctuations has been estimated at ca. 42 m (Maynard and Leeder, 1992), 60 m (Church and Gawthorpe, 1994) or 65 ± 15 m (Crowley and Baum, 1991). Based on the depth of incision of palaeovalleys, Rygel et al. (2008) reported glacio-eustatic sea-level oscillations of 60-100 m during the Namurian. Magnitudes and periodicities of eustatic modulation during the Namurian were similar to those of Late Quaternary glacial-interglacial cycles (Brettle, 2001).

5.4 Methods

5.4.1 Database

A synthesis of data from 18 interpreted incised-valley fills (IVFs) from Namurian successions of the UK and Ireland is undertaken here. Data on the sedimentology of fluvial deposits forming part of these IVFs are included in a relational database, the Fluvial Architecture Knowledge Transfer System (FAKTS; Colombera et al., 2012). FAKTS stores data on the geometry, spatial relationships, and hierarchical relationships of genetic units such as 'depositional elements', 'architectural elements' and 'facies units'; these genetic units are assigned to subsets of fluvial systems, themselves classified on multiple parameters (e.g., climate, tectonic setting, catchment area) and metadata (e.g., data quality, data types). Facies units in FAKTS represent lithofacies classified by grainsize and sedimentary structures, and delimited by bounding surfaces that correspond to a change in lithofacies type or palaeocurrent direction, or to erosional contacts or element boundaries (Colombera et al., 2013).

The sedimentological data relating to the studied IVFs in this work have been derived from 27 literature sources and one original field study. A detailed account of the IVFs considered in this work, their corresponding published-source references, the types of the data available for each, and their geographic location is shown in **Table 5.1**; the age and stratigraphic level of the studied IVFs is reported in **Fig. 5.2**. For the studied examples, investigations of the facies architecture of their fluvial deposits are generally based on outcrop exposures in South Wales, North Wales, northern England, Scotland and Northern Ireland, and on subsurface datasets from the East Midlands Shelf and the Southern North Sea (**Table 5.1**).

The scheme for the classification of facies units adopted in FAKTS (Colombera et al., 2013) is adapted and extended from the earlier scheme by Miall (1996); the facies types identified in the studied IVF fluvial deposits are reported in **Table 5.2**. The classifications of facies types in the database rely upon interpretations given in the original works. To facilitate analysis and to establish an audit trail, the detailed facies descriptions reported in the original sources are also recorded, but are not used in this work. The relative proportion of each facies type within IVF fluvial deposits has been calculated based on the sum of their measured thicknesses.

Table 5.1. *Namurian incised-valley fills of the UK and Ireland stored in the Fluvial Architecture Knowledge Transfer System (FAKTS) database and considered in this study. For each example, the table reports its acronym as used in this work (column IVF), location, basin name, lithostratigraphic unit, published literature sources and data types. Fm. = formation; Gp. = Group.*

IVF	Location	Basin	Lithostratigraphic unit	Data source	Data type	Spatial type
MVS	Scotland	Midland Valley Basin	Spireslack Sandstone, Upper Limestone Fm.	Ellen et al. (2019)	Outcrops	2D section
TCL	Western Ireland	Shannon Basin (Clare Basin)	Tullig Sandstone	Stirling (2003); Best et al. (2016)	Outcrops	2D section
KCL	Western Ireland	Shannon Basin (Clare Basin)	Kilkee Sandstone	Pulham (1988)	Outcrops	2D section
AGN	North Wales	Pennine Basin (North Wales Shelf)	Aqueduct Grit, Gwespyr Sandstone	Jerrett and Hampson (2007)	Outcrops	2D section
LKG 6	England	Pennine Basin	Lower Kinderscout Grit, Millstone Grit Gp.	Hampson (1997)	Outcrops	1D vertical
LKG 8	England	Pennine Basin	Lower Kinderscout Grit, Millstone Grit Gp.	Hampson (1997)	Outcrops	1D vertical
LRRP	England	Pennine Basin	Lower Rough Rock, Millstone Grit Gp.	Hampson et al. (1996); Hampson (1995)	Outcrops	2D section
URRP	England	Pennine Basin	Upper Rough Rock, Millstone Grit Gp.	Hampson et al. (1996); Hampson (1995)	Outcrops	2D section
URRE	England	Pennine Basin (East Midlands Shelf)	Upper Rough Rock, Millstone Grit Gp.	Hampson et al. (1996); Church and Gawthorpe (1994);	Outcrops	2D section

				Hampson (1995)		
ASHP	Southern England	Pennine Basin (East Midlands Shelf)	Ashover Grit, Millstone Grit Gp.	Church and Gawthorpe (1994); Jones and Chisholm (1997)	Cores	1D vertical
CGE	Southern England	Pennine Basin (East Midlands Shelf)	Chatsworth Grit, Millstone Grit Gp.	O'Beirne (1996); Waters et al. (2008)	Outcrops	2D section
MGP	Northern England	Pennine Basin	Midgley Grit, Millstone Grit Gp.	Brettle et al. (2002); Brettle (2001)	Outcrops	2D section
UHEP	Northern England	Pennine Basin	Upper Howgate Edge Grit, Millstone Grit Gp.	Martinsen (1993)	Outcrops	1D vertical
LFGP	Northern England	Pennine Basin	Lower Follifoot Grit, Millstone Grit Gp.	Martinsen et al. (1995); Martinsen (1990)	Outcrops	1D vertical
BGP	Northern England	Pennine Basin	Bearing Grit, Millstone Grit Gp.	Bijkerk (2014)	Outcrops	2D section
LNS	Southern North Sea	Southern North Sea Basin	Millstone Grit Gp.	George (2001)	Cores, Well logs	1D vertical
LTSS	Southern North Sea	Southern North Sea Basin	Lower Trent Sandstone, Millstone Grit Gp.	O'Mara et al. (1999)	Cores, Well logs	1D vertical
FRS	South Wales	South Wales Basin	Farewell Rock, Upper Sandstone Gp.	original field study; George (2001)	Outcrops	2D section

Table 5.2. *Scheme adopted for the classification of lithofacies of fluvial deposits. The facies types are employed in FAKTS (Colombera et al., 2012, 2013), and are adapted and extended from those by Miall (1996).*

Code	Characteristics
G-	Conglomerate with undefined structure and undefined additional textural characteristics.
Gmm	Matrix-supported, massive or crudely bedded conglomerate.
Gmg	Matrix-supported, graded conglomerate.
Gcm	Clast-supported, massive conglomerate.
Gci	Clast-supported, inversely graded conglomerate.
Gh	Clast-supported, horizontally or crudely bedded conglomerate; possibly imbricated.
Gt	Trough cross-stratified conglomerate.
Gp	Planar cross-stratified conglomerate.
S-	Sandstone with undefined structure.
St	Trough cross-stratified sandstone.
Sp	Planar cross-stratified sandstone.
Sr	Current ripple cross-laminated sandstone.
Sh	Horizontally bedded sandstone.
Sl	Low-angle (<15°) cross-bedded sandstone.
Ss	Faintly laminated, cross-bedded, massive or graded sandstone fill of a shallow scour.
Sm	Massive sandstone; possibly locally graded or faintly laminated.
Sd	Soft-sediment deformed sandstone.
F-	Fine-grained deposits (siltstone, claystone) with undefined structure.
Fl	Interlaminated very-fine sandstone, siltstone and claystone; might include thin cross-laminated sandstone lenses.
Fsm	Laminated to massive siltstone and claystone.
Fm	Massive claystone.
Fr	Fine-grained rooted bed.
C	Coal or highly carbonaceous mudstone.

5.4.2 Dune-scale cross-set thickness

The thickness of cross-sets in dune-scale cross-stratification (planar and trough cross-stratification) has been measured directly on logged sections or outcrop panels using image-analysis software (ImageJ; Schneider et al., 2012) for the fluvial deposits of each IVF. Only dune-scale cross sets in sandstones and conglomerates are included in the dataset; sedimentary structures that are interpreted to represent preserved macroforms (bars, *sensu* Jackson, 1975; Bridge, 2003) or microforms (ripple cross-laminations; *sensu* Allen, 1982; Bartholdy et al., 2015) have not been considered. Isolated cross-sets that were originally interpreted to be formed by unit bars (Bridge and Tye, 2000) are also excluded. Cross-sets interpreted as the expression of smaller dunes superimposed on larger dunes are also not considered, since these bedforms might reflect local flow conditions over the larger host bedforms (Jackson, 1975; Soltan and Mountney, 2016).

5.4.3 Incised-valley-fill dimensions

IVF dimensions are derived from the original source work, either obtained from the primary text or measured directly on figures using image-analysis software (ImageJ; Schneider et al., 2012). The measurement of IVF dimensions follows the method by Wang et al. (2019). IVF thickness (T) is defined as the vertical distance between the elevation of the lower most point of the erosional IVF base and the interfluves at the valley margins. IVF width (W) is defined as the maximum horizontal distance between the valley walls as measured perpendicular to the valley axis. IVF thickness usually differs from the thickness of IVF fluvial deposits, for example because incised valleys are partly filled by estuarine deposits (e.g., Farewell Rock IVF in South Wales, Lower Trent Sandstone IVF in the southern North Sea). Based on the reported geometry of IVF fluvial sandstones, the IVF cross-sectional area is approximated by a half-elliptical or rectangular shape (respectively, π/4*T*W or T*W, where T is IVF thickness and W is IVF width, both in metres), depending on the reported geometry of the sedimentary unit. For instance, the IVF geometries for the lower and upper Rough Rock examples from the Pennine Basin and for the Upper Rough Rock example from the East Midlands Shelf (LRRP, URRP and URRE in **Table 5.1**) are originally described as sheet-like, and accordingly the corresponding IVF cross-sectional areas are approximated as rectangular.

5.4.4 Estimation of drainage-area size

To estimate the size of the drainage area upstream of the location where the studied IVF is characterized, two integrative approaches are employed in this work.

5.4.4.1 Estimation of drainage area from cross-set thickness

5.4.4.1.1 Scaling between cross-set thickness, dune height and formative flow depth

Previous theoretical, experimental (Jerolmack and Mohrig, 2005; Bridge and Tye, 2000; Leclair and Bridge, 2001; Leclair, 2002) and numerical studies (Ganti et al., 2013; Jerolmack and Mohrig, 2005; Leclair, 2002) have demonstrated that the mean thickness (s_m) of a cross set, considered relative to the mean formative bedform height (h_m), and that the coefficient of variation (ratio of standard deviation to mean) of the preserved cross-set thickness (CV (d_{st})) remains relatively constant under steady flow conditions ($s_m / h_m \approx 0.3$; CV (d_{st}) ≈ 0.88).

The following scaling relation has been used to estimate the formative bedform height:

$h_m = 2.9(\pm 0.7)\, s_m$ (Bridge and Tye, 2000; Leclair and Bridge, 2001)

This empirical equation is indicated to be only applicable when the coefficient of variation of cross-set thickness CV (d_{st}) equals to 0.88 ± 0.3 (Bridge and Tye, 2000).

A scaling relation derived from field observations by Bradley and Venditti (2017) has been used to estimate the formative flow depth (d), from estimated dune height (h) as:

d = 6.7 h (Bradley and Venditti, 2017)

In this work, these empirical equations have been used to estimate the mean bankfull depth for the formative rivers of the studied IVFs from mean dune height, themselves estimated from the mean value of measured cross-set thickness (Bridge and Tye, 2000; Holbrook and Wanas, 2014; Buller et al., 2018; Ganti et al., 2019a).

5.4.4.1.2 Regional hydraulic-geometry curves for estimating drainage areas

For the prediction of drainage areas, Davidson and North (2009) recommend the use of regional hydraulic-geometry curves obtained from modern drainage-basin surveys, which relate mean bankfull depth to drainage area under differing climatic, physiographic and latitudinal conditions. In this work, the approach of Davidson and North (2009) is employed to estimate the drainage areas from the estimated mean bankfull depth.

During the Namurian, the study areas were located a few degrees north of the palaeo-equator (Scotese and McKerrow, 1990; Blakey, 2016) and were characterized by predominantly humid tropical conditions and short-term seasonally drier intervals (Davies, 2008; Davies et al., 2012; Boucot et al., 2013). The Pennine drainage system is interpreted to have derived sediments from Caledonian uplands, which were located to the north of the Pennine Basin, in an area corresponding to present-day Greenland and lying between ca. 10° and 20° latitude (Hallsworth et al., 2000). This implies that a part of the drainage basin might have been located in the seasonal tropical climate zone and is likely to have received variable, possibly monsoonal, precipitation throughout the year (Bijkerk, 2014). A regional curve that is ideally suited to the palaeoclimate or palaeolatitude of the Namurian basins of the UK and Ireland is not available among those presented by Davidson and North (2009), whose compilations relating to coastal-plain regions of north Florida, northwest Florida, North Carolina and Maryland (USA) can be considered as relatively close analogues. The Amazon basin, whose regional curve can be compiled from Beighley and Gummadi (2011), is considered as perhaps a more appropriate analogue, since the Amazon catchment is located near the equator and is predominantly characterized by tropical rainforest climate, with subordinate

tropical monsoon climate. Even though these modern analogues may not perfectly match the palaeoclimate or palaeolatitude of the studied Namurian basins, they allow an assessment of the likely range in size of drainage areas.

The approach proposed by Davidson and North (2009) is based on inversion of the direct relations between mean bankfull depth and drainage area to reconstruct drainage areas from mean bankfull depth, which can be estimated from observations from the rock record. However, to be able to present prediction intervals, corresponding relations have been recompiled based on the data reported in the original sources whereby mean bankfull depth and drainage area are independent and dependent variables respectively (**Fig. 5.3**). Unlike Davidson and North (2009), who quantified these two variables in imperial units, metric units are here used in representing the scaling relations (**Fig. 5.3**). To present the uncertainty in the estimated size of drainage areas for the ancient rivers feeding the studied IVFs, 95% confidence and prediction intervals are constructed for relationships between the two variables (**Fig. 5.3**). 95% prediction intervals are utilized in the subsequent analyses to carry the sample variability forward as a form of uncertainty (cf. James et al., 2013).

A scaling relation between drainage area versus mean bankfull depth has also been derived for all the data from all the aforementioned modern analogues (‘average modern analogue’, hereafter). The resultant estimated drainage areas are used in the subsequent analyses, for investigating the relationships between facies architecture within incised-valley fluvial deposits and the size of the drainage basins feeding their formative river systems.

Based on the reconstructed scaling relationships for individual modern analogues (**Fig. 5.3A-E**) and for their collective dataset (**Fig. 5.3F)**, drainage areas for 15 IVFs considered in this work (15 of 18 valley fills studied) are estimated from reconstructions of mean bankfull depth based on mean values of cross-set thickness. Few examples (Ashover Grit, East Midlands Shelf; Bearing Grit, Pennine Basin; late Namurian IVF, the southern North Sea Basin) are not considered for this part of the analysis due to the unavailability of data on dune-scale cross-set thickness.

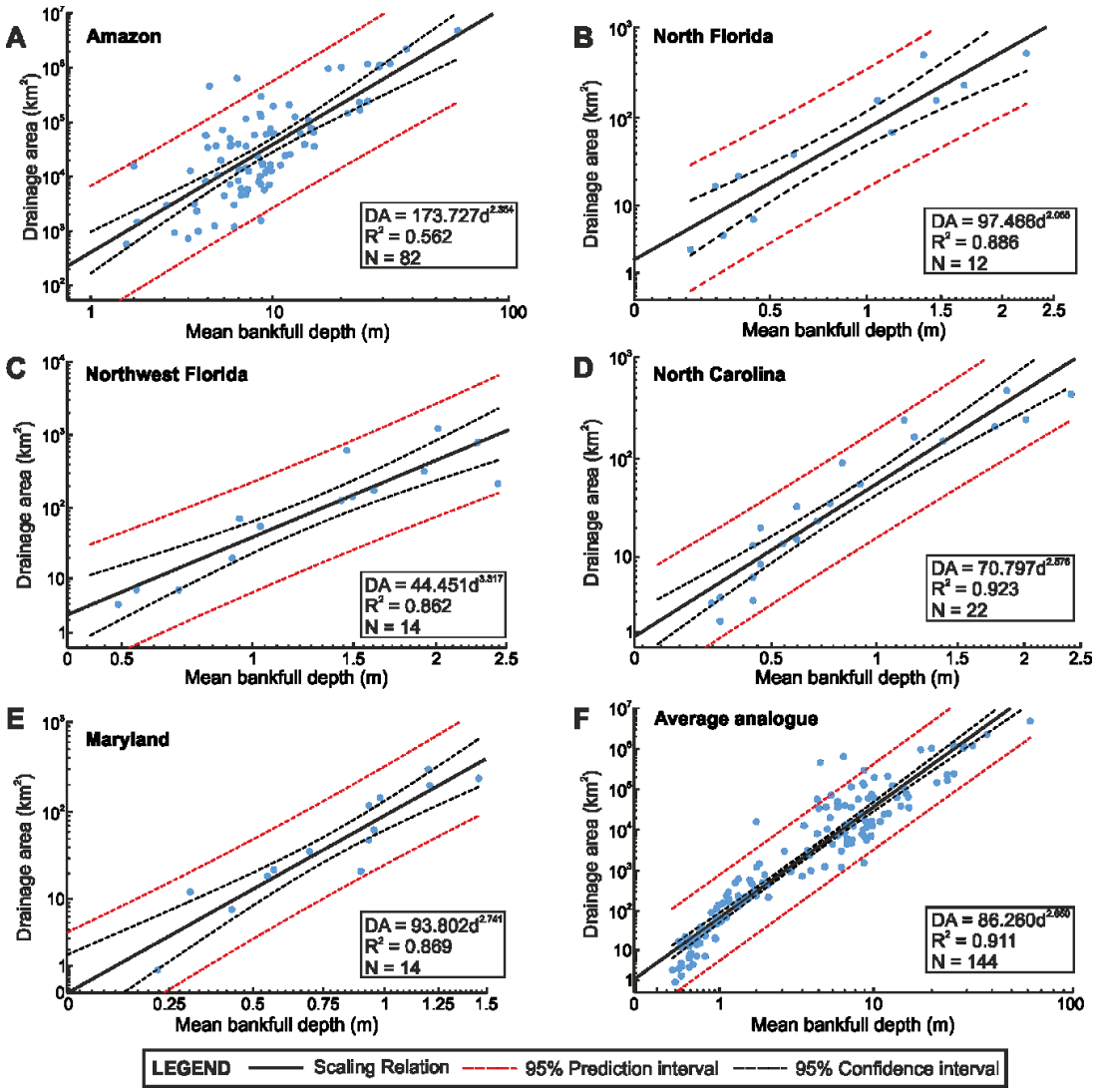

Fig. 5.3. *Cross-plots of drainage area versus mean bankfull depth for selected modern analogues: Amazon basin(A), north Florida (B), northwest Florida (C), North Carolina (D), Maryland (E), and the cumulative dataset from all these modern analogues (F). Data in (B-E) are available in Davidson and North (2009). Original data taken from Beighley and Gummadi (2011), Metcalf (2004), Metcalf and Shaneyfelt (2005), Sweet and Geratz (2003) and McCandless (2003). 'N' denotes the number of readings. The results of regression analysis between these two variables (power-law relationship and R2) are reported in respective boxes. Considering the results herein are extra analyses of the data from other approaches and will be used in the subsequent sections, this figure is introduced here and not in the Results section.*

5.4.4.2 Estimation of drainage area from incised-valley-fill dimensions

The dimensions of nearshore incised valleys are determined by a number of factors, including the magnitude and rate of relative base-level fall, contributing

drainage-basin size, climate, basin physiography, substrate types and tectonics (Talling, 1998; Posamentier, 2001; Gibling 2006; Strong and Paola, 2006, 2008; Martin et al., 2011; Blum et al., 2013; Wang et al., 2019). Based on statistical analysis of late-Quaternary incised valleys, previous workers (Mattheus et al., 2007; Mattheus and Rodriguez, 2011; Phillips, 2011; Wang et al., 2019) have demonstrated that, for a relative sea-level fall of a given magnitude, valley dimensions at comparable locations along their dip extent are strongly correlated with the drainage-basin area of their formative rivers, and that for passive margins, water discharge exerts a primary control on valley-fill shape and size. Considering the similarity in magnitude and frequency of eustatic sea-level changes during Namurian and late-Quaternary times, and given the relatively quiescent tectonic context of the Namurian basins of the UK and Ireland, the drainage areas of 10 incised valleys considered in this work have been tentatively estimated based on the approximated IVF cross-sectional area. A scaling relation between drainage area and IVF cross-sectional area for late-Quaternary IVFs from passive continental margins (**Fig. 5.4**) is derived on the basis of data from Wang et al. (2019). Ideally, IVF thickness should be used as predictor, since it is generally easier to constrain in the stratigraphic record. However, since the relationship between drainage area and IVF cross-sectional area for late-Quaternary IVFs is stronger than that between drainage area and IVF thickness or width (Wang et al., 2019), and considering that valley incision is more sensitive to basin physiography (Bijkerk, 2014; Wang et al., 2019), the IVF cross-sectional area is utilized in this work for prediction of valley drainage areas. However, IVF cross-sectional areas are estimated based on the extrapolation of local observations and not measured directly.

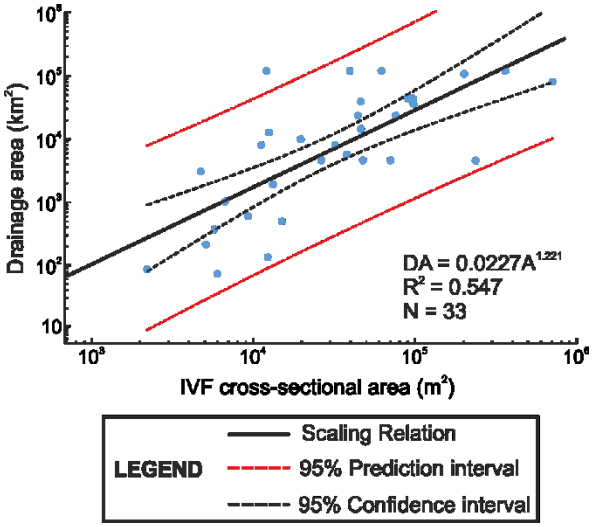

Fig. 5.4. *Cross-plots of drainage area versus reconstructed IVF cross-sectional area for late-Quaternary incised-valley fills along passive continental margins. Data taken from Wang et al. (2019). 'N' denotes the number of readings. The results of regression analysis between these two variables (power-law relationship and R2) are reported. Considering the results herein are extra analyses of the existing data from other approaches and will be used in the subsequent sections, this figure is introduced here and not in the Results section.*

5.4.5 Statistical analyses

Statistical analyses have been performed in Minitab 18 and SPSS Statistics 25. The regression analysis and computation of the prediction of drainage areas have been performed in SPSS Statistics 25. Statistical analyses have also been carried out to investigate relationships between continuous variables. Pearson or Spearman correlation coefficients (R and r hereafter) are utilized to quantify linear and monotonic relationships, respectively, between pairs of continuous variables. Their statistical significance is expressed by P-values (P hereafter). P-values are compared with significance levels (α hereafter) that equal 0.05 or 0.1. Further explanation of statistical methods can be referred to the work by Davies (2002) and James et al. (2013).

5.5 Results

5.5.1 Facies proportions in incised-valley fluvial deposits

Data on the proportions of facies types can provide information on the relative predominance of types of depositional and post-depositional processes and of

possible formative bedforms, which themselves might relate to river-discharge characteristics and drainage-area size. Database outputs on facies proportions in fluvial deposits of each IVF are presented in **Fig. 5.5**. When distributions in facies proportions in fluvial deposits across all the studied IVFs are considered (**Fig. 5.6**), it is noted that planar cross-stratified sandstones (mean proportion: avgP = 0.40) and trough cross-stratified sandstones (avgP = 0.19) are the most abundant types of facies.

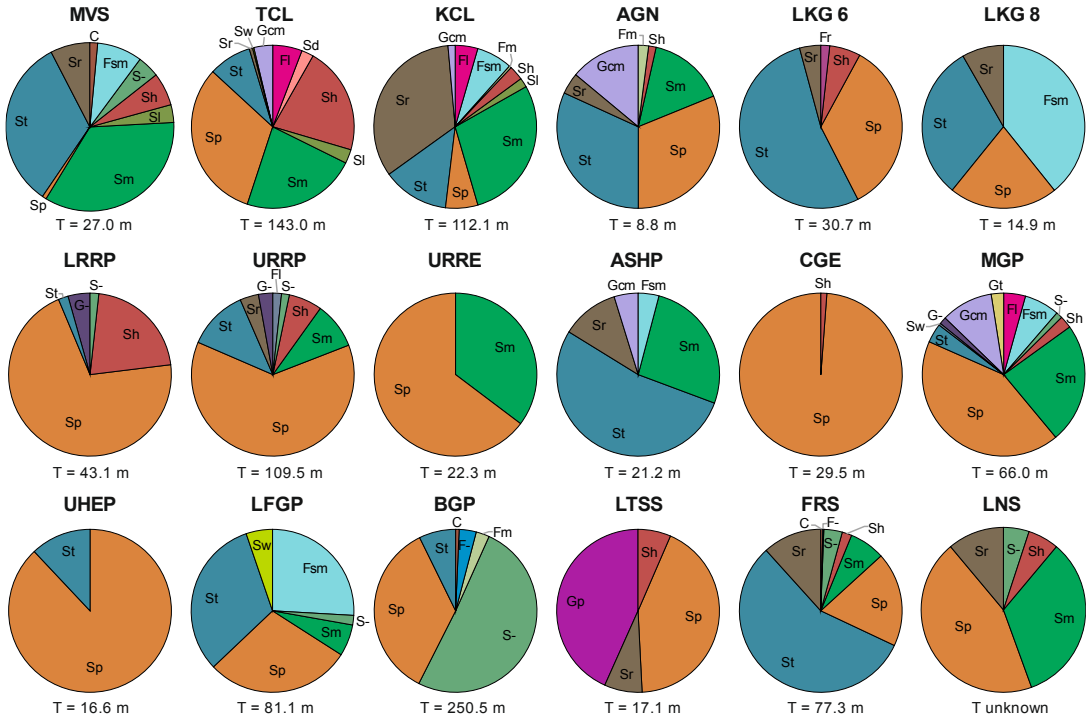

Fig. 5.5. *Proportions of facies types in fluvial deposits of the studied IVFs. T denotes the sum of the thickness of all measured facies units for each incised-valley fill. See Table 5.2 for facies codes.*

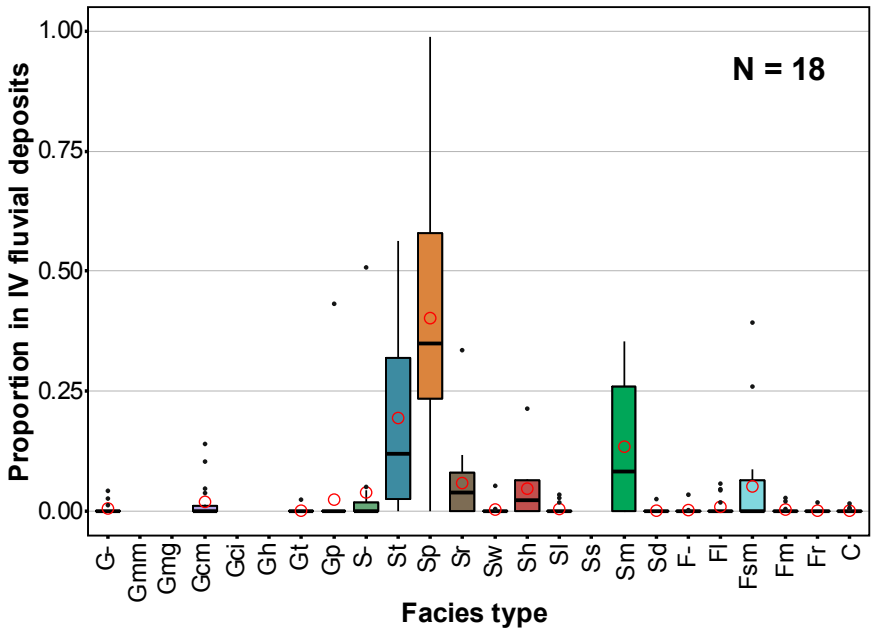

Fig. 5.6. *Box plots that present distributions in facies proportions in fluvial deposits across the studied incised-valley (IV) fills. For each box plot, boxes represent interquartile ranges, red open circles represent mean values, horizontal bars within the boxes represent median values and black dots represent outliers (values that are more than 1.5 times the interquartile range). 'N' denotes the number of studied incised-valley fills. See Table 2 for facies codes.*

5.5.2 Distribution of cross-set thickness in incised-valley fluvial deposits

Figure 5.7 illustrates the distributions in the measured dune-scale cross-set thickness, from planar and trough cross-stratified sandstones or conglomerates in fluvial deposits of the studied IVFs. The results indicate that the mean values of the measured thickness of dune-scale cross-sets for the studied IVFs, range from 0.32 ± 0.07 m to 1.94 ± 0.52 m. The coefficients of variation of cross-set thickness in the fluvial deposits of the studied IVFs are calculated and illustrated in **Fig. 5.8**. The results indicate that all the estimated values of CV (d_{st}) for the studied IVFs are lower than 0.88. Only two IVFs (Chatsworth Grit, East Midlands Shelf; Midgley Grit, Pennine Basin) are reported to have CV (d_{st}) within the range of 0.58 to 1.18 (0.61 and 0.78, respectively), and therefore yield cross-set thickness statistics suitable for derivation of mean formative-dune height (Bridge and Tye, 2000). All values of CV (d_{st}) for the other IVFs are below 0.58 (**Fig. 5.8**). Notwithstanding, the empirical equation of Bridge and Tye (2000) (cf. Leclair and Bridge, 2001) has been tentatively applied in this work to all the studied IVFs.

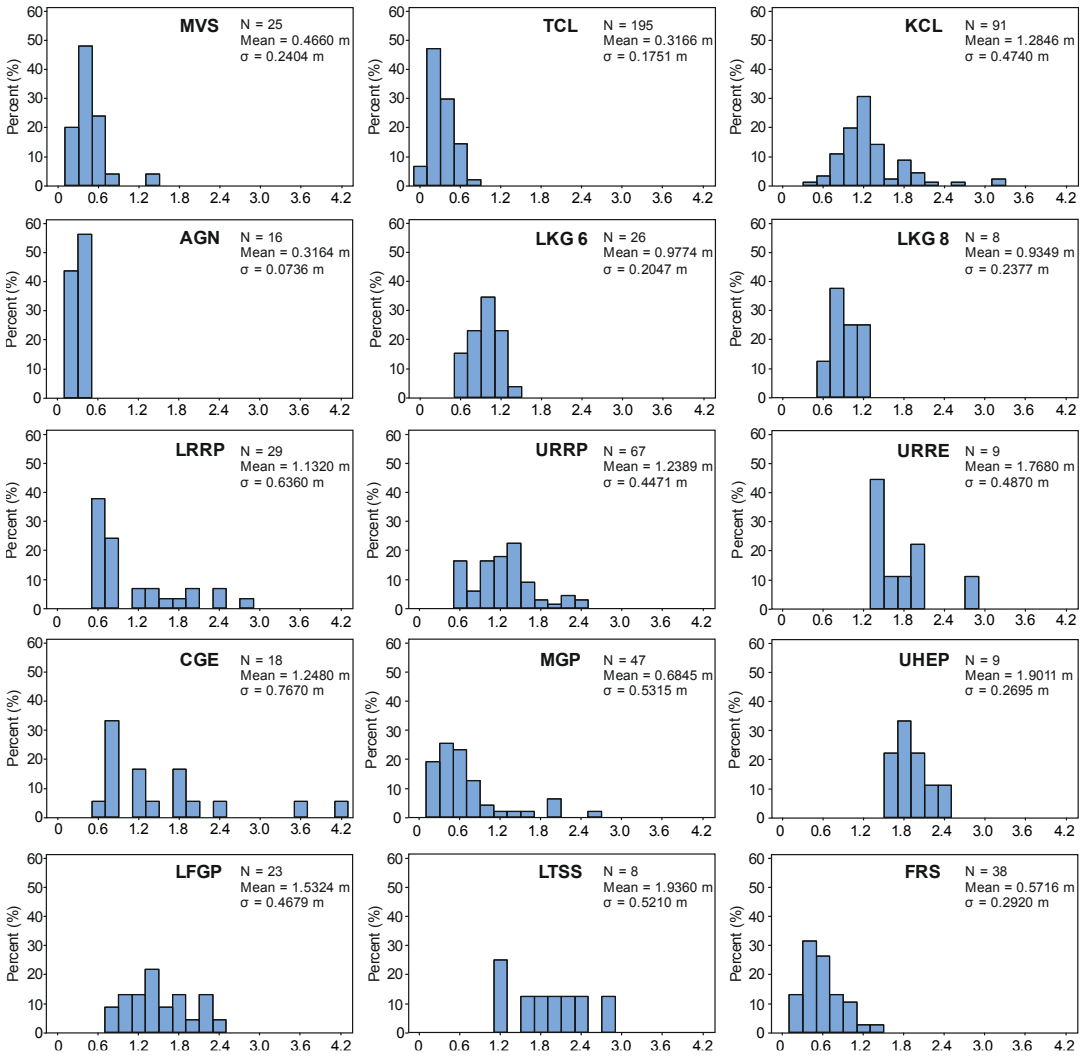

***Fig. 5.7**. Histograms that present distributions in the measured thickness of dune-scale cross-sets, from planar and trough cross-stratified sandstones and conglomerates in fluvial deposits of each IVF. 'N' denotes the number of readings and 'σ' denotes the standard deviation.*

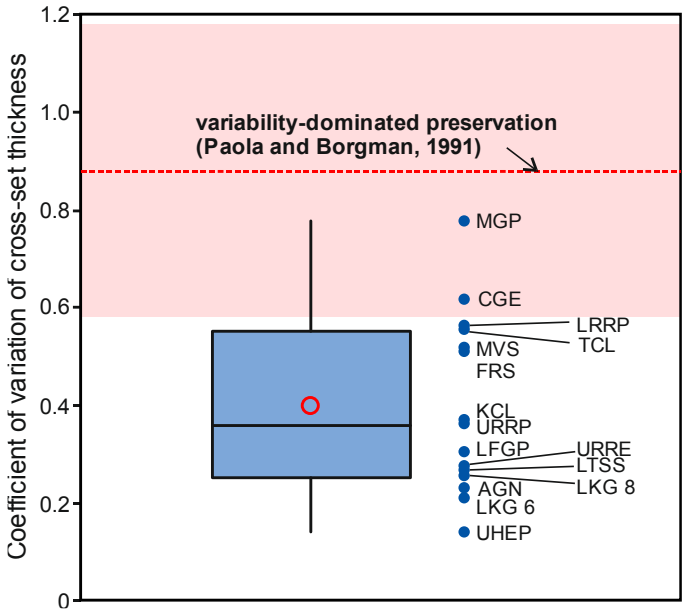

Fig. 5.8. *Box plot of the distribution in the coefficient of variation of measured cross-set thickness for 15 IVFs considered in this work. Individual values are also shown next to the boxplot for each IVF. For the boxplot, boxes represent interquartile ranges, red open circles represent mean values, horizontal bars within the boxes represent median values, and black dots represent outliers (values that are more than 1.5 times the interquartile range). The pink band indicates the 0.58-1.18 range, wherein data are considered suitable for calculating mean dune height, according to the method of Bridge and Tye (2000). The red dashed line denotes the value indicated by the variability-dominated preservation model of Paola and Borgman (1991).*

5.5.3 Estimation of formative flow depth

Estimation of mean bankfull depth for the formative rivers of the studied IVFs from measured cross-set thickness is represented in **Fig. 5.9**. The results indicate that the estimated mean bankfull depth of these rivers ranges from 6 to 38 m, with an average value of 21 m. The estimated mean bankfull depth for the formative rivers of the Farewell Rock (FRS), Spireslack Sandstone (MVS), Tullig Sandstone (TCL) and Aqueduct Grit (AGN) IVFs is smaller than or equal to 10 m. The estimated mean bankfull depth for IVFs of the Upper Rough Rock of the East Midlands Shelf (URRE), Upper Howgate Edge Grit (UHEP) and Lower Trent Sandstone (LTSS) is larger than 30 m. The mean bankfull depth estimated for rivers draining into the Pennine valleys ranges from 13 m to 38 m.

In the fluvial deposits of the studied IVFs, recognition of bar and channel-fill elements whose vertical profile is completely preserved is limited, since these units

are commonly amalgamated laterally and vertically to form multistorey architectures. For the very few cases where complete bar and channel-fill elements are recognized, estimates of maximum bankfull depth can be attempted by assuming a compaction factor of 10% (after Ethridge and Schumm, 1978), which yield values of 6.1 m, 4.0 m, 8.6 m and 6.2 m for the Spireslack Sandstone (MVS), the Tullig Sandstone (TCL), the Midgley Grit (MGP) and the Chatsworth Grit (CGE) respectively. It is significant that the projected values of mean bankfull depths based on these maximum bankfull depths (obtained assuming the channel cross-sectional area approximated by a half-elliptical shape, and hence the mean bankfull depth as being equal to π/4 times the maximum bankfull depth) are consistently smaller than the mean bankfull depths estimated from measured cross-set thickness.

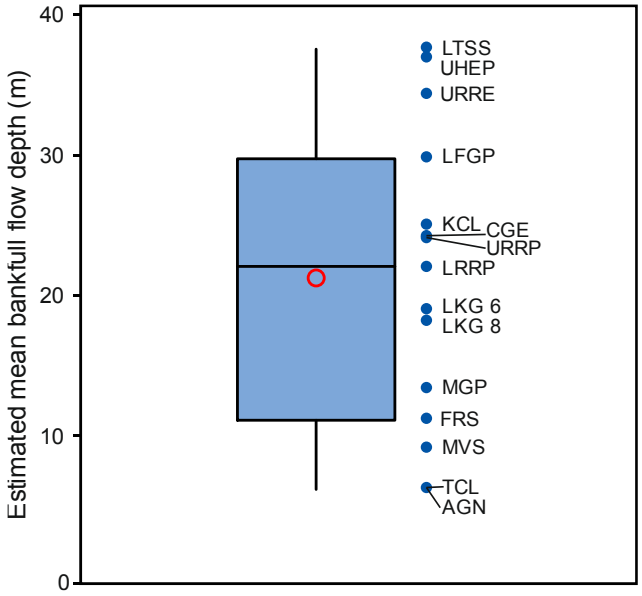

Fig. 5.9. *Box plot of the distribution in the estimated mean bankfull depth for 15 incised-valley fills considered in this work. Individual values are also shown next to the boxplot for each incised-valley fill. For the boxplot, boxes represent interquartile ranges, red open circles represent mean values, horizontal bars within the boxes represent median values, and black dots represent outliers (values that are more than 1.5 times the interquartile range).*

5.5.4 Estimation of drainage area

Two independent approaches are employed to estimate the drainage areas for the studied IVFs. The first method is based on the empirical equations that use measured mean cross-set thickness (S_m) to estimate mean dune height (h_m), itself

used to derive values of mean bankfull depth (d_m) that can be applied to regional curves to predict catchment size. The second method employs scaling relationships between IVF dimension and drainage area (**Fig. 5.4**), based on a compilation of data from late-Quaternary examples (Wang et al., 2019).

As the original published datasets vary significantly with respect to the availability of data on cross-set thickness and IVF dimension, both methods for the estimation of drainage areas could only be applied to eight IVFs.

The results of estimated drainage areas for the studied IVFs are represented in **Fig. 5.10.** Estimations of drainage area based on the northwest Florida and Maryland coastal-plain analogues are larger than the value obtained using the Amazon basin as analogue, whereas predicted values of drainage area based on the North Carolina and north Florida coastal-plain analogues are smaller than that based on the Amazon regional curve (**Fig. 5.10A**). The orders of magnitude of drainage-area size for the studied IVFs range from 10^3 km^2 to 10^6 km^2, but prediction intervals cover a wider range, from 10^3 km^2 to the order of 10^7 km^2. Estimations of the size of drainage areas based on the average modern analogue range in order of magnitude from 10^4 km^2 to 10^6 km^2 (**Fig. 5.10B**). The estimated drainage areas for the Farewell Rock (FRS), Spireslack Sandstone (MVS), Tullig Sandstone (TCL) and Aqueduct Grit (AGN) IVFs is in the order of 10^4 km^2; only three IVFs (URRE, UHEP, LTSS) have estimated drainage area in the order of 10^6 km^2. For all eight IVFs with available data on both dune-scale cross-set thickness and IVF dimension, 95% prediction interval of drainage areas estimated from the average modern analogue and 95% prediction interval of drainage areas estimated from IVF dimensions overlap significantly (**Fig. 5.10B**); the base-case predicted values based on these two methods fall within the range of the prediction interval of the alternative method respectively, except for one case (MGP). Specifically, for the Farewell Rock (FRS) and Chatsworth Grit (CGE) IVFs, the two approaches to the estimation of their drainage areas return broadly similar values (50,887 km^2 versus 47,547 km^2 for FRS; 402,564 km^2 versus 525,819 km^2 for CGE).

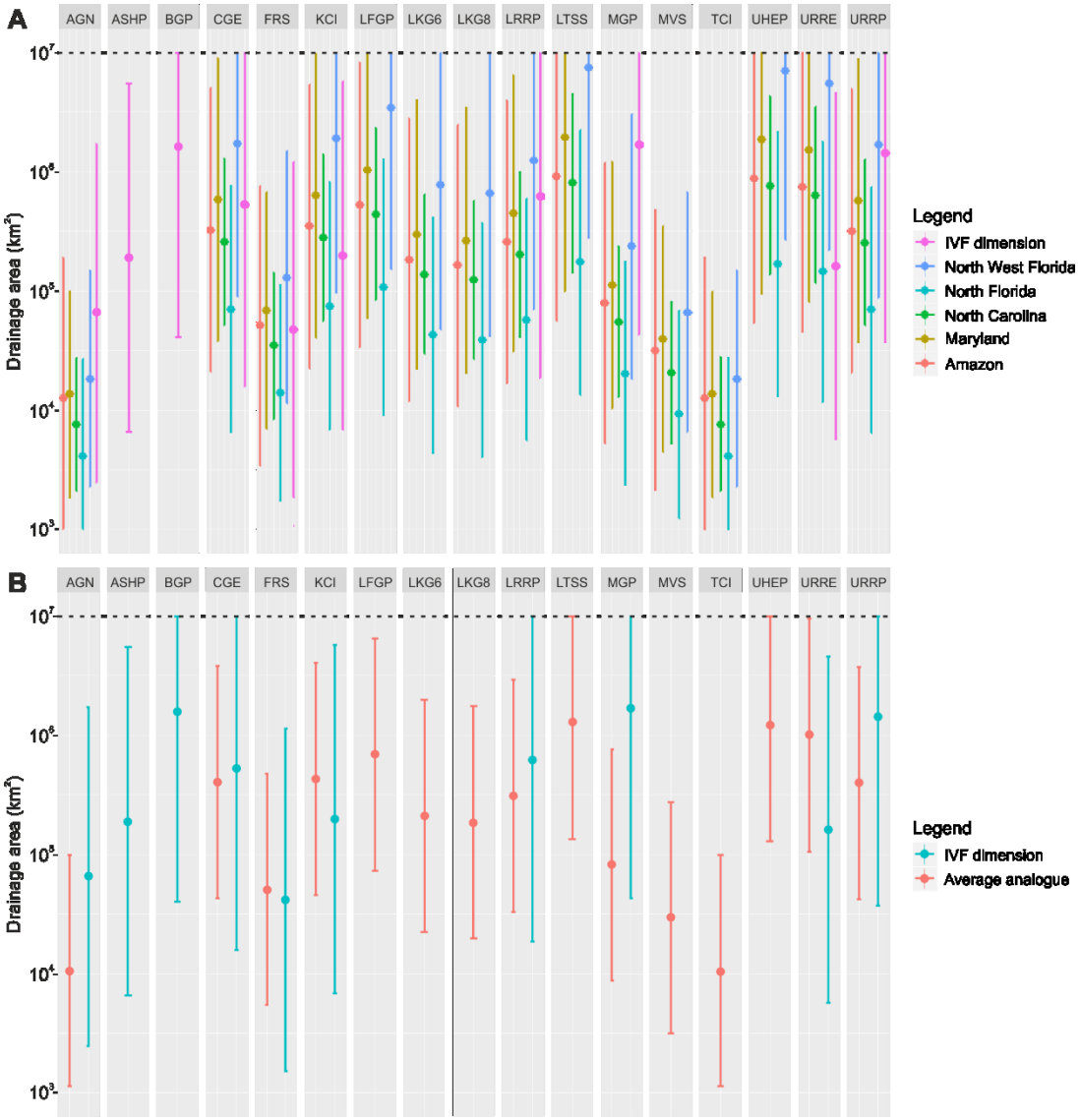

Fig. 5.10. *Range plots of estimated drainage area from measured cross-set thickness and IVF dimension. Solid dots represent the predicted values; vertical bars represent 95% prediction intervals. Note that prediction intervals are truncated at 107 km2, since it is deemed unrealistic that the studied Namurian IVFs could be fed by drainage areas larger than this value, based on palaeogeographic considerations. The size of the drainage basin of the modern Amazon, the largest river in the world in terms of catchment size, is 7,050,000 km2, but larger values of drainage area can be expected for lowstand landscapes because of amalgamation of separate river systems as they meet on the continental shelf. However, the truncation of prediction intervals at 107 km2 carries uncertainties as the Carboniferous was a time of supercontinent assembly (Pangea) (Blakey, 2007) implying that there was a larger single landmass to drain and therefore the potential for the development of larger rivers.*

5.5.5 Facies architecture in incised-valley fluvial deposits and drainage-basin size

Considering that the manner in which river systems are expected to respond to flood waves and undergo modulation of water discharge depends in part on the size of their drainage areas (Syvitski et al., 2003; Sømme et al., 2009; Hansford et al., 2020), relationships are investigated between the size of the drainage-basin areas of each IVF, as estimated from data on dune-scale cross-set thickness, and both the proportion of selected facies types in incised-valley fluvial deposits (**Fig. 5.11**) and cross-set thickness variability (**Fig. 5.12**).

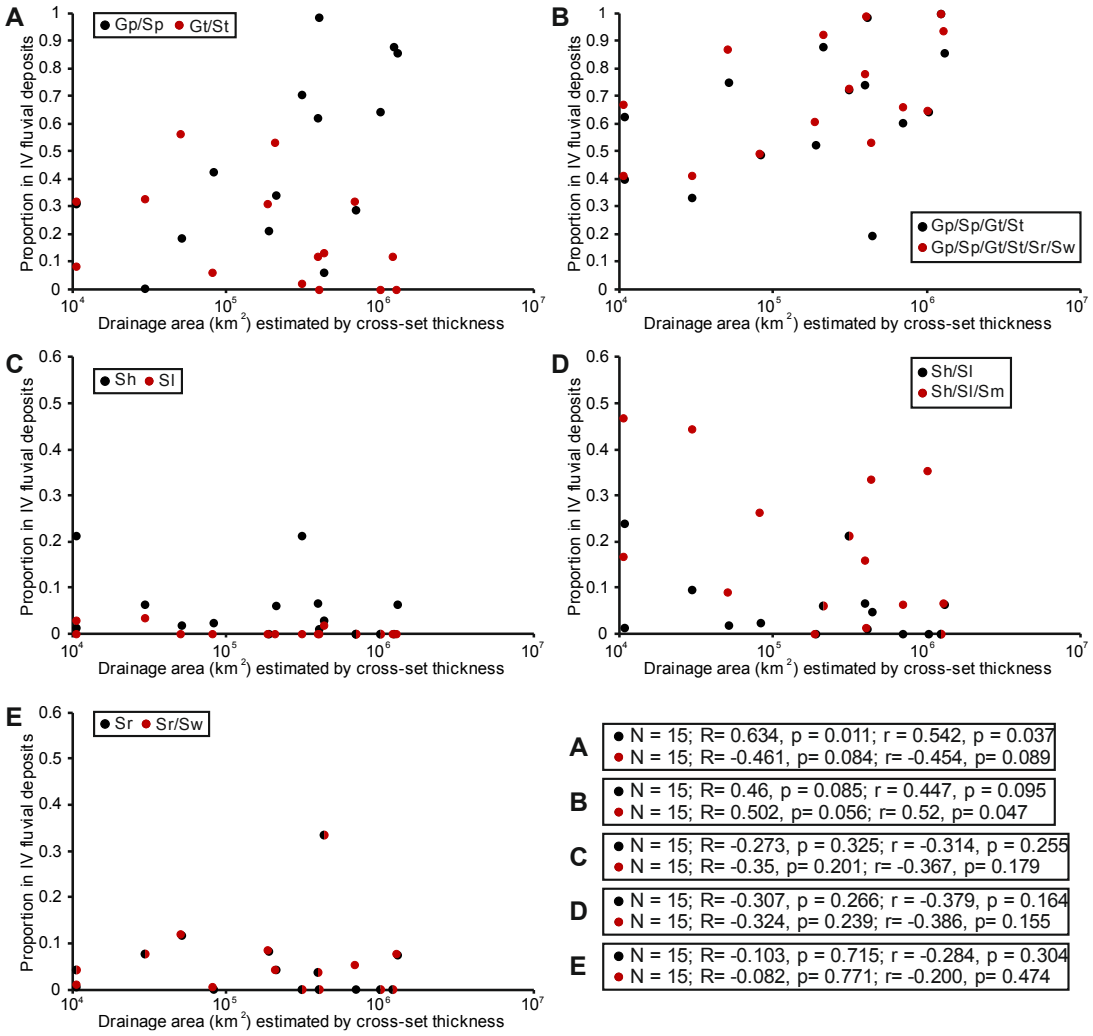

Fig. 5.11. *Cross-plots of proportions of facies types within fluvial deposits of the studied incised-valley fills versus drainage areas estimated from mean cross-set thickness of each. (A) Cumulative proportions of facies Gp and Sp, and of facies Gt and St versus drainage area. (B) Cumulative proportions of facies Gp, Sp, Gt and St and of facies Gp, Sp, Gt, St, Sr and Sw versus drainage area. (C) Proportions of facies Sh and Sl versus drainage area. (D) Cumulative proportions of facies Sh and Sl and of facies Sh, Sl and Sm versus drainage area. (E) Proportion of facies Sr and cumulative proportions of Sr and Sw versus drainage area. Half-and-half dots represent IVFs for which the two proportions are the same. For each pair of variables, the correlation coefficients of determination and p-values are reported in respective boxes on the bottom right. 'N' denotes the number of readings, 'R' denotes Pearson's R, and 'r' denotes Spearman's rho.*

A positive correlation is noted between the cumulative proportion of planar cross-stratified sandstones and conglomerates (Gp/Sp) in incised-valley fluvial deposits and the estimated drainage area (**Fig. 5.11A**). A modest negative correlation is

noted between the cumulative proportion of trough cross-stratified sandstones and conglomerates (Gt/St) and the estimated drainage area (**Fig. 5.11A**).

When Gp, Sp, Gt and St facies are considered jointly, a modest positive relationship is seen between the cumulative proportion of these facies and the estimated drainage area (**Fig. 5.11B**); when Gp, Sp, Gt, St, Sr (current ripple-laminated sandstones) and Sw (wave ripple-laminated sandstones) facies are considered together, a modest positive correlation is seen between the cumulative proportion of these facies and the estimated drainage area (**Fig. 5.11B**).

A weak negative correlation is noted between the proportion of planar horizontally bedded sandstones (Sh) or of low-angle cross-stratified sandstones (Sl) and the estimated drainage area (**Fig. 5.11C**). A weak negative correlation is noted between the proportion of low-angle cross-stratified sandstones (Sl) and the estimated drainage area (**Fig. 5.11C**).

When Sh and Sl facies are considered jointly, a weak negative relationship is seen between the cumulative proportion of these facies and the estimated drainage area (**Fig. 5.11D**); when Sh, Sl and Sm (massive sandstones) facies are considered together, a weak negative correlation is noted between the cumulative proportion of these facies and the estimated drainage area (**Fig. 5.11D**).

No correlation or a very weak correlation is identified between the proportion of current ripple-laminated sandstones (Sr) and the estimated drainage area (**Fig. 5.11E**); when Sr and Sw are considered jointly, no correlation or a very weak correlation is noted between their cumulative proportion and the estimated drainage area (**Fig. 5.11E**).

A modest negative relationship is noted between the coefficient of variation of dune-scale cross-set thickness and the size of drainage areas estimated from cross-set thickness (**Fig. 5.12A**), whereas a modest positive relationship is noted between the coefficient of variation of cross-set thickness and the size of drainage areas estimated from IVF dimension, albeit not statistically significant at the level of 0.1 (**Fig. 5.12B**).

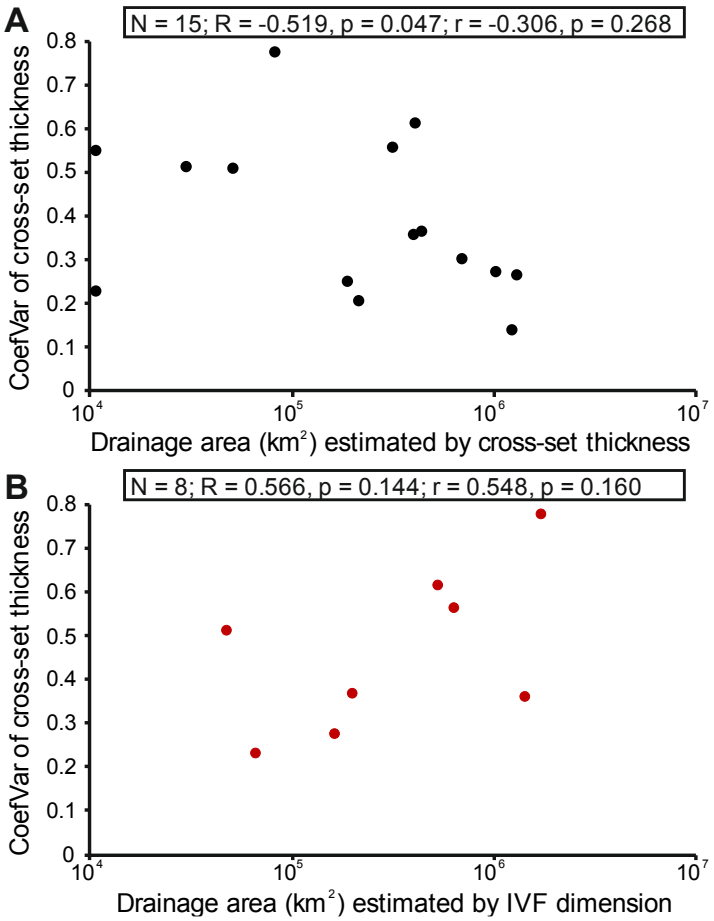

Fig. 5.12. *Cross-plots of the coefficient of variation of cross-set thickness versus (A) drainage area estimated by cross-set thickness and (B) drainage area estimated by IVF dimension. For each pair of variables, the correlation coefficients of determination and p-values are reported in respective boxes. 'N' denotes the number of readings, 'R' denotes Pearson's R, and 'r' denotes Spearman's rho.*

5.6 Discussion

5.6.1 Palaeohydrological characteristics

Previous workers have argued that discharge variability can exert a primary control on the alluvial stratigraphy from bedform to basin scales (Fielding et al., 2009 and 2018; Plink-Björklund, 2015; Nicholas et al., 2016; Trower et al., 2018; Colombera and Mountney, 2019; Ganti et al., 2019b; Leary and Ganti, 2020). Perennial rivers with low discharge variability are typically characterized by the predominance of Froude subcritical flow structures (cross-stratification and ripple cross-lamination) and subordinance of Froude supercritical and transcritical flow structures (planar horizontal lamination and low-angle cross-stratification; cf. Fielding et al., 2009,

2018; Plink-Björklund, 2015; Colombera and Mountney, 2019). Mean and median values of facies proportions in the fluvial deposits of the studied IVFs indicate the predominance of sandstones with planar and tabular cross stratification and ripple cross lamination (**Fig. 5** and **Fig. 5.6**), which are consistent with what is generally represented in classical facies models for sandy river channel deposits (e.g., Walker, 1976; Collinson, 1996; Miall, 1996; Bridge, 2006), and consistently with the notion that the palaeoriver-systems feeding the Namurian IVFs of the UK and Ireland are likely perennial and characterized by relatively low discharge variability. This is reconciled with the inference of a predominantly equatorial humid tropical climate prevailing in the study areas during the Namurian (Davies, 2008; Davies et al., 2012; Boucot et al., 2013; Blakey, 2016). Based on global quantitative analyses of modern river discharge variability and hydrograph shape with respect to climate types, Hansford et al. (2000) indicated that due to intense perennial precipitation, rivers in tropical rainforest climate are typically characterized by large discharge, low discharge variability and broad flood hydrograph, whereby the flood discharge tends to build slowly and decline gradually over the course of several months.

The values of mean bankfull depth for the formative rivers of the studied IVFs estimated from mean values of measured dune-scale cross-set thickness ranges from 6 m to 38 m, with an average of 21 m (**Fig. 5.9**). However, the values of mean bankfull depths projected from the maximum bankfull depth based on limited complete bar and channel-fill elements in fluvial deposits for few examples (MVS, TCL, MGP, CGE) studied in this work are consistently smaller than the values estimated from measured cross-set thickness. Furthermore, in some cases (LRRP, URRE, UHEP, LTSS) values of maximum bankfull depths projected from the mean bankfull depths (themselves estimated from mean cross-set thicknesses) are even larger than the restored thickness of the IVFs themselves, even assuming a compaction factor of 10%. In addition, the fluvial deposits of the studied IVFs are commonly characterized by multistorey architectures (Hampson et al., 1997; Hampson et al., 1999; Davies et al., 1999), and this should support the idea that the fluvial fill of each of these valleys should be significantly thicker than the palaeodepth of the river that formed it. These inconsistencies might arise in part because flow depth estimated from mean cross-set thickness tends to yield an overestimation of the mean bankfull depth, due to preferential preservation of thicker dune-scale cross-sets in portions of channel deposits that represent deeper channel areas (Holbrook and Wanas, 2014), and perhaps because estimation of dune height from cross-set thickness has been attempted in this work despite the fact that the method may not be applicable under the observed conditions of limited variability in cross-set thickness (Bridge and Tye, 2000). Misidentification of cross-sets that represent the preserved product of unit bars (Reesink, 2019), as dunes, is

another possible explanation. Estimations of flow depth larger than the restored thickness of IVFs might also be attributed in part to the fact that IVF fluvial strata are prone to be truncated at the top by wave or tidal ravinement (e.g., O'Mara et al., 1999; Wignall and Best, 2000; George, 2001; Brettle et al., 2002; cf. Wellner and Bartek, 2003; Wang et al., 2020).

Considering similar prevailing humid tropical climate conditions for the studied IVFs, negative relationships between estimated drainage area and the proportions of facies that may have been deposited under upper-flow-regime conditions (horizontally bedded, low-angle cross-stratified and massive sandstones) and positive relationships between drainage area and proportions of facies that may have been deposited under lower-flow-regime conditions (planar cross-stratified, trough cross-stratified and ripple-laminated sandstones or conglomerates) (**Fig. 5.11**) might reflect the fact that the size of drainage areas might leave a record in the facies architecture of fluvial deposits within incised valleys through its control on variability in water discharge (cf. Colombera and Mountney, 2019). Based on global quantitative analyses of modern rivers, Hansford et al. (2020) indicated that water discharge variability tends to decrease with increasing drainage areas. This is attributed to the fact that smaller and steeper drainage basins are more prone to larger differences between flood and base-flow discharge (Smith, 1992; Robinson and Sivapalan, 1997; Sømme et al., 2009) as external flood drivers (e.g., storms) are more likely to affect the entire drainage basin.

Values of the coefficient of variation of measured cross-set thickness for the studied Namurian incised-valley fluvial deposits are consistently lower than what is expected for steady flow state, based on theoretical, experimental and numerical studies (e.g. Paola and Borgman, 1991; Bridge and Tye, 2000; Leclair and Bridge, 2001; Leclair, 2002; Jerolmack and Mohrig, 2005; Ganti et al., 2013) (**Fig. 5.8**). Theoretical analyses and flume experiments under steady and unsteady flows by Leary and Ganti (2020) indicate that preserved fluvial cross strata tend to record bedform evolution during flood recession. Given a characteristic bedform disequilibrium timescale $T^* = Tf / Tt$, where Tf is the duration of the prevailing flow and Tt is the bedform adjustment timescale (Myrow et al., 2018), steady flows with broad flood hydrographs, having a gradual decline in flood discharge and $T^* \geq 1$, tend to result in CV (d_{st}) ≈ 0.88, whereas flashy flood hydrographs, with abrupt decrease in flood discharge and $T^* \ll 1$, tend to result in CV (d_{st}) that is significantly lower than 0.88 (Leary and Ganti, 2020). The cross-set thickness variability can therefore yield information on the ratio of the timescales of formative flood variability and bedform adjustment, and hence can act as a potential signature of disequilibrium in the sedimentary record (Leary and Ganti, 2020). In this

perspective, the low variability (coefficients of variation) of cross-set thickness for the studied Namurian incised-valley fluvial deposits could be attributed to bedform disequilibrium relative to formative flows, reflecting the record of bedform evolution under flashy flood hydrographs. However, this is a condition that appears unlikely to apply to the studied Namurian IVFs, based on their palaeoclimatic context and facies architecture. Given the scale and likely hydrodynamics of the studied river systems, it can be hypothesized that the low inter-annual discharge variability of these rivers may be responsible for the observed low values of CV (d_{st}). One possible explanation might be that, for the studied palaeorivers, cross-set-forming dunes tended to accumulate their deposits under limited disequilibrium, so that the low variability in cross-set thickness would merely reflect the limited variability in magnitude across different flood events.

The negative correlation between the coefficient of variation of cross-set thickness versus the size of drainage areas estimated from mean values of cross-set thickness (**Fig. 5.12A**) might reflect how river systems with drainage areas of different sizes are expected to respond to flood and modulate water discharge (e.g., in terms of inter-annual discharge variability), since these factors might control the preservation of cross strata. Because of the control exerted by inter-annual discharge variability on resulting alluvial stratigraphy (Fielding et al., 2018), the relationship between inter-annual discharge variability and drainage area for modern rivers is also investigated (**Fig. 5.13**), in order to derive insight that could be applied to IVFs in the rock record. To characterize inter-annual discharge variability, Fielding et al. (2018) proposed to use the coefficient of variation of annual peak flood discharge CVQp: based on daily discharge data reported in Fielding et al. (2018), a modest negative relationship is seen between CVQp and drainage area for 26 modern rivers distributed across different climatic zones (**Fig. 5.13**). However, when a corresponding analysis is exclusively made for modern rivers in rainforest climatic types based on daily discharge data by Hansford et al. (2020), no correlation is noted between the coefficient of variation of peak discharge and drainage area (**Fig. 5.13**). Hansford et al. (2020) proposed the use of an index of yearly discharge variability (DVI_y), equal to the average of the difference between the highest and the lowest daily discharge in the same year divided by the average discharge across many years, to characterize discharge variability from the annual to inter-annual scale. Based on data from several modern rivers, a weak negative relationship is noted between DVI_y and drainage area for rivers across all climate zones (regression with $R^2 = 0.22$), but stronger negative correlations are seen for rivers in rainforest climate zones ($R^2 = 0.39$) and for persistent rivers ($R^2 = 0.39$). Notwithstanding, a conclusive explanation of the cause for the consistently low

values of the coefficients of variation of cross-set thickness (**Fig. 5.8** and **Fig. 5.12A**) appears elusive.

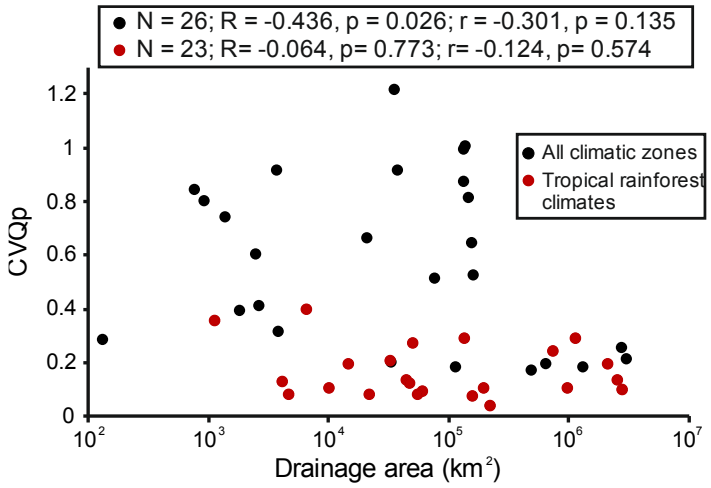

Fig. 5.13. *Cross-plots of the coefficient of variation of annual peak discharge (CVQp) versus drainage area for modern rivers across all climate zones and in tropical rainforest climates, respectively. Black spots denote examples from all climatic zones with data taken from Fielding et al. (2018). Red spots denote examples in tropical rainforest climates with data taken from Hansford et al. (2020). For each pair of variables, the correlation coefficients of determination and p-values are reported in respective boxes. 'N' denotes the number of readings, 'R' denotes Pearson's R, and 'r' denotes Spearman's rho.*

5.6.2 Palaeogeographic reconstructions

Sedimentological data such as palaeocurrent vectors or palaeoslope indicators (e.g., interpreted movement directions of slumps, orientation of facies belts), provide information on directions of sediment transport, but tend to be affected by local topographic variations. Provenance studies based on detrital zircon age dating and heavy-mineral analyses can provide key information on the source areas at a larger scale. The proposed estimations of the size of drainage areas form a dataset that can be used to integrate existing provenance and sedimentological data, to improve understanding of likely source areas, enable reconstruction of source-to-sink systems, and contribute to the refinement of regional palaeogeographic reconstructions for the Namurian (**Fig. 5.14**). Implications of the results for selected basins are presented in the following section. The size of drainage areas for each IVF used for regional palaeogeographic reconstructions represents either (i) the average of the base-case predicted value estimated from the average modern analogue and that estimated from IVF dimension, or (ii) the value obtained with

either of these two methods if data on cross-set thickness or IVF dimension are lacking.

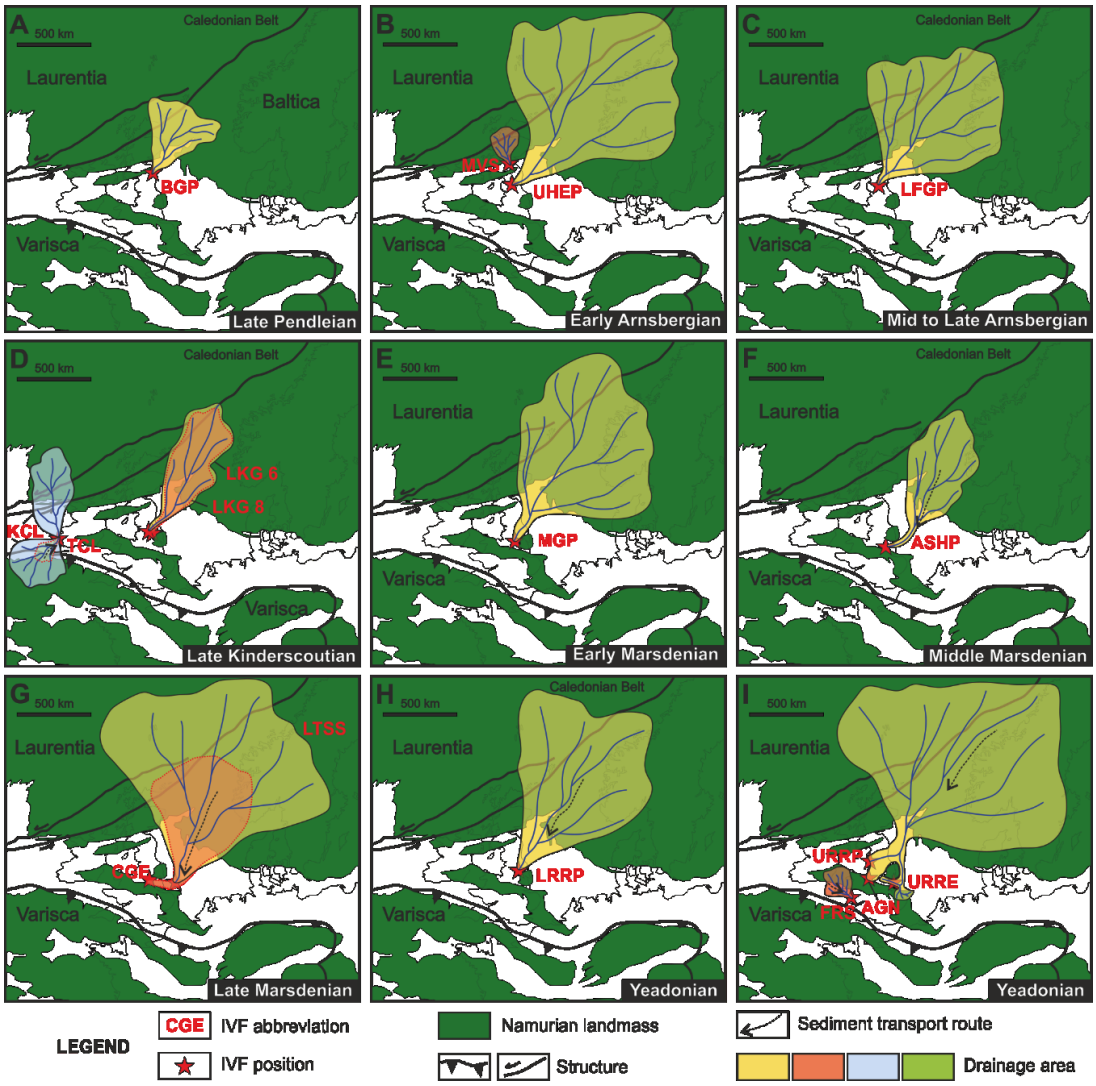

Fig. 5.14. *Palaeogeographic reconstruction maps for basins in the UK and Ireland during Namurian time, presented by regional substage. Green outlines of palaeo-landmasses adapted from reconstructions of R. Blakey, and Colorado Plateau Geosystems (2016). Black dashed arrows denote sediment transport paths inferred from existing provenance studies (detrital zircon age dating, heavy mineral analyses, petrographic data) and sedimentological data (palaeocurrent or palaeogradient indicators). Note that the size of drainage areas for each IVF used for regional palaeogeographic reconstructions represents either (i) the average of the base-case predicted value estimated from the average modern analogue and that estimated from IVF dimension, or (ii) the value obtained with either of these two methods if data on cross-set thickness or IVF dimension are lacking.*

5.6.2.1 Pennine Basin

The integration of heavy-mineral analysis and detrital-zircon dating for late Carboniferous sandstones of the Pennine Basin by Hallsworth et al. (2000) indicates that during the Namurian, the majority of sediment was derived from the north, with subordinate amounts of sediment supplied from the Wales-Brabant High, on the southern margin of the basin. The northern source areas lay within the part of Laurentia-Baltica affected by the Caledonian orogeny, which is considered to locate to the north of the present-day North Sea and has extended to present-day Greenland. Based on combined analyses of heavy minerals, garnet geochemistry and palaeocurrent directions of late Carboniferous (Yeadonian) fluvial sandstones in the Pennine Basin, Hallsworth and Chisholm (2008) proposed that the fluvial sandstones of the Rough Rock of the central Pennines were mainly supplied with sediment of northerly provenance. Additional local sediment sources can be inferred at the northern and southern basin margins and from an intrabasinal high, the Market Weighton High. The main north branch of the drainage system extended into the North Staffordshire area, whereas the south branch did not extend beyond the Widmerpool Gulf. Estimations of drainage areas for the lower Rough Rock and Upper Rough Rock IVFs in the Pennine Basin (LRRP, URRP) and for the Upper Rough Rock IVF in the East Midlands Shelf (URRE) yield average predicted values of approximately 470,000 km^2, 910,000 km^2 and 590,000 km^2, respectively. Taking into account the studies on the provenance of the Rough Rock IVFs and the average value of base-case estimations of drainage areas based on the average modern analogue and IVF dimension, palaeogeographic map that illustrates the possible Yeadonian drainage configurations has been proposed (**Fig. 5.14H and I**). The sum of the estimated drainage area for the URRP and URRE IVFs is used when reconstructing the palaeogeography. The estimated drainage areas are of a size that is compatible with the extent of the source terranes recorded by the detrital zircon age spectra and heavy-mineral analysis. The proposed reconstruction accommodates the hypothesis that the northern drainage system bifurcated into two branches near the Market Weighton High because of the existence of this topographic high (Hallsworth and Chisholm, 2008; Waters et al., 2009). The northern branch fed the Upper Rough Rock in northern England (URRP) and the Aqueduct Grit in North Wales (AGN); the southern branch diverted westwards due to the existence of the Wales-Brabant High on the south margin of the basin, as recorded in palaeocurrent data (Bristow, 1988; Hallsworth and Chisholm, 2008), and alimented the Upper Rough Rock in the Widmerpool Gulf (URRE).

5.6.2.2 Clare Basin

The provenance of Namurian sedimentary strata of the Clare basin remains highly contentious despite decades of research. Contrasting interpretations are derived on the basis of sedimentological data, i.e., palaeocurrent indicators and interpreted movement directions of slumps: Collinson et al. (1991) envisaged a source from the west or northwest, whereas Wignall and Best (2000) suggested sediment influx from a southerly provenance. Based on detrital-zircon age data from three Namurian sandstone units (Ross Formation, Tullig Sandstone, Doonlicky Sandstone), Pointon et al. (2012) suggested that from the time of deposition of the uppermost Ross Formation (early Kinderscoutian) until the deposition of the Doonlicky Sandstone (late Kinderscoutian to early Marsdenian), a major sediment source (over 35%-40%) for the Clare basin was represented by a number of small terranes of Gondwanan affinity (Avalonia/Ganderia, Armorica and Iberia) located to the south; yet, it is recognized that the possibility of a combined source from peri-Gondwanan terranes and Laurentia to the north of the basin cannot be discredited. Drainage area estimates for the Tullig sandstone IVF (TCL) from mean cross-set thickness yield a range (95% prediction interval) from ca. 1,140 km^2 to 99,000 km^2, with a base-case predicted value of ca. 10,600 km^2. Avalonia was of sufficient size to host a catchment of such limited extent. Drainage area estimates for the Kilkee sandstone IVF (KCL) yield a range (95% prediction interval) from ca. 46,000 km^2 to 4,108,000 km^2 with a most-likely predicted value of ca. 435,000 km^2. This reveals that the Kilkee sandstones of the Clare Basin must have been deposited by a river system with a continental-scale or at least regional-scale catchment. The relatively small terrane of Avalonia might have been too limited in size to host the entirety of this drainage basin, supporting the hypothesis of a combined source from both Avalonia and Laurentia. Palaeogeographic reconstructions (**Fig. 5.14D**) indicate that, during the late Kinderscoutian, a river network draining from Laurentia might have reached the Clare Basin and flowed into the basin eastward or southeastward, while drainage networks sourced from the south flowed northeastward into Clare Basin, as indicated by palaeocurrent data (Pulham, 1989). In the Clare Basin, these two catchments amalgamated into a single larger catchment, which might potentially have acted as a source to contemporaneous deep-water turbidites.

5.6.2.3 South Wales Basin

A speculative palaeogeographic model by George (2001) proposed that the late Yeadonian Farewell Rock IVF of South Wales (FRS) might represent a preserved part of the routing system for the late Namurian turbidites (Crackington Formation) of the Culm Basin. Other authors (Freshney et al., 1979; Melvin, 1986; Burne, 1995; Hartley, 1993) have demonstrated a northerly provenance for these turbidites on

the basis of sedimentological data. However, based on channel orientation and palaeoflow analysis, Rippon (1996) inferred that the deposits of Westphalian A-B sedimentary strata of the Culm Basin and South Wales Basin were derived from a common, distant southerly source. This implies that combined northerly-southerly sources for the late Namurian turbidites of the Culm basin cannot be ruled out on the basis of the available data. The estimated average value of mean bankfull depth for the formative rivers of the Farewell Rock incised valley is ca. 10 m, returning an estimated drainage area with a base-case value of ca. 50,000 km^2. Hence, this regional-scale river system, being derived from the emergent Wales-Brabant High, a localised high (George, 2001), could only provide limited supply of sediment to the late Namurian turbidites of the Culm basin. The hypothesis of an additional sediment source from the south appears therefore likely. However, mass-balance analysis of the sediment volume derivable from the source and deposited in the basin is necessary to substantiate this assumption.

5.7 Conclusions

A database-driven synthesis of data from 18 Namurian incised-valley fills in the UK and Ireland has been performed to quantitatively estimate palaeohydrological characteristics of their formative river systems, and to attempt refinement of the regional palaeogeographic reconstructions of their basins. The main findings are summarized as follows.

(i) The facies architecture of fluvial deposits of the studied IVFs suggests that the palaeorivers feeding the Namurian IVFs of the UK and Ireland were likely perennial and characterized by relatively low discharge variability. This is in accord with inferences of a predominantly humid tropical climate prevailing in the study areas, located near the equator during the Namurian. The coefficient of variation of the thickness of sets of dune-scale cross-stratification for the studied deposits is characteristically low, possibly because of the low inter-annual discharge variability of these palaeorivers.

(ii) In four examples, inferences on river bathymetry based on limited observations of the thickness of bar and channel-fill elements return consistently smaller channel depths than estimations based on cross-set thickness statistics. In other four cases, projected values of maximum bankfull depths are larger than the decompacted thickness of the IVFs. Limitations in data and interpretations are acknowledged as possible

causes, but a conclusive explanation of these inconsistencies has not been reached.

(iii) Reconstruction of the size of IVF drainage areas has been attempted based on integration of flow-depth estimations from dune-scale cross-set thickness statistics with scaling relationships of IVF dimensions derived from late-Quaternary IVFs (Wang et al., 2019). This approach allowed effective consideration of a range of uncertainties in rock-record observations and in resulting extrapolations.

(iv) Relationships between estimated drainage areas and the relative proportions of facies that may have been deposited under lower- *versus* upper-flow-regime conditions might reflect the fact that the size of drainage areas controls the facies architecture of fluvial deposits within incised valleys through its effect on variability in water discharge.

(v) The proposed estimations of the size of drainage areas provide complementary insight to existing provenance and sedimentological data, as they enable tentative reconstructions of source-to-sink systems in the context of the regional palaeogeographic configuration for the Namurian.

The approaches illustrated in this work can be replicated to the study of palaeohydrologic characteristics and palaeogeographic reconstructions of incised-valley fills globally and through geological time.

6 Discussion

This chapter integrates the main findings of the previous chapters and presents a wider discussion of the implications of these results for sequence-stratigraphic models and source-to-sink analyses, and of their applied significance.

6.1 Geological controls on incised-valley-fill geometry and implications for sequence-stratigraphic models

Previous research on near-shore incised-valley systems (e.g., Schumm, 1993; Talling, 1998; Posamentier and Allen, 1999; Blum and Törnqvist, 2000; Posamentier, 2001; Van Heijst and Postma, 2001; Gibling 2006; Strong and Paola, 2006, 2008; Loget and Van Den Driessche, 2009; Martin et al., 2011; Blum et al., 2013) has highlighted that a wide variety of factors such as the magnitude and rate of relative base-level fall, basin physiography (gradients and convexity along the depositional profile and shelf-break depth), contributing drainage-basin size, climate, substrate characteristics and tectonics, play key roles in determining the geometry of near-shore incised-valley fills.

The tectonic context of a continental margin controls valley incision and widening through its effects on base level and relative sea-level fluctuations, distinct characteristics of basin physiography, climate, water discharge and sediment delivery rates (Posamentier and Allen, 1999; Jain and Tandon, 2003; Ishihara et al., 2011, 2012; Wohl et al., 2012; Tropeano et al., 2013; Vandenberghe, 2003; Ishihara and Sugai, 2017). In Chapter 3, incised-valley fills developed along active continental margins are demonstrated to be thicker and wider, on average, than those along passive continental margins, implying that the tectonic type of a continental margin has a significant influence – at least indirectly – in determining the dimensions of near-shore incised-valley systems.

Climate is known to have significant influence in controlling valley incision and widening, especially through variations in temperature, peak precipitation, vegetation and permafrost in drainage-basin areas, which in turn determines water discharge, rates of sediment supply and bank stability (Blum et al., 1994; Blum and Törnqvist, 2000; Vandenberghe, 2003; Bogaart et al., 2003a, b; Blum et al., 2013). Similarly, the drainage-basin area can affect incised-valley-fill dimensions through

its control on water discharge and sediment yield, which in turn might influence river-system size and mobility, and in turn valley-fill dimensions. Recent research by Mattheus et al. (2007), Mattheus and Rodriguez (2011) and Phillips (2011) has demonstrated that factors that act upstream, in particular, the size of the drainage basin, act as primary controls in determining the dimensions of incised-valley-fill systems whereas factors such as shelf-break depth, or coastal-plain and shelf gradients is considered to be less important. In Chapter 3, strong scaling relations between contributing drainage area and incised-valley-fill geometry, and distinctive differences in incised-valley-fill geometry across catchments dominated by different vegetation patterns support the dominant role of drainage-basin characteristics in dictating incised-valley-fill dimensions, especially for passive continental margins, and reveal possible controls by the size and dominant vegetation patterns of drainage areas.

The physiography of the depositional profile over which incised valleys develop also exerts a key control on the dimensions of incised-valley fills (Summerfield, 1985; Talling, 1998; Posamentier and Allen, 1999; Posamentier, 2001; Blum and Törnqvist, 2000; Törnqvist et al., 2006; Blum et al., 2013). Along continental margins, valley incision typically tends to begin developing when a relative sea-level fall exposes a convex-up topographic surface (Summerfield, 1985; Talling, 1998; Blum and Törnqvist, 2000; Blum et al., 2013; **Fig. 2.2**), notably either at the depositional shoreline break of the highstand shoreline, or at the shelf-slope break. Conceptual models (Talling, 1998; Posamentier and Allen, 1999; Posamentier, 2001; Törnqvist et al., 2006) predict that incised valleys tend to develop across the whole continental shelf if a relative sea-level fall exposes the entire shelf; by contrast, valleys tend to only incise near the coastal prism region if a relative sea-level fall does result in exposure of the shelf break. Additionally, a consideration made in sequence-stratigraphic thinking (e.g., Posamentier and Allen, 1999; **Fig. 6.1**) is that the magnitude of incision in relation to the generation of sequence boundaries is associated with the degree of exposure of the continental shelf: when a relative sea-level fall exposes the entire shelf, valley incision tends to be deeper compared to that associated with partial shelf exposure. In this work, potential effects of basin physiography (gradients and convexity along the depositional profile and shelf-break depth) on valley incision and widening are explored based on the assumption that the physiography of the continental shelf and nearshore during modern times serve as a proxy for the physiography of the shelf and nearshore during the Last Interglacial (LI) highstand. This analysis is undertaken with awareness that the present-day basin physiography might differ from that during the LI, notably arising from spatial variations in isostatic adjustment or in post-glacial shelf and shelf-break accretion, and because of differences in process regime,

variable styles of fluvial and shoreline responses linked to the diversity of climatic and tectonic settings, and autogenic dynamics. Although the maximum sea-level fall during the LGM is recorded to vary between 120 m to 130 m (Fairbanks, 1989; Yokoyama et al., 2000; Lambeck and Chappell, 2001; Peltier and Fairbanks, 2006; Simms et al., 2007b), geographically and across estimates by different authors, a 120-m fall is utilized as the representative value for scopes of analysis. In Chapter 3, shelves with breaks currently deeper than 120 m are demonstrated to contain thicker and wider incised-valley fills, on average, than shelves with breaks shallower than 120 m (**Fig. 6.1**). This finding challenges the notion that the magnitude of incision in relation to sequence boundaries is generally associated with the degree of exposure of the continental shelf. This might be due to the fact that the studied continental shelves with shelf breaks that are deeper than 120 m are associated with contributing drainage areas that are larger on average than those linked to shallower shelves. Yet, negative correlation between valley-fill thickness and shelf-break depth for cross-shelf valley fills in relation to continental shelf margin shallower than 120 m is noted (**Fig. 3.7A**), probably suggesting that valley fills from shallow shelves still record a causal link between magnitude of exposure, incision, and resulting valley-fill thickness. According to Talling (1998), along passive margins and in foreland basins, if the sea level remains above the continental shelf break, the magnitude of valley incision near the shoreline tends to be determined by the geometry of the coastal prism and valley incision depth will increase with the coastal-prism convexity. However, lack of correlation between valley-fill thickness and present-day coastal-prism convexity is documented in Chapter 3. This discrepancy could be attributed to the influence of overriding factors, or to the fact that convexity for present-day costal prisms might not be a good proxy for the coastal-prism convexity established during the LI.

The possible effects of shoreline hydrodynamic conditions on valley widening has also been explored. Mattheus and Rodriguez (2011) highlight that during episodes of relative sea-level rise, bay-ravinement, or estuarine shoreline erosion can widen incised valleys through the erosion of waves and tides near the shoreline. However, no correlation is seen between incised-valley-fill width and mean wave height at modern shorelines, as shown in Chapter 4. This might due to the fact that wave ravinement is prone to truncate the topmost part of the interfluves of some incised valleys, where each valley is expected to have been widest (**Fig. 4.16A**), counteracting the effects of any widening of the incised valleys by wave erosion. This inconsistency might also be explained by the fact that present-day hydrodynamic conditions at the shoreline may not be comparable to those that existed during the late TST, or by the influence of other overriding factors. Positive correlation between incised-valley-fill width and mean tidal range at modern

shorelines (**Fig. 4.14A**) might be due to the fact that tidal ravinement tends to result in erosion of valley margins, which in turn leads to the widening of the incised valleys (**Fig. 4.16B**). The results of this research also corroborate the notion that the basal surfaces of incised-valley fills are highly diachronous, composite erosional features (Strong and Paola, 2006, 2008; Martin et al., 2011; Blum et al., 2013).

In summary, the type of continental margin (active versus passive) appears to act as a predictor of the dimensions of incised-valley fills, potentially because of controls operated by factors such as the nature of basin physiography, climate, water discharge and sediment delivery. In addition, the findings in Chapter 3, and additional analysis between valley geometry and shoreline hydrodynamic conditions in Chapter 4, might imply that upstream controls (e.g., contributing drainage-basin area and dominant vegetation type prevailing in the catchment) could be more important in modulating the incision and widening of near-shore incised-valley systems, compared to the characteristics of the receiving basin (e.g., coastal-prism convexity, shelf-break depth, substrate lithology and shoreline hydrodynamic conditions), especially for passive continental margins.

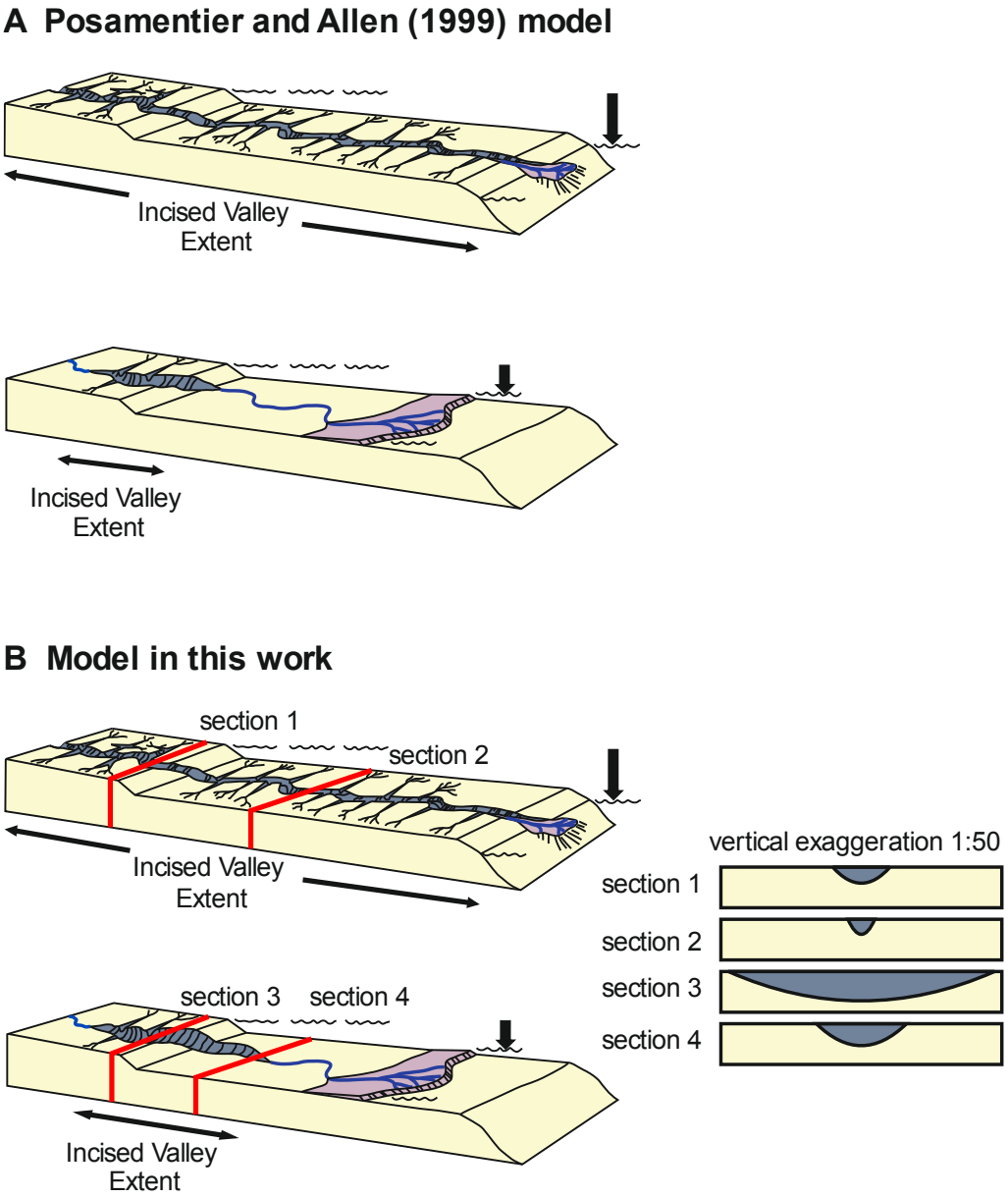

Fig. 6.1. *Comparison between a model (A) illustrating differences in incised-valley development depending on the degree of shelf exposure (modified from Posamentier and Allen, 1999), and a corresponding model (B) revised according to the findings of this research. Note that the thickness and width of valley fills shown for section 1-4 on the right are scaled with the estimated means of the dimensions of valley fills measured beneath the coastal plain and on the shelf corresponding to shelf-break depth shallower or deeper than 120 m respectively in Chapter 3.*

6.2 Geological controls on incised-valley-fill stratigraphic architecture

Classical facies models pertinent to coastal-plain incised-valley fills (Dalrymple et al., 1992; Allen and Posamentier, 1994b; Zaitlin et al., 1994) typically recognize three segments: (i) a landward segment typically characterized by fluvial systems throughout its depositional history, (ii) a middle segment exhibiting a drowned-valley estuarine complex that existed around the time of maximum transgression, overlying a lowstand to transgressive succession of fluvial and estuarine deposits, and (iii) a seaward segment commonly comprising basal fluvial deposits overlain by estuarine deposits and capped by fully marine deposits. Quantitative analysis of the internal fills of late-Quaternary incised-valley fills in this work suggests that the general stratigraphic organization of these IVFs is overall consistent with the qualitative depictions in the widely adopted classical facies models (e.g., Dalrymple et al., 1992; Zaitlin et al., 1994; Allen and Posamentier, 1994b), which confirms the primary control of sea-level on the internal fills of near-shore incised-valley systems. However, on the basis of a large composite dataset, a wide variability in stratigraphic architectures of the internal fills of incised valleys has been recognized in this work (**Fig. 6.2**; cf. Chaumillon et al., 2008; 2010), which is not captured by these classical models. Variations in the facies architecture of coastal-plain and cross-shelf valley fills can be accounted for factors other than relative sea-level change, such as tectonic setting (continental-margin type), basin physiography, catchment area, river-system size and shoreline hydrodynamics (**Fig. 6.2**).

The tectonic setting of the host continental margins exert a critical control on IVF stratigraphic architecture, notably through its modulation of basin physiography, rates and mode of sediment supply, and nature of sediment load. This is supported by the observation that compared to their counterparts on passive margins, coastal-plain IVFs hosted on active margins contain, on average, a higher proportion of fluvial deposits and a lower proportion of central-basin estuarine deposits; estuarine deposits tend however to be thicker.

Contributing drainage-basin size and incised-valley dimensions also show relationships with the stratigraphic architecture of IVFs. Positive correlations between the thickness and proportion of lowstand systems tracts versus coastal-plain IVF dimensions identified in this work might suggest a control exerted by contributing drainage-basin area on the scale of the fluvial systems that carved and infilled the valleys. Positive relationships between the thickness of fluvial deposits, bayhead-delta deposits and central-basin estuarine deposits, versus coastal-plain IVF dimensions and valley catchment area are noted in Chapter 4; these relationships are interpreted to reflect the roles of the river-system scale and

contributing drainage area in dictating the rates of sediment supply, and of valley size in controlling accommodation.

Shelf gradient is suggested to be a significant control on the thickness and proportion of barrier-complex deposits and estuarine muds in cross-shelf valley fills. Equilibrium in sandy shorelines is reported by previous workers (Cowell and Thom, 1994; Stive and de Vriend, 1995) to be attained over timescales of 10^2 to 10^3 years. The magnitude of horizontal shoreline shifts tends to increase with decreasing shelf gradient, for a given relative sea-level change. Hence, any high-energy environment located in the area of the coastline across steeper-gradient shelves tends to stabilize at a location for longer periods compared to lower-gradient shelves, during periods of negligible or slow rates of relative sea-level rise, which could possibly result in the accumulation of barrier-complex deposits within cross-shelf valleys (e.g., Posamentier, 2001; Reijenstein et al., 2011; Wetzel et al., 2017). Shelf gradient influences the nature of transgression, and also exerts an indirect control on the erodibility of barrier deposits when considered together with climate. Also, warm tropical or sub-tropical climates are typically characterized by particularly high rates of shoreline cementation, which is documented to occur on a scale of months to decades (Frankel, 1968; Hopley, 1986; Moore, 2001; Vousdoukas et al., 2007; Cawthra and Uken, 2012): longer periods of early barrier cementation taking place along steeper shelves before barrier overstepping might result in the accumulation of barrier deposits that are notably more resistant to transgressive erosion. Positive relationships are noted in this work between the thickness and proportion of barrier-complex deposits within incised-valley fills versus present-day average shelf gradient, and this may indicate a control by the continental shelf physiography on the development and preservation of barrier-island environments within incised valleys. The gradient of the continental shelf might also play a role in the establishment and preservation of the thickness of estuarine muds in cross-shelf valley fills by partly controlling the magnitude of valley incision and resultant in-valley accommodation. Positive correlations between the proportion of estuarine bay/lagoon elements and the average shelf gradient noted in this work might reflect the fact that steeper shelves tend to promote larger differences between shelf gradient and the fluvial equilibrium profile, which in turn could promote deeper fluvial incision for a given relative sea-level fall (Schumm and Brackenridge, 1987; Leckie, 1994; Posamentier and Allen, 1999; Wang et al., 2019), and therefore provide increased accommodation for estuarine bay/lagoon deposits that can be preserved in incised valleys.

Shoreline hydrodynamics is also demonstrated to act as a control on the stratigraphic architecture of IVFs. In particular, incised-valley-fill geometry, coastal

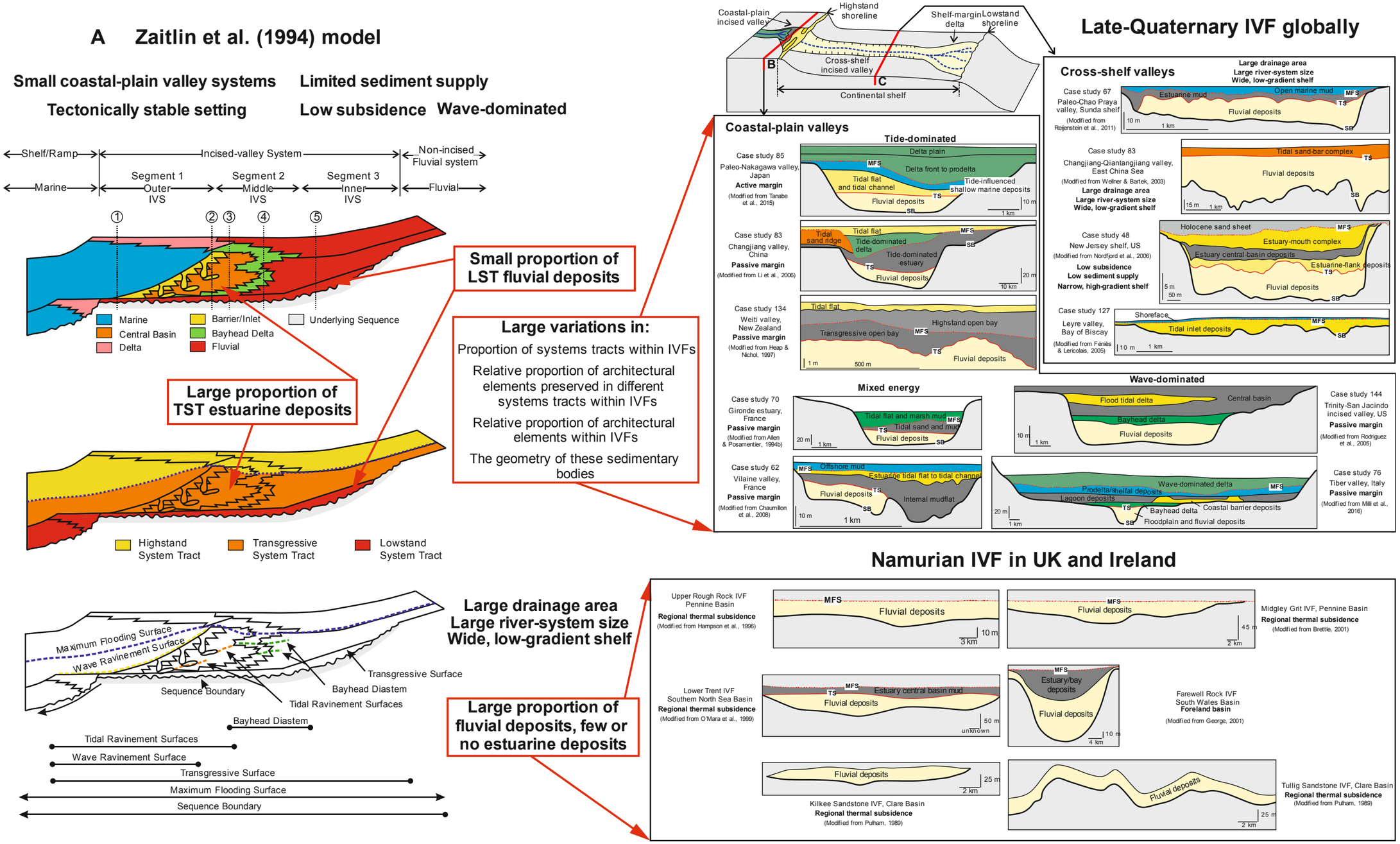

Fig. 6.2. *Comparison between representative stratigraphic architectures of late-Quaternary incised-valley fills and Namurian valley fills in the UK and Ireland, considered in this work, versus stratigraphic organization of valley fills depicted in the model by Zaitlin et al. (1994). In (B), for each example, information on the geological context is reported. Key sequence-stratigraphic bounding surfaces (SB, TS and MFS) are shown for examples for which sequence-stratigraphic interpretations were presented in the original source work. SB denotes the sequence boundary, TS denotes the transgressive surface, and MFS denotes the maximum flooding surface.*

physiography (open-ocean settings and enclosed or semi-enclosed seas) and shelf physiography (shelf width, shelf-break depth and shelf gradient) can indirectly influence the stratigraphic architecture of IVFs by affecting hydrodynamic conditions near the shoreline. Correlations between incised-valley-fill width and present-day mean tidal range or mean wave height at the shoreline suggest that tidal dynamics at the shoreline may play a role in the widening of the incised valleys. Correlation between the proportion of tide-dominated elements within incised-valley fills and incised-valley-fill width might attributed to the reciprocal controls between hydrodynamic conditions at the shoreline and valley geometry. Distinctive differences in proportion of elements recording different process regimes between valley fills from open-ocean settings and those from enclosed or semi-enclosed seas are identified in this study (**Fig. 4.11**), which might reflect differences in hydrodynamic conditions across these settings.

6.3 Importance of other controls

A wide range of other factors that have not been examined in this work can control valley-fill dimensions and stratigraphic architecture. These include, for example, pre-existing structures, inherited topography along the base of incised valleys, valley shape, different tectonic regimes of tectonically active settings, and variations of substrate type. Inherited topography and the morphology of the bedrock exposed along the base of incised valleys might have a potential control on local hydrodynamics and resultant sedimentation in the valley fill. In tectonically active settings, extensional, compressional and strike-slip tectonic regimes can variably exist and determine differences in rates of subsidence or uplift, which might influence the resultant incised-valley-fill dimensions and stratigraphic architecture. For example, subsidence can control the dimensions, stratigraphic architecture and preservation potential of incised-valley fills, whereby higher subsidence rates increase the preservation potential of the valley forms. Many of the late-Quaternary examples considered in this Thesis might have relatively low preservation potential due to long-term relative sea-level fluctuations and the limited rates of subsidence to which their host margins are subject. By contrast, the Carboniferous examples discussed in Chapter 5 are located in sedimentary basins that were largely subject to continuous and prolonged regional thermal subsidence, which largely allowed preservation of their fluvial infill. The significance of subsidence on the dimensions and stratigraphic architecture of incised-valley fills can be manifested in two ways through its effects on relative sea-level change. Firstly, subsidence counteracts the effects of eustatic sea-level falls in consuming accommodation, and this can impact

the vertical shifts of river profiles that promote vertical fluvial incision. Secondly, subsidence reinforces the effect of eustatic sea-level rise on the generation of accommodation, which in turn can have an influence on channel-belt stacking patterns as well as on the morphology of the formative river channels. Additionally, higher rates of relative sea-level rise tend to induce rapid shoreline migration in response to transgression, which can cause any high-energy environment (wave and/or tide dominated environment) at the shoreline to transit rapidly along the path of the extant cross-shelf incised valleys, therefore favouring the preservation potential of basal fluvial deposits in the valley fills. Furthermore, key stratigraphic markers that characterize interfluves, such as palaeosols, and that characterize the internal fills of incised valleys, such as wave/tidal ravinement surfaces, might not develop in rapidly subsiding basin: during eustatic sea-level fall subaerial exposure and related pedogenesis might have limited temporal duration, whereas during eustatic sea-level rise rapid shoreline migration can limit the length of time over which erosion by wave and tidal processes can take place at the shoreline (Blum and Törnqvist, 2000). Finally, factors such as pre-existing structures, gradient, local topography, and variations in substrate type could control the location, morphology, and orientation of an incised valley-fill along a margin, in turn influencing incised-valley-fill dimensions and stratigraphic architecture. Future research could attempt a detailed analysis of these aspects to further improve our understanding of geological controls on the geometry and stratigraphic architecture of incised-valley fills.

6.4 Incised-valley-fill dimensions and lessons for the ancient rock record

Data on morphometric parameters of incised-valley fills studied in this work, including both late-Quaternary examples distributed globally and Carboniferous incised-valley systems in UK and Ireland, have been plotted in **Fig. 6.3**. For comparison, data on the scales of ancient incised-valley systems interpreted in the preserved stratigraphic record based on a literature compilation by Gibling (2006) have been included. Results (**Fig. 6.3**) indicate that late-Quaternary examples cover a wider range of width and thickness values, compared to the ancient examples studied in this work and documented in the database of Gibling (2006), with width varying over three orders of magnitude (from 142 to 90, 000 m) and thickness over two orders of magnitude (from 6 m to 92 m). The studied Carboniferous valley systems from UK and Ireland demonstrate a narrower range of width and thickness values, with width-to-thickness ratios mainly in the ~100-1000 range. The widths of these Carboniferous examples fall within the upper end

of the spectrum of width of late-Quaternary examples. Compared to the datasets from Gibling (2006), Carboniferous valley systems studied in this work are comparable in scale to other documented Carboniferous incised valleys. Most ancient incised valleys within Gibling (2006) database are comparable in scale to the larger late-Quaternary examples considered in this work. Additionally, Gibling (2006) demonstrates that Carboniferous incised-valley fills tend to be thicker and wider than Jurassic and Cretaceous examples (mean value of thickness: 31.0 m vs. 21.2 m; mean value of width: 10.0 km vs. 5.6 km).

The discrepancy between the dimensions of late-Quaternary incised-valley fills and those of ancient examples interpreted from the ancient rock record (**Fig. 6.3**) can be attributed to several factors. First, large incised-valley fills tend to be more easily identified in the preserved stratigraphic record than smaller valley systems. Second, thicker ancient valley systems in the dataset by Gibling (2006) might represent multiple cycles of eustatic sea-level fluctuations, unlike the late-Quaternary examples documented in this Thesis, and especially those formed during the last glacial-interglacial cycle. Third, this discrepancy might relate to the preservation potential of late-Quaternary examples. One possibility is that large valley systems may have higher preservation potential than smaller valley systems. Moreover, as noted in section 6.3, subsidence rates control the preservation of incised-valley fills in the ancient rock record. Specifically, for a relative sea-level fall of given magnitude, and therefore for a given scale of incised-valley incision at late lowstand, incised-valley fills associated with more rapidly subsiding basin are expected to be more limitedly affected by wave and tidal erosion when the shoreline backsteps across the extant incised valley during sea-level rise (see details in section 6.3). Fourth, intrinsic differences in the scale of incised-valley systems might exist between Icehouse vs. Greenhouse periods of the Earth history, and in relation to the timing of advent of land plants and bank-stabilizing deeply rooted vegetation. Icehouse periods are typically characterized by high-frequency and high-magnitude (> 100 m) sea-level changes driven by the waxing and waning of continental ice sheets, whereas greenhouse periods are characterized by high-frequency but limited-amplitude (< 10 m) sea-level fluctuations (Lehrmann and Goldhammer, 1999; Séranne, 1999). Gibling (2006) highlights that the larger scale of Carboniferous incised valleys (icehouse) compared to those formed in Jurassic or Cretaceous period (greenhouse) might be due to the influence of the higher magnitude glacioeustatic fluctuations experienced by the Carboniferous examples.

Vegetation types have evolved throughout the Earth History: the land plants that characterize the Earth today are different from those in the geological past. Vegetation types and density in both catchment areas and basins, and their effects

on bank stabilization and river hydrology, control fluvial morphodynamics and planform styles (Davies and Gibling, 2010a, 2010b, 2011; Mial, 2014; Santos et al., 2017). Hence, care must be taken when extrapolating the insight derived from the late-Quaternary icehouse examples to the ancient stratigraphic record. Insight derived from late-Quaternary examples might have only a limited applicability to the ancient past, especially in application to the Palaeozoic, when land plants had only recently colonised the land masses and had only shallow root systems (Santos et al., 2017). To improve our understanding of geological controls on the dimensions and stratigraphic architecture of incised-valley fills, future research could concentrate on quantitative analysis incised-valley-fill characteristics for: (i) icehouse vs. greenhouse periods and (ii) successions accumulated before and after the advent of land plants and under variable conditions of vegetation types and density.

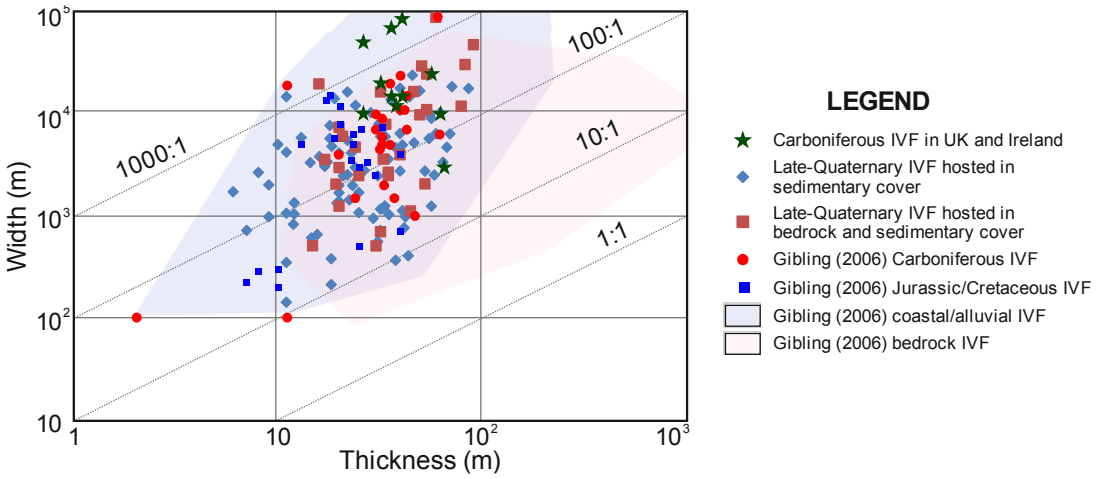

Fig. 6.3. *Scales of late-Quaternary incised-valley fills and Namurian incised-valley fills in the UK and Ireland considered this work vs. valley fills interpreted in the ancient stratigraphic record as extracted from the published literature by Gibling (2006).*

6.5 Lessons for 'source-to-sink' studies

The source-to-sink concept focuses on quantification of the main components of siliciclastic sedimentary systems, from sediment-producing source areas, through the dispersal system, to deposition within a wide range of potential sedimentary sinks, which are typically considered to be related in analytical approaches that use mass-balance theory (Sømme et al., 2009a; **Fig. 2.19** and **2.20**). On the basis of a compilation of modern and late-Quaternary siliciclastic systems from different tectonic and climatic settings, previous research on source-to-sink systems

(Anderson et al., 2004, 2016; Syvitski and Milliman, 2007; Sømme et al., 2009a,b; Blum et al., 2013; Xu et al., 2016; Sweet and Blum, 2016) has illustrated positive scaling relationships between the scale of drainage-basin area, water discharge, river-driven sediment flux, fluvial channel-belt dimensions, and the scale of distal components of sediment-dispersal systems (e.g. submarine canyons and basin-floor fans). For instance, Sømme et al. (2009a, 2009b) recorded morphometric parameters of 29 submodern source-to-sink systems, which characterize the scale of contributing drainage-basin areas, fluvial systems and shelf to deepwater systems, and identified strong positive relationships between drainage area, river length and gradient, shelf gradient, shelf width, dimensions of submarine canyons and scale of basin-floor fans. Considering the data on submarine-fan scale and drainage-area size reported in Sømme et al. (2009a), it becomes possible to recognize that strong positive correlations exist between the scale of submarine fans (fan area, fan width, fan length and fan volume) and their contributing drainage-basin areas, based on 28 submodern source-to-sink systems distributed across different climatic zones and tectonic settings (**Fig. 6.4**). A regression analysis between pairs of variables relating to these attributes (**Fig. 6.4**) has been performed in order to describe scaling between the size of submarine fans and the size of their contributing drainage-basin areas.

Incised-valley systems have long been recognized to play an important part in transferring sediments from sediment-producing source areas to deep-marine environments, especially during relative sea-level fall (Posamentier and Allen, 1999; Blum and Törnqvist, 2000; Blum et al., 2013). Positive correlations between incised-valley-fill dimensions and contributing drainage-basin area recognized in the compilation of late-Quaternary examples presented in Chapter 3 can broaden existing source-to-sink scaling relationships to incised-valley fills. Notably, the scale of incised-valley fills could be utilized to infer or predict the scales of their contributing drainage-basin areas based on the regression analysis reported in Chapter 5 (**Fig. 5.4**), which is derived from the scaling relationships of late-Quaternary examples. The reconstructed drainage-basin areas can subsequently employed to predict the scale and grainsize character of linked downdip coarse-grained lowstand deltas or basin-floor fans based on the scaling relationships derived from the data by Sømme et al. (2009a; **Fig. 6.4**).

Analyses of source-to-sink systems have recently been applied to deep-time stratigraphic systems, which largely are based on facies architectures in the ancient record using the empirical equations derived from theoretical or experimental studies (Bhattacharya and Tye, 2004; Carvajal and Steel, 2012; Miller et al., 2013; Holbrook and Wanas, 2014). Methods for the estimation of drainage-basin area

based on the scaling relations of dimensions of late-Quaternary IVF can provide a tool that integrates existing approaches. In Chapter 5, the resultant database-derived power-law relationships between late-Quaternary incised-valley-fill dimensions and drainage-basin area have been applied to the estimation of the size of contributing drainage areas that fed river systems forming incised-valley fills recognized in the ancient rock record (Namurian of the United Kingdom and Ireland), in combination with palaeohydrological estimations based on dune-scale cross-set thickness statistics.

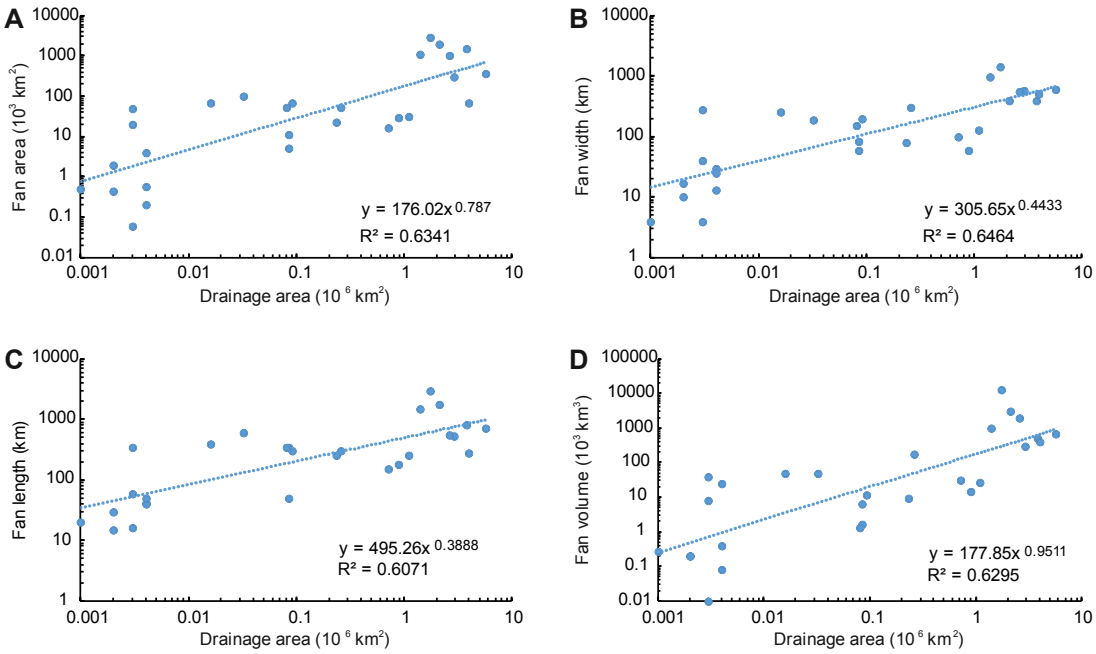

***Fig. 6.4**. Cross-plots of the scale of submarine fan (fan area, fan width, fan length and fan volume) versus drainage-basin area for 28 submodern source-to-sink systems. Data taken from Sømme et al. (2009a). For each pair of variables, the results of regression analysis (power-law relationship and coefficient of determination, R^2) are reported.*

However, two considerations should be made on the feasibility of employing this approach to link contributing drainage areas to both IVF characteristics and the scale of linked downdip components of sediment-dispersal systems. Firstly, Amazon-scale river systems are not always associated with Amazon-scale fans (e.g., Rough Rock Formation in Chapter 5). This is because sediment bypassing across a shelf might be limited due to the large amount of sediment storage on the continental shelf itself. The amount of shelf storage in sediment budgets is indicated to be primarily determined by wave and shelfal current patterns, inherited bathymetry, local topography and temporal variations in shelf morphology, which in turn is mainly controlled by the balance between sediment supply, subsidence/uplift

and eustatic sea level (Sømme et al., 2009a). As for the Rough Rock Formation, discussed in Chapter 5, the relatively limited volume of deep-water deposits in the downdip components of this area is attributed to the fact that large volumes of sediments could be permanently sequestered in the large composite valleys that formed across the shelf during eustatic sea-level fall, due to the regional thermal subsidence prevailing in the area. Secondly, for tectonically active systems, the size of contributing drainage areas might not be a good predictor of incised-valley-fill dimensions or of the scale of submarine fans. Tectonically active margins are typically associated with small drainage areas (Fig. 3.5) and tend to have high specific sediment yield and narrow, steep shelves, which appear to be associated with large incised-valley systems (**Fig. 3.5**). Furthermore, small source-to-sink systems associated with tectonically active margins, with narrower and steeper shelves, might be much more efficient in bypassing sediment to the continental slope and basin floor than larger source-to-sink systems (Sømme et al., 2009a). However, these considerations need to be corroborated by further analysis.

6.6 Implications for applied resource geology

Some results of this work have applied significance for subsurface characterization, for example in contexts of hydrocarbon exploration and production, groundwater exploitation and clean-up, and underground carbon sequestration (**Fig. 6.5**). The ability to link the scale of incised-valley fills to characteristics of catchments and shelves provides key insight for the development of semi-quantitative guidelines, which can be utilized to infer or predict the size, location and timing of accumulation of potential downdip shallow- to deep-marine hydrocarbon reservoirs (**Fig. 6.5A**). Additionally, incised-valley fills themselves can form important hydrocarbon reservoirs or groundwater aquifers. Typically, during the episodes of relative sea-level fall and lowstand, incised valleys tend to be filled with coarse-grained fluvial deposits first, which are subsequently overlain by estuarine and marine deposits during the ensuing relative sea-level rise (Roy, 1984; Dalrymple et al., 1992; Allen and Posamentier, 1993; Wright and Marriott, 1993; Shanley and McCabe, 1993, 1994; Dalrymple et al. 1994; Zaitlin et al., 1994; Blum and Törnqvist, 2000; Blum et al., 2013). Thus, many valley fills are sand prone, and are in some cases sealed by offshore mud-prone deposits; this architectural configuration makes them potential hydrocarbon reservoirs, groundwater aquifers and sites for the underground storage of CO_2 (Wright and Marriott, 1993; Shanley and McCabe, 1994; Dalrymple et al. 1994; Zaitlin et al., 1994; Blum et al., 2013; **Fig. 6.5B**). In Chapter 3, incised-valley-fill dimensions are demonstrated to be affected by a wide variety of geological controls and hence this should be taken into account when exploration of

incised-valley-fill plays is performed across different tectonic, physiographic and climatic settings. Notably, results illustrating that incised-valley fills along active continental margins tend to be thicker and wider than their counterparts along passive continental margins in this work might imply that the incised-valley fills along active continental margins could be considered as potential exploration targets.

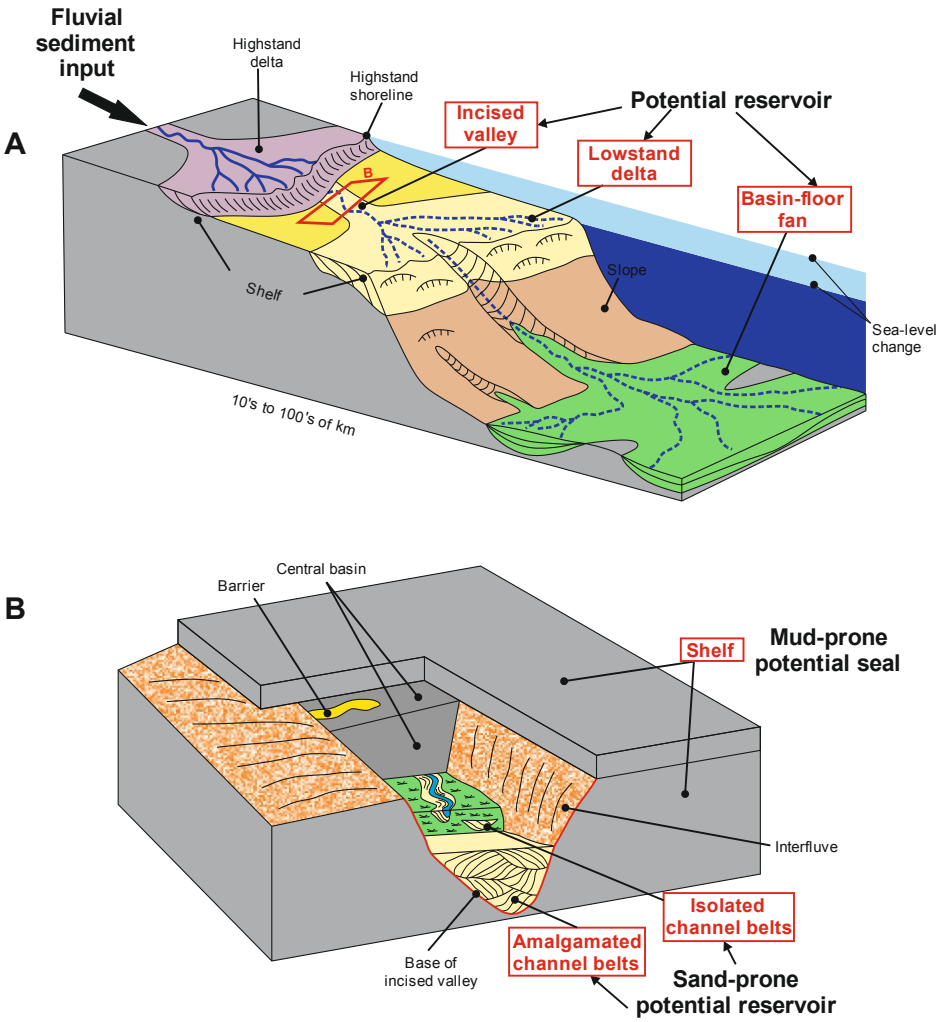

Fig. 6.5. *Schematic diagram A illustrating the importance of incised-valley fills for the inference or prediction of linked downdip lowstand delta and basin-floor fan systems, all of which might serve as potential applied subsurface hydrocarbon reservoirs. Inset map B exhibits the general characteristics of architectural configuration in typical cross-shelf incised-valley fills, which makes incised-valley fills potential exploration targets from a petroleum-system perspective. Sand-prone basal fluvial deposits might act as potential reservoirs and the widely developed offshore muds on the top could be considered as potential top seal rocks. Diagram A modified from Blum and Womack, 2009; originally after Posamentier and Kolla, 2003.*

In the characterization and modelling of subsurface hydrocarbon reservoirs, both modern and outcrop analogues are routinely employed to constrain the geometry, spatial relationships and complexity of sedimentary bodies (e.g., Reynolds, 1999; Bridge and Tye, 2000; Bhattacharya and Tye, 2004; Tye, 2004; Pranter et al., 2009; Deveugle et al., 2014). Quantitative analysis of the different possible geological controls on the stratigraphic architecture of incised-valley fills presented in Chapter 4 indicates that the relative proportion and geometry of different architectural elements within incised-valley fills are determined by a wide variety of factors, notably catchment size, river-system size, tectonic setting, shoreline hydrodynamics, coastal physiography, shelf width, shelf-break depth and shelf gradient. These findings highlight the importance of selecting suitable modern and outcrop analogues for reservoir or aquifer characterization, and that the late-Quaternary case studies themselves constitute a large pool of potential analogues, which can be used for predicting the architecture of subsurface successions of the same type. The variability in architectural motifs in incised-valley fills documented in this research can be employed in subsurface studies for purposes of uncertainty quantification.

Based on the facies architecture of incised-valley-fill fluvial deposits in the preserved stratigraphic record, reconstruction of palaeohydraulic characteristics of valley-forming river systems and estimation of their drainage-basin area in combination with provenance analysis and sedimentological data (as exemplified in Chapter 5) can provide key insight into potential characteristics of the source areas (e.g., composition of exposed rock formation and climate in the source area). This approach exemplified in Chapter 5 has significant implications for the predictions of hydrocarbon reservoir lithology and quality in hydrocarbon prospects. Typically, sediment composition of reservoir units is primarily determined by its provenance, notably the composition of exposed rock formations in the source areas (e.g., Pettijohn et al., 1987). For instance, erosion of volcanic arc terranes commonly yield clay-rich volcanic litharenites with an abundance in unstable framework grains, such as volcanic rock fragments and labile minerals such as mica, plagioclase and amphiboles (Marsaglia and Ingersoll, 1992; Critelli and Ingersoll, 1995). These sandstones generally have low reservoir quality due to the widespread occlusion of primary porosity during burial and compaction. By contrast, shield terranes, such as stable continental interiors, tend to result in multi-cycle quartz-rich sandstones that commonly have higher reservoir quality (Dickinson, 1985; Johnson, 1993). Composition of the reservoir rocks is also influenced by the climatic conditions prevailing in the source area or the intermediate sinks (Johnson, 1990a, 1990b, 1993; Franzinelli and Potter, 1983). For example, in humid tropical climates, high rates of chemical weathering could lead to the labile minerals in siliciclastic and

igneous rocks to be more readily weathered and thus produce clay instead of sand or gravel; carbonate rocks tend to experience extensive dissolution. In this perspective, for hydrocarbon plays with available 1D core data, the approach stated above can be replicated to provide key information of the source areas such as composition of exposed rock formation and climate, which can itself be applied for predictions of reservoir lithology and quality in hydrocarbon prospects located away from available datasets. For hydrocarbon plays with only available seismic data, estimation of drainage-basin area could be tentatively reconstructed based on incised-valley-fill geometry identified in the seismic data and can thus yield some insight into the characteristics of potential source areas, which might provide some important guidelines for predictions of reservoir lithology and quality in the local hydrocarbon prospects.

7 Conclusions and future work

This chapter provides a brief summary of the work in this Thesis, presenting conclusions with regard to the overarching Thesis aim and research objectives stated in Chapter 1. Recommendations are also given for possible areas of future research, which might be undertaken to further build upon the findings presented and discussed in this Thesis.

7.1 Summary

Chapter 2 provided a brief review of published literature pertinent to the research topics investigated in this work, including an overview of external controls (sea-level change, climate and tectonics) on fluvial geometry and architecture and the current understanding relating to incised-valley-fill systems. This forms the essential basis to investigate the geological controls of geometry and stratigraphic organization of valley fills and to decipher their prevailing boundary conditions from the preserved alluvial stratigraphic record, which is the focus of Chapters 3-5.

Chapter 3 concentrated on the investigation and evaluation of the relative roles of potential controlling factors (e.g., magnitude and rate of relative base-level fall, basin physiography, contributing drainage-basin size, climate, substrate characteristics, tectonic setting), which might interplay in determining the geometry of incised-valley-fill systems. This was accomplished via a novel database-driven statistical analysis of 151 globally distributed late-Quaternary incised-valley fills from the published literature, which is considered to be the largest study of this type undertaken so far.

By means of a quantitative analysis of a very large composite dataset, trends were identified to attempt to decipher the relative roles of potential geological controls in determining the geometry of incised-valley-fill systems. The results of the analysis presented in Chapter 3 were built upon some assumptions: (i) the magnitude of valley incision is considered to be primarily controlled by the degree of shelf or coastal-plain incision, which itself is determined by the vertical shifts in fluvial longitudinal equilibrium profile possibly arising from changes in base level, water discharge and sediment supply, and by the degree to which the graded profile is approximated through knickpoint retreat, together with potential truncation by ravinement processes; (ii) valley widening is significantly influenced by the rate of

lateral migration of channel belts hosted within them, which in turn is expected to be controlled by water discharge and sediment supply, and by valley-wall erodibility.

Database-driven quantitative analysis of the studied late-Quaternary incised-valley fills yielded the following main findings: (i) incised-valley fills hosted on active continental margins are demonstrated to be thicker and wider, on average, than those hosted on passive continental margins, suggesting the important role of the tectonic setting of continental margins in controlling the geometry of incised-valley-fill systems, possibly via effects on relative sea-level change, basin physiography, climate, water discharge and modes of sediment delivery; (ii) positive relationships are noted between incised-valley-fill geometry and the contributing drainage-basin area, which highlights the key role of drainage-basin area, serving as a proxy of water discharge, in dictating valley-fill dimensions; (iii) climate is also indicated to exert potential controls on the geometry of incised-valley-fill systems, especially by means of modulation of characteristics in catchment area, such as temperature, peak precipitation, vegetation and permafrost; (iv) continental shelves with shelf-slope breaks currently deeper than 120 m are found to contain thicker and wider incised-valley fills, on average, than shelves with shelf-slope breaks shallower than 120 m. This result contrasts with the notion, embedded in sequence-stratigraphic thinking, that the degree of exposure of the continental shelf dictates the magnitude of vertical incision preserved in sequence boundaries. This discrepancy might be attributed to the fact that the studied continental shelves with shelf-slope breaks that are documented to be deeper than 120 m are primarily associated with larger drainage-basin areas, compared to those with shallower shelf-slope breaks. However, negative scaling relation between valley-fill thickness and shelf-break depth for cross-shelf valley fills hosted on continental shelves with shelf-slope breaks that are shallower than 120 m are identified, which likely reflects a causal link between magnitude of exposure, incision, and resulting valley-fill thickness; (v) the lack of correlation between valley-fill thickness and present-day coastal-prism convexity challenges the view that magnitude and location of valley incision are primarily determined by the coastal-prism convexity at the highstand shoreline, if the sea-level does not drop below the shelf break. This might be due to the potential influence of other overriding factors (e.g., the size of contributing drainage areas), or to the fact that the form of present-day coastal prisms might differ significantly from that of coastal prisms developed along the same coasts during the Last Interglacial.

These findings challenge some paradigms that are widely adopted in sequence-stratigraphic studies, and have significant implications for analysis and improved understanding of source-to-sink sediment route-ways, as positive scaling relations

between incised-valley-fill dimensions and contributing drainage-basin area recognized in this work extend existing source-to-sink scaling relationships to incised-valley fills. The applied significance of these results is also discussed: notably the incised-valley-fill systems themselves can form potential hydrocarbon reservoirs or groundwater aquifers and in consideration of the various controls in determining the geometry of incised-valley-fill systems, care should be taken during exploration of incised-valley-fill plays across different tectonic, physiographic and climatic settings. Additionally, incised-valley-fill systems could act as reference for the prediction of the size, location and timing of accumulation of potential downdip shallow- to deep-marine hydrocarbon reservoirs in consideration of the scaling relationship between valley-fill dimensions and drainage-basin area and the existing scaling relations between drainage-basin area and the scale of downdip shallow- to deep-marine systems, such as submarine canyons and basin-floor fans reported by previous workers (e.g., Syvitski and Milliman, 2007; Sømme et al., 2009a,b; Blum et al., 2013; Sweet and Blum, 2016).

Chapter 4 focused on the assessment of the general validity of classical facies models for incised-valley fills and on the investigation of the relative importance of different potential controls on their stratigraphic organization. This was achieved through a database-driven statistical analysis on the basis of a literature compilation of 87 late-Quaternary incised-valley fills, distributed across different tectonic, climatic and physiographic settings. Different geological factors such as continental-margin type, contributing drainage-basin area, valley-fill geometry, coastal physiography, shelf physiography and shoreline hydrodynamics – in addition to the role of sea level – were assessed and evaluated as potential controls of the internal architecture of incised valley fills.

The following main findings are summarized: (i) the overall stratigraphic organization of the studied coastal-plain incised-valley fills is considered to be in agreement with what represented in popular facies models, but significant variability in stratigraphic architectures is identified; (ii) positive relationships between the thickness or proportion of LST deposits and incised-valley-fill geometry might indicate potential controls exerted by the size of catchment areas and water discharge in dictating the scale of lowstand fluvial deposits. The thickness of fluvial, bayhead-delta, and estuarine bay/lagoon elements and incised-valley-fill dimensions are positively correlated with the size of contributing drainage areas, suggesting the key role of catchment size in determining the scale of these deposits, likely through its effects on water discharge, sediment supply, sediment-load type, and incised-valley geometry; (iii) positive relations between the thickness or proportion of barrier-complex deposits within incised-valley fills and the present-

day average shelf gradient might reflect a potential control exerted by the continental-shelf physiography on the development and preservation of barrier-island environments within incised valleys. The gradient of the continental shelf may also have an indirect influence on the establishment and preservation of the geometry of estuarine muds in cross-shelf valley fills by its effects on magnitude of incisions and resultant in-valley accommodation; (iv) correlations between incised-valley-fill width versus present-day mean tidal range or mean wave height at the shoreline are also explored and demonstrate that tidal dynamics at the shoreline might play a role in driving the widening of the incised valleys; (v) correlation between the proportion of tide-dominated elements within incised-valley fills and incised-valley-fill width might be attributed to the interplay of hydrodynamic conditions and valley geometry; (vi) valley fills from open-ocean settings and those from enclosed or semi-enclosed seas are found to show significant differences with respect to the proportion of elements relating to different process regimes; these differences are consistent with differences in hydrodynamic conditions across these settings.

This chapter revealed the complexity of the internal sedimentary fills of incised valleys to a level of detail that is not accounted for by traditional facies and sequence-stratigraphic models. These results are important for guiding interpretations and predictions of the architecture of ancient paralic successions, in the subsurface and in outcrop. Nevertheless, it should be taken into account that results derived from late-Quaternary examples could only be limitedly utilized as templates for interpreting or predicting the stratigraphic architecture of ancient paralic successions, especially for those developed under greenhouse climates and subject to modest sea-level fluctuations.

In **Chapter 5**, the focus was shifted to the analysis of the internal fills of Namurian incised-valley fills of the United Kingdom and Ireland. Scaling relationships derived from late-Quaternary examples, presented in Chapter 3, were applied to tentatively reconstruct the contributing drainage areas of the rivers feeding the studied Namurian incised-valley fills. This was accomplished in consideration of the similarity in magnitude and frequency of eustatic sea-level fluctuations during Namurian and late-Quaternary times. The facies architecture of these ancient examples was also studied, to help decipher palaeohydraulic characteristics of their formative rivers and to attempt a refinement of regional palaeogeographic reconstructions.

The main findings derived from this chapter are summarized below: (i) the facies organization recorded in the studied valley-fill fluvial deposits indicate that their formative palaeorivers were likely perennial and characterized by relatively low

discharge variability, which is consistent with the dominantly equatorial humid tropical climate inferred for the study areas during the Namurian; (ii) observed variations in proportions of facies indicative of likely upper- vs. lower-flow-regime conditions and in the thickness distributions of dune-scale cross sets recorded in the valley-fill fluvial deposits might reflect a control exerted by the size of drainage areas on river hydrology; (iii) estimations of the size of contributing drainage areas in combination with existing provenance and sedimentological data have been considered in order to understand the potential extent of source areas, for the refinement of regional palaeogeographic reconstructions for the Namurian.

The approach employed in this chapter could be extended to the study of palaeohydrologic characteristics and to palaeogeographic reconstructions of other incised-valley fills.

In **Chapter 6**, an integration of the primary findings of the previous chapters of the Thesis was presented, and the implications of these results for sequence-stratigraphic models and source-to-sink analyses and their applied significance were discussed in a wider context. In particular, in terms of applied significance, the main findings of this work can provide key insight into potential characteristics of the source areas, which control hydrocarbon-reservoir lithology and quality.

7.2 Future research

The work presented in this Thesis has set the stage for further research about incised-valley fills developed in the Quaternary and in the ancient past, which could be undertaken in a number of ways to further improve our understanding of geological controls on the geometry and stratigraphic architecture of incised-valley fills.

7.2.1 Quantitative analysis of incised-valley-fill characteristics for Icehouse versus Greenhouse periods

The research presented in this Thesis has mainly focused on the quantitative analysis of late-Quaternary examples, with only limited consideration of deep-time incised-valley fills. The applicability of quantitative facies models based on late-Quaternary examples to the ancient rock record remains unclear. One issue of considerable concern is the fact that late-Quaternary icehouse periods are characterized by high-frequency (<400 kyr) and high-amplitude (>50 m) global eustatic sea-level changes, unlike the majority of the Cenozoic and Mesozoic (Miller et al., 2005). This implies that insight derived from late-Quaternary examples, i.e., icehouse depositional systems, might not be applicable to the interpretation or

prediction of the stratigraphic architecture of ancient greenhouse depositional systems, deposited at times when more limited sea-level fluctuations occurred (Miller et al., 2005; Sømme et al., 2009c; Miall, 2014). Blum et al. (2013) propose that, during icehouse times, relative sea-level fall across a low-gradient shelf tends to expose large areas and leads to the development of a wide coastal plain over newly emergent shelves, which could result in the significant amalgamation of drainage-basin areas during sea-level fall. Instead, during Greenhouse periods, the potential for drainage-basin amalgamation might be considerably less due to significantly shorter transverse distances of drainage rivers (**Fig. 2.22**), resulting in smaller, less-integrated drainage basins at lowstands. Based on limited data on deep-time incised-valley-fill dimensions, Gibling (2006) indicated that upper Palaeozoic valley fills are typically larger than Mesozoic examples in scale and highlight that this difference might be attributed to the influence of the higher-magnitude glacioeustatic fluctuations experienced by the Palaeozoic examples. As a follow-on study, a quantitative analysis could be performed of the geometry and stratigraphic architecture of incised-valley fills developed during icehouse versus greenhouse periods of the Earth history; such analysis could yield important insights into the effects of glacioeustatic fluctuations on incised-valley-fill dimensions and stratigraphic architecture and further augment the current understanding of the different possible geological controls on IVF geometry and stratigraphic architecture based on late-Quaternary examples.

7.2.2 Quantitative analysis of the characteristics of incised-valley fills developed before and after the advent of land plants and with respect to vegetation types and density

Another possible direction for future research lies in the quantitative analysis of the geometry and stratigraphic architecture of incised-valley-fill developed before and after the advent of land plants, and with respect to the evolution of vegetation types and density through Earth history. Vegetation types have evolved throughout the Earth history and the vegetation types that characterize the earth in most recent period (i.e., present-day times and late-Quaternary times) are different from those in the geological past. For example, the establishment of large land plants at the Devonian times, of plants that can survive under seasonal climatic conditions at the Mesozoic times, and of grasses at the Miocene times, all contributed to significant changes in fluvial hydrologic characteristics and channel style (Schumm, 1968; Davies and Gibling, 2010a, 2010b, 2011; Mial, 2014; Santos et al., 2017). Hence, modern or late-Quaternary analogues have only a limited applicability to the ancient past, especially in parts of the Palaeozoic when land plants had only recently colonised the land masses and had only shallow root systems (e.g., Santos et al.,

2017). A follow-on study could focus on the quantitative analysis of incised-valley-fill geometry and stratigraphic architecture to improve our understanding of the influence of the evolution of vegetation in controlling earth-surface processes.

7.2.3 Quantitative analysis of incised-valley-fill characteristics along dip and with respect to the valley shape

Marked variations in incised-valley-fill architecture and geometry exist along their dip extent (Dalrymple et al., 1992; Zaitlin et al., 1994; Chaumillon et al., 2010; Blum et al., 2013; Strong and Paola, 2008; Martin et al., 2011; Phillips, 2011). In future, possible research efforts, grounded on the results of the late-Quaternary examples studied in this work, might be directed towards improved analyses of the variation of IVF architecture and geometry along the dip profile of incised-valley systems, to improve our understanding of the geological controls of incised-valley-fill geometry and stratigraphic architecture and to guide hydrocarbon-reservoir characterization and modelling.

Additionally, characteristics relating to the shape of incised valleys and to their variations in shape along their dip profile are beyond the scope of this work. Previous work (Heap and Nichol, 1997; Rodriguez et al., 2005; Rodriguez et al., 2008) has shown that the shape of incised valleys might control IVF architecture; for example, the progressive inundation of terraces in terraced IVFs can cause step-wise changes in accommodation space and in variations of hydrodynamic processes, which in turn can influence the valley-fill architecture. In future, it is desirable to attempt further analysis with additional metrics of valley-shape variability along dip to consider its potential control on stratigraphic architectures.

References

Abrahim, G.M., Nichol, S.L., Parker, R.J., Gregory, M.R., 2008. Facies depositional setting, mineral maturity and sequence stratigraphy of a Holocene drowned valley, Tamaki Estuary, New Zealand. Estuar. Coast. Shelf. Sci. 79, 133-142.

Adams, J.M., Faure, H., 1997. Preliminary vegetation maps of the world since the Last Glacial Maximum: an aid to archaeological understanding. J. Archaeol. Sci. 24, 623–647.

Allard, J., Chaumillon, E., Féniès, H., 2009. A synthesis of morphological evolutions and Holocene stratigraphy of a wave-dominated estuary: The Arcachon lagoon, SW France. Cont. Shelf Res. 29, 957-969.

Allen, G.P., 1991. Sedimentary processes and facies in the Gironde estuary: a recent model for macrotidal estuarine systems. In: Smith, D.G., Zaitlin, B.A., Reinson, G.E., Rahmani R.A. (Eds.), Clastic Tidal Sedimentology — Recognition Criteria and Facies Models. Mem. Can. Soc. Petrol. Geol. 16, 29–39.

Allen, G.P., Posamentier, H.W., 1993. Sequence stratigraphy and facies model of an incised valley fill: the Gironde Estuary, France. J. Sed. Res. 63, 378-391.

Allen, G.P., Posamentier, H.W., 1994a. Sequence stratigraphy and facies model of an incised valley fill: The Gironde Estuary, France: Reply. J. Sed. Res. B64, 81-84.

Allen, G.P., Posamentier, H.W., 1994b. Transgressive facies and sequence architecture in mixed tide-and wave-dominated incised valleys: example from the Gironde Estuary, France. In: Dalrymple, R.W., Boyd, R., Zaitlin, B.A. (Eds.), Incised-valley systems: Origin and sedimentary sequences. SEPM Spec. Publ. 51, 225-239.

Allen, J.R.L., 1982. Sedimentary Structures: Their Character and Physical Basis. Elsevier, New York.

Alqahtani, F.A., Johnson, H.D., Jackson, C.A.L., Som, M.R.B., 2015. Nature, origin and evolution of a Late Pleistocene incised valley-fill, Sunda Shelf, Southeast Asia. Sedimentology 62, 1198-1232.

Amorosi, A., Sarti, G., Rossi, V., Fontana, V., 2008. Anatomy and sequence stratigraphy of the late quaternary Arno valley fill (Tuscany, Italy). In: Amorosi, A., Haq, B.U., Sabato, L. (Eds.), Advances in Application of Sequence Stratigraphy in Italy. GeoActa Spec. Publ. 1, 117-128.

Amorosi, A., Pacifico, A., Rossi, V., Ruberti, D., 2012. Late Quaternary incision and deposition in an active volcanic setting: The Volturno valley fill, southern Italy. Sed. Geol. 282, 307-320.

Amorosi, A., Rossi, V., Sarti, G., Mattei, R., 2013. Coalescent valley fills from the late Quaternary record of Tuscany (Italy). Quatern. Int. 288, 129-138.

Amorosi, A., Bracone, V., Campo, B., D'Amico, C., Rossi, V., Rosskopf, C.M., 2016. A late Quaternary multiple paleovalley system from the Adriatic coastal plain (Biferno River, Southern Italy). Geomorphology 254, 146-159.

Anderson, J.B., Siringan, F.P., Taviani, M., Lawrence, J., 1991. Origin and Evolution of Sabine Lake, Texas-Louisiana. Trans. Gulf Coast Assoc. Geol. Soc. 41, 12-16.

Anderson, J.B., Rodriguez, A., Abdulah, K.C., Fillon, R.H., Banfield, L.A., McKeown, H.A., Wellner, J.S., 2004. Late Quaternary stratigraphic evolution of the northern Gulf of Mexico margin: a synthesis. In: Anderson, J.B., Fillon, R.H. (Eds.), Late Quaternary Stratigraphic Evolution of the Northern Gulf of Mexico Margin: A Synthesis. SEPM Spec. Publ. 79, 1–23.

Anderson, J.B., Wallace, D.J., Simms, A.R., Rodriguez, A.B., Weight, R.W., Taha, Z.P., 2016. Recycling sediments between source and sink during a eustatic cycle: Systems of late Quaternary northwestern Gulf of Mexico Basin. Earth-Sci. Rev. 153, 111–138.

Aquino da Silva, A.G., Stattegger, K., Schwarzer, K., Vital, H., 2016. Seismic stratigraphy as indicator of late Pleistocene and Holocene sea level changes on the NE Brazilian continental shelf. J. S. Am. Earth Sci. 70, 188-197.

Bartholdy, J., Ernstsen, V.B., Flemming, B.W., Winter, C., Bartholomä, A., Kroon, A., 2015. On the formation of current ripples. Sci. Rep. 5, 11390.

Becker, J.J., Sandwell, D.T., Smith, W.H.F., Braud, J., Binder, B., Depner, J., Fabre, D., Factor, J., Ingalls, S., Kim, S. H., Ladner, R., Marks, K., Nelson, S., Pharaoh, A., Trimmer, R., Von Rosenberg, J., Wallace, G., Weatherall, P., 2009. Global Bathymetry and Elevation Data at 30 Arc Seconds Resolution: SRTM30_PLUS. Mar. Geodesy 32, 355-371.

Beighley, R.E., Gummadi, V., 2011. Developing channel and floodplain dimensions with limited data: a case study in the Amazon Basin. Earth Surf. Proc. Land. 36, 1059–1071.

Belknap, D.F., Kraft, J.C., 1981. Preservation potential of transgressive coastal lithosomes on the US Atlantic shelf. Mar. Geol. 42, 429–442.

Bellotti, P., Caputo, C., Davoli, L., Evangelista, S., Garzanti, E., Pugliese, F., Valeri, P., 2004. Morpho-sedimentary characteristics and Holocene evolution of the emergent part of the Ombrone River delta (southern Tuscany). Geomorphology 61, 71-90.

Benallack, K., Green, A.N., Humphries, M.S., Cooper, J.A.G., Dladla, N.N., Finch, J.M., 2016. The stratigraphic evolution of a large back-barrier lagoon system with a non-migrating barrier. Mar. Geol. 379, 64-77.

Berné, S., Vagner, P., Guichard, F., Lericolais, G., Liu, Z., Trentesaux, A., Yin, P., Yi, H.I., 2002. Pleistocene forced regressions and tidal sand ridges in the East China Sea. Mar. Geol. 188, 293-315.

Best, J., Wignall, P.B., Stirling, E.J., Obrock, E., Bryk, A., 2006. The Tullig and Kilkee Cyclothems in Southern County Clare. In: Best, J.L., Wignall, P.B. (Eds.), A Field Guide to the Carboniferous Sediments of the Shannon Basin, Western Ireland. IAS Field Guide, 240-328.

Bhattacharya, J.P., Tye, R.S., 2004. Searching for modern ferron analogs and application to subsurface interpretation. In: Chidsey Jr., T.C., Adams, R.D., Morris, T.H. (Eds.), The Fluvial-Deltaic Ferron Sandstone: Regional to Wellbore-Scale Outcrop Analog Studies and Application to Reservoir Modeling. AAPG Studies in Geology 50, 39-57.

Bijkerk J.F., 2014. External controls on sedimentary sequences: a field and analogue modelling-based study. Unpublished PhD Thesis, University of Leeds, UK.

Blakey, R., 2016. Library of Paleogeography, Colorado Plateau Geosystems™, Arizona, USA. http://deeptimemaps.com/global-paleogeography-and-tectonics-in-deep-time-series/ (accessed 21 November 2019).

Blakey, R.C., Wong, T.E., 2007. Carboniferous–Permian paleogeography of the assembly of Pangaea. In: Wong, T.E. (Ed.), Proceedings of the XVth International Congress on Carboniferous and Permian Stratigraphy. Utrecht, 10-16 August 2003, pp. 443-456. Royal Netherlands Academy of Arts and Sciences, Amsterdam.

Blum, M.D., 1993. Genesis and architecture of incised valley fill sequences: a Late Quaternary example from the Colorado River, Gulf Coastal Plain of Texas. In: Weimer, P., Posamentier, H. W. (Eds.), Siliciclastic Sequence Stratigraphy: Recent Developments and Applications. Mem. Am. Assoc. Petrol. Geol. 58, 259-283.

Blum, M.D., Valastro, S. Jr., 1994. Late Quaternary sedimentation, lower Colorado River, Gulf Coastal Plain of Texas. Geol. Soc. Am. Bull. 106, 1002–1016.

Blum, M.D., Price, D.M., 1998. Quaternary alluvial plain construction in response to interacting glacio-eustatic and climatic controls, Texas Gulf Coastal Plain. In: Shanley, K.W., McCabe P.J. (Eds.), Relative Role of Eustasy, Climate and Tectonism in Continental Rocks. SEPM Spec. Publ. 59, 31–48.

Blum, M.D., Törnqvist, T.E., 2000. Fluvial responses to climate and sea-level change: A review and look forward. Sedimentology 47, 2–48.

Blum, M.D., Womack, J.H., 2009. Climate change, sea-level change, and fluvial sediment supply to deepwater systems. In: Kneller, B., Martinsen, O.J., McCaffrey, B. (Eds.), External Controls on Deep Water Depositional Systems: Climate, Sea-Level, and Sediment Flux. SEPM Spec. Publ. 92, 15–39.

Blum, M.D., Martin, J., Milliken, K., Garvin, M., 2013. Paleovalley systems: insights from Quaternary analogs and experiments. Earth-Sci. Rev. 116, 128–169.

Bogaart, P. W., Balen, R. T. V., Kasse, C., Vandenberghe, J., 2003a. Process-based modelling of fluvial system response to rapid climate change—I: model formulation and generic applications. Quatern. Sci. Rev. 22, 2077-2095.

Bogaart, P. W., Balen, R. T. V., Kasse, C., Vandenberghe, J., 2003b. Process-based modelling of fluvial system response to rapid climate change II. Application to the River Maas (The Netherlands) during the Last Glacial–Interglacial Transition. Quatern. Sci. Rev. 22, 2097-2110.

Bogaart, P.W., Tucker, G.E., De Vries, J.J., 2003c. Channel network morphology and sediment dynamics under alternating periglacial and temperate regimes: a numerical simulation study. Geomorphology 54, 257-277.

Boucot, A.J., Xu, C., Scotese, C.R., Morley, R.J., 2013. Phanerozoic paleoclimate: an atlas of lithologic indicators of climate. In: Nichols G. J., Ricketts B. (Eds.), SEPM Concepts in Sedimentology and Paleontology. SEPM, Tulsa, Oklahoma, pp. 478.

Bowen, D.W., Weimer, P., 2003. Regional sequence stratigraphic setting and reservoir geology of Morrow incised-valley sandstones (lower Pennsylvanian), eastern Colorado and western Kansas. AAPG Bull. 87, 781–815.

Boyd, R., Dalrymple, R.W., Zaitlin, B.A., 2006. Estuarine and incised-valley facies model. In: Posamentier H.W., Walker R.G. (Eds), Facies Models Revisited. SEPM Spec. Publ. 84, 171–235.

Bradley, R. W., Venditti, J. G., 2017. Reevaluating dune scaling relations. Earth-Sci. Rev. 165, 356–376.

Braudrick, C.A., Dietrich, W.E., Leverich, G.T., Sklar, L.S., 2009. Experimental evidence for the conditions necessary to sustain meandering in coarse-bedded rivers. Proc. Nat. Acad. Sci. 106, 16936–16941.

Breda, A., Amorosi, A., Rossi, V., Fusco, F., 2016. Late-glacial to Holocene depositional architecture of the Ombrone palaeovalley system (Southern Tuscany, Italy): Sea-level, climate and local control in valley-fill variability. Sedimentology 63, 1124-1148.

Brettle, M. J., 2001. Sedimentology and high-resolution sequence stratigraphy of shallow water delta systems in the early Marsdenian (Namurian) Pennine Basin, Northern England. Unpublished PhD Thesis, University of Liverpool, UK.

Brettle, M. J., McIlroy, D., Elliott, T., Davies, S. J., Waters, C. N., 2002. Identifying cryptic tidal influences within deltaic successions: an example from the Marsdenian (Namurian) interval of the Pennine Basin, UK. J. Geol. Soc. 159, 379-391.

Bridge, J.S., Mackey, S.D., 1993. A theoretical study of fluvial sandstone body dimensions. In: Flint, S., Bryant, I.D. (Eds.), The geological modeling of hydrocarbon reservoirs and outcrop analogues. Int. Assoc. Sedimentol. Spec. Publ. 15, 213–236.

Bridge, J.S., Tye, R.S., 2000. Interpreting the dimensions of ancient fluvial channel bars, channels, and channel belts from wireline-logs and cores. AAPG Bull. 84, 1205-1228.

Bridge, J.S., 2003. Rivers and Floodplains: Forms, Processes, and Sedimentary Record. John Wiley & Sons, Malden, Massachusetts, pp. 491.

Bridge, J.S., 2006. Fluvial facies models: recent developments. In: Posamentier, H.W., Walker, R.G. (Eds.), Facies Models Revisited. SEPM Spec. Publ. 84, 85–170.

Bridge, J., Demicco, R., 2008. Earth surface processes, landforms and sediment deposits. Cambridge University Press, pp. 815.

Bristow, C.S., 1988. Controls on the sedimentation of the Rough Rock Group (Namurian) from the Pennine Basin of northern England. In: Besly, B.M., Kelling, G., (Eds.), Sedimentation in a Synorogenic Basin Complex: The Upper Carboniferous of Northwest Europe. Blackie, Glasgow, pp. 114-131.

Bristow, C.S., Myers, K.J., 1989. Detailed sedimentology and gamma-ray log characteristics of a Namurian deltaic succession I: Sedimentology and facies analysis. In: Whateley, M. K. G., Pickering, K. T. (Eds), Deltas: Sites and Traps for Fossil Fuels. Geol. Soc. London Spec. Publ. 41, 75-80.

Bristow, C.S., 1993. Sedimentology of the Rough Rock: a Carboniferous braided river sheet sandstone in northern England. In: Best, J. L., Bristow, C. S. (Eds), Braided Rivers. Geol. Soc. London Spec. Publ. 75, 291-304.

Broecker, W. S., 1995. Cooling the tropics. Nature 376, 212-213.

Buller, T., Eriksson, K.A., McClung, W.S., 2018. Upstream controls on incised-valley dimensions and fill: Examples from the Upper Mississippian Mauch Chunk Group, Central Appalachian Basin, USA. Palaeogeogr. Palaeoclimatol. Palaeoecol. 490, 355-374.

Burgess, P.M., Hovius, N., 1998. Rates of delta progradation during highstands: consequences for timing of deposition in deep-marine systems. J. Geol. Soc. London 155, 217–222.

Burgess, P.M., Steel, R.J., Granjeon, D., 2008. Stratigraphic forward modeling of basin-margin clinoform systems: Implications for controls on topset and shelf width and timing of formation of shelf-edge deltas. In: Hampson, G.J., Steel, R.J., Burgess, P.M., Dalrymple, R.W. (Eds.), Recent Advances in Models of Siliciclastic Shallow-Marine Stratigraphy. SEPM Spec. Publ. 90, 35–45.

Burne, R.V., 1995. The return of the fan that never was: Westphalian turbidite systems in the Variscan Culm Basin: Bude Formation (southwest England). In: A.G. Plint (Ed.), Sedimentary Facies Analysis. Int. Assoc. Sedimentol. Spec. Publ. 22, 101-135.

Caputo, R., Bianca, M., D'Onofrio, R., 2010. Ionian marine terraces of southern Italy: insights into the Quaternary tectonic evolution of the area. Tectonics 29, 24.

Carlin, J.A., Dellapenna, T.M., Strom, K., Noll, C.J.I., 2015. The influence of a salt wedge intrusion on fluvial suspended sediment and the implications for sediment transport to the adjacent coastal ocean: a study of the lower Brazos River TX, USA. Mar. Geol. 359, 134–147.

Carvajal, C., Steel, R., 2012. Source-to-sink sediment volumes within a tectonostratigraphic model for a Laramide shelf-to-deep-water basin: Methods and results. In: Busby, C., Azor, A. (Eds.), Tectonics of Sedimentary Basins: Recent Advances. John Wiley & Sons, Ltd., Chichester, UK, pp. 131–151.

Cattaneo, A., Steel, R.J., 2003. Transgressive deposits: a review of their variability. Earth-Sci. Rev. 62, 187–228.

Catuneanu, O., Elango, H.N., 2001. Tectonic control on fluvial styles: the Balfour Formation of the Karoo Basin, South Africa. Sed. Geol. 140, 291-313.

Catuneanu, O., 2006. Principles of Sequence Stratigraphy. Elsevier, Amsterdam.

Catuneanu, O., Abreu, V., Bhattacharya, J.P., Blum, M.D., Dalrymple, R.W., Eriksson, P.G., Fielding, C.R., Fisher,W.L., Galloway,W.E., Gibling, M.R., Giles, K.A., Holbrook, J.M., Jordan, R., Kendall, C.G., St, C., Macurda, B., Martinsen, O.J., Miall, A.D., Neal, J.E., Nummedal, D., Pomar, L., Posamentier, H.W., Pratt, B.R., Sarg, J.F., Shanley, K.W., Steel, R.J., Strasser, A., Tucker, M.E., Winker, C., 2009. Toward the standardization of sequence stratigraphy. Earth-Sci. Rev. 92, 1-33.

Cawthra, H.C., Uken, R., 2012. Modern beachrock formation in Durban, KwaZulu-Natal. S. Afr. J. Sci. 108, 1–5.

Cecil, C.B., 1990. Paleoclimate controls on stratigraphic repetition of chemical and siliciclastic rocks. Geology 18, 533-536.

Cecil, C.B., 2003. The concept of autocyclic and allocyclic controls on sedimentation and stratigraphy, emphasizing the climatic variable. In: Cecil, C.B., Edgar, N.T. (Eds.), Climate Controls on Stratigraphy. SEPM Spec. Publ. 77, 13–20.

Chatanantavet, P., Lamb, M.P., Nittrouer, J.A., 2012. Backwater controls of avulsion location on deltas. Geophys. Res. Lett. 39, L01402.

Chaumillon, E., Proust, J.N., Menier, D., Weber, N., 2008. Incised-valley morphologies and sedimentary-fills within the inner shelf of the Bay of Biscay (France): a synthesis. J. Mar. Syst. 72, 383-396.

Chaumillon, E., Weber, N., 2006. Spatial variability of modern incised valleys on the French Atlantic Coast: comparison between the Charente and the Lay–Sèvre incised valleys. In: Dalrymple R.W., Leckie D.A., Tillman R.W. (Eds.), Incised valleys in time and space. SEPM Spec. Publ. 85, 57–85.

Chaumillon, E., Tessier, B., Reynaud, J.Y., 2010. Stratigraphic records and variability of incised valleys and estuaries along French coasts. Bull. Soc. Géol. Fr. 181, 75-85.

Church, K. D., Gawthorpe, R. L., 1994. High resolution sequence stratigraphy of the late Namurian in the Widmerpool Gulf (East Midlands, UK). Mar. Petrol. Geol. 11, 528-544.

Church, M., 1983. Pattern of instability in a wandering gravel bed channel. In: Collinson, J.D., Lewin, J. (Eds.), Modern and Ancient Alluvial Systems. Int. Assoc. Sedimentol. Spec. Publ. 6, 169–180.

Cilumbriello, A., Sabato, L., Tropeano, M., Gallicchio, S., Grippa, A., Maiorano, P., Mateu-Vicens, G., Rossi, C.A., Spilotro, G., Calcagnile, L., Quarta, G., 2010. Sedimentology, stratigraphic architecture and preliminary hydrostratigraphy of the Metaponto coastal-plain subsurface (Southern Italy). In: Bersezio, R., Amanti, M.

(Eds.), Proceedings of the National Workshop “Multidisciplinary approach for porous aquifer characterization”. Memorie descrittive della Carta Geologica d'Italia, XC, pp. 67–84.

Cilumbriello, A., Tropeano M., Sabato, L., 2008. The Quaternary terraced marine-deposits of the Metaponto area (Southern Italy) in a sequence stratigraphic perspective. In: Amorosi, A., Haq, B.U., Sabato, L. (Eds.), Advances in Application of Sequence Stratigraphy in Italy. GeoActa Spec. Publ. 1, 29–54.

Clement, A.J., Fuller, I.C., 2018. Influence of system controls on the Late Quaternary geomorphic evolution of a rapidly-infilled incised-valley system: The lower Manawatu valley, North Island New Zealand. Geomorphology 303, 13-29.

Clement, A.J., Fuller, I.C., Sloss C.R., 2017. Facies architecture, morphostratigraphy, and sedimentary evolution of a rapidly-infilled Holocene incised-valley estuary: The lower Manawatu valley, North Island New Zealand. Mar. Geol. 390, 214-233.

Coe, M.T., Latrubesse, E.M., Ferreira, M.E., Amsler, M.L., 2011. The effects of deforestation and climate variability on the streamflow of the Araguaia River, Brazil. Biogeochemistry 105, 119-131.

Collier, J.S., Oggioni, F., Gupta, S., García-Moreno, D., Trentesaux, A., De Batist, M., 2015. Streamlined islands and the English Channel megaflood hypothesis. Global Planet. Change 135, 190-206.

Collinson, J.D., 1996. Alluvial sediments. In: Reading, H.G. (Ed.), Sedimentary Environments: Processes, Facies and Stratigraphy. Blackwell Science, Oxford, pp. 37–82.

Collinson, J.D., Evans, D.J., Holliday, D.W., Jones, N.S., 2005. Dinantian and Namurian depositional systems in the southern North Sea. In: Collinson, J.D., Evans, D.J., Holliday, D.W., Jones, N.S. (Eds), Carboniferous Hydrocarbon Geology: The Southern North Sea and Surrounding Onshore Basins. Yorks. Geol. Soc. Spec. Publ. 7, 35-56.

Collinson, J.D., Martinsen, O., Bakken, B., Kloster, A. 1991. Early fill of the western Irish Namurian Basin; a complex relationship between turbidites and deltas. Basin Res. 3, 223–242.

Colman, S.M., Mixon, R.B., 1988. The record of major Quaternary sea-level changes in a large coastal plain estuary, Chesapeake Bay, eastern United States. Palaeogeogr. Palaeoclimatol. Palaeoecol. 68, 99-116.

Colman, S.M., Halka, J.P., HOBBS III, C.H., Mixon, R.B., Foster, D.S., 1990. Ancient channels of the Susquehanna River beneath Chesapeake Bay and the Delmarva peninsula. Geol. Soc. Am. Bull. 102, 1268-1279.

Colombera, L., Mountney, N.P., McCaffrey, W.D., 2012. A relational database for the digitization of fluvial architecture: concepts and example applications. Petrol. Geosci. 18, 129–140.

Colombera, L., Mountney, N.P., McCaffrey, W.D., 2013. A quantitative approach to fluvial facies models: methods and example results. Sedimentology 60, 1526–1558.

Colombera, L., Mountney, N.P., Hodgson, D.M., McCaffrey, W.D., 2016. The Shallow-Marine Architecture Knowledge Store: A database for the characterization of shallow-marine and paralic depositional systems. Mar. Petrol. Geol. 75, 83–99.

Colombera, L., Mountney, N.P., 2019. The lithofacies organization of fluvial channel deposits: A meta-analysis of modern rivers. Sed. Geol. 383, 16-40.

Cooper, J.A.G., 1991. Beachrock formation in low latitudes: implications for coastal evolutionary models. Mar. Geol. 98, 145–154.

Cooper, J.A.G., Green, A.N., Wright, C.I., 2012. Evolution of an incised valley coastal plain estuary under lowsediment supply: a “give-up” estuary. Sedimentology 59, 899–916.

Cooper, J. A. G., Green, A. N., Meireles, R. P., Klein, A. H., Souza, J., Toldo, E. E., 2016. Sandy barrier overstepping and preservation linked to rapid sea level rise and geological setting. Mar. Geol. 382, 80-91.

Cooper, W.S., 1958. Coastal sand dunes of Oregon and Washington. Geol. Soc. Am. Mem. 72, 144.

Cowell, P.J., Thom, B.G., 1994. Morphodynamics of coastal evolution. In: Carter, R.W.G., Woodroffe, C.D. (Eds.), Coastal Evolution, Late Quaternary Shoreline Morphodynamics. Cambridge University Press, Cambridge, pp. 33–86.

Critelli, S., Ingersoll, R.V., 1995. Interpretation of neovolcanic versus palaeovolcanic sand grains: an example from Miocene deep-marine sandstone of the Topanga group (Southern California). Sedimentology 42, 783–804.

Crockett, J.S., Nittrouer, C.A., Ogston, A.S., Naar, D.F., Donahue, B. T., 2008. Morphology and filling of incised submarine valleys on the continental shelf near the mouth of the Fly River, Gulf of Papua. J. Geophys. Res. 113, no. F1.

Crowley, T.J., North, G.R., 1991. Palaeoclimatology. Oxford University Press, Oxford.

Crowley, T.J., Baum, S.K., 1991. Estimating Carboniferous sea-level fluctuations from Gondwanan ice extent. Geology 19, 975-977.

Crumeyrolle, P., Renaud, I., 2003. Quaternary incised valleys and low stand deltas imaged with 3D seismic and 2D HR profiles, Mahakam delta, Indonesia. AAPG International Conference, Barcelona, Spain, Extended Abstracts, 8.

Dalrymple, R.W., 2006. Incised valleys in space and time: an introduction to the volume and an examination of the controls on valley formation and filling. In: Dalrymple R.W., Leckie D.A., Tillman R.W. (Eds.), Incised valleys in time and space. SEPM Spec. Publ. 85, 5–12.

Dalrymple, R.W., Baker, E.K., Harris, P.T., Hughes, M., 2003. Sedimentology and stratig- raphy of a tide-dominated, foreland-basin delta (Fly River, Papua New Guinea). In: Sidi, F.H., Nummedal, D., Imbert, P., Darman, H., Posamentier, H.W. (Eds.), Tropical Deltas of Southeast Asia – Sedimentology, Stratigraphy, and Petroleum Geology. SEPM Spec. Publ. 76, 147–173.

Dalrymple, R.W., Boyd, R., Zaitlin, B.A., 1994. Preface. In: Dalrymple, R.W., Boyd, R., Zaitlin B.A. (Eds.), Incised valley systems: Origins and sedimentary sequences. SEPM Spec. Publ. 51, iii.

Dalrymple, R.W., Leckie, D.A., Tillman, R.W., 2006. Incised valleys in time and space. SEPM Spec. Publ. 85.

Dalrymple, R.W., Mackay, D.A., Ichaso, A.A., Choi, K.S., 2012. Processes, morphodynamics, and facies of tide- dominated estuaries. In: Davis Jr, R.A., Dalrymple R.W. (Eds.), Principles of Tidal Sedimentology. Springer, Dordrecht, Heidelberg, pp. 79–107.

Dalrymple, R.W., Zaitlin, B.A., 1994. High-resolution sequence stratigraphy of a complex, incised valley succession, the Cobequid Bay–Salmon River estuary, Bay of Fundy, Canada. Sedimentology 41, 1069–1091.

Dalrymple, R.W., Zaitlin, B.A., Boyd, R., 1992. Estuarine facies models: conceptual basis and stratigraphic implications. J. Sed. Petrol. 62, 1130–1146.

Daniell, J.J., 2008. Development of a bathymetric grid for the Gulf of Papua and adjacent areas: A note describing its development. J. Geophys. Res. 113, F1.

Davidson, S.K., North, C.P., 2009. Geomorphological regional curves for prediction of drainage area and screening modern analogues for rivers in the rock record. J. Sediment. Res. 79, 773-792.

Davies, S.J., 2008. The record of Carboniferous sea-level change in low-latitude sedimentary successions from Britain and Ireland during the onset of the late

Paleozoic ice age. In: Fielding, C.R., Frank, T.D., Isbell, J.L. (Eds.), Resolving the Late Paleozoic Ice Age in Time and Space. Geol. Soc. Am. Spec. Pap. 441, 187–204.

Davies, N.S., Gibling, M.R., 2010a. Cambrian to Devonian evolution of alluvial systems: the sedimentological impact of the earliest land plants. Earth-Sci. Rev. 98, 171-200.

Davies, N.S., Gibling, M.R., 2010b. Paleozoic vegetation and the Siluro-Devonian rise of fluvial lateral accretion sets. Geology 38, 51-54.

Davies, N.S., Gibling, M.R., 2011. Evolution of fixed-channel alluvial plains in response to Carboniferous vegetation. Nat. Geosci. 4, 629-633.

Davies, S.J., Hampson, G.J., Elliott, T., Flint, S.S., 1999, Continental scale sequence stratigraphy of the Upper Carboniferous and its applications to reservoir prediction. In: Fleet, A.J., Boldy, S.A.R. (Eds.), Petroleum Geology of NW Europe. Proceedings of the 5th Conference: London, Geological Society of London, pp. 757–770.

Davis Jr., R.A., Hayes, M.O., 1984. What is a wave-dominated coast? Mar. Geol. 60, 313–329.

Davis Jr, R.A., Clifton, H.E., 1987. Sea-level change and the preservation potential of wave- dominated and tide-dominated coastal sequences. In: Nummedal, D., Pilkey, O.H., Howard, J.D. (Eds.), Sea-level fluctuation and coastal evolution. SEPM Spec. Publ. 41, 167–178.

Davis Jr, R.A., FitzGerald, D.M., 2009. Beaches and coasts. John Wiley & Sons.

Davis, J.C., 2002. Statistics and Data Analysis in Geology, third ed. Wiley, New York.

Dean, M.T., Browne, M.A.E., Waters, C.N., Powell, J.H., 2011. A lithostratigraphical framework for the Carboniferous successions of northern Great Britain (onshore). British Geological Survey Research Report, RR/10/07.

Deveugle, P.E., Jackson, M.D., Hampson, G.J., Stewart, J., Clough, M.D., Ehighebolo, T., Farrell, M.E., Calver, C.S., Miller, J.K., 2014. A comparative study of reservoir modeling techniques and their impact on predicted performance of fluvial-dominated deltaic reservoirs. AAPG Bull. 98, 729-763.

Dickinson, W.R., 1985. Interpreting provenance relations from detrital modes of sand- stones. In: Zuffa, G.G. (Ed.), Provenance of arenites. Springer, Netherlands, pp. 333–361.

Dietrich, W.E., Whiting, P., 1989. Boundary shear stress and sediment transport in river meanders of sand and gravel. In: Ikeda, H., Parker, G. (Eds.), River Meandering. AGU Water Resources Monograph, 12, 1–50.

Doglioni, C., Tropeano, M., Mongelli, F. and Pieri, P., 1996. Middle-late Pleistocene uplift of Puglia: an “anomaly” in the Apenninic foreland. Mem. Soc. Geol. Ital. 51, 101–117.

Dyke, A.S., 2004. An outline of North American deglaciation with emphasis on central and northern Canada. Dev. Quat. Sci. 2, 373–424.

Easterbook, D.J., 1999. Surface Processes and Landforms. Prentice Hall, New Jersey, pp. 546.

Einsele, G., 2000. Sedimentary basins: evolution, facies, and sediment budget. Springer, Berlin, pp. 628.

Ellen, R., Browne, M.A.E., Mitten, A.J., Clarke, S.M., Leslie, A.G., Callaghan, E., 2019. Sedimentology, architecture and depositional setting of the fluvial Spireslack Sandstone of the Midland Valley, Scotland: insights from the Spireslack surface coal mine. In: Corbett, P.W.M., Owen, A., Hartley, A.J., Pla-Pueyo, S., Barreto, D., Hackney, C., Kape, S.J. (Eds.), River to Reservoir: Geoscience to Engineering. Geol. Soc. Spec Publ., 488, SP488-2.

Emery, D., Myers, K. J., 1996. Sequence stratigraphy. Blackwell Science, Oxford.

Fairbanks, R.G., 1989. A 17,000-year glacio-eustatic sea level record: influence of glacial melting rates on the Younger Dryas event and deep-ocean circulation. Nature 342, 637–642.

Fenies, H., Tastet, J., 1998. Facies and architecture of an estuarine tidal bar (the Trompeloup bar, Gironde Estuary, SW France). Mar. Geol. 150, 149–169.

Féniès, H., Lericolais, G., 2005. Internal architecture of an incised valley-fill on a wave-and tide-dominated coast (the Leyre incised valley, Bay of Biscay, France). CR Acad. Sci. Paris 337, 1257-1266.

Féniès, H., Lericolais, G., Posamentier, H.W., 2010. Comparison of wave-and tide-dominated incised valleys: specific processes controlling systems tract architecture and reservoir geometry. Bull. Soc. Géol. Fr. 181, 171-181.

Ferrer, P., Benabdellouahed, M., Certain, R., Tessier, B., Barusseau, J. P., Bouchette, F., 2010. The Late Holocene sediment infilling and beach barrier dynamics of the Thau lagoon (Gulf of Lions, Mediterranean Sea, SE France). Bull. Soc. Géol. Fr. 181, 197-209.

Fielding, C.R., Crane, R.C., 1987. An application of statistical modelling to the prediction of hydrocarbon recovery factors in fluvial reservoir sequences. In: Ethridge, F.G., Flores R.M., Harvey M.D. (Eds.), Recent Developments in Fluvial Sedimentology. SEPM Spec. Publ. 39, 321–327.

Fielding, C.R., Trueman, J.D., Alexander, J., 2006. Holocene depositional history of the Burdekin river delta of northeastern australia: a model for a low accommodation, highstand delta. J. Sed. Res. 76, 411–428.

Fielding, C.R., Allen, J.P., Alexander, J., Gibling, M.R., 2009. Facies model for fluvial systems in the seasonal tropics and subtropics. Geology 37, 623–626.

Fielding, C.R., Alexander, J., Allen, J.P., 2018. The role of discharge variability in the formation and preservation of alluvial sediment bodies. Sed. Geol. 365, 1–20.

Fisk, H.N., 1944. Geological investigation of the alluvial valley of the lower Mississippi River. Vicksburg, Mississippi, U.S. Army Corps of Engineers Mississippi River Commission, 78 p., 33 plates.

Flint, J.J., 1974. Stream gradient as a function of order, magnitude, and discharge. Water Resour. Res. 10, 969–973.

Forbes, D.L., Orford, J.D., Carter, R.W.G., Shaw, J., Jennings, S.C., 1995. Morphodynamic evolution, self-organisation, and instability of coarse-clastic barriers on paraglacial coasts. Mar. Geol. 126, 63–85.

Foreman, B.Z., Heller, P.L., Clementz, M.T., 2012. Fluvial response to abrupt global warming at the Palaeocene/Eocene boundary. Nature 491, 92-95.

Foyle, A.M., Oertel, G.F., 1992. Seismic stratigraphy and coastal drainage patterns in the Quaternary section of the southern Delmarva Peninsula, Virginia, USA. Sed. Geol. 80, 261-277.

Foyle, A.M., Oertel, G.F., 1997. Transgressive systems tract development and incised-valley fills within a Quaternary estuary-shelf system: Virginia inner shelf, USA. Mar. Geol. 137, 227-249.

Frankel, E., 1968. Rate of formation of beachrock. Earth Planet. Sci. Lett. 4, 439–440.

Franzinelli, E., Potter, P.E., 1983. Petrology, chemistry, and texture of modern river sands, amazon river system. J. Geol. 91, 23–39.

Freshney, E.C., Edmonds, E. A., Taylor, R. T., Williams, B. J., 1979. Geology of the country around Bude and Bradworthy. Geol. Surv. Great Brit. Mem. HMSO, London.

Galloway, W. E., 1986. Reservoir facies architecture of microtidal barrier systems. AAPG Bull. 70, 787-808.

Galloway, W.E., Hobday, D.K., 1996. Terrigenous Clastic Depositional Systems: Ap- plications to Fossil Fuel and Groundwater Resources. Springer, New York, pp. 489.

Ganti, V., Paola, C., Foufoula-Georgiou, E., 2013. Kinematic controls on the geometry of the preserved cross sets. J. Geophys. Res. Earth Surf. 118, 1296–1307.

Ganti, V., Whittaker, A. C., Lamb, M. P., Fischer, W. W., 2019a. Low-gradient, single- threaded rivers prior to greening of the continents. Proc. Nat. Acad. Sci. 116, 11652–11657.

Ganti, V., Lamb, M. P., Chadwick, A. J., 2019b. Autogenic Erosional Surfaces in Fluvio- deltaic Stratigraphy from Floods, Avulsions, and Backwater Hydrodynamics. J. Sediment. Res. 89, 815–832.

Gardner, J.V., Dartnell, P., Mayer, L.A., Hughes-Clarke, J.E., Calder, B.R., Duffy, G., 2005. Shelf-edge deltas and drowned barrier–island complexes on the northwest Florida outer continental shelf. Geomorphology 64, 133–166.

Gardner, J.V., Calder, B.R., Hughes Clark, J.E., Mayer, L.A., Elston, G., Rzhanov, Y., 2007. Drowned shelf-edge deltas, barrier islands and related features along the outer continental shelf north of the head of De Soto Canyon, NE Gulf of Mexico. Geomorphology 89, 370–390.

Geehan, G., Underwood, J., 1993. The use of shale length distributions in geological modeling. In: Flint, S., Bryant, I.D. (Eds.), The geological modeling of hydrocarbon reservoirs and outcrop analogues. Int. Assoc. Sedimentol. Spec. Publ. 15, 205–212.

George, G.T., 2001. Late Yeadonian (Upper Sandstone Group) incised valley supply and depositional systems in the South Wales peripheral foreland basin: implications for the evolution of the Culm Basin and for the Silesian hydrocarbon plays of onshore and offshore UK. Mar. Petrol. Geol. 18, 671-705.

Gibling, M.R., 2006. Width and thickness of fluvial channel bodies and valley fills in the geological record: A literature compilation and classification. J. Sed. Res. 76, 731–770.

Gibling, M.R., Fielding, C.R., Sinha, R., 2011. Alluvial valleys and alluvial sequences: towards a geomorphic assessment. In: Davidson, S.K., Leleu, S., North, C. (Eds.), From River to Rock Record: The Preservation of Fluvial Sediments and Their Subsequent Interpretation. SEPM Spec. Publ. 97, 423–447.

Gilbert, G.K., 1877. Geology of the Henry Mountains. Government Printing Office, Washington, D.C., pp. 160.

Goldsmith, S.T., Carey, A.E., Lyons, W.B., Kao, S.J., Chen, J., 2008. Geochemical fluxes from the ChoShui River during Typhoon Mindulle, July 2004. Geology 36, 483-486.

Gomes, M. P., Vital, H., Stattegger, K., Schwarzer, K., 2016. Bedrock control on the Assu Incised Valley morphology and sedimentation in the Brazilian Equatorial Shelf. Int. J. Sed. Res. 31, 181-193.

Gonzalez, R., Dias, J.M.A., Lobo, F., Mendes, I., 2004. Sedimentological and paleoenvironmental characterisation of transgressive sediments on the Guadiana Shelf (Northern Gulf of Cadiz, SW Iberia). Quatern. Int. 120, 133-144.

Green, A.N., 2009. Palaeo-drainage, incised valley fills and transgressive systems tract sedimentation of the northern KwaZulu-Natal continental shelf, South Africa, SW Indian Ocean. Mar. Geol. 263, 46-63.

Green, A.N., Garlick, G.L., 2011. A sequence stratigraphic framework for a narrow, current-swept continental shelf: The Durban Bight, central KwaZulu-Natal, South Africa. J. Afr. Earth Sci. 60, 303-314.

Green, A.N., Cooper, J.A.G., Leuci, R., Thackeray, Z., 2013a. Formation and preservation of an overstepped segmented lagoon complex on a high-energy continental shelf. Sedimentology 60, 1755-1768.

Green, A.N., Dladla, N., Garlick, G.L., 2013b. Spatial and temporal variations in incised valley systems from the Durban continental shelf, KwaZulu-Natal, South Africa. Mar. Geol. 335, 148-161.

Green, A.N., Cooper, J.A.G., Salzmann, L., 2014. Geomorphic and stratigraphic signals of postglacial meltwater pulses on continental shelves. Geology 42, 151-154.

Green, A.N., Cooper, J.A.G., Wiles, E.A., De Lecea, A.M., 2015. Seismic architecture, stratigraphy and evolution of a subtropical marine embayment: Maputo Bay, Mozambique. Mar. Geol. 369, 300-309.

Green, A.N., Cooper, J.A.G., Salzmann, L., 2018. The role of shelf morphology and antecedent setting in the preservation of palaeo-shoreline (beachrock and aeolianite) sequences: the SE African shelf. Geo-Mar. Lett. 38, 5-18.

Greene, D.L. Jr, Rodriguez, A.B., Anderson, J.B., 2007. Seaward-branching coastal-plain and piedmont incised-valley systems through multiple sea-level

cycles: Late Quaternary examples from Mobile Bay and Mississippi Sound, USA. J. Sed. Res. 77, 139-158.

Grippa, A., Bianca, M., Tropeano, M., Cilumbriello, A., Gallipoli, M.R., Mucciarelli, M., Sabato, L., 2011. Use of the HVSR method to detect buried paleomorphologies (filled incised-valleys) below a coastal plain: the case of the Metaponto plain (Basilicata, southern Italy). B. Geofis. Teor. Appl. 52, 225-240.

Gupta, S., Collier, J. S., Palmer-Felgate, A., Potter, G., 2007. Catastrophic flooding origin of shelf valley systems in the English Channel. Nature 448, 342-345.

Hallsworth, C.R., Chisholm, J.I., 2008. Provenance of late Carboniferous sandstones in the Pennine Basin (UK) from combined heavy mineral, garnet geochemistry and palaeocurrent studies. Sed. Geol. 203, 196-212.

Hallsworth, C.R., Morton, A.C., Claoué-Long, J., Fanning, C.M., 2000. Carboniferous sand provenance in the Pennine Basin, UK: constraints from heavy mineral and detrital zircon age data. Sed. Geol. 137, 147–185.

Hampson, G.J., 1995. Incised valley fills and sequence stratigraphy of selected carboniferous delta systems in the UK. Unpublished PhD Thesis, University of Liverpool.

Hampson, G.J., 1997. A sequence stratigraphic model for deposition of the Lower Kinderscout Delta, an Upper Carboniferous turbidite-fronted delta. Proc. Yorkshire Geol. Soc. 51, 273-296.

Hampson, G.J., Elliott, T., Flint, S.S., 1996. Critical application of high resolution sequence stratigraphic concepts to the Rough Rock Group (Upper Carboniferous) of northern England. In: Howell, J. A., Aitken, J. F. (Eds.), High resolution sequence stratigraphy: innovations and applications. Geol. Soc. London Spec. Publ., 104, 221-246.

Hampson, G.J., Davies, S.J., Elliott, T., Flint, S.S., Stollhofen, H., 1999. Incised valley fill sandstone bodies in Upper Carboniferous fluvio–deltaic strata: recognition and reservoir characterization of Southern North Sea analogues. In: Fleet, A.J., Boldy, S.A.R. (Eds), Petroleum Geology of Northwest Europe: Proceedings of the 5th Conference. Geological Society of London, pp. 771-788.

Hansford, M.R., Plink-Björklund, P., Jones, E.R., 2020. Global quantitative analyses of river discharge variability and hydrograph shape with respect to climate types. Earth-Sci. Rev. 102977.

Harris, P.T., Macmillan-Lawler, M., Rupp, J., Baker, E.K., 2014. Geomorphology of the oceans. Mar. Geol. 352, 4-24.

Hartley, A.J., 1993. Silesian sedimentation in south-west Britain: sedimentary responses to the developing Variscan Orogeny. In: Gayer, R. A., Greiling, R. O., Voger, A. K. (Eds.), Rhenohercynian and Subvariscan Fold Belts. Braunschweig, Vieweg, pp. 159-196.

Hayes, M.O., 1979. Barrier island morphology as a function of tidal and wave regime. In: Leatherman, S.P. (Ed.), Barrier Islands from the Gulf of Mexico to the Gulf of St. Lawrence. Academic Press, New York, pp. 1-28.

Healy, T., Werner, F., 1987. Sediment budget for a semi-enclosed sea in a near homogeneous lithology; example of Kieler Bucht, Western Baltic. Senckenb. Marit 19, 32-70.

Healy, T., Harada, K., 1991a. Definition and physical characteristics of the world's enclosed coastal seas. Mar. Pollut. Bull. 23, 639-644.

Healy, T., Harada, K., 1991b. Enclosed and Semi-Enclosed Coastal Seas. J. Coastal Res. 7, i-vi.

Heap, A.D., Nichol, S.L., 1997. The influence of limited accommodation space on the stratigraphy of an incised-valley succession: Weiti River estuary, New Zealand. Mar. Geol. 144, 229-252.

Helland-Hansen, W., Martinsen, O.J., 1996. Shoreline trajectories and sequences: description of variable depositional-dip scenarios. J. Sed. Res. 66, 670–688.

Helland-Hansen, W., Steel, R.J., Somme, T.O., 2012. Shelf genesis revisited. J. Sed. Res. 82, 133–1148.

Hickin, E.J., Nanson, G.C., 1975. The character of channel migration of the Beatton River, northeast British Columbia, Canada. Geol. Soc. Am. Bull. 86, 487–494.

Hickin, E.J., Nanson, G.C., 1984. Lateral migration rates of river bends. J. Hydraul. Eng. 110, 1557–1567.

Hill, J.C., Driscoll, N.W., 2008. Paleodrainage on the Chukchi shelf reveals sea level history and meltwater discharge. Mar. Geol. 254, 129-151.

Hill, J.C., Driscoll, N.W., Brigham-Grette, J., Donnelly, J. P., Gayes, P. T., Keigwin, L., 2007. New evidence for high discharge to the Chukchi shelf since the Last Glacial Maximum. Quatern. Res. 68, 271-279.

Holbrook, J., Schumm, S.A., 1999. Geomorphic and sedimentary response of rivers to tectonic deformation: a brief review and critique of a tool for recognizing subtle epeirogenic deformation in modern and ancient settings. Tectonophysics 305, 287-306.

Holbrook, J.M., Scott, R.W., Oboh-Ikuenobe, F.E., 2006. Base-level buffers and buttresses: a model for upstream verses downstream control on preservation of fluvial geometry and architecture within sequences. J. Sed. Res. 76, 162–174.

Holbrook, J., Wanas, H., 2014. A fulcrum approach to assessing source-to-sink mass balance using channel paleohydrologic paramaters derivable from common fluvial data sets with an example from the Cretaceous of Egypt. J. Sediment. Res. 84, 349-372.

Holdsworth, B.K., Collinson, J.D., 1988. Millstone Grit cyclicity revisited. In: Besly, B.M., Kelling, G., (Eds.), Sedimentation in a Synorogenic Basin Complex: The Upper Carboniferous of Northwest Europe. Blackie, Glasgow, pp. 132-152.

Hooke, J.M., 1979. An analysis of the processes of river bank erosion. J. Hydrol. 42, 39– 62.

Hooke, J.M., 1980. Magnitude and distribution of rates of river bank erosion. Earth Surf. Proc. 5, 143– 157.

Hopley, D., 1986. Beachrock as a sea-level indicator. In: van de Plassche, O. (Ed.), Sea level Research: A Manual for the Collection and Evaluation of Data. Geo Books, Regency House, Norwich, pp. 157–173.

Houbolt, J.J.H.C., 1968. Recent sediments in the southern bight of the North Sea. Geol. Mijnb. 47, 245-273.

Howard, A.D., 1998. Long profile development of bedrock channels: interaction of weathering, mass wasting, bed erosion, and sediment transport. In: Tinkler, J., Wohl, E. (Eds.), Rivers over Rock: Fluvial Processes in Bedrock Channels. AGU Geophysical Monograph, 107, pp. 297–313.

Howard, A.D., Dietrich, W.E., Seidl, M.A., 1994. Modeling fluvial erosion on regional to continental scales. J. Geophys. Res. 99, 13971–13986.

Huisink, M., 2000. Changing river styles in response to Weichselian climate changes in the Vecht valley, eastern Netherlands. Sed. Geol. 133, 115–134.

Huisink, M., de Moor, J.J.W., Kasse, C., Virtanen, T., 2002. Factors influencing periglacial morphology in the northern European Russian tundra and taiga. Earth Surf. Proc. Land. 27, 1223–1235.

Hume, T.M., 2005. Tidal Prism. In: Schwartz, M.L. (Eds), Encyclopedia of Coastal Science. Encyclopedia of Earth Science Series. Springer, Dordrecht.

IBM Corp. Released 2015. IBM SPSS Statistics for Windows, Version 23.0. Armonk, NY: IBM Corp.

Ishihara, T., Sugai, T., Hachinohe, S., 2011. Buried surfaces during the Last Glacial Age in the middle and upper part of the Arakawa Lowland and the Menuma Lowland, Central Japan. The Quatern. Res. (Japan) 50, 113–128.

Ishihara, T., Sugai, T., Hachinohe, S., 2012. Fluvial response to sea-level changes since the latest Pleistocene in the near-coastal lowland, central Kanto Plain, Japan. Geomorphology 147, 49-60.

Ishihara, T., Sugai, T., 2017. Eustatic and regional tectonic controls on late Pleistocene paleovalley morphology in the central Kanto Plain, Japan. Japan. Quatern. Int. 456, 69-84.

Jackson, R.G., 1975. Hierarchical attributes and a unifying model of bed forms composed of cohesionless material and produced by shearing flow. Geol. Soc. Am. Bull. 86, 1523–1533.

Jain, M., Tandon, S. K., 2003. Fluvial response to Late Quaternary climate changes, western India. Quatern. Sci. Rev. 22, 2223-2235.

James, G., Witten, D., Hastie, T., Tibshirani, R., 2013. An introduction to statistical learning. Springer, New York.

Jerolmack, D.J., Mohrig, D., 2005. Frozen dynamics of migrating bedforms. Geology 33, 57–60.

Jerrett, R.M., Hampson, G.J., 2007. Sequence stratigraphy of the upper Millstone Grit (Yeadonian, Namurian), North Wales. Geol. J. 42, 513-530.

Jervey, M.T., 1988. Quantitative geological modeling of siliciclastic rock sequences and their seismic expression. In: Wilgus, C.K., Hastings, B.S., Kendall, C.G.S.C., Posamentier, H.W., Ross, C.A., Van Wagoner, J.C. (Eds.), Sea-level changes: an integrated approach. SEPM spec. Publ. 42, 47–69.

Joeckel, R.M., 1999. Tectonic Uplift and Climate Change. Bull. Am. Meteorol. Soc. 80, 936.

Johnson, M.J., 1990a. Overlooked sedimentary particles from tropical weathering environments. Geology 18, 107–110.

Johnson, M.J., 1990b. Tectonic versus chemical-weathering controls on the composition of fluvial sands in tropical environments. Sedimentology 37, 713–726.

Johnson, M.J., 1993. The system controlling the composition of clastic sediments. Geol. Soc. Am. Spec. Pap. 284, 1–20.

Jones, C.M., Chisholm, J.I., 1997. The Roaches and Ashover Grits: sequence stratigraphic interpretation of a 'turbidite-fronted delta' system. Geol. J. 32, 45-68.

Karisiddaiah, S.M., Veerayya, M., Vora, K.H., 2002. Seismic and sequence stratigraphy of the central western continental margin of India: late-Quaternary evolution. Mar. Geol. 192, 335-353.

Kassambara, A., Mundt, F., 2017. factoextra: Extract and Visualize the Results of Multivariate Data Analyses. R package version 1.0.5. https://CRAN.R-project.org/package=factoextra (accessed 21 August 2019).

Kasse, C., 1997. Cold-climate aeolian sand-sheet formation in north-western Europe (c. 14–12.4 ka): a response to permafrost degradation and increased aridity. Permafrost Periglac. Process. 8, 295–311.

Kennedy, D.M., Paulik, R., Millar, M., 2008. Infill of a structurally controlled estuary: an example from southern Whanganui Inlet, New Zealand. N. Z. Geogr. 64, 20–33.

Kennish, M.J., 1991. Ecology of estuaries: anthropogenic effects. CRC press, Boca Raton.

Kolla, V., Posamentier, H.W., Eichenseer, H., 1995. Stranded parasequences and the forced regressive wedge systems tract: deposition during base-level fall-discussion. Sed. Geol. 95, 139-145.

Korus, J.T., Kvale, E.P., Eriksson, K.A., Joeckel, R.M., 2008. Compound paleovalley fills in the Lower Pennsylvanian New River Formation, West Virginia, USA. Sed. Geol. 208, 15-26.

Labaune, C., Tesson, M., Gensous, B., 2005. Integration of High and Very High-resolution Seismic Reflection Profiles to Study Upper Quaternary Deposits of a Coastal Area in the Western Gulf of Lions, SW France. Mar. Geophys. Res. 26, 109-122.

Labaune, C., Tesson, M., Gensous, B., Parize, O., Imbert, P, Delhaye-Prat, V., 2010. Detailed architecture of a compound incised valley system and correlation with forced regressive wedges: Example of Late Quaternary Têt and Agly rivers, western Gulf of Lions, Mediterranean Sea, France. Sed. Geol. 223, 360-379.

Lamb, M.P., Nittrouer, J.A., Mohrig, D., Shaw, J., 2012. Backwater and river plume controls on scour upstream of river mouths: Implications for fluvio-deltaic morphodynamics. J. Geophys. Res. 117, F01002.

Lambeck, K., Chappell, J., 2001. Sea level change through the last glacial cycle. Science 292, 679-86.

Lane, E.W., 1955. The importance of fluvial morphology in hydraulic engineering. Am. Soc. Civil Eng. Proc. 81, 1-17.

Lawler, D.M., Grove, J.R., Couperthwaite, J.S., Leeks, G.J.L., 1999. Downstream change in river bank erosion rates in the Swale-Ouse system, northern England. Hydrol. Process. 13, 977–992.

Leary, K., Ganti, V., 2020. Preserved fluvial cross strata record bedform disequilibrium dynamics. Geophys. Res. Lett. 47, e2019GL085910. https://doi.org/10.1029/2019GL085910.

Leckie, D.A., 1994. Canterbury Plains, New Zealand — implications for sequence strati- graphic models. AAPG Bull. 78, 1240–1252.

Leclair, S.F., 2002. Preservation of cross-strata due to the migration of subaqueous dunes: an experimental investigation. Sedimentology 49, 1157–1180.

Leclair, S.F., Bridge, J.S., 2001. Quantitative Interpretation of Sedimentary Structures Formed by River Dunes. J. Sediment. Res. 71, 713–716.

Lee, G.S., Cukur, D., Yoo, D.G., Bae, S.H., Kong, G.S., 2017. Sequence stratigraphy and evolution history of the continental shelf of South Sea, Korea, since the Last Glacial Maximum (LGM). Quatern. Int. 459, 17-28.

Leeder, M.R., Harris, T., Kirkby, M.J., 1998. Sediment supply and climate change: implications for basin stratigraphy. Basin Res. 10, 7–18.

Legarreta, L., Uliana, M.A., 1998. Anatomy of hinterland depositional sequences: Upper Cretaceous fluvial strata, Neuquen Basin, west-central Argentina. In: Shanley, K.W., McCabe, P.J. (Eds.), Relative Role of Eustasy Climate and Tectonism in Continental Rocks. SEPM Spec. Publ. 59, 83–92.

Lericolais G., Berné S., Féniès H., 2001. Seaward pinching out and internal stratigraphy of the Gironde incised valley on the shelf (Bay of Biscay). Mar. Geol. 175, 183-197.

Li, C.X., Wang, P.X., 1998. Late Quaternary stratigraphy of the Yangtze Delta. China Science Press, Beijing, pp. 222.

Li, C.X., Wang, P., Sun, H., Zhang, J., Fan, D., Deng, B., 2002. Late Quaternary incised-valley fill of the Yangtze delta (China): its stratigraphic framework and evolution. Sed. Geol. 152, 133-158.

Li, C.X., Wang, P., Fan, D., Yang, S., 2006. Characteristics and formation of Late Quaternary incised-valley-fill sequences in sediment-rich deltas and estuaries: case studies from China. In: Dalrymple R.W., Leckie D.A., Tillman R.W. (Eds.), Incised valleys in time and space. SEPM Spec. Publ. 85, 141-160.

Lin, C.M., Zhuo, H.C., Gao, S., 2005. Sedimentary facies and evolution in the Qiantang River incised valley, eastern China. Mar. Geol. 219, 235-259.

Lloret, E., Dessert, C., Gaillardet, J., Albéric, P., Crispi, O., Chaduteau, C., Benedetti, M.F., 2011. Comparison of dissolved inorganic and organic carbon yields and fluxes in the watersheds of tropical volcanic islands, examples from Guadeloupe (French West Indies). Chem. Geol. 280, 65-78.

Lobo, F.J., Hernández-Molina, F.J., Somoza, L., del Río, V.D., 2001. The sedimentary record of the post-glacial transgression on the Gulf of Cadiz continental shelf (Southwest Spain). Mar. Geol. 178, 171-195.

Lobo, F.J., García, M., Luján, M., Mendes, I., Reguera, M.I., Van Rooij, D., 2018. Morphology of the last subaerial unconformity on a shelf: insights into transgressive ravinement and incised valley occurrence in the Gulf of Cádiz. Geo-Mar. Lett. 38, 33-45.

Lockhart, D.A., Lang, S.C., Allen, G.P., 1996. Stratal Architecture and Seismic Stratigraphy of Late Quaternary Bedrock-Controlled Incised Valley Systems, Southern Moreton Bay, Australia. Proceedings, the International Symposium on Sequence Stratigraphy, S.E. Asia, May 1995.

Loget, N., Van Den Driessche, J., 2009. Wave train model for knickpoint migration. Geomorphology 106, 376–382.

Luketina, D., 1998. Simple tidal prism models revisited. Estuar. Coast. Shelf. Sci. 46, 77-84.

Mackey, S.D., Bridge, J.S., 1995. Three-dimensional model of alluvial stratigraphy: theory and application. J. Sed. Res. 65, 7-31.

Mackin, J.H., 1948. Concept of the graded river. Geol. Soc. Am. Bull. 59, 463–512.

Makinouchi, T., Mori, S., Danhara, T., Takemura, K., 2006. Stratigraphic horizon and formational process of the first gravel formation (BG) in the Nobi Plain. Memoirs Geol. Soc. Jpn. 59, 129–140 (in Japanese, with English abstract).

Marlianingrum, P. R., Kusumastanto, T., Adrianto, L., Fahrudin, A., 2019. Economic analysis of management option for sustainable mangrove ecosystem in Tangerang District, Banten Province, Indonesia. In IOP Conference Series: Earth and Environmental Science (Vol. 241, No. 1, p. 012026). IOP Publishing.

Marsaglia, K.M., Ingersoll, R.V., 1992. Compositional trends in arc-related, deep-marine sand and sandstone: a reassessment of magmatic-arc provenance. Geol. Soc. Am. Bull. 104, 1637–1649.

Martin, J., Cantelli, A., Paola, C., Blum, M., Wolinsky, M., 2011. Quantitative modeling of the evolution and geometry of incised valleys. J. Sed. Res. 81, 64–79.

Martinsen, O.J., 1990. Interaction Between Eustacy, Tectonics and Sedimentation with Particular Reference to the Namurian E1c-H2c of the Craven-Askrigg Area, Northern England. Unpublished PhD Thesis, Universitetet i Bergen, Norway.

Martinsen, O.J., 1993. Depositional systems of the Craven-Askrigg Area, northern England: implications for sequence-stratigraphic models. In: Posamentier, H.W., Summerhayes, C.P., Haq, B.U., Allen, G.P. (Eds.), Sequence Stratigraphy and Facies Associations. Int. Assoc. Sedimentol. Spec. Publ. 18, 247-281.

Martinsen, O.J., Collinson, J.D., Holdsworth, B.K., 1995. Millstone Grit cyclicity revisited, II: sequence stratigraphy and sedimentary responses to changes of relative sea-level. In: Plint, A.G. (Ed.), Sedimentary Facies Analysis: A Tribute to the Research and Teaching of Harold G. Reading. Int. Assoc. Sedimentol. Spec. Publ. 22, 305-327.

Maselli, V., Trincardi, F., 2013. Large-scale single incised valley from a small catchment basin on the western Adriatic margin (central Mediterranean Sea). Global Planet. Change 100, 245-262.

Maselli, V., Trincardi, F., Asioli, A., Ceregato, A., Rizzetto, F., Taviani, M., 2014. Delta growth and river valleys: the influence of climate and sea level changes on the South Adriatic shelf (Mediterranean Sea). Quatern. Sci. Rev. 99, 146-163.

Masselink, G., Hughes, M.G., 2003. Introduction to Coastal Processes and Geomorphology. Oxford University Press, New York, pp. 354.

Mattheus, C.R., Rodriguez, A.B., Greene, D.L., Simms, A.R., Anderson, J.B., 2007. Control of upstream variables on incised-valley dimension. J. Sed. Res. 77, 213–224.

Mattheus, C.R., Rodriguez, A.B., 2011. Controls on late Quaternary incised-valley dimension along passive margins evaluated using empirical data. Sedimentology 58, 1113-1137.

Mattheus, C.R., Rodriguez, A.B., 2014. Controls on lower-coastal-plain valley morphology and fill architecture. J. Sed. Res. 84, 314-325.

Maynard, J.R., 1992. Sequence stratigraphy of the upper Yeadonian of northern England. Mar. Petrol. Geol. 9,197-207.

Maynard, J.R., Leeder, M.R., 1992. On the periodicity and magnitude of Late Carboniferous glacio-eustatie sea-level changes. J. Geol. Soc. London 149, 303-311.

McCandless, T.L., 2003. Maryland Stream Survey: Bankfull Discharge and Channel Characteristics of Streams in the Coastal Plain Hydrologic Region. U.S. Fish and Wildlife Service, Report CBFO-S03-02.

Melvin, J., 1986. Upper Carboniferous fine-grained turbiditic sandstones from Southwest England; a model for growth in an ancient, delta-fed subsea fan. J. Sediment. Res. 56, 19-34.

Menier, D., 2004. Morphologie et remplissage des vallées fossiles sud-armoricaines: apport de la stratigraphie sismique. PhD Thesis, Université de Bretagne Sud.

Menier, D., Reynaud, J.Y., Proust, J.N., Guillocheau, F., Guennoc, P., Bonnet, S., Tessier, B., Goubert, E., 2006. Basement control on shaping and infilling of valleys incised at the southern coast of Brittany, France. In: Dalrymple, R.W., Leckie, D.A., Tillman, R.W. (Eds.), Incised valleys in time and space. SEPM Spec. Publ. 85, 37-55.

Menier, D., Tessier, B., Proust, J.N., Baltzer, A., Sorrel, P., Traini, C., 2010. The Holocene transgression as recorded by incised-valley infilling in a rocky coast context with low sediment supply (southern Brittany, western France). Bull. Soc. Géol. Fr. 181, 115-128.

Metcalf, C., 2004. Regional channel characteristics for maintaining natural fluvial geomorphology in Florida streams. U.S. Fish and Wildlife Service, Panama City Fisheries Resource Office.

Metcalf, C., Shaneyfelt, R., 2005. Alabama Riparian Reference Reach and Regional Curve Study. U.S. Fish and Wildlife Service, Panama City Fisheries Resource Office.

METOCEAN 2019: https://app.metoceanview.com/hindcast/ (accessed 1 March 2019)

Miall, A.D., 1996. The Geology of Fluvial Deposits: Sedimentary Facies, Basin Analysis, and Petroleum Geology. Springer-Verlag, Heidelberg.

Miall, A.D., 2002. Architecture and sequence stratigraphy of Pleistocene fluvial systems in the Malay Basin, based on seismic time-slice analysis. AAPG Bull. 86, 1201–1216.

Miall, A.D., 2014. Fluvial depositional systems. Springer, Berlin.

Millar, R.G., 2000. Influence of bank vegetation on alluvial channel patterns. Water Resour. Res. 36, 1109–1118.

Miller, E.L., Soloviev, A.V., Prokopiev, A.V., Toro, J., Harris, D., Kuzmichev, A.B., Gehrels, G.E., 2013. Triassic river systems and the paleo-Pacific margin of northwestern Pangea. Gondwana Res. 23, 1631-1645.

Miller, K.G., Kominz, M.A., Browning, J.V., Wright, J.D., Mountain, G.S., Katz, M.E., Sugarman, P.J., Cramer, B.S., Christie-Blick, N., Pekar, S.F., 2005. The Phanerozoic record of global sea-level change. Science 310, 1293–1298.

Milli, S., D'Ambrogi, C., Bellotti, P., Calderoni, G., Carboni, M.G., Celant, A., Di Bella, L., Di Rita, F., Frezza, V., Magri, D., Pichezzi, R.M., Ricci, V., 2013. The transition from wave-dominated estuary to wave-dominated delta: the Late Quaternary stratigraphic architecture of Tiber River deltaic succession (Italy). Sed. Geol. 284, 159-180.

Milli, S., Mancini, M., Moscatelli, M., Stigliano, F., Marini, M., Cavinato, G.P., 2016. From river to shelf, anatomy of a high-frequency depositional sequence: The Late Pleistocene to Holocene Tiber depositional sequence. Sedimentology 63, 1886-1928.

Milliman, J.D., 1995. Sediment discharge to the ocean from small mountainous rivers: the New Guinea example. Geo-Mar. Lett. 15, 127-133.

Milliman, J.D., Syvitski, J.P.M., 1992. Geomorphic/tectonic control of sediment discharge to the oceans: The importance of small mountainous rivers. J. Geol. 100, 525–544.

Mitchum Jr, R.M., Van Wagoner, J.C., 1991. High-frequency sequences and their stacking patterns: sequence-stratigraphic evidence of high-frequency eustatic cycles. Sed. Geol. 70, 131-160.

Mitchum, R.M., 1985. Seismic stratigraphic expression of submarine fans. In: Berg, O.R., Woolverton, D.G. (Eds.), Seismic Stratigraphy II—An Integrated Approach. AAPG Memoir 39, 116–136.

Moore, C.H., 2001. Carbonate reservoir porosity evolution and diagenesis in a sequence stratigraphic framework. In: van Loon, A.J. (Ed.), Developments in Sedimentology. Elsevier, Doorwerth, Netherlands, 55, pp. 185–244.

Morton, R.A., Suter, J.R., 1996. Sequence stratigraphy of composition of late Quaternary shelf-margin deltas, northern Gulf of Mexico. AAPG Bull. 80, 505-530.

Mulder, T., Syvitski, J.P.M., 1996. Climatic and morphologic relationships of rivers: implications of sea-level fluctuations on river loads. Journal of Geology 104, 509–523.

Muto, T., Swenson, J.B., 2005. Large-scale fluvial grade as a nonequilibrium state in linked depositional systems: Theory and experiment. J. Geophys. Res. 110, F3.

Myrow, P. M., Jerolmack, D. J., Perron, J. T., 2018. Bedform Disequilibrium. J. Sediment. Res. 88, 1096–1113.

Nanson, G.C., Hickin, E.J., 1983. Channel migration and incision on the Beatton River. J. Hydraul. Eng. 109, 327-337.

Nanson, G.C., Hickin, E.J., 1986. A statistical analysis of bank erosion and channel migration in western Canada. Geol. Soc. Am. Bull. 97, 497-504.

Ngueutchoua, G., Giresse, P., 2010. Sand bodies and incised valleys within the Late Quaternary Sanaga–Nyong delta complex on the middle continental shelf of Cameroon. Mar. Petrol. Geol. 27, 2173-2188.

Nichol, S.L., Boyd, R., Penland, S., 1996. Sequence stratigraphy of a coastal-plain incised valley estuary, Lake Calcasieu, Louisiana. J. Sed. Res. 66, 847-857.

Nicholas, A. P., Smith, G. H. S., Amsler, M. L., Ashworth, P. J., Best, J. L., Hardy, R. J., et al., 2016. The role of discharge variability in determining alluvial stratigraphy. Geology 44, 3–6.

NOAA 2019: https://tidesandcurrents.noaa.gov/map/index.html (accessed 1 March 2019)

Nordfjord, S., Goff, J.A., Austin, J.A., Sommerfield, C.K., 2005. Seismic geomorphology of buried channel systems on the New Jersey outer shelf: assessing past environmental conditions. Mar. Geol. 214, 339-364.

Nordfjord, S., Goff, J.A., Austin, J.A., Gulick, S.P.S., 2006. Seismic facies of incised-valley fills, New Jersey continental shelf: implications for erosion and preservation processes acting during latest Pleistocene–Holocene transgression. J. Sed. Res. 76, 1284-1303.

O'Beirne, A.M., 1996. Controls on Silesian sedimentation in the Pennine Basin, UK and Appalachian Basin, Eastern Kentucky. Unpublished PhD Thesis, Oxford Brookes University, UK.

Oertel, G.F., Foyle, A.M., 1995. Drainage displacement by sea-level fluctuation at the outer margin of the Chesapeake Seaway. J. Coastal Res. 11, 583-604.

Olariu, C., Steel, R.J., 2009. Influence of point-source sediment-supply on modern shelf-slope morphology: implications for interpretation of ancient shelf margins. Basin Res. 21, 484–501.

Olariu, C., Steel, R.J., Dalrymple, R.W., Gingras, M.K., 2012. Tidal dunes versus tidal bars: the sedimentological and architectural characteristics of compound

dunes in a tidal seaway, the lower Baronia Sandstone (Lower Eocene), Ager Basin, Spain. Sediment. Geol. 279, 134e155.

O'Mara, P. T., Merryweather, M., Stockwel, M., Bowler, M. M., 1999. The Trent Gas Field: correlation and reservoir quality within a complex Carboniferous stratigraphy. In: Fleet, A.J., Boldy, S.A.R. (Eds.), Petroleum Geology of Nortwest Europe. Proceedings of the 5th Petroleum Geology Conference, 809-821.

Paola, C., Borgman, L., 1991. Reconstructing random topography from preserved stratification. Sedimentology 38, 553–565.

Paola, C., Heller, P.L. , Angevine, C.L., 1992. The large-scale dynamics of grain-size variation in alluvial basins, 1: Theory. Basin Res. 4, 73-90.

Patacca, E., Scandone, P., 2001. Late thrust propagation and sedimentary response in the thrust belt-foredeep system of the Southern Apennines (Pliocene–Pleistocene), In: Vai, G.B., Martini, I.P. (Eds.), Anatomy of an Orogen. Kluwer Academic Publication, 401–440.

Payenberg, T.H., Boyd, R., Beaudoin, J., Ruming, K., Davies, S., Roberts, J., Lang, S.C., 2006. The filling of an incised valley by shelf dunes — An example from Hervey Bay, east coast of Australia. In: Dalrymple, R.W., Leckie, D.A., Tillman, R.W. (Eds.), Incised valleys in time and space. SEPM Spec. Publ. 85, 87-98.

Peakall, J., Ashworth, P.J., Best, J.L., 2007. Meanderbend evolution, alluvial architecture, and the role of cohesion in sinuous river channels: a flume study. J. Sed. Res. 77, 197–212.

Peltier, W.R., Fairbanks, R.G., 2006. Global glacial ice volume and Last Glacial Maximum Duration from an extended Barbados sea level record. Quatern. Sci. Rev. 25, 3322–3337.

Perlmutter, M.A., Matthews, M.D., 1990. Global cyclostratigraphy—a model. In: Cross, T.A. (Ed.), Quantitative dynamic stratigraphy. Prentice Hall, Englewood Cliffs, pp. 233–260.

Petter, A.L., 2011. Reconstructing backwater reaches of paleorivers and their influence on fluvial facies distribution, Campanian Lower Castlegate Sandstone, Utah. Geological Society of America Annual Meeting, Minneapolis, Paper 149-12.

Pettijohn, F.J., Potter, P.E., Siever, R., 1987. Sand and Sandstone. Springer Science & Business Media, NewYork, pp. 553.

Phillips, J.D., 2011. Drainage area and incised valley fills in Texas rivers: A potential explanation. Sed. Geol. 242, 65–70.

Plink-Björklund, P., 2015. Morphodynamics of rivers strongly affected by monsoon precipitation: review of depositional style and forcing factors. Sed. Geol. 323, 110–147.

Pointon, M.A., Cliff, R.A., Chew, D.M., 2012. The provenance of Western Irish Namurian Basin sedimentary strata inferred using detrital zircon U–Pb LA-ICP-MS geochronology. Geol. J. 47, 77-98.

Portela, L.I., Ramos, S., Teixeira, A.T., 2013. Effects of salinity on the settling velocity of fine sediments of a harbour basin. J. Coastal Res. 65, 1188–1193.

Posamentier, H.W., Jervey, M.T., Vail, P.R., 1988. Eustatic controls on clastic deposition I —conceptual framework. In: Wilgus, C.K., Hastings, B.S., Kendall, C.G.C., Posamentier, H.W., Ross, C.A., Van Wagoner, J.C. (Eds.), Sea-Level Changes: An Integrated Approach. SEPM Spec. Publ. 42, 109–124.

Posamentier, H.W., Vail, P.R., 1988. Eustatic control on clastic deposition II— sequence and system tract models. In: Wilgus, C.K., Hastings, B.S., Kendall, C.G.C., Posamentier, H.W., Ross, C.A., Van Wagoner, J.C. (Eds.), Sea-Level Changes: An Integrated Approach. SEPM Spec. Publ. 42, 125–154.

Posamentier, H.W., Allen, G.P., James, D.P., Tesson, M., 1992. Forced regressions in a sequence stratigraphic framework: concepts, examples and exploration significance. AAPG Bull. 76, 1687-1709.

Posamentier, H. W., Allen, G. P., 1999. Siliciclastic sequence stratigraphy: concepts and applications. SEPM, Tulsa, Oklahoma.

Posamentier, H.W., 2001. Lowstand alluvial bypass systems: incised vs. unincised. AAPG Bull. 85, 1771–1793.

Posamentier, H.W., Kolla, V., 2003. Seismic geomorphology and stratigraphy of deposi- tional elements in deep-water settings. J. Sed. Res. 73, 367–388.

Powell, J.W., 1875. Exploration of the Colorado River of the West and Its Tributaries. U.S. Government Printing Office, Washington, D.C., pp. 291.

Pranter, M.J., Cole, R.D., Panjaitan, H., Sommer, N.K., 2009. Sandstone-body dimensions in a lower coastal-plain depositional setting: lower Williams fork formation, coal canyon, piceance basin, Colorado. AAPG Bull. 93, 1379-1401.

Pretorius, L., Green, A., Cooper, A., 2016. Submerged shoreline preservation and ravinement during rapid postglacial sea-level rise and subsequent “slowstand”. Geol. Soc. Am. Bull. 128, 1059-1069.

Proust, J.N., Menier, D., Guillocheau, F., Guennoc, P., Bonnet, S., Rouby, D., Le Corre, C., 2001. Fossil valleys in the bay of Vilaine (Brittany, France): Nature and

evolution of the Pleistocene coastal sediment wedge of Brittany. Bull. Soc. Géol. Fr. 172, 737-749.

Proust J.N., Renault M., Guennoc P., Thinon I., 2010. Sedimentary architecture of the Loire River drowned valleys of the French Atlantic shelf. Bull. Soc. Géol. Fr. 181, 129-149.

Pulham A.J., 1988. Depositional and syn-sedimentary deformation processes in Namurian deltaic sequences of West County Clare, Ireland. Unpublished PhD Thesis, University College of Swansea, UK.

Pulham, A.J., 1989. Controls on internal structure and architecture of sandstone bodies within Upper Carboniferous fluvial-dominated deltas, County Clare, western Ireland, In: Whateley, M. K. G., Pickering, K. T. (Eds.), Deltas: Sites and Traps for Fossil Fuels. Geol. Soc. London Spec. Publ. 41, 179-203.

R Core Team, 2019. R: A language and environment for statistical computing. R Foundation for Statistical Computing, Vienna, Austria. https://www.R-project.org/ (accessed 21 August 2019).

Ray, N., Adams, J., 2001. A GIS-based vegetation map of the world at the last glacial maximum (25,000-15,000 BP). Int. Archaeol., 11. http://intarch.ac.uk/journal/issue11/bristowpindex.html (accessed 21 April 2018). DOI: 10.11141/ia.11.2.

Reading, H.G., Collinson, J.D., 1996. Clastic Coasts. In: Reading, H.G. (Ed.), Sedimentary Environments: Processes, Facies and Stratigraphy. Blackwell Science, Oxford, pp.154-231.

Reesink, A. J. H., 2019. Interpretation of cross strata formed by unit bars. In: Ghinassi et al. (Eds.), Fluvial Meanders and Their Sedimentary Products in the Rock Record. Int. Assoc. Sedimentol. Spec. Publ. 48, 173-200.

Reijenstein, H.M., Posamentier, H.W., Bhattacharya, J.P., 2011. Seismic geomorphology and high-resolution seismic stratigraphy of inner-shelf fluvial, estuarine, deltaic, and marine sequences, Gulf of Thailand. AAPG Bull. 95, 1959-1990.

Reynolds, A.D., 1999. Dimensions of paralic sandstone bodies. AAPG Bull. 83, 211-229.

Richard, G. A., Julien, P. Y., Baird, D. C., 2005. Statistical analysis of lateral migration of the Rio Grande, New Mexico. Geomorphology 71, 139-155.

Riley, N.J., Claoué-Long, J.C., Higgins, A.C., Owens, B., Spears, A., Taylor, L., Varker, W.J., 1995. Geochronometry and geochemistry of the European mid-

Carboniferous boundary global stratotype proposal, Stonehead Beck, North Yorkshire, UK. Ann. Soc Géol. Belg., 116, 275–289.

Rippon, J.H., 1996. Sand body orientation, palaeoslope analysis and basin-fill implications in the Westphalian A–C of Great Britain. J. Geol. Soc. London 153, 881-900.

Roberts, H.H., Sydow, J., 2003. Late Quaternary stratigraphy and sedimentology of the offshore Mahakam delta, east Kalimantan (Indonesia). In: Sidi, F.H., Nummedal, D., Imbert, P., Darman, H., Posamentier, H.W. (Eds.), Tropical Deltas of Southeast Asia—Sedimentology, Stratigraphy, and Petroleum Geology. SEPM Spec. Publ. 76, 125-145.

Rodriguez, A.B., Anderson, J.B., Simms, A.R., 2005. Terrace inundation as an autocyclic mechanism for parasequence formation: Galveston Estuary, Texas, USA. J. Sed. Res. 75, 608-620.

Rodriguez, A.B., Duran, D.M., Mattheus, C.R., Anderson, J.B., 2008. Sediment accommodation control on estuarine evolution: An example from Weeks Bay, Alabama, USA. In: Anderson, J.B., Rodriguez, A.B. (Eds.), Response of upper Gulf Coast estuaries to Holocene climate change and sea-level rise. Geol. Soc. Am. Spec. Pap. 443, 31-42.

Rossi, V., Amorosi, A., Sarti, G., Mariotti, S., 2017. Late Quaternary multiple incised-valley systems: An unusually well-preserved stratigraphic record of two interglacial valley-fill successions from the Arno plain (northern Tuscany, Italy). Sedimentology 64, 1901-1928.

Roy, P.S., 1984. New South Wales Estuaries: their origin and evolution. In: Thom B.G. (Eds.), Coastal Geomorphology in Australia. Academic Press, Sydney, NSW, pp. 99–121.

Ruddiman, W.F., 2013. Tectonic uplift and climate change. Springer Science & Business Media.

Rygel, M.C., Fielding, C.R., Frank, T.D., Birgenheier, L.P., 2008. The magnitude of Late Paleozoic glacioeustatic fluctuations: a synthesis. J. Sediment. Res. 78, 500-511.

Sakai, T., Fujiwara, O., Kamataki, T., 2006. Incised-valley-fill succession affected by rapid tectonic uplifts: An example from the uppermost Pleistocene to Holocene of the Isumi River lowland, central Boso Peninsula, Japan. Sed. Geol. 185, 21-39.

Salem, A. M., Ketzer, J. M., Morad, S., Rizk, R. R., Al-Aasm, I. S., 2005. Diagenesis and reservoir-quality evolution of incised-valley sandstones: evidence from the Abu

Madi gas reservoirs (Upper Miocene), The Nile Delta Basin, Egypt. J. Sed. Res. 75, 572-584.

Salzmann, L., Green, A., Cooper, J. A. G., 2013. Submerged barrier shoreline sequences on a high energy, steep and narrow shelf. Mar. Geol. 346, 366-374.

Santos, M.G., Mountney, N.P., Peakall, J., 2017. Tectonic and environmental controls on Palaeozoic fluvial environments: reassessing the impacts of early land plants on sedimentation. J. Geol. Soc. London 174, 393-404.

Schneider, C.A., Rasband, W.S., Eliceiri, K.W., 2012. NIH Image to ImageJ: 25 years of image analysis. Nat. Methods 9, 671.

Schumm, S.A., 1968. Speculations concerning paleohydrologic controls of terrestrial sedimentation. Geol. Soc. Am. Bull. 79, 1573-1588.

Schumm, S.A., Harvey, M.D., Watson, C.C., 1984. Incised Channels: Morphology, Dynamics and Control. Water Resources Publication, Chelsea, MI, pp. 200.

Schumm, S.A., Brackenridge, S.A., 1987. River response. In: Ruddiman, W.F., Wright H.E. Jr (Eds.), North America and Adjacent Oceans during the Last Deglaciation. Geol. Soc. Am., The Geology of North America, K-3, 221–240.

Schumm, S.A., 1993. River response to base-level change: Implications for sequence stratigraphy. J. Geol. 101, 279–294.

Schwartz, M.L. (2005-2011) Encyclopedia of Coastal Science. Kluwer Academic Publishers, Dordrecht.

Scotese, C.R., McKerrow, W.S., 1990. Revised world maps and introduction. In: McKerrow, W.S., Scotese, C.R. (Eds.), Palaeozoic Palaeogeography and Biogeography. Geol. Soc. London Mem. 12, 1–21.

Shanley, K.W., 2004. Fluvial reservoir description for a giant, low-permeability gas field. Jonah Field, Green River Basin, WY.

Shanley, K.W., McCabe, P.J., 1994. Perspectives on the sequence stratigraphy of continental strata: report of a working group at the 1991 NUNA conference of high resolution sequence stratigraphy. AAPG Bull. 78, 544–568.

Sheets, B.A., Hickson, T.A., Paola, C., 2002. Assembling the stratigraphic record: depositional patterns and timescales in an experimental alluvial basin. Basin Res. 14, 287–301.

Shideler, G.L., Ludwick, J.C., Oertel, G.F., Finkelstein, K., 1984. Quaternary stratigraphic evolution of the southern Delmarva Peninsula coastal zone, Cape Charles, Virginia. Geol. Soc. Am. Bull. 95, 489-502.

Simms, A.R., 2005. Late Quaternary/Holocene evolution of the Nueces incised valley, central Texas. PhD Thesis, Rice University, Houston.

Simms, A.R., Anderson, J.B., Taha, Z.P., Rodriguez, A.B., 2006. Overfilled versus underfilled incised valleys: examples from the Quaternary Gulf of Mexico. In: Dalrymple, R.W., Leckie, D.A., Tillman, R.W. (Eds.), Incised valleys in time and space. SEPM Spec. Publ. 85, 117-139.

Simms, A.R., Anderson, J.B., Milliken, K.T., Taha, Z.P., Wellner, J.S., 2007a. Geomorphology and age of the OIS2 (last lowstand) sequence boundary on the northwestern Gulf of Mexico continental shelf. In: Davies, R.J., Posamentier, H.W., Wood, L.J., Cartwright, J.A. (Eds.), Seismic Geomorphology: Applications to Hydrocarbon Exploration and Production. Geol. Soc. London Spec. Publ. 277, 29–46.

Simms, A.R., Lambeck, K., Purcell, A., Anderson, J.B., Rodriguez, A.B., 2007b. Sea-level history of the Gulf of Mexico since the Last Glacial Maximum with implications for the melting history of the Laurentide Ice Sheet. Quatern. Sci. Rev. 26, 920-940.

Simms, A.R., Aryal, N., Miller, L., Yokoyama, Y., 2010. The incised valley of Baffin Bay, Texas: a tale of two climates. Sedimentology 57, 642–669.

Sinclair, H.D., Allen, P.A., 1992. Vertical versus horizontal motions in the Alpine orogenic wedge: stratigraphic response in the foreland basin. Basin Res. 4, 215-232.

Sloss, C.R., Jones, B.G., Murray-Wallace, C.V., McClennen, C.E., 2005. Holocene sea level fluctuations and the sedimentary evolution of a barrier estuary: Lake Illawarra, New South Wales, Australia. J. Coastal Res. 21, 943-959.

Sloss, C.R., Jones, B.G., McClennen, C.E., de Carli, J., Price, D.M., 2006. The geomorphological evolution of a wave-dominated barrier estuary: Burrill Lake, New South Wales, Australia. Sed. Geol. 187, 229-249.

Sloss, C.R., Jones, B.G., Switzer, A.D., Nichol, S., Clement, A.J., Nicholas, A.W., 2010. The Holocene infill of Lake Conjola, a narrow incised valley system on the southeast coast of Australia. Quatern. Int. 221, 23-35.

Smyth, W.C., 1991. Seismic facies analysis and depositional history of an incised valley system, Galveston Bay area, Texas. PhD Thesis, Rice University, Houston.

Soltan, R., Mountney, N.P., 2016. Interpreting complex fluvial channel and barform architecture: Carboniferous Central Pennine Province, northern England. Sedimentology 63, 207-252.

Sømme, T.O., Helland-Hansen, W., Martinsen, O.J., Thurmond, J.B., 2009a. Relationships between morphological and sedimentological parameters in source-to-sink systems: A basis for predicting semi-quantitative characteristics in subsurface systems. Basin Res. 21, 361–387

Sømme, T.O., Martinsen, O.J., Thurmond, J.B., 2009b. Reconstructing morphological and depositional characteristics in subsurface sedimentary systems: An example from the Maastrichtian-Danian Ormen Lange system, Møre Basin, Norwegian Sea. AAPG Bull. 93, 1347–1377.

Sømme, T.O., Helland-Hansen, W., Granjeon, D., 2009c. Impact of eustatic amplitude variations on shelf morphology, sediment dispersal, and sequence stratigraphic interpretation: Icehouse versus greenhouse systems. Geology 37, 587-590.

Stallard, R.F., Edmond, J.M., 1983. Geochemistry of the Amazon: 2. The influence of geology and weathering environment on the dissolved load. J. Geophys. Res. 88, 9671-9688.

Stephen, K.D., Dalrymple, M., 2002. Reservoir simulations developed from an outcrop of incised valley fill strata. AAPG Bull. 86, 797–822.

Stirling, E. J., 2003. Architecture of fluvio-deltaic sandbodies: the Namurian of Co. Clare, Ireland, as an analogue for the Plio-Pleistocene of the Nile Delta. Unpublished PhD Thesis, University of Leeds, UK.

Stive, M.J.F., De Vriend, H.J., 1995. Modelling shoreface profile evolution. Mar. Geol. 126, 235–248.

Stockmaster, B.A., 2017. Paleodrainage insights into the fluvial and glacial history of the western Chukchi margin, Arctic Alaska. Ph.D. Thesis, Coastal Carolina University, pp. 45-73.

Storms, J.E.A., Weltje, G.J., Terra, G.J., Cattaneo, A., Trincardi, F., 2008. Coastal dynamics under conditions of rapid sea-level rise: Late Pleistocene to Early Holocene evolution of barrier–lagoon systems on the northern Adriatic shelf (Italy). Quatern. Sci. Rev. 27, 1107–1123.

Strong, N., Paola, C., 2006. Fluvial landscapes and stratigraphy in a flume. Sed. Rec. 4, 4–8.

Strong, N., Paola, C., 2008. Valleys that never were: time surfaces versus stratigraphic surfaces. J. Sed. Res. 78, 579–593.

Stuart, J.Y., 2015. Subsurface architecture of fluvial-deltaic deposits in high-and low-accommodation settings. Unpublished PhD Thesis, University of Leeds, UK.

Sugai, T., Sugiyama, Y., 1998. Deep Seismic Reflection Survey of Concealed Active Structures in the Nobi Basin Dynamics and Subsidence History of the Nobi Plain, Central Japan. Geological Survey of Japan Interim Report EQ/98/1, 55-66 (in Japanese with English abstract).

Sugai, T., Sugiyama, Y., 1999. Basin Dynamics and Subsidence History of the Nobi Plain, Central Japan, Revealed by 600 M Deep Core Analysis and Deep Seismic Reflection Survey. Geological Survey of Japan Interim Report EQ/99/3, 77-87 (in Japanese with English abstract).

Summerfield, M.A., 1985. Plate tectonics and landscape development on the African continent. Tectonic Geomorphology, 27–51.

Sweet, M. L., Blum, M. D., 2016. Connections Between Fluvial To Shallow Marine Environments and Submarine Canyons: Implications For Sediment Transfer To Deep Water. J. Sed. Res. 86, 1147-1162.

Sweet, W.V., Geratz, J.W., 2003. Bankfull hydraulic geometry relationships and recurrence intervals for North Carolina's Coastal Plain. American Water Resources Association Journal 39, 861–871.

Sydow, J.C., 1996. Holocene to Late Pleistocene Stratigraphy of the Mahakam Delta, Kalimantan, Indonesia. Ph.D. Thesis, Louisiana State University.

Syvitski, J.P.M., Milliman, J.D., 2007. Geology, geography, and humans battle for dominance over the delivery of fluvial sediment to the coastal ocean. J. Geol. 115, 1–19.

Syvitski, J.P.M., Peckham, S.D., Hilberman, R., Mulder, T., 2003. Predicting the terrestrial flux of sediment to the global ocean: a planetary perspective. Sediment. Geol. 162, 5–24.

Takashimizu, Y., Shibuya, T., Abe, Y., Otsuka, T., Suzuki, S., Ishii, C., Miyama, Y., Konishi H., Hu, S.G., 2016. Depositional facies and sequence of the latest Pleistocene to Holocene incised valley fill in Kushiro Plain, Hokkaido, northern Japan. Quatern. Int. 397, 159-172.

Talling, P.J., 1998. How and where do incised valleys form if sea level remains above the shelf edge? Geology 26, 87–90.

Tanabe, S., Saito, Y., Vu, Q.L., Hanebuth, T.J., Ngo, Q.L., Kitamura, A., 2006. Holocene evolution of the Song Hong (Red River) delta system, northern Vietnam. Sed. Geol. 187, 29-61.

Tanabe, S., Nakanishi, T., Matsushima, H., Hong, W., 2013. Sediment accumulation patterns in a tectonically subsiding incised valley: Insight from the Echigo Plain, central Japan. Mar. Geol. 336, 33-43.

Tanabe, S., Nakanishi, T., Ishihara, Y., Nakashima, R., 2015. Millennial-scale stratigraphy of a tide-dominated incised valley during the last 14 kyr: Spatial and quantitative reconstruction in the Tokyo Lowland, central Japan. Sedimentology 62, 1837-1872.

Tessier, B., Delsinne, N., Sorrel, P., 2010a. Holocene sedimentary infilling of a tide-dominated estuarine mouth. The example of the macrotidal Seine estuary (NW France). Bull. Soc. Géol. Fr. 181, 87–98.

Tessier, B., Billeaud, I., Lesueur, P., 2010b. Stratigraphic organization of a composite macrotidal wedge: the Holocene sedimentary infill of the Mont-Saint-Michel Bay. Bull. Soc. Géol. Fr. 181, 99–113.

Tessier, T., Billeaud, I., Sorrel, P., Delsinne, N., Lesueur, P., 2012. Infilling stratigraphy of macrotidal tide-dominated estuaries. Controlling mechanisms: sea-level fluctuations, bedrock morphology, sediment supply and climate changes (the examples of the Seine estuary and the Mont-Saint-Michel Bay, English Channel, NW France). Sediment. Geol. 279, 62–73.

Tesson, M., Labaune, C., Gensous, B., Suc, J. P., Melinte-Dobrinescu, M., Parize, O., Imbert, P., Delhaye-Prat, V., 2011. Quaternary "Compound" Incised Valley In A Microtidal Environment, Roussillon Continental Shelf, Western Gulf of Lions, France. J. Sed. Res. 81, 708-729.

Tesson, M., Posamentier, H., Gensous, B., 2015. Compound incised-valley characterization by high-resolution seismics in a wave-dominated setting: Example of the Aude and Orb rivers, Languedoc inner shelf, Gulf of Lion, France. Mar. Geol. 367, 1-21.

Thieler, E.R., Butman, B., Schwab, W.C., Allison, M.A., Driscoll, N.W., Donnelly, F.P., Uchupi, E., 2007. A catastrophic meltwater flood event and the formation of the Hudson Shelf Valley. Palaeogeogr. Palaeoclimatol. Palaeoecol. 246, 120–136.

Thomas, M.A., Anderson, J.B., 1994. Sea-level controls on the facies architecture of the Trinity/Sabine incised-valley system, Texas continental shelf. In: Dalrymple, R.W., Boyd, R., Zaitlin, B.A. (Eds.), Incised-Valley Systems: Origin and Sedimentary Sequences. SEPM Spec. Publ. 51, 63–82.

Thorne, J., 1994. Constraints on riverine valley incision and the response to sea-level change based on fluid mechanics. In: Dalrymple, R.W., Boyd, R., Zaitlin, B.A.

(Eds.), Incised-Valley Systems: Origin and Sedimentary Sequences. SEPM Spec. Publ. 51, 29–45.

Tjallingii, R., Stattegger, K., Wetzel, A., Van Phach, P., 2010. Infilling and flooding of the Mekong River incised valley during deglacial sea-level rise. Quatern. Sci. Rev. 29, 1432-1444.

Törnqvist, T.E., 1998. Longitudinal profile evolution of the Rhine-Meuse system during the last deglaciation: interplay of climate change and glacio. Terra Nova 10, 11-15.

Törnqvist, T. E., Wortman, S. R., Mateo, Z. R. P., Milne, G. A., Swenson, J. B., 2006. Did the last sea level lowstand always lead to cross-shelf valley formation and source-to-sink sediment flux? J. Geophys. Res. 111, F04002.

Trincardi, F., Correggiari, A., Roveri, M., 1994. Late Quaternary transgressive erosion and deposition in a modern epicontinental shelf: the Adriatic semi-enclosed Basin. Geo-Mar. Lett. 14, 41–51.

Tropeano, M., Cilumbriello, A., Sabato, L., Gallicchio, S., Grippa, A., Longhitano, S.G., Bianca, M., Gallipoli, M.R., Mucciarelli, M., Spilotro, G., 2013. Surface and subsurface of the Metaponto Coastal Plain (Gulf of Taranto—southern Italy): Present-day- vs LGM-landscape. Geomorphology 203, 115-131.

Trower, E. J., Ganti, V., Fischer, W. W., Lamb, M. P., 2018. Erosional surfaces in the Upper Cretaceous Castlegate Sandstone (Utah, USA): Sequence boundaries or autogenic scour from backwater hydrodynamics? Geology 46, 707–710.

Twichell, D. C., Cross, V. A., Peterson, C. D., 2010. Partitioning of sediment on the shelf offshore of the Columbia River littoral cell. Mar. Geol. 273, 11-31.

Tye, R.S., 2004. Geomorphology: an approach to determining subsurface reservoir dimensions. AAPG Bull. 88, 1123-1147.

Vail, P.R., Todd, R.G., Sangree, J.B., 1977. Seismic stratigraphy and global changes of sea level, part 5: chronostratigraphic significance of seismic reflections. In: Payton, C.E. (Ed.), Seismic Stratigraphy — Applications to Hydrocarbon Exploration. AAPG Spec. Publ. 26, 99–116.

Van Heijst, M.W.I.M., Postma, G., 2001. Fluvial response to sea-level changes: a quantitative analogue, experimental approach. Basin Res. 13, 269-292.

Van Wagoner, J.C., Posamentier, H.W., Mitchum, R.M., Vail, P.R., Sarg, J.F., Loutit, T.S., Hardenbol, J., 1988. An overview of sequence stratigraphy and key definitions. In: Wilgus, C.K., Hastings, B.S., Kendall, C.G.St.C., Posamentier, H.W.,

Ross, C.A., Van Wagoner, J.C. (Eds.),Sea-level Changes: An Integrated Approach. SEPM Spec. Publ. 42, 39–45.

Van Wagoner, J.C., Mitchum, R.M., Campion, K.m., Rahmanian, V.D., 1990. Siliciclastic sequence stratigraphy in well logs, core, and outcrops: concepts for high resolution correlation of time and facies. AAPG Meth. Explor. Ser. 7, 55.

Vandenberghe, J., 2003. Climate forcing of fluvial system development: an evolution of ideas. Quatern. Sci. Rev. 22, 2053-2060.

Vis, G.J., Kasse, C., 2009. Late Quaternary valley fill succession of the Lower Tagus Valley, Portugal. Sed. Geol. 221, 19–39.

Vis, G.J., Kasse, C., Vandenberghe, J., 2008. Late Pleistocene and Holocene palaeogeography of the Lower Tagus Valley (Portugal): effects of relative sea level, valley morphology and sediment supply. Quatern. Sci. Rev. 27, 1682-1709.

Vital, H., Furtado, S.F.L., Gomes, M.P., 2010. Response of the Apodi-Mossoró estuary-incised valley system (NE Brazil) to sea-level fluctuations. Braz. J. Oceanog. 58, 13–24.

Vousdoukas, M.I., Velegrakis, A.F., Plomaritis, T.A., 2007. Beachrock occurrence, characteristics, formation mechanisms and impacts. Earth-Sci. Rev. 85, 23–46.

Vu, V.Q., 2011. ggbiplot: A ggplot2 based biplot. R package version 0.55. http://github.com/vqv/ggbiplot (accessed 21 August 2019).

Walker, R.G., 1976. Facies Models 3. Sandy fluvial systems. Geoscience Canada 3, 101–109.

Wang, R., Colombera, L., Mountney, N.P., 2019. Geologic controls on the geometry of incised-valley fills: Insights from a global dataset of late-Quaternary examples. Sedimentology 66, 2134-2168.

Wang, R., Colombera, L., Mountney, N.P., 2020. Database-Driven Quantitative Analysis of the Stratigraphic Architecture of Incised-Valley Fills. Earth-Sci. Rev. 102988, 1-25.

Waters, C.N., Chisholm, J.I., Benfield, A.C., O'Beirne, A.M., 2008. Regional evolution of a fluviodeltaic cyclic succession in the Marsdenian (late Namurian Stage, Pennsylvanian) of the Central Pennine Basin, UK. Proc. Yorkshire Geol. Soc. 57, 1-28.

Waters, C.N., Waters, R.A., Barclay, W.J., Davies, J.R., 2009. A lithostratigraphical framework for the Carboniferous successions of southern Great Britain (Onshore). British Geological Survey Research Report, RR/09/01.

Waters, C.N., Condon, D.J., 2012. Nature and timing of Late Mississippian to Mid-Pennsylvanian glacio-eustatic sea-level changes of the Pennine Basin, UK. J. Geol. Soc. London 169, 37-51.

Weber, N., Chaumillon, E., Tesson, M., Garlan, T., 2004. Architecture and morphology of the outer segment of a mixed tide and wave-dominated-incised valley, revealed by HR seismic reflection profiling: the paleo-Charente River, France. Mar. Geol. 207, 17-38.

Wellner, R.W., Bartek, L.R., 2003. The effect of sea level, climate, and shelf physiography on the development of incised-valley complexes: a modern example from the East China Sea. J. Sed. Res. 73, 926-940.

Weschenfelder, J., Baitelli, R., Corrêa, I.C., Bortolin, E.C., dos Santos, C.B., 2014. Quaternary incised valleys in southern Brazil coastal zone. J. S. Am. Earth Sci. 55, 83-93.

Wescott, W.A., 1993. Geomorphic thresholds and complex response of fluvial systems—some implications for sequence stratigraphy. AAPG Bull. 77, 1208-1218.

Wetzel, A., Szczygielski, A., Unverricht, D., Stattegger, K., 2017. Sedimentological and ichnological implications of rapid Holocene flooding of a gently sloping mud-dominated incised valley–an example from the Red River (Gulf of Tonkin). Sedimentology 64, 1173-1202.

Wickham H., 2016. ggplot2: Elegant Graphics for Data Analysis, second ed. Springer, New York.

Wignall, P.B., Best, J.L., 2000. The Western Irish Namurian Basin reassessed. Basin Res. 12, 59–78.

Wilkinson, B.H., Byrne, J.R., 1977. Lavaca Bay – Transgressive deltaic sedimentation in central Texas estuary. AAPG Bull. 61, 527-545.

Wilson, K., Berryman, K., Cochran, U., Little, T., 2007. A Holocene incised valley infill sequence developed on a tectonically active coast: Pakarae River, New Zealand. Sed. Geol. 197, 333-354.

Wohl, E., Barros, A., Brunsell, N. et al., 2012. The hydrology of the humid tropics. Nat. Clim. Change. 2, 655-662.

Wong, H.K., Lüdmann, T., Haft, C., Paulsen, A.-M., Hübscher, C., Geng, J., 2003. Quaternary sedimentation in the Molengraaff paleo-delta, northern Sunda Shelf (southern South China Sea). In: Sidi, F.H., Nummedal, D., Imbert, P., Darman, H., Posamentier, H.W.(Eds.), Tropical Deltas of Southeast Asia Pacific Region—

Sedimentology, Stratigraphy, and Petroleum Geology. SEPM Spec. Publ. 76, 201–216.

Woo, M.K., 1986. Permafrost hydrology in North America. Atmosphere-Ocean 24, 201-234.

Woo, M.K., Winter, T.C., 1993. The role of permafrost and seasonal frost in the hydrology of northern wetlands in North America. J. Hydrol. 141, 5–31.

Wood, L.J., Ethridge, F.G., Schumm, S.A., 1993. The effects of base-level fluctuations on coastal plain-shelfslope depositional systems: an experimental approach. In: Posamentier, H.W., Summerhayes, C.P., Haq, B.U., Allen G.P. (Eds.), Sequence Stratigraphy and Facies Associations. Int. Assoc. Sedimentol. Spec. Publ. 18, 43–54.

Woolfe, K.J., Larcombe, P., Naish, T., Purdon, R.G., 1998. Lowstand rivers need not incise the shelf: an example from the Great Barrier Reef, Australia, with implications for sequence stratigraphic models. Geology 26, 75-78.

Wright, V.P., Marriott, S.B., 1993. The sequence stratigraphy of fluvial depositional systems: the role of floodplain sediment storage. Sed. Geol. 86, 203-210.

Wright, V.P., Vanstone, S.D., 2001. Onset of Late Palaeozoic glacio-eustasy and the evolving climates of low latitude areas: a synthesis of current understanding. J. Geol. Soc. London 158, 579-582.

Xu, J., Snedden, J.W., Galloway, W.E., Milliken, K.T., Blum, M.D., 2017. Channel-belt scaling relationship and application to early Miocene source-to-sink systems in the Gulf of Mexico basin. Geosphere 13, 179-200.

Yokoyama, Y., Lambeck, K., De Deckker, P., Johnston, P., Fifield, L.K., 2000. Timing of the Last Glacial Maximum from observed sea-level minima. Nature 406, 713–716.

Yoshida, S., Steel, R., Dalrymple, R., Maceachern, J., 2005. Facies change between wave/storm- and tide/current-generated deposits within a relative sea level cycle: Outcrop examples from the Cretaceous Western Interior Seaway in North America—A Review: International Geological Correlation Programme 475 Delta conference.

Zaitlin, B.A., Dalrymple, R.W., Boyd, R., 1994. The stratigraphic organization of incisedvalley systems associated with relative sea-level change. In: Dalrymple, R.W., Boyd, R., Zaitlin, B.A. (Eds.), Incised-Valley Systems: Origin and Sedimentary Sequences. SEPM Spec. Publ. 51, 45–60.

Zhang, G.J., Li, C.X., 1996. The fills and stratigraphic sequences in the Qiantangjiang incised paleovalley, China. J. Sed. Res. 66, 406-414.

Zhang, X., Lin, C.M., Dalrymple, R.W., Gao, S., Li, Y.L., 2014. Facies architecture and depositional model of a macrotidal incised-valley succession (Qiantang River estuary, eastern China), and differences from other macrotidal systems. Geol. Soc. Am. Bull. 126, 499-522.

Zhang, X., Dalrymple, R. W., Lin, C.M., 2017. Facies and stratigraphic architecture of the late Pleistocene to early Holocene tide-dominated paleo-Changjiang (Yangtze River) delta. Geol. Soc. Am. Bull. 130, 455-483.

Zhuo, H.T., Wang, Y.M., Shi, H.S., He, M., Chen, W.T., Li, H., Wang, Y., Yan, W.Y., 2015. Contrasting fluvial styles across the mid-Pleistocene climate transition in the northern shelf of the South China Sea: evidence from 3D seismic data. Quatern. Sci. Rev. 129, 128–146.

List of digital appendices

In the attached CD, additional material is included as spreadsheets named as follows:

- **Digital appendix A:** contains a Microsoft Excel spreadsheet that gives a detailed account of case studies and the associated parameters stored in the Shallow-Marine Architecture Knowledge Store (SMAKS) database on the dimensions of late-Quaternary incised-valley fills presented in Chapter 3.

- **Digital appendix B:** contains a Microsoft Excel spreadsheet that details all case studies and the associated parameters stored in the Shallow-Marine Architecture Knowledge Store (SMAKS) database on the stratigraphic architecture of late-Quaternary incised-valley fills presented in Chapter 4.

- **Digital appendix C:** contains a Microsoft Excel spreadsheet that includes datasets relating to proportions of facies types in fluvial deposits of Namurian incised-valley fills in UK and Ireland, measured thickness of dune-scale cross sets for each incised-valley fill and dimensions of incised-valley fills presented in Chapter 5.